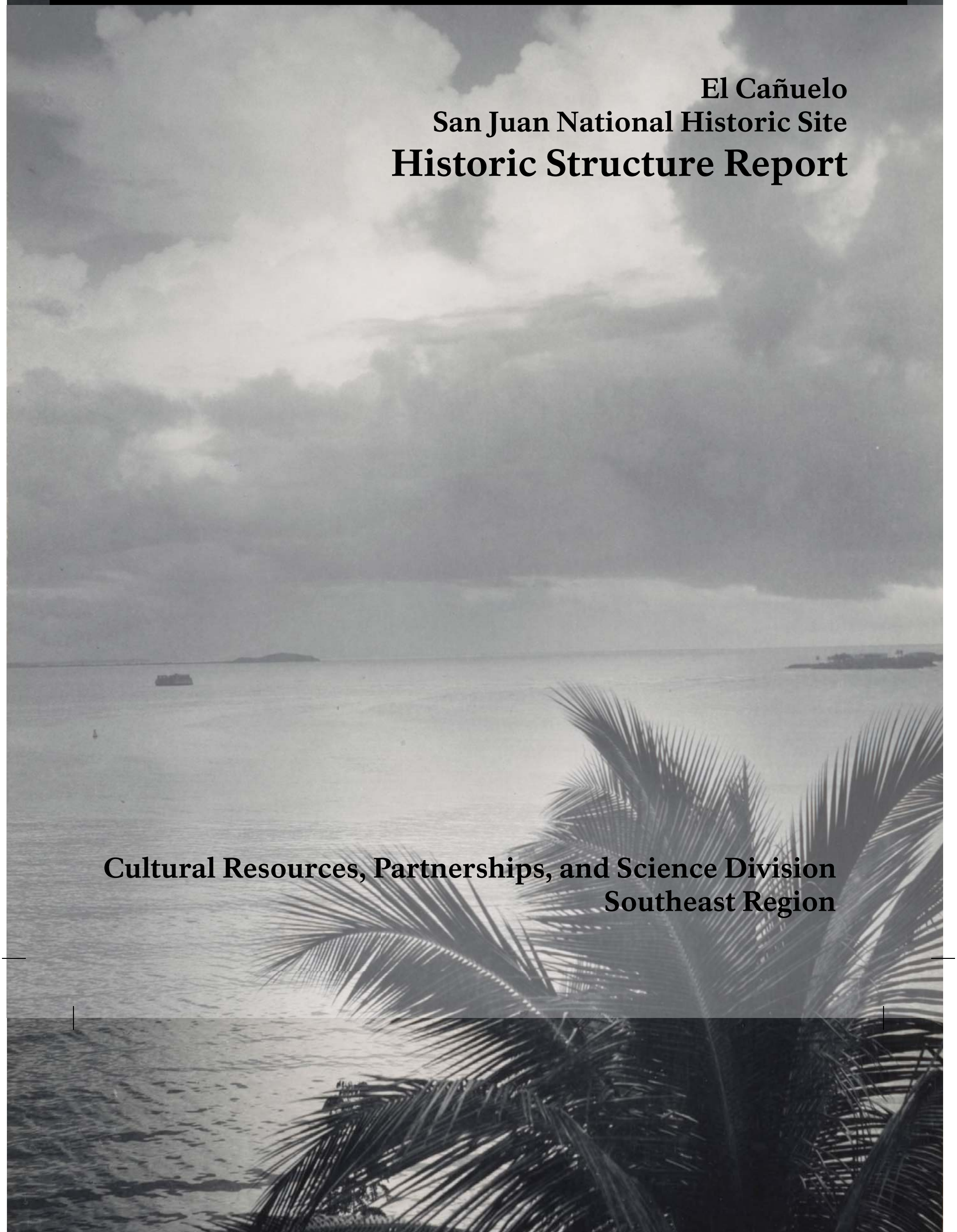
saju_hsr_front.ai crop marks are black .5 pt lines

National Park Service
U.S. Department of the Interior

San Juan National Historical Site

El Cañuelo
San Juan National Historic Site
Historic Structure Report



Cultural Resources, Partnerships, and Science Division
Southeast Region

El Cañuelo

San Juan National Historic Site

Historic Structure Report

May 2018
Prepared by:
WLA Studio
RATIO
Palmer Engineering
Building Conservation Associates, Inc.

Under the direction of
National Park Service
Southeast Regional Office
Cultural Resources, Partnerships, & Science Division



The report presented here exists in two formats. A printed version is available for study at the park, the Southeastern Regional Office of the National Park Service, and at a variety of other repositories. For more widespread access, this report also exists in a web-based format through ParkNet, the website of the National Park Service. Please visit www.nps.gov for more information.

Cultural Resources, Partnerships, & Science Division
Southeast Regional Office
National Park Service
100 Alabama Street, SW
Atlanta, Georgia 30303
(404)507-5847

San Juan Historic Site
501 Norzagaray Street
San Juan, PR 00901

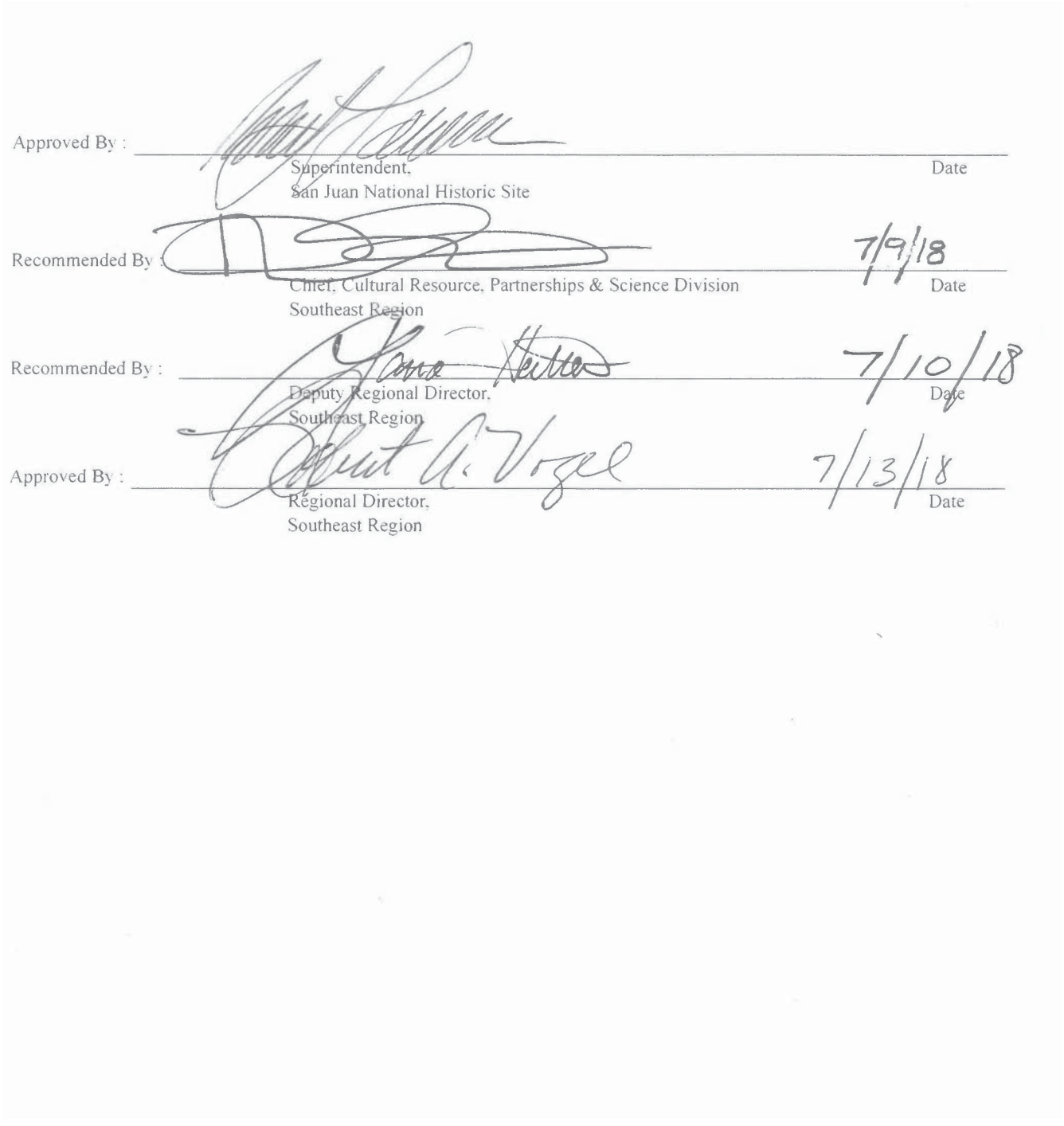
www.nps.gov/saju

About the cover: Eleanor Butler Roosevelt, "View from E's window looking northwest," Library of Congress.

El Cañuelo

San Juan National Historic Site

Historic Structure Report



Approved By : _____ Date
Superintendent,
San Juan National Historic Site

Recommended By : _____ 7/9/18 Date
Chief, Cultural Resource, Partnerships & Science Division
Southeast Region

Recommended By : _____ 7/10/18 Date
Deputy Regional Director,
Southeast Region

Approved By : _____ 7/13/18 Date
Regional Director,
Southeast Region

Page intentionally left blank.

Table of Contents

Foreword xv

Management Summary 1

Executive Summary 2
Purpose and Scope 2
Historical Overview 2
Statement of Significance 3
Project Methodology 3
Conclusions and Recommendations 3
Administrative Data 5
Locational Data 5
Related NPS Studies 5
Real Property Information 5
Size Information 5
Cultural Resource Data 5
Proposed Treatment 6

I.A Historical Background and Context 7

Introduction 7
The Conquest Period 1493-1625 8
Colony Evolves: From Frontier Post to Fortified City--1625-1812 12
From Age of Enlightenment to American Territory--1812-1898 16
War Department Era--1898-1949 18
Early National Park Service Period 1949-1985 22
Recent National Park Service Period 1985-2017 27

I.B Chronology of Development and Use 31

Military Use of El Cañuelo Island 31
Drake's Attack 31
First Fort Constructed on El Cañuelo 31
First Masonry Fort at El Cañuelo 1664 32
Ongoing Repairs to Fort at El Cañuelo 1665-1785 33
Spanish Non-Military Use of Fort El Cañuelo 1785-1898 34
Spanish Abandon Fort at El Cañuelo 1785-1840 34
Lazaretto 34
Spanish American War 1898 35
United States Agencies Management of El Cañuelo 35
United States War Department Period 1898-1949 35
Early National Park Service Period 1949-1985 36
Recent National Park Service Period 1985-2017 39
Timeline 47

I.C Physical Description 49

El Cañuelo: The Site 49
Las Cabras Island 49
El Cañuelo Landscape 50
El Cañuelo: Building 53
Exterior 53
Interior 61
Structural Analysis 68
Exterior 68
Interior 74
Structural Observation 79
El Cañuelo: Material Analysis 84
Introduction 84
Background Information 84
Archival Record 85
Methodology 86
Summary of Findings 86

I.D Significance and Integrity 97

San Juan National Historic Site Purpose and Significance 97
Significance Criteria 97
National Register Significance Evaluation 97
Character-Defining Features 97
Assessment of Integrity 99

II Treatment and Use 101

San Juan National Historic Site Preservation Philosophy 101
Alternatives for Treatment and Use 101
Requirements for Treatment and Use 102
Ultimate Treatment and Use 102
The Secretary of the Interior's Standards for Preservation 103
The Secretary of the Interior's Standards for Rehabilitation 104
Prioritization of Treatment Recommendations 104
Repair Mortar, Stucco, and Plaster Mixes 107
Resilience to Natural Hazards 111
Impact on El Cañuelo 112
Implications – Adapting to
Natural Hazards and Increased Climate Variability 112

Bibliography 115

List of Figures

About the cover: Eleanor Butler Roosevelt, "View from E's window looking northwest," Library of Congress. ii

Foreword xv

Management Summary 1

I.A Historical Background and Context 7

Figure 1: Site Map (NPS) 7
Figure 2: "Plano del asiento y del puerto de la ciudad de Puerto Rico [12 de septiembre de 1519]," (Archivo General de Indias) 8
Figure 3: "Remitido por Juan Ponce de León, con carta de 31 de julio de 1579,"(Archivo General de Indias) 9
Figure 4: "Plano de los puertos y barras de San Juan y Toa, [1660]" (Archivo General de Indias) 10
Figure 5: Drake's Attack 1595 (NPS) 11
Figure 6: Cumberland's Attack 1598 (NPS) 11
Figure 7: Dutch Attack 1625 (NPS) 12
Figure 8: "Puerto Rico… el año del señor de 1678 años," (Archivo General de Indias) 13
Figure 9: Detail of "Puerto Rico… el año del señor de 1678 años," (Archivo General de Indias) 13
Figure 10: "De Hoofdstad en Haven, van't Eiland Porto Rico [1731]" 14
Figure 11: "Port et Ville de Porto-Rico dans l'Isle de ce nom [1764]," (Library of Congress) 14
Figure 12: "Plano de ciudad de S. Juan [1770]," (Library of Congress) 14
Figure 13: "Plano de Pto. Rico [1780]," (Library of Congress) 14
Figure 14: English Attack 1797 (NPS) 15
Figure 15: Detail of "Plano de Pto. Rico [1780]," (Library of Congress) 15
Figure 16: "San Juan Puerto Rico [1794]," (Library of Congress) 16
Figure 17: 1841 Drawing (Image proved by Wanda Bobonis) 17
Figure 18: "El Canuelo, pre-1935 photograph, c. 1920-1934" (Archivo General de Puerto Rico) 17
Figure 19: "Plano de la Plaza de San Juan Puerto Rico [1886]", Archivo Digital Nacional de Puerto Rico) 18
Figure 20: Detail from "Plano de la Plaza de San Juan Puerto Rico [1886]", Archivo Digital Nacional de Puerto Rico) 18
Figure 21: "The Bombardment of San Juan by the American Fleet Porto Rico, [1898]" (Library of Congress) 18
Figure 22: "Before El Canuelo was connected to Las Cabras, [January 1935]" (Library of Congress) 20
Figure 23: "Fort Amezquita, [1958]" (NPS) 21
Figure 24: 1887 map overlaid on 2017 aerial 21

Figure 25: 1958 map overlaid on 2017 aerial 21
Figure 26: Aerial View San Juan Bay [circa 1954], (Archivo General de Puerto Rico) 22
Figure 27: "HABS: April 19, 1954 EAST AND NORTH ELEVATIONS", (Library of Congress) 22
Figure 28: "HABS: April 19, 1954 NORTH ELEVATION," (Library of Congress) 22
Figure 29: "HABS: April 19, 1954 DETAIL OF SENTRY BOX CORDON AND MASONRY, NE CORNER," (Library of Congress) 23
Figure 30: "HABS: April 19, 1954 DETAIL OF KITCHEN AND LATRINE SOUTHWEST CORNER," (Library of Congress) 23
Figure 31: "HABS: April 19, 1954 DETAIL OF SENTRY BOX CORDON AND MASONRY, NE CORNER," (Library of Congress) 23
Figure 32: "HABS: April 19, 1954 DETAIL OF ENTRANCE, EAST ELEVATION," (Library of Congress) .. 24
Figure 33: "HABS: April 19, 1954 WEST AND SOUTH ELEVATIONS," (Library of Congress) 24
Figure 34: "HABS: April 19, 1954 DETAIL OF ENTRANCE, EAST ELEVATION," (Library of Congress) .. 24
Figure 35: "Mario J. Buschiazzo inspecciona gran brecha en la bas del fortin del Cañulo," (University of Puerto Rico) 24
Figure 36: "Area adyacente al Fortin El Cañuelo en Isla de Cabras," (University of Puerto Rico) 25
Figure 37: "View of El Canuelo" (Archivo General de Puerto Rico) 26
Figure 38: "View of El Canuelo" (Archivo General de Puerto Rico) 26
Figure 39: "View of El Canuelo" (Archivo General de Puerto Rico) 26
Figure 40: "Restoration of Fort Wall [1960]," (National Park Service) 26
Figure 41: "View of Stairs at El Cañuelo [circa 1962]," (National Park Service) 27
Figure 42: "Stairs and Grate [1962]," (National Park Service) 27
Figure 43: Photograph showing El Cañuelo [undated] 27
Figure 44: "Sketch of Proposed Work, [circa 1991-1992]" (Puerto Rico State Historic Preservation Office) 28
Figure 45: "Fort Amezquita Survey [1991]," (NPS) 28
Figure 46: "HABS PR,7-SAJU,11—10," (Library of Congress) 28
Figure 47: "HABS PR,7-SAJU,11—11," (Library of Congress) 28
Figure 48: "HABS PR,7-SAJU,11—10," (Library of Congress) 28
Figure 49: "HABS PR,7-SAJU,11—13," (Library of Congress) 29
Figure 50: "HABS PR,7-SAJU,11—14," (Library of Congress) 29
Figure 51: "HABS PR,7-SAJU,11—15," (Library of Congress) 29
Figure 52: "HABS PR,7-SAJU,11—16," (Library of Congress) 29
Figure 53: "1992-2012 Maintenance, North Elevation," (San Juan National Historic Site) 30
Figure 54: "1992-2012 Maintenance," (San Juan National Historic Site) 30
Figure 55: "2012 Project," (San Juan National Historic Site) 30
Figure 56: "2012 Project," (San Juan National Historic Site) 30
Figure 57: "2012 Project," (San Juan National Historic Site) 30

I.B Chronology of Development and Use 31

Figure 58: Pre-1935, (Archivo General de Puerto Rico Annotated WLA Studio, 2017) 42
Figure 59: Circa 1935, (Library of Congress, Annotated WLA Studio, 2017) 42
Figure 60: HABS 1954, (Library of Congress, Annotated WLA Studio, 2017) 43

Figure 61: HABS 1954, (Library of Congress, Annotated WLA Studio, 2017) 43
Figure 62: HABS 1954, (Library of Congress, Annotated WLA Studio, 2017) 44
Figure 63: HABS, (Library of Congress, Annotated WLA Studio, 2017)..... 44
Figure 64: Circa 1954-1962, (Archivo General de Puerto Rico, Annotated WLA Studio, 2017)..... 45
Figure 65: HABS 1998, (Library of Congress, Annotated WLA Studio, 2017) 45
Figure 66: HABS 1998, (Annotated WLA Studio, 2017) 46
Figure 67: Google Map 2017, (Annotated WLA Studio, 2017)..... 46

I.C Physical Description..... 49

Figure 68: El Cañuelo Breakwaters, November 2016 (WLA Studio)..... 49
Figure 69: El Cañuelo Floating Debris in Lagoon, November 2016 (WLA Studio) 49
Figure 70: El Cañuelo Shoreline Erosion, November 2016 (WLA Studio) 49
Figure 71: El Cañuelo Access Road, November 2016 (WLA Studio) 50
Figure 72: El Cañuelo South Elevation, November 2016 (WLA Studio) 50
Figure 73: El Cañuelo Stone and Concrete Apron along South Elevation, November 2016 (WLA Studio)..... 50
Figure 74: El Cañuelo Sheet Pile Revetment at South Corner, November 2016 (WLA Studio)..... 50
Figure 75: El Cañuelo Picnic Shelters north of Fort, November 2016 (WLA Studio)..... 51
Figure 76: El Cañuelo Open Space with Lawn and Trees, November 2016 (WLA Studio)..... 51
Figure 77: El Cañuelo Debris Deposited on Shore, November 2016 (WLA Studio) 51
Figure 78: El Cañuelo Park Sign, November 2016 (WLA Studio)..... 51
Figure 79: El Cañuelo Interpretive Sign, November 2016 (WLA Studio)..... 51
Figure 80: View of El Cañuelo from El Morro (RATIO Architects) 52
Figure 81: East and north elevations of El Cañuelo from jetty (RATIO Architects)..... 52
Figure 82: North elevation (RATIO Architects) 52
Figure 83: Detail of north elevation showing stucco loss (RATIO Architects) 52
Figure 84: Detail of north elevation showing stucco loss and sentry box (RATIO Architects)..... 52
Figure 85: East and north elevations (RATIO Architects)..... 52
Figure 86: Detail of sentry box and northeast corner (RATIO Architects)..... 54
Figure 87: Detail of sentry box from southeast (RATIO Architects)..... 54
Figure 88: Detail of entry door (RATIO Architects) 54
Figure 89: Detail of cordón at east elevation (RATIO Architects) 54
Figure 90: View of grade conditions at east elevation (RATIO Architects)..... 54
Figure 91: West and south elevations from dock at Cabras Island gatehouse (RATIO Architects)..... 55
Figure 92: View of grade conditions at south elevation (RATIO Architects) 55
Figure 93: Gap in cordón at south elevation (RATIO Architects)..... 55
Figure 94: Detail of stucco loss at south elevation; typical brick infill patch (retaining stucco) to right of center (RATIO Architects)..... 55
Figure 95: West elevation (RATIO Architects)..... 56
Figure 96: Detail of latrine at west elevation (RATIO Architects) 56
Figure 97: Typical range of stucco conditions at west elevation (RATIO Architects) 56
Figure 98: Detail of cracks at west elevation (RATIO Architects)..... 56

Figure 99: View of terreplein looking northeast (RATIO Architects) 57
Figure 100: View of terreplein looking southwest (RATIO Architects) 57
Figure 101: Battlements of west and north walls (RATIO Architects) 57
Figure 102: Detail of stair scuttle door and sentry box (RATIO Architects) 58
Figure 103: Detail of sentry box (RATIO Architects) 58
Figure 104: Floor of sentry box (RATIO Architects) 58
Figure 105: View of El Morro and entry to San Juan Bay from sentry box corner window (RATIO Architects) 58
Figure 106: Detail of sentry box south window (RATIO Architects) 58
Figure 107: Overview of kitchen (202) and latrine (203) (RATIO Architects) 59
Figure 108: Detail of ***fogón*** at kitchen (RATIO Architects) 59
Figure 109: Detail of ***fogón*** at kitchen (RATIO Architects) 59
Figure 110: Latrine (203) (RATIO Architects) 60
Figure 111: Detail of latrine bench (RATIO Architects) 60
Figure 112: Detail of south chute of latrine with deck drains below (RATIO Architects) 60
Figure 113: Detail of east wall showing gap between 1992 concrete slab and walls (RATIO Architects) 60
Figure 114: Detail of rounded southwest corner between kitchen and latrine (RATIO Architects) 60
Figure 115: Detail rounded southwest corner from top of parapet (RATIO Architects) 60
Figure 116: View of Rooms 100 and 101, facing west (RATIO Architects) 62
Figure 117: View of Rooms 101 and 100 from terreplein, facing east (RATIO Architects) 62
Figure 118: Exterior brick threshold at Room 100 (RATIO Architects) 62
Figure 119: Detail of ruined brick masonry staircase at Room 101, facing northwest (RATIO Architects) 62
Figure 120: Door to Room 102 at west wall of Room 101 (RATIO Architects) 62
Figure 121: Ceiling at southwest corner of Room 101 showing 1992 concrete slab and 2012 wood beam (RATIO Architects) 63
Figure 122: Detail of former beam location at southwest corner of Room 101 (RATIO Architects) 63
Figure 123: Detail flooring of Rooms 102 (foreground) and 101 (RATIO Architects) 63
Figure 124: View of Room 102, facing east (RATIO Architects) 63
Figure 125: View of Room 102 facing west (RATIO Architects) 64
Figure 126: Detail of termite tube at north wall of Room 102 (RATIO Architects) 64
Figure 127: Room 103 looking into Room 100, facing north (RATIO Architects) 64
Figure 128: Room 103, facing south (RATIO Architects) 65
Figure 129: Floor of Room 103, facing south (RATIO Architects) 65
Figure 130: Upper north wall of Room 103 showing recess and pocket at left and graffiti above door (RATIO Architects) 65
Figure 131: View into pocket in northwest corner of Room 103, facing west (RATIO Architects) 65
Figure 132: Detail of pocket in east wall of Room 103, facing east (RATIO Architects) 65
Figure 133: Design team and NPS staff in Room 104, facing west (RATIO Architects) 66
Figure 134: Door from Room 104 to Room 103, facing east (RATIO Architects) 66
Figure 135: Northeast corner of Room 104 showing large crack (RATIO Architects) 66
Figure 136: Debris at floor of Room 104, facing northwest (RATIO Architects) 66

Figure 137: Large crack at south wall of Room 104, facing southwest (RATIO Architects)..... 67
Figure 138: View up into crack in ceiling of Room 104 showing debris in crack (RATIO Architects) .. 67
Figure 139: North Elevation, closeup of base of wall showing erosion of vertical head joints between stones (Palmer Engineering)..... 68
Figure 140: North Elevation, showing several of the holes that have been filled with brick pieces (Palmer Engineering)..... 68
Figure 141: East Corner, showing Sentry Box, Entry Door, Exterior Wood Platform and Stair. Note patches above door and to the left of door, as well as debris from storm waves (Palmer Engineering). 68
Figure 142: Entry Door in East Elevation, showing multiple patches of walls around door. Note missing cable in guardrail (Palmer Engineering). 69
Figure 143: East Elevation, showing cracks in render with white efflorescence outines, and close-up of patched cordon and parapet (Palmer Engineering). 69
Figure 144: South Corner looking at South Elevation, showing cracks (Palmer Engineering). 69
Figure 145: South Corner, viewed from parapet looking down at breakwater and steel sheet piles (Palmer Engineering)..... 69
Figure 146: South Elevation, close-up of cordon showing location where cordon was omitted (Palmer Engineering). 70
Figure 147: South Elevation, showing mortared crack (Palmer Engineering)..... 70
Figure 148: South Elevation looking at South Corner, showing erosion of breakwater (Palmer Engineering). 70
Figure 149: West Corner, looking at West Elevation. Note patched area, as well as mortared stones at grade, with rip rap breakwater beyond (Palmer Engineering). 70
Figure 150: West Corner, looking at West Elevation (Palmer Engineering)..... 71
Figure 151: West elevation at central crack. Note previous mortar patch, with new crack through patch (Palmer Engineering)..... 71
Figure 152: West Elevation at top of parapet, at central crack. Note remains of crack monitor (Palmer Engineering). 71
Figure 153: West elevation at central crack. Note two crack monitors. Note crack widens as it climbs the wall (Palmer Engineering). 71
Figure 154: Concrete Slab, from Interior Stair Room. Note termite infestation of wood beam. Note welded wire fabrix located at bottom of slab (Palmer Engineering).. 72
Figure 155: Scuttle Door in Concrete Slab, edge on top of North exterior wall, showing brick pavers (Palmer Engineering). 72
Figure 156: Concrete Slab at Privy, showing gap between concrete and exterior walls. Because the layer of sand and stone beneath has been eroded by water, this gap extends down the wall and under the slab (Palmer Engineering). 72
Figure 157: Concrete Slab at East Elevation, showing gap (Palmer Engineering). 72
Figure 158: Concrete Slab at Privy, showing gap between concrete and exterior walls. There is a void below slab at this location that extends down the wall (Palmer Engineering). 72
Figure 159: Scuttle Door in Concrete Slab. Note arch beyond (Palmer Engineering). 73
Figure 160: Sentry Box, soor, note step down from concrete slab (Palmer Engineering). 73
Figure 161: Kitchen, at West Corner, with Privy on the right. Note opening with plug that has shifted out of place (Palmer Engineering)..... 73

Figure 162: Privy, looking at top. Exterior is on the right. CMU cells are visible, filled with mortar. Note that intersecting wall is not attached (Palmer Engineering). 73
Figure 163: Privy, showing sloped concrete and openings to drain concrete slab (Palmer Engineering). 74
Figure 164: Privy from West Elevation (Palmer Engineering). 74
Figure 165: Privy from West Elevation. Water from Concrete Top has eroded brick, concrete and stone allowing water to flow back into building (Palmer Engineering). 74
Figure 166: Interior Stair Room looking at Interior Entry Vestibule. Note opening to Ramp to East Magazine on the right. Brown line is a termite tube, not a crack (Palmer Engineering). 75
Figure 167: : Interior Entry Vestibule, wall to the left of Entry Door. Note notches in wall near door, hole at left corner of door, and spalling at individual bricks (Palmer Engineering). 75
Figure 168 Interior Entry Vestible, ceiling (Palmer Engineering). 75
Figure 169: Interior Entry Vestibule, hole in wall at left corner of Entry Door (Palmer Engineering). . 75
Figure 170: Interior Stair Room, low ceiling close to North Magazine. Note curved wall, and impressions in underside of masonry where wood beam or formwork was placed (Palmer Engineering). 76
Figure 171: North Magazine, looking out at opening to Interior Stair Room (Palmer Engineering). .. 76
Figure 172: North Magazine, lintel blocks above opening looking into room (Palmer Engineering). 76
Figure 173: North Magazine, jamb to the right of opening (Palmer Engineering). 76
Figure 174: Ramp to East Magazine. Note door to East Magazine in the right wall (Palmer Engineering). 77
Figure 175: East Magazine, base of crack to the left of opening (Palmer Engineering). 77
Figure 176: East Magazine, upper portion of crack to the left of opening. Note wall protruding into room. Note where render coating on wall has split at crack (Palmer Engineering). 77
Figure 177: East Magazine, close-up of upper portion of crack to the left of opening. Note remains of crack monitor, and brick and stone inside crack (Palmer Engineering). 78
Figure 178: East Magazine, crack above opening. Note bricks that form barrel vault. Brown line is a termite tube (Palmer Engineering). 78
Figure 179: East Magazine, upper portion of crack to the right of opening (Palmer Engineering). ... 78
Figure 180: East Magazine, lower portion of crack to the right of opening. 78
Figure 181: East Magazine, upper portion of crack to the right of opening, with crack monitor. 79
Figure 182: East Magazine, looking directly up into crack above opening (Palmer Engineering). 79
Figure 183: East Elevation, close-up of left hand crack. Left side is at corner, and right side is toward midsection of wall. Right side is proud or pushed more forward than left side. Note that line runs up the side of a vertical line in the render (Palmer Engineering). 80
Figure 184: West Elevation, close-up of left hand crack. Left side is at corner, and right side is toward midsection of wall. Right side is proud or pushed more forward than left side (Palmer Engineering). . 81
Figure 185. View of El Cañuelo, looking south, 2016 (Photograph by BCA). 85
Figure 186. East Elevation of El Cañuelo (Drawing courtesy of RATIO Architects, Inc. Annotated BCA). 87
Figure 187. Terreplein Plan of El Cañuelo (Drawing courtesy of RATIO Architects, Inc. Annotated BCA). 87

Figure 188. West Elevation of El Cañuelo (Drawing courtesy of RATIO Architects, Inc, Annotated BCA). 87
Figure 189. Lower Entrance Section of El Cañuelo (Drawing courtesy of RATIO Architects,Inc. Annotated BCA). 87
Figure 190. "Beachrock" facing stones with lime-brick mortar (Photograph by BCA). 89
Figure 191. Interior passageway with plaster-coated brick walls (Photograph by BCA). 89
Figure 192. M01 sample location, northeast rampart (Photograph by BCA). 92
Figure 193. Sample M01, rampart stucco (Photograph by BCA). 92
Figure 194. M01 sample location, pre-1962 (Courtesy of General Archives of Puerto Rico). 92
Figure 195. M01 sample location, 2008 (Courtesy of Section 106 survey). 92
Figure 196. M01 sample location, 2016 (Photograph by BCA). 92
Figure 197. M02 sample location; northwest battlement (Photograph by BCA). 93
Figure 198. Sample M02, bedding mortar (Photograph by BCA). 93
Figure 199. M02 sample location, 2008 (Courtesy of Section 106 survey). 93
Figure 200. M02 sample location, 2016 (Photograph by BCA). 93
Figure 201. M03a sample location; northwest latrine (Photograph by BCA). 94
Figure 202. Sample M03b, latrine stucco (Photograph by BCA). 94
Figure 203. M04 sample location; southeast cordón (Photograph by BCA). 94
Figure 204. Sample M04a, cordón stucco (Photograph by BCA). 94
Figure 205. M04 sample location, c. 1930 (Courtesy of General Archives of Puerto Rico). 95
Figure 206. M04 sample location, 1998 (Courtesy of Historic American Building Survey). 95
Figure 207. M04 sample location, 2008 (Courtesy of Section 106 survey). 95
Figure 208. M04 sample location, 2012 (Courtesy of National Park Service, San Juan National Historic Site). 95
Figure 209. M04 sample location, 2016 (Photograph by BCA). 95
Figure 210. M05 sample location; interior passage wall (Photograph by BCA). 96
Figure 211. Sample M05a, interior stucco body (Photograph by BCA). 96
Figure 212. Sample M05b, interior stucco finish (Photograph by BCA). 96

Page intentionally left blank.

Foreword

In 2012, the National Park Service decided to restore access to Fort San Juan de la Cruz. This fortification, located on the opposite side of Castillo San Felipe del Morro, was instrumental in preserving Spanish dominion over Puerto Rico until the 19th Century. Occupying the whole extension of the small island of El Cañuelo, the fort allowed the Spanish to control the entrance to the San Juan Bay as well as the mouth of the Bayamón River, which was crucial for communications with the interior of Puerto Rico. The historical significance of this fort and its contribution to the overall defensive strategy of the Spanish Empire has been well established, particularly in the events related to the 1625 Dutch Attack.

There is a saying in Puerto Rico that states: "Good perfume comes in small flasks, but so does venom". This is a good description for El Cañuelo. The fort, together with El Morro, represented an almost impossible obstacle for those trying to force their way into the San Juan Harbor. It was, as the saying goes, perfume for the Spanish but venom to their enemies.

During its long life, El Cañuelo has been used for multiple purposes. This rich history however, has not prevented long periods of disrepair and lack of maintenance resulting in a progressive deterioration that was not addressed until the National Park Service acquired the fortification from the U.S. Army in the 1960's. After initial repairs and the conditioning of the spaces surrounding it to accommodate visitation, the fort was never the subject of a well-planned preservation program. There were, for sure, important interventions such as the construction of a breakwater to minimize the effects of coastal erosion; the construction of a cap to prevent vandals from accessing the fortification; and its reopening to the public in 2012. However, these approaches to the rehabilitation of the fortification did not respond to an organized and prioritized treatment plan. This is the main goal of this historic structure report.

This report will serve as the guide for future treatment of the fortification. It is meant to work in conjunction with other planning efforts such as the *Ethnographic Assessment of San Juan National Historic Site*, which has tied the preservation of the fortification with public engagement in the Palo Seco community. The park wants to raise awareness of the conditions of the fortification while highlighting its significance to world history. This is an important step to make Fort San Juan de la Cruz relevant to the community, and to educate the public about the threats it is facing. Through this concerted effort, the park and the fort can represent an economic and social development tool for this gateway community while preserving it for this and future generations.

Randolph Lavasseur
Superintendent
Caribbean National Parks

Page intentionally left blank.

Management Summary

Project Team

Building Investigation/ Building Condition Assessment	David Kroll Historical Architect Benjamin Ross, Historic Preservation Specialist RATIO Architects, Inc., Indianapolis, IN Baku Patel, Structural Engineer Angela Booth, Structural Engineer Palmer Engineering Co., Tucker, GA Kevin Wohlgemuth, Architectural Conservator Building Conservation Associates, Inc., Philadelphia, PA Melody S. Padrah, Project Manager Existing Conditions Survey, Inc., Boston, MA Keyes Williamson, Principal Historian WLA Studio, Athens, GA
Research	Keyes Williamson, Principal Historian WLA Studio, Athens, GA
Building Recordation	David Kroll Historical Architect Benjamin Ross, Historic Preservation Specialist RATIO Architects, Inc., Indianapolis, IN Angela Booth, Structural Engineer Palmer Engineering Co., Tucker, GA
Contracting Officer Representative	Eric López, Park Historian San Juan National Historic Site San Juan, Puerto Rico
Program Review	Ali Miri, Historical Architect National Park Service Southeast Regional Office Atlanta, GA

Executive Summary

At the request of the National Park Service (NPS), WLA Studio has developed this Historic Structure Report (HSR) for fort San Juan de la Cruz (El Cañuelo). WLA Studio consulted with RATIO Design, Building Conservation Associates, and Palmer Engineering Company in preparing this document. Dr. Ali Miri, Historical Architect with the NPS Southeast Region, assisted in the management of the project and facilitated important conversations with San Juan National Historic Site staff, in particular Felix Lopez, Cultural Resources Manager, Eric Lopez, Park Historian, and Elvis Babilonia, Supervisory Facility Operations Specialist.

Purpose and Scope

The purpose of this Historic Structure Report is to document the construction history and current condition of fort San Juan de la Cruz (El Cañuelo) at San Juan National Historic Site (SAJU) and to provide recommendations for the structure's treatment and use. This HSR will guide the National Park Service (NPS) in the stewardship of this historic resource.

The report includes *Part I: Developmental History* and *Part II: Treatment and Use*. Part I provides a brief review of the historical development of the historic fortifications of San Juan, Puerto Rico; known historical information about El Cañuelo's construction and use, and transfer of the property to the National Park Service. A chronology of the structure's physical development and use provides information on the known evolution of the building over time. This information derives largely from physical investigations with the addition of limited, available historical documentation. The HSR provides information about the why the structure was constructed, who constructed it, and how it was constructed. The HSR also provides a chronology of changes that have been made to the structure, from its original construction to 2018.

A current physical description based on building investigations and assessment using non-destructive methods provides a systemic accounting of all features, materials, and spaces. A list of character-defining features and a summary assessment of the building's current condition are also included.

Part II provides recommendations for the treatment and use of El Cañuelo. The Treatment and Use chapter presents alternative uses and treatments for the historic structure. It emphasizes preservation of existing historic material while conforming to applicable laws, regulations, planning, and functional requirements. Treatment recommendations address foundation conditions, masonry conditions, and deterioration of the physical structure.

A bibliography provides all sources of information this report references. An appendix contains scaled drawings of the existing building plan and elevations.

Historical Overview

Fort San Juan de la Cruz (El Cañuelo) is an 80-foot-square foot masonry fortification currently located on Isla de Cabras (Cabras Island, Goat Island) across the entrance into the Bay of San Juan from the historic city of San Juan. The building originally occupied a small island, isolated in the bay, called El Cañuelo. In 1943, the United States Army connected Cabras Island and El Cañuelo Island as part of a land fill project. Cabras Island is in Palo Seco, a sector within the municipality of Toa Baja, Puerto Rico.

The Spanish officials in Puerto Rico completed the fort by 1644. The fort features rubble masonry walls and a load-bearing veneer of local sandstone. The top of the walls reach approximately 17-feet above mean low tide. Spanish military officials constructed a stockade at El Cañuelo Island during the time of Francis Drake's raid of San Juan in 1595. The Spanish subsequently constructed a wooden artillery tower built on a masonry foundation on the island around 1608. The walls, embrasures, and sentry box of the existing building date to its construction in 1644. Around 1841, Spanish officials converted the building to serve as a lazaretto to shelter infirmed passengers arriving to San Juan and to serve as a facility for leprosy patients. Elements of the 1841 lazaretto are visible today. Puerto Rican officials constructed another lazaretto complex in the 1870s; they presumably abandoned El Cañuelo during this period.

In 1898, the building became the property of the United States and was under the jurisdiction of the War Department. The army made limited

repairs to the building before transferring it to the National Park Service in 1949 to become part of San Juan National Historic Site. NPS made repairs and modifications over the decades as part of an effort to preserve and restore features of the structure. NPS provided access into the building around 1962, but they closed the entrance into the structure in 1992. NPS reopened the building for limited visitation in 2012.

Statement of Significance

El Cañuelo is a contributing feature of the San Juan National Historic Site (SAJU), listed on the National Register of Historic Places in 1966. SAJU was listed as a National Historic Landmark in 2013 as part of the Old San Juan Historic District. SAJU and La Fortaleza were designated a UNESCO World Heritage Site in 1983. The fortifications of SAJU are historically significant as representing major Caribbean fortifications of the Spanish Empire, constructed to protect Spain's imperial interests in the Western Hemisphere. The colonial fortifications are significant under National Register Criteria A and C. Collectively, the fortifications are considered significant in the areas of architecture, engineering, and military history.

The National Register of Historic Places Inventory—Nomination Form, completed by Frederick Gjessing and Loretta Schmidt in 1974, classifies the building as deserving "First Order of Significance." The Nomination Form lists the period of significance as 1539 to 1945; its area of significance included Historic, Architecture, Engineering, and Military.

Project Methodology

The scope of work for this HSR defined the required level of the historical research and the architectural investigation, analysis, and documentation as "limited." Research was to be conducted referring to primary-source documents and public records, with most resources derived directly from the NPS Archives at SAJU. Additional research was conducted at the General Archives of Puerto Rico and the Puerto Rico State Historic Preservation Office. Building investigation was directed to be "non-destructive," but did include the collection of materials as part of an analysis of historic mortar and render.

Documentation of the building began in September 2016. Consultants from several disciplines including historical architects, structural engineers, material analysts, and historians conducted the initial site visit for this project in October and November 2016 and included a project kick-off meeting with NPS staff. Documentation of the building began in October 2016 with field drawings of the existing conditions, notes about exterior and interior materials and architectural features, structural conditions, and digital photographs. Research at local archives and historic preservation agencies, with the help of SAJU Archives staff, obtained useful documentation, maps and photographs of the building. The available NPS documents provided important information on the historic context of El Cañuelo, documentation to-date of the structure, and management plans that are guiding the management of the resource.

The historical architects referred to existing drawings such as HABS recordation documents, as available, for the preliminary analysis of the building's evolution and to prepare for fieldwork. The October/November 2016 site investigation included thorough building investigation, comprised of an examination of construction techniques and building development, comparison of existing conditions to HABS records, and digital photography. The consultants also recorded features for a site plan during this site visit. The historical architect and staff prepared the existing conditions plans based on these field investigations and the digital scan, and drafted them using AutoCAD.

The project historian conducted further research on El Cañuelo using online scholarly sources. These sources included historical texts, several academic theses, and articles published in numerous academic journals. The project historian also obtained historic photographs from the Library of Congress and the General Archives of Puerto Rico.

Conclusions and Recommendations

It is the consensus of the project team that water infiltrating through cracks in the masonry walls and through open joints in the concrete cap is having a negative impact on the structural integrity

of the fort. The increase in moisture content in the backfill is likely resulting in lateral pressure against the fort's walls.

The treatment recommendations include immediate stabilization that includes filling the crack between the 1992 concrete cap and the historic parapet walls. This will stop the ongoing infiltration of water into the interior of the fort. The treatment recommendations also propose removing the concrete cap as a more long-term preservation solution. A condition assessment of the terreplein surface is recommended after the removal of the concrete cap. The recommendations call for repairing the historic drain system that would more effectively shed water from the terreplein surface, whereas today, water is flowing into and being trapped in the interior backfill of the fort.

The project team also has concerns about the condition and composition of the subgrade below the fort. Geotechnical exploration of the subsurface conditions and composition of the interior backfill would provide information critical to determining the pressures on the walls. The future research section includes recommended studies that would inform future maintenance and preservation decisions.

Administrative Data

Locational Data

Building Name: Fort San Juan de la Cruz (El Cañuelo)

Location: San Juan National Historic Site

State/Territory: Puerto Rico

Related NPS Studies

Edwin Bearss, *Historic Structures Report, Historical Data Section, San Juan Fortifications, 1899-1958*, Denver, CO: National Park Service, 1984.

Berkowitz, et. al. *The Fortifications of San Juan National Historic Site, 3 volumes*. Atlanta, GA: National Park Service, 1991.

F. Ross Holland and Russell Jones. *Masonry Forts of the National Park Service: Special History Study*. Denver, CO: National Park Service, 1973.

Frank Sales, et. al. *Spanish Exploration and Settlement: National Historic Landmark Theme Studies*. Santa Fe, NM: National Park Service, 1959.

Real Property Information

Acquisition Date: 1949

LCS ID: 006075

Size Information

Total Terreplein Area: 3,984 square feet ± (excluding latrine and sentry box)

100 Vestibule: 34 square feet ±

101 Stair Hall: 61 square feet ±

102 Vault 1: 115 square feet ±

103 Passage: 28 square feet ±

104 Vault 2: 45 square feet ±

Parcel Area: 3.4 Acres ±

Cultural Resource Data

National Register Status: Listed as the San Juan National Historic Site on October 15, 1966. Updated documentation accepted in 1973. Listed as a National Historic Landmark on February 27, 2013.

Proposed Treatment

The Secretary of the Interior's Standards for the Treatment of Historic Properties guided the development of treatment recommendations for significant exterior and interior features of the building, as well as for the surrounding landscape. Following the overall treatment approaches of Preservation for the structure and Rehabilitation for the landscape, specific treatment recommendations are included to address the observed conditions of El Cañuelo. The treatment recommendations specifically focus on preventing additional infiltration of water into the interior of the building.

I.A Historical Background and Context

Introduction

Fort San Juan de la Cruz, also commonly called El Cañuelo, is located on Isla de Cabras (Cabras Island), on the west side of the San Juan Bay, Puerto Rico. El Cañuelo was originally a low-lying island in the shallow waters between the Puerto Rican mainland near Palo Seco and Cabras Island. The United States Army connected El Cañuelo and Cabras Island in 1943. The primary channel into San Juan Bay lies between Cabras Island and the tip of San Juan islet (today's Old San Juan). Ships entering the harbor pass between these two points of land. (Figure 1).



Figure 1: Site Map (NPS)

The Spanish located a stockade on the small island at the time of Francis Drake's raid in 1595. During a subsequent effort to enhance the defensive fortifications around San Juan, Spanish Governor Gabriel de Rojas Párano (in office 1608-1614) approved the construction of a fort on El Cañuelo island in 1608. "After 1609 Roxas y Paramo began the reconstruction of El Cañuelo following a square plan with battlements which was finished by his successor Felipe de Viamonte y Navarra."[1] Governor Felipe de Beaumont y Navarra was in office from 1614 to 1620. This building was a wooden tower built on a rubble masonry foundation. According to one source, the Spanish "built the 'Torreon del Cañuelo,' (tower of the small channel) under the name 'San Juan de la Cruz' (St. John of the Cross) fronting the entrance to the river Bayamón."[2]

The fort's location near the mouth of the bay opposite Castillo San Felipe del Morro provided for strategic crossfire upon enemy ships attempting to enter the San Juan Bay. Additionally, it defended the mouth of the Bayamón River, an important transportation link into the interior of the island of Puerto Rico. El Cañuelo also defended the city of San Juan from an attack from the west by protecting the shallow channel between Palo Seco Point and Cabras Island.

This fort saw significant action during the Dutch attack on San Juan in 1625. During the battle, the Spanish partially destroyed the fort during their counter offensive to recapture the island from the Dutch. In 1664, the Spanish rebuilt the fort, replacing the wooden tower with a quadrilateral fort featuring ashlar and rubble masonry. The Spanish abandoned the structure in 1785. In 1841, San Juan officials converted the building into a lazaretto and facility to isolate patients suffering from leprosy. As part of this project, they added a structure on the upper level of the fort to provide shelter for the patients.

The United States took possession of Puerto Rico in 1898 as part of the treaty ending the Spanish-American War. Little is known about the island and the fort during the first half of the twentieth century aside from two photographs taken prior to 1935. Since 1949, the fort has been part of the San Juan National Historic Site. Along with the other Spanish fortifications in San Juan, El Cañuelo was listed on the National Register of Historic Places in 1966, designated a UNESCO World Heritage Site

1. Juan Blanco, "A Study of the Morphological Structure of the System of Fortifications of San Juan de Puerto Rico with a Special Emphasis on the Development of the 'Frente de Tierra de San Cristobal," (copyrighted by author, 1988), 127. This report is at the research library at National Park Service Southeastern Regional Office.
2. Charles Hartzel, *Register of Porto Rico for 1903* (San Juan, Puerto Rico: Louis E Tuzo and Company, 1903), 202.



Figure 2: "Plano del asiento y del puerto de la ciudad de Puerto Rico [12 de septiembre de 1519]," (Archivo General de Indias)

in 1983, and designated part of the Old San Juan National Historic Landmark in 2013.

The Conquest Period 1493-1625

Spanish Settlement of Puerto Rico

Prior to the arrival of European explorers, the island now known as Puerto Rico was home to thousands of native Taíno Indians who called the island "Boriquén." Christopher Columbus encountered the island on November 19, 1493 during his second voyage to explore the New World. Columbus christened the island "San Juan Bautista."[3]

The island of Puerto Rico is among a chain of islands known as the West Indies that stretch from Florida to South America along the eastern edge of the Caribbean Sea. The islands forming the northern half of this chain include the Bahamas and the Greater Antilles (including Cuba, Jamaica, Haiti, the Dominican Republic, and Puerto Rico). The southern half include large number of small islands, collectively known as the Lesser Antilles.

At the beginning of the sixteenth century, Spain used ports they established among the Greater Antilles as bases from which to explore and settle Central and South America. Ships, carrying precious metals and other raw materials from continental expeditions, would often shelter within harbors in the Greater Antilles prior to making the return trip to Spain.

Juan Ponce de León, who accompanied Columbus on the 1493 voyage, returned to the island in August 1508 with 50 soldiers to settle the island. Ponce de León entered a protected harbor on the north coast of the island that he called "Puerto Rico" ("Rich Port"); but he moved his troops approximately two miles inland from the harbor to establish the first European settlement on the island, which he called "Caparra." In 1511, the Taíno Indians rebelled against the Spanish settlers, but the Spanish soundly defeated the Taíno, after which many fled to join tribes on neighboring islands.

Because the conditions at Caparra proved undesirable, the Spanish government instructed Ponce de León to relocate the settlement. The colonists chose the small islet between the Atlantic Ocean on the north and the deep bay of "Puerto Rico" on the south. (The name Puerto Rico, originally assigned to the bay, later became the accepted name of the entire island; the name San Juan, originally assigned to the island, later became the accepted name of the bay and the islet upon which the Spanish built the city of San Juan.) The San Juan islet is approximately three and a half miles long and about a mile wide. The steep cliffs overlooking the harbor were an important geographic feature for the Spanish military as they considered developing the harbor as a naval outpost in the Caribbean. (Figure 2).

The Spanish began the move from Caparra to San Juan in 1519. They completed the move by 1521, the year Ponce de León left on an expedition to colonize Florida. Ponce de León never returned, though his remains are interred at the Cathedral de San Juan Bautista in San Juan.

Early Fortification of San Juan under Tejeda and Antonelli

From the beginning of Spain's efforts to colonize the Americas and Caribbean islands, other nations, particularly the English, French, and Dutch, challenged Spanish settlements and harassed Spanish fleets transporting goods to and from the western hemisphere. Spain and France were at war for many decades of the sixteenth century, and French privateers successfully raided Spanish ships travelling through Caribbean waters. The French

3. National Park Service, *The Forts of Old San Juan, Official National Park Handbook. San Juan National Historic Site* (Washington, D.C.: NPS, nd), 15-22.

attacked and destroyed San Germán, a Spanish settlement on the west coast of Puerto Rico, in 1528.

In response to these challenges, the Spanish declared the Caribbean Sea closed to outside nations and established a convoy system where Spanish commercial vessels would sail under the protection of armed, Spanish Navy ships. Spain also fortified key ports in the Caribbean, including the port at San Juan. The fortification of important commercial and military harbors was an essential component of the Spanish efforts to maintain control of their colonial claims in the Western Hemisphere. The development of harbor fortified military settlements or "presidios" borrowed architecture and layout from Spanish harbor towns in Europe and in the Mediterranean.[4]

The Spanish authorized a fort at San Juan in 1529, but construction of the building known as La Fortaleza began 1537. In 1539, the Spanish began construction on a more strategically located fortification at the headland overlooking the entrance into the bay. This 140-foot-high promontory or "el morro," became the location of a massive fortification that grew over the years into Castillo San Felipe del Morro (El Morro). A 1579 map of the area shows the placement of cannon overlooking the narrow channel entering the bay. (Figure 3).

As rival nations effectively challenged Spanish naval supremacy in Europe, particularly after England's naval victory over Spain in 1588, the Spanish adjusted their geopolitical strategy to maintain control over the territory under their claim in the Americas and the Caribbean. Beginning in the late sixteenth century, Spain identified military strongholds from which they would initiate offensive maneuvers and which would serve as defensive outposts for their fleets. San Juan was one of the most important of these presidios, because of its location along the prevailing wind and water currents and because of its location guarding the primary route through the Caribbean Sea.

4. Fernando Cobos-Guerra, "Technical and systemic keys and context of Hispanic fortifications on Western Mediterranean coast," in *Defensive Architecture of the Mediterranean XV to XVII Centuries*, ed. Rodriquez-Navarro, (accessed online 2/27/2017: http://dx.doi.org/10.4995/FORTMED2015.2015.1803).



Figure 3: "Remitido por Juan Ponce de León, con carta de 31 de julio de 1579," (Archivo General de Indias)

After King Philip II decided to create a presidio at San Juan, Spain sent Captain General Diego Menéndez de Valdés to be the island's military governor. He arrived in 1582 with 50 soldiers. Menéndez de Valdés prepared a report describing how to effectively defend San Juan. His primary concern was protecting the harbor from enemy invaders. Under his direction, the Spanish built gun batteries, including one at Santa Elena, between El Morro and La Fortaleza, overlooking the harbor.

Spain sent a series of military experts and engineers to the West Indies to oversee the construction of fortifications at their most important ports and settlements. Field Marshal Juan de Tejeda, a military strategist, and Juan Bautista Antonelli, a military engineer and architect, inspected Spanish strongholds in the Caribbean and Florida in 1586 and 1587. They recommended the development of major fortifications at ten sites, including San Juan. Philip II approved their plan in November 1588, just months after England's resounding defeat of the Spanish Armada.

Tejeda and Antonelli returned to Puerto Rico in March 1589, bringing along dozens of artisans including stonecutters and masons. Tejeda and Antonelli's plans for defenses around San Juan focused on securing the bay and protecting against an overland assault from the east. Using soldiers, slaves, and hired laborers, the Spanish began construction of a defensive wall across the San Juan islet from La Fortaleza to the north coast. Antonelli designed additions to El Morro to provide shelter for up to 3,000 soldiers. As more soldiers arrived

from Spain, the San Juan garrison grew to around 1,500 men by the end of the century.[5]

Captain Pedro de Salazar arrived in San Juan in May 1591 to oversee the construction projects proposed by Tejeda and Antonelli. Construction projects included a series of bastions on the hills and cliffs overlooking approaches from both overland and through the entrance into the harbor. Defending San Juan Bay was a critical concern in these early years. There are four water entrances into San Juan Bay: two to the east of San Juan islet at Boquerón Bay and San Antonio Channel; the main channel at El Morro; and from the west, a shallow channel along the coastline near the entrance of the Bayamón River. This western approach was between the mainland and a series of reef islands that included Cabras and El Cañuelo. The Bayamón River was an important transportation route to the interior of the island. The military and citizens of San Juan depended upon goods brought from the interior. Also, the military used the Bayamón River to communicate with and transport troops located at settlements on the mainland.

Ponce de León had mentioned fortifying the islands across the entrance into the bay as early as 1579. He recommended building a redoubt on El Cañuelo and an artillery tower on Cabras Island.[6] Tejeda and Antonelli, however, did not share this opinion and they did not approve the construction of a redoubt during this time.

England Invades Puerto Rico in 1595 and 1598

England tested the fortifications at San Juan, when Queen Elizabeth I authorized Sir Francis Drake and John Hawkins to command an expedition against Puerto Rico in 1595. Drake had attained great fame for his circumnavigation of the world, completed in 1580, and was second in command when England defeated the Spanish Armada in 1588. The English learned of a Spanish galleon loaded with treasure anchored in San Juan Bay for repairs. In August 1595, Drake set sail for the Caribbean to steal the silver believed to be in San Juan. The Spanish also sent an expedition led by Admiral Pedro de Guzmán to San Juan to guard and return the treasure to Spain. While en route to Puerto Rico, Guzmán encountered Drake's



Figure 4: "Plano de los puertos y barras de San Juan y Toa, [1660]" (Archivo General de Indias)

fleet and learned the intent of the English mission. Guzmán arrived in time to warn of San Juan's defenders of the impending invasion. The military governor of San Juan, Pedro Suarez Coronel, sank a damaged galleon to block the channel into the bay and anchored several Spanish frigates just inside the bay below the cliffs south of El Morro.

Drake arrived off the coast of Puerto Rico on November 22, 1595 and anchored his ships at El Escambrón, near the Boquerón Inlet leading into San Juan Bay east of the city. Spanish batteries fired against his ships, hitting Drake's flagship and killing several sailors and officers. On November 23, Drake moved his force west of San Juan, anchoring off Cabras Island beyond the range of the cannon at El Morro. He sent sailors to take measurements of the water depth in search of a back entrance into the bay along the shallows behind Cabras Island.[7] A map of San Juan from 1660 depicts Cabras Island, El Cañuelo Island, and the shallow waters providing a possible western entrance into the bay (Figure 4).

Admiral Guzmán sent forces to the west side of the bay to engage Drake's forces from locations on the mainland, near the Bayamón River and from a low lying island called El Cañuelo. Firing from these locations, the Spaniards drove Drake's men back to their boats, forcing them to abandon their attack on San Juan. (Figure 5).

5. Blanco, *Fortifications*, 68.
6. Blanco, *Fortifications*, 68.
7. NPS, *The Forts of Old San Juan,* 32.

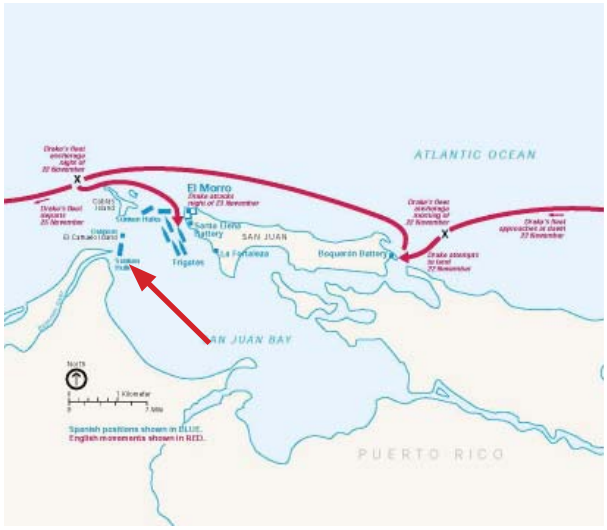


Figure 5: Drake's Attack 1595 (NPS)

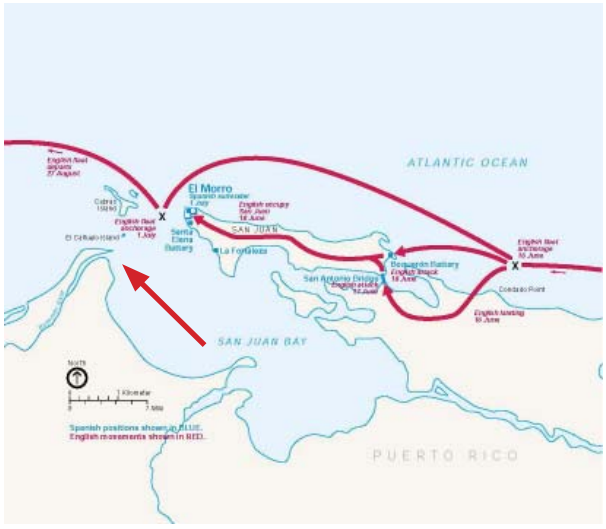


Figure 6: Cumberland's Attack 1598 (NPS)

Following Drake's attack, Admiral Guzmán returned to Spain, carrying with him the treasure. He left behind 200 men and 150 volunteers to protect San Juan. A new military governor, Captain Antonio de Mosquera, arrived in June 1597. He had no funds available to improve the city defenses and found its garrison depleted by disease. An outbreak of dysentery swept through San Juan, reducing the city's population to around 180.

With San Juan and its garrison depleted through troop reductions and disease, England approved another direct assault on Puerto Rico led by Sir George Clifford, Third Earl of Cumberland. Sailing from England in March 1598 aboard this ship, the *Scourge of Malice*, Clifford arrived off the coast of Puerto Rico in June. Hoping to improve upon Drake's failed assault, Clifford anchored near Condado Point, farther away from Spanish batteries east of San Juan. He disembarked his force and marched overland towards San Juan. On June 17, he attacked Spanish defenders at the Boquerón Battery protecting the bridge over the inlet. After the Spanish repelled the initial attack, Clifford moved his ships into position to bombard the battery. Clifford successfully captured the bridge and forced the Spanish into a retreat towards San Juan. Clifford entered the abandoned city unopposed on the morning of June 18. Most of the citizens had fled into the mainland of the island or into El Morro, guarded by about 80 soldiers. Despite being low on water and supplies, Governor de Mosquera refused Clifford's demand for surrender.

Clifford set up batteries on high ground surrounding El Morro and shelled the fort for several days. The Spanish surrendered on July 1 and Clifford imprisoned Governor de Mosquera at La Fortaleza. Clifford's occupation of San Juan lasted only a few weeks, because dysentery sickened and killed many of his troops. On August 14, Clifford's remaining force pillaged the city, setting fire to many buildings, before departing Puerto Rico.[8] (Figure 6).

After learning of the surrender of San Juan and subsequent departure of Clifford, the Spanish sent 400 soldiers and 46 cannon to refortify the city's defenses. They also named a new military governor, Alonso de Mercado, whose priority was to strengthen the city fortifications. De Mercado arrived in March 1599. Many of his projects focused on rebuilding the batteries and defenses on the east end of the island.

Between 1599 and 1619, the Spanish rebuilt and improved San Juan's fortifications. Spanish workers expanded and increased the size of El Morro. The Spanish also repaired and expanded the defenses on the east side of the islet. It was at this time that the Spanish constructed a wooden artillery tower on a masonry foundation on El Cañuelo Island.

8. National Park Service, *Spanish Exploration and Settlement: The National Survey of Historic Sites and Buildings* (Washington, D.C.: NPS, 1959), 74.

Colony Evolves: From Frontier Post to Fortified City--1625-1812

Dutch Attack in 1625

In 1625, Dutch forces attacked multiple Spanish settlements in South America and in the Caribbean. In September, Dutch General Boudewijn Hendricksz, the Burgomaster of Edam, led a flotilla of 17 ships to attack San Juan. The Dutch sailed directly into the entrance of the harbor passing close to and directly below El Morro. On September 26, after anchoring beyond the range of San Juan's batteries, Dutch ships bombarded the town in preparations of an assault which included 800 soldiers. Only 330 men defended the garrison at El Morro and the Governor, Juan de Haro, sent messages to the interior of the island hoping to raise support. Hendricksz captured La Fortaleza and prepared to besiege El Morro. To isolate the Spanish in the fortress, Hendricksz captured the San Antonio Bridge, blocking the eastern route into the city. Then, the Dutch captured the fort at El Cañuelo because it controlled the mouth of the Bayamón River and San Juan's main line of communication with the interior of the island.[9]

For the next month, as Hendricksz dug trenches towards El Morro, the Spanish troops made several attempts to break the siege. According to one account, on "October 16th, the [Spanish] Governor commissioned Captain Botello to make an attack on El Cañuelo. With two launches and thirty men, the captain made the assault, moving on the fort from the western or Bayamón side of the harbor entrance. The ensuing engagement lasted two hours. In spite of the fact that the Dutch had artillery and were inside a strong little fort, the Puerto Ricans finally captured the position with its garrison of eighteen men, two of whom had been killed. They reduced the fort, as the Spanish account has it, 'by putting fire into it.'"[10] De Haro also successfully drove the Dutch garrison away from the San Antonio Bridge.

Encouraged by their success, the Spanish governor and troops in El Morro increased their counter attacks against Hendricksz's troops entrenched in front of El Morro. On October 21, Hendricksz



Figure 7: Dutch Attack 1625 (NPS)

demanded surrender again and Haro again refused. The Dutch ransacked the city, stealing anything valuable before setting fire to many of the buildings. Haro sent another counter attack from El Morro, driving the Dutch to their ships anchored in the bay. Hendricksz kept his ships out of range from Spanish cannon until November 2, when they sailed past El Morro, leaving San Juan behind in ruins.[11] (Figure 7).

After the Dutch attack, San Juan experienced another burst of construction as the Spanish worked to improve rebuild the city and its fortifications. In 1645, King Philip IV of Spain described the importance of Puerto Rico. "It is the front and vanguard of all my West Indies, and consequently the most important of them all—and the most coveted by my enemies."

The Dutch attack reinforced to the Spanish the need to defend San Juan against attacks from the south and west. Under the leadership of Governors Enrique Enríquez de Sotomayor and Iñigo de la Mota Sarmiento, the Spanish accelerated the construction of projects to protect the city. During this time, the Spanish rebuilt La Fortaleza and repaired el Morro. They built large masonry walls around the south and east sides of the city. In 1634, they started construction on a major fortification, San Cristóbal, to protect the city from another overland attack from the east. A map from 1678 shows the two forts and walls surrounding the city. El Cañuelo is included among fortifications

9. Edward Hoyt, ed., *A History of the Harbor Defenses of San Juan, P.R., under Spain 1509-1898: including a brief history of artillery and a guide to the ancient fortifications* (San Juan: United States Army Puerto Rico Coast Artillery Command, 1943), 63.
10. Hoyt, *A History of the Harbor Defenses*, 65.
11. NPS, *The Forts of Old San Juan*, 44-45.



Figure 8: "Puerto Rico… el año del señor de 1678 años," (Archivo General de Indias)



Figure 9: Detail of "Puerto Rico… el año del señor de 1678 años," (Archivo General de Indias)

repaired during this time. It also appears on the map. (Figure 8).

In 1658, Governor José Novoa y Moscosa recommended rebuilding a fort on the site of El Cañuelo. It is unclear if they rebuilt the structure at this time; however, according to Juan Blanco, the Spanish stationed twelve soldiers on the island during this period.[12]

By 1663, the Spanish considered constructing stronger, more permanent fort on El Cañuelo to defend the western passage into San Juan Bay. According to Blanco,

> This was the great lesson of the Dutch siege. If el Morro and the batteries along the channel castigated any vessel traveling its length, el Cañuelo provided crossfire by prohibiting retreat onto the shallows deeper in the bay; permitted the closure of the harbor entrance and kept the communication into the interior of the island open. El Cañuelo dominated a principle avenue of approach to the city in these ways. El Cañuelo also served as a transplaced ravelin for San Juan Gate and curtain wall due to its location directly perpendicular to this front and more. This redoubt served as the location for a beacon for vessels navigating the entrance into the bay and channel.[13]

By 1664, the Spanish had completed Fortín San Juan de la Cruz on the island and outfitted it with 20 guns "five to a side."[14] The fort appears on a 1678 map of San Juan. The map shows the fort flying the Spanish Cross of Burgundy flag. (Figure 9).

Expansion of San Juan Fortifications under O'Reilly

Despite a series of wars that entangled many European nations, the eighteenth century was a period of relative calm, progress, and prosperity in San Juan. The ascension of the French Bourbons to the Spanish throne in 1701 resulted in an alliance between Spain and France; but it also led to a series of wars with Great Britain. San Juan steadily grew in population during the century, reaching a population of 6,000 civilians, protected by a garrison of approximately 3,000 regular soldiers by 1776. As a result of the period of peace, records suggest a reduction of construction activity in San Juan over the first half of the eighteenth century. However, around the middle of the century, England resumed sailing through the Caribbean challenging Spain's colonies. As a result, Spain renewed construction on San Juan's fortifications. In 1765, Spain's King Charles III declared San Juan as a "Defense of the First Order." He declared that "San Juan in Puerto Rico shall be a city of the first order of support for the Island; bulwark of the Antilles; safeguard of the Gulf of Mexico; depository; point of acclimatization; port of call and naval station of the navigating fleets; favorable to foster and secure the commerce that will improve industry, agriculture, and art—the foundation of true wealth."[15] A 1731 Map of San

12. Blanco, *Fortifications*, 172.
13. Blanco, *Fortifications,* 174-175.
14. Blanco, *Fortifications*, 277.
15. Joan Berkowitz, et. al. "The City Walls of San Juan," in *The Fortifications of San Juan National Historic Site, Historic Structures Report, Volume III* (Atlanta: Southeastern Regional Office, National Park Service, 1991), 21.

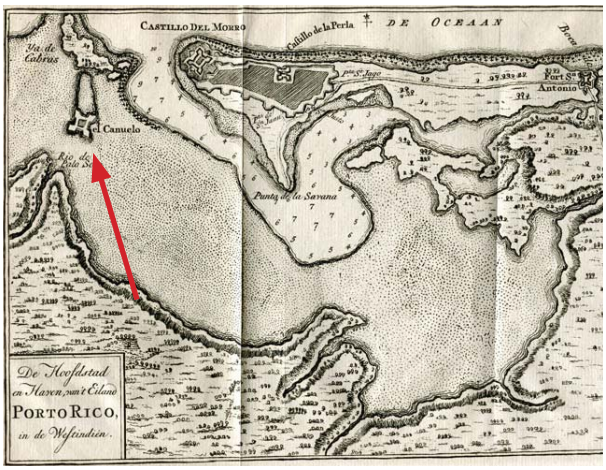


Figure 10: "De Hoofdstad en Haven, van't Eiland Porto Rico [1731]"



Figure 11: "Port et Ville de Porto-Rico dans l'Isle de ce nom [1764]," (Library of Congress)



Figure 12: "Plano de ciudad de S. Juan [1770]," (Library of Congress)

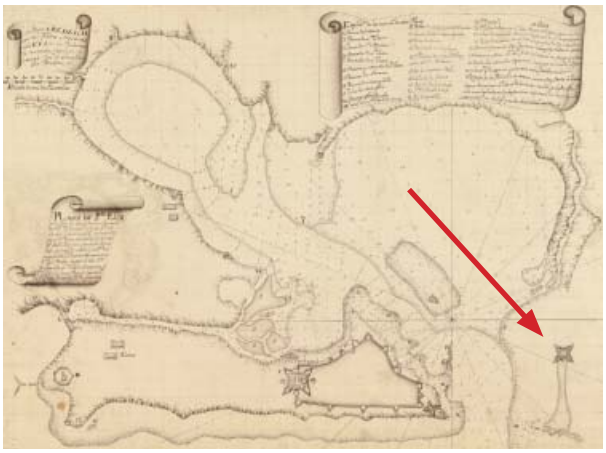


Figure 13: "Plano de Pto. Rico [1780]," (Library of Congress)

Juan shows the channel into the bay and depicts "el Canuelo" as a quadrilateral fort with bastions projecting from its four corners. (Figure 10).

A 1764 map lists El Cañuelo as "Petit Fort" and notes that is was equipped with 18 cannons. (Figure 11) In early 1765, Field Marshall Alexander O'Reilly arrived in Puerto Rico to inspect the defenses at San Juan. In his report to King Charles III, he recommended a major reorganization of the forces and a construction campaign to strengthen the city against another foreign attack. In general, O'Reilly's plan shifted the defensive focus from the water to defending against a land attack. In particular, O'Reilly recommended the creation of a "defense-by-depth" series of fortifications to protect the eastern approach to the city that previous invaders had used effectively. He also emphasized the need to complete a wall that would completely encircle the city of San Juan. In September, Charles III approved the "General Fortification Plan" for San Juan. Chief Engineers Thomas O'Daly and Juan Francisco Mestre oversaw the implementation of the plan. Existing walls were rebuilt, while new outerworks and batteries were constructed east of the city. They made improvements to the main forts, El Morro and San Cristobal. Once completed, the city walls enclosed a space of approximately 62 acres, turning San Juan into a fortified bastion. A 1770 map depicts the fort as a simple square, but a 1780 map reproduces the bastioned fort depicted on the 1731 map (Figure 12), (Figure 13).

On May 2, 1787, a large earthquake struck offshore of Puerto Rico, damaging several forts, including El Morro and San Cristóbal, and many buildings in the city of San Juan.[16]

English Attack 1797

In early 1793, following the execution of King Louis XVI of France, the King of Spain, Charles IV, joined a coalition against Revolutionary France. In July 1795, Spain switched allegiances and signed

16. http://www.discoveringpuertorico.com/puerto-rico-earthquakes/.



Figure 14: English Attack 1797 (NPS)



Figure 15: Detail of "Plano de Pto. Rico [1780]," (Library of Congress)

treaty with France; a year later, on October 5, 1796, Charles IV declared war on Great Britain.

The following February 1797, Great Britain sent a naval force towards Puerto Rico. They first captured Trinidad to establish a base from which to launch armed expeditions against Spanish colonies in the Americas. Led by Sir Ralph Abercrombie, a large armada of English vessels sailed into view off the coast of Puerto Rico in April 1797. Abercrombie anchored his force near Cangrejos and sent two frigates to guard the entrance into San Juan Bay.

In 1797, approximately 3,000 to 4,000 Spanish soldiers defended San Juan, but only 200 to 300 of these were experienced veterans. Puerto Rican Governor, don Ramón de Castro sent messages to communities across the island, imploring volunteers and militia to reinforce the San Juan garrison.

On April 18, Abercrombie launched his attack, leading 3,000 soldiers onto the beach at Cangrejos. Following a similar strategy used by Lord George Clifford, Abercrombie's force marched overland towards the San Antonio Bridge and San Juan. Abercrombie also sent several of his ships west of the city to search for a second landing location. On April 19, a British frigate explored the waters around El Cañuelo and Cabras Island. Governor de Castro dispatched a body of infantry and militia to defend against an attack from the west.

A 1943 history of harbor defenses describes the English movements.

> The harbor of San Juan, it will be recalled, was immediately at the beginning of the siege placed under the blockade of ships of the British fleet. These vessels kept, of course, out of range of the guns at El Morro and San Cristóbal, with the result that there was little exchange of fire between them and the forts. . . . However, the day after the blockade was established, that is, the 19th, a small action took place against a British launch. It had been sent in from one of the blockading ships to scout Cabras Island and the fort of El Cañuelo. El Morro fired on it to drive it away or to warn it not to make another scouting, and it was seen to retire to its mother-ship. . . . On the night of the following day another action took place. At about nine o'clock in the evening it was observed that the enemy blockade ship and frigates were moving toward Punta Salinas. El Morro and El Cañuelo fired at them but did not sustain their fire because the ships were out of range. . . . Later that night a brigantine anchored near the north side of Cabras Island. El Cañuelo and San Fernando battery, with its thirty six pounders, were ordered to conduct rapid fire to harass the enemy ship. The results were not observed until dawn, when the brigantine moved off out of range as quickly as possible, using both sail and oars.[17]

While the passage quoted above mentions artillery firing from El Cañuelo, other descriptions of the battle do not mention soldiers at the island fort. The main action of the battle was at the line of defenses east of the city. Abercrombie attacked the batteries at Boquerón Inlet. For seven days, he used artillery to bombard San Gerónimo and the Spanish soldiers defending San Antonio Bridge.

17. Hoyt, *A History of the Harbor Defenses*, 92.

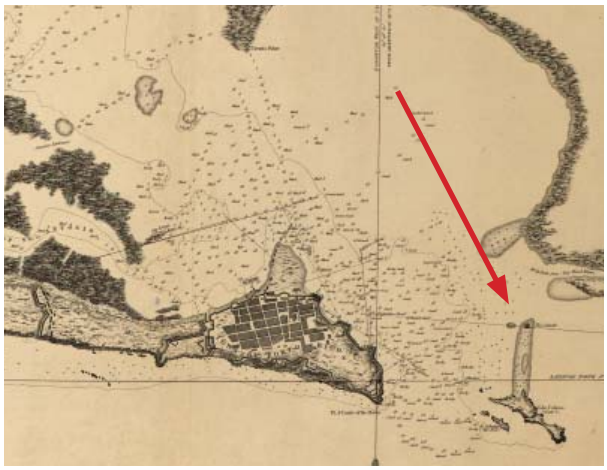


Figure 16: "San Juan Puerto Rico [1794]," (Library of Congress)

The Spanish successfully counter-attacked on the 29 and the 30, forcing Abercrombie to withdraw to his ships anchored at Cangrejos. On May 1, Abercrombie set sail from Puerto Rico, abandoning the expedition.[18] (Figure 14); (Figure 15).

After the failed English attack of 1797, Puerto Rico enjoyed another century of relative calm before the next major conflict. Following the 1797 attack, Governor Ramón de Castro prepared a report on the condition of the defensive fortifications. In the following decades, Spain completed repairs to the redoubt at San Gerónimo and to the bridge at San Antonio. The Spanish also built additional batteries on the eastern defensive front, including a new battery at Point Escambrón. A 1794 map shows the extents of the fortifications at this time. (Figure 16).

From Age of Enlightenment to American Territory--1812-1898

Evolution of San Juan's Fortifications

San Juan's system of defensive fortifications was largely complete by the beginning of the nineteenth century. During the nineteenth century, the Spanish would maintain the fortifications and add new military-related buildings, including hospitals and barracks for the troops. The most important development during the century was a series of revisions to the artillery. The major upgrade to the artillery began in the 1850s, followed by a second revision that began in the 1870s and continued into the 1890s.

18. Wanda López Bobonis, "A Preservation Plan for Fort El Cañuelo, San Juan National Historic Site, Isla de Cabras, Puerto Rico" (master's thesis, University of Pennsylvania, 2005).

By 1822, according to a report by De Córdoba, "the fortifications were in a state of abandonment." The walls had structural cracks and vegetation covering them. Between 1824 and 1832, the entire system of fortifications were "cleaned, refaced, and the external bridges and gates replaced."[19] Beginning around 1850, the Spanish installed a new artillery system in San Juan. The system consisted of coastal artillery batteries on the cliffs overlooking the Atlantic, at El Morro and San Cristóbal. They also establish (or planned) batteries on high ground inland from Bayamón and on the hills of Cabras Island. These new weapons fired with a "high trajectory that were designed to fall on the wood decks of ships that were then beginning to be made with metal armour."[20] The low trajectory shots capable from El Cañuelo did not fit in with the "new technologies of warfleets and coastal defenses."[21]

Temporary Lazaretto 1841-1898

According to Blanco's history of San Juan's fortifications, several treatises about hygiene and disease influenced military architecture in San Juan in the eighteenth and nineteenth centuries.[22] In the nineteenth century, after a series of outbreaks of yellow fever and cholera, the Spanish constructed a number of new barracks and hospitals designed to improve living conditions and sanitary conditions for soldiers.[23] In 1838, Puerto Rico, under the governorship of Miguel López de Baños, passed anti-vagrancy legislation aimed at clearing the streets of San Juan of people unwilling to or incapable of working. According to Adriana Garriga López, anti-vagrancy laws often targeted those inflicted with leprosy, who local governments at the time often labeled vagrants.[24]

Wanda López Bobonis, in her "Preservation Plan for Fort El Cañuelo," reproduces a document from the Archivo General de Puerto Rico showing El Cañuelo modified to serve as a leper hospital or "lazaretto" in 1841.[25] Lazarettos were common features in coastal ports like San Juan. In addition

19. Blanco, *Fortifications*, 745.
20. Blanco, *Fortifications*, 774.
21. Blanco, *Fortifications,* 774 and 779.
22. Blanco, *Fortifications*, 752.
23. Blanco, *Fortifications*, 773.
24. Adriana María Garriga López, "Colonial Palimpsest: the biopolitical history of Isla de Cabras leper colony and the problematics of the memorialization of suffering" (final seminar paper: Columbia University, 2003), 3.
25. Bobonis, *Preservation Plan*, 10.

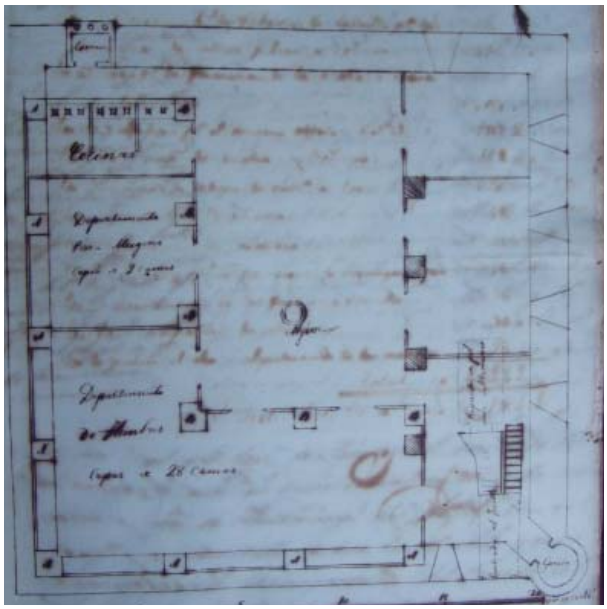


Figure 17: 1841 Drawing (Image proved by Wanda Bobonis)

to serving those with leprosy, a lazaretto would serve as a quarantine station to isolate passengers believed to have an infectious disease. [26] (Figure 17). (Figure 18).

Another earthquake struck off the east coast of Puerto Rico in November 1867, damaging buildings across the island.[27] In 1876, the Governor of Puerto Rico, Segundo de la Portilla, authorized a new, larger quarantine facility and leper hospital on the adjacent island, Cabras Island. This expanded facility, which replaced the small building on El Cañuelo, served as "a maritime quarantine station for isolating passengers on ships arriving in San Juan who were sick or suspected of being ill with diseases like yellow fever, cholera, bubonic plague."[28] This complex opened in 1877.

Presumably, Puerto Rican officials abandoned the facility at El Cañuelo around the time the facility on Cabras Island opened in 1877. However, Spanish records mention El Cañuelo as housing soldiers who inspected incoming vessels. "Passengers, equipment, cargo were to dock at Islas del Cabras… to vent the content scrupulously… by detachments stationed on guard

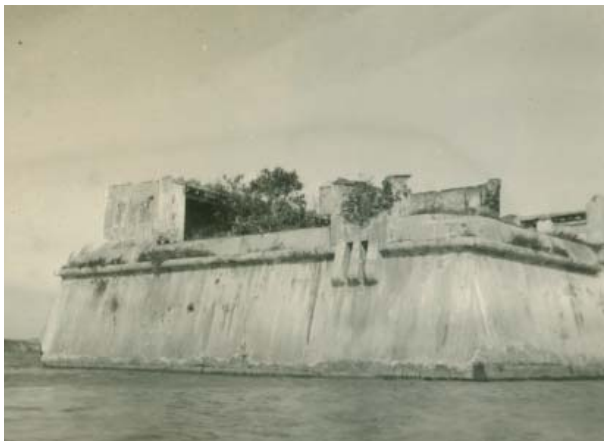


Figure 18: "El Canuelo, pre-1935 photograph, c. 1920-1934" (Archivo General de Puerto Rico)

at the El Canuelo[sic] at the point of Palo Seco."[29] Two major hurricanes struck Puerto Rico in August 1916. The hurricanes inflicted major damage on the buildings at Cabras Island, beginning a concerted effort to relocate the quarantine facility. Despite their uninhabitable condition, the Isla de Cabras facility remained in operation until 1926, when the hospital moved to a new complex constructed in Trujillo Alto, southeast of San Juan.

The population of San Juan expanded during the nineteenth century, reaching 26,000 by 1875 and literally outgrowing the confines of the old city walls. The Spanish military continued making routine repairs to San Juan's fortifications and, towards the end of the century, the Spanish upgraded the artillery again, installing new weapons in locations around San Juan harbor.

Spanish American War

Beginning in the 1870s, the Spanish installed a second system of advanced artillery around the fortifications of San Juan. According to Blanco, the Spanish military considered the ancient system of fortifications built in the seventeenth and eighteenth centuries to be increasingly obsolete against the threat posed by a new generation of warships and naval artillery.[30] The new weapons the Spanish planned for San Juan included larger guns with even greater range than those installed just a few decades earlier. The Spanish upgraded the guns at El Morro, built new batteries at San Cristobal, and designed a series of new batteries at different locations along the coast to engage

26. Bobonis, *Preservation Plan*, 10.
27. http://www.discoveringpuertorico.com/puerto-rico-earthquakes/
28. López, *Colonial Palimpsest*, 3.
29. Leslie Paul Walker, "Narrating Climate Change at San Juan National Historic Site," (masters thesis, University of South Florida, 2015), 16-17.
30. Blanco, *Fortifications*, 779.



Figure 19: "Plano de la Plaza de San Juan Puerto Rico [1886]", Archivo Digital Nacional de Puerto Rico)



Figure 20: Detail from "Plano de la Plaza de San Juan Puerto Rico [1886]", Archivo Digital Nacional de Puerto Rico)

enemy ships before they could get close enough to bombard the city. A map produced in 1887 shows the topography of the area around San Juan Bay (Figure 19).

The new system was under construction when the United States declared war on Spain in April 1898, in part to support political revolutions in Cuba and the Philippines. Admiral William T. Sampson, who commanded the Atlantic Fleet, was sent into the Caribbean to locate and destroy the Spanish Atlantic fleet under the command of Rear Admiral Pascual Cervera y Topete. On May 11, Sampson's squadron sailed into the waters off Puerto Rico believing the Spanish fleet to be there. Sampson probed the Spanish defenses with smaller vessels, to confirm reports of new weapons in El Morro and San Cristobal. By the following day, May 12, Sampson concluded that the Spanish fleet was not in San Juan Bay, but he decided to bombard the Spanish batteries defending the harbor. (Figure 20).

The fleet made successive passes between San Cristobal and El Morro firing shells into the historic forts. During the engagement, the cruiser USS *Montgomery* entered the channel of the bay, reaching "Fort Cañuelo" before withdrawing and rejoining the rest of the fleet stationed off the coast. In three hours, the Americans fired almost a thousand shells into the Spanish defenses. Some of the shells over shot their targets hitting churches and private homes in the Old City. Satisfied with the damage, Sampson's squadron sailed away



Figure 21: "The Bombardment of San Juan by the American Fleet Porto Rico, [1898]" (Library of Congress)

before nightfall and headed to Cuba.[31] (Figure 21).

Later, in July 1898, American forces invaded Puerto Rico, landing on the south coast of the island near the port of Guánica. After a series of skirmishes, the American army marched across the island towards San Juan. Spain and the United States reached an armistice suspending fighting on August 12. On December 10, 1898, the two countries signed the Treaty of Paris, officially ending the war. The treaty transferred ownership of Spain's colonies, including the Philippines, Guam, Cuba and Puerto Rico, to the United States.

War Department Era--1898-1949

On December 15, 1900, U.S. Secretary of War Elihu Root issued the declaration, "That Cabras and Cañuelo islands in San Juan Harbor and all lands and buildings on San Juan Island belonging

31. Edwin Bearss, *Historic Structure Report: Historical Data Section* (Denver: Denver Service Center, National Park Service, 1984), 5-15.

to the United States… [are] to be retained by the War Department for military uses." El Cañuelo remained under War Department administration for the next half century, during which the army faced numerous challenges maintaining the historic masonry fortifications in San Juan. Throughout this period, army officials dealt with structural failures in the city walls and with the deterioration of materials at the individual fortifications. Additionally, during World War I and World War II, the army treated the fortifications around San Juan as part of Fort Brooke, an active military reservation and headquarters for the coastal defenses of Puerto Rico.

Soon after taking possession of San Juan in 1898, army ordinance engineers performed an inventory of armament left by the Spanish, but they do not list any artillery at El Cañuelo and do not list the fort as an active coastal defense installation.[32] While there are very few mentions of El Cañuelo during this period, it did appear in a report of the American Military Governor of Puerto Rico in 1900. He described the fort, "The little Canuelo [sic] situated on an islet in the bay, was built by Governor Roxas about 1610, but it was captured by the Dutch and retaken by the Spaniards in 1625."[33]

Caring for the monumental masonry structures proved to be a difficult and expensive responsibility for the army. Within the first few years of occupying San Juan, the army discovered that large sections of the old city wall were structurally unsound. Captain Clement A. F. Flagler arrived in San Juan in October 1900 to inspect the physical condition of the Spanish fortifications. In his report, he noted multiple locations where walls were failing and he provided an itemized list of necessary repairs. As early as 1901, Flagler led a department in charge of overseeing ongoing maintenance to the Spanish structures. Among his duties, Flagler was to provide "preservation and repair of fortifications, care and issuing of instruments, preparation of estimates and projects."[34] Projects completed under Flagler's supervision included the repair of deteriorated sentry boxes, repair of broken concrete, and replacement of damaged doors, ramps, and bridges. In 1902, Flagler received funds specifically for preservation of the fortifications. For the next few years, workers completed multiple projects patching broken masonry, repairing failing plaster, and rebuilding failing sections of city walls.

By 1902, the army installed their own weapons among the fortifications, including guns at El Morro and at other bastions along the city walls. Military plans mentioned mounting guns "along the channel and sea fronts of San Juan to the neighboring islets of Cabras and Cañuelo."[35] In July 1903, President Theodore Roosevelt signed General Order No. 97 authorizing the Army to use the Spanish fortifications for military purposes.[36] A 1912 geodetic survey map notes a flagstaff at El Cañuelo.

By 1913, the army was undertaking major maintenance and restoration projects at El Morro and San Cristóbal, including filling of cavities in the walls. During this period, one work project proposed covering walls in a protective "coat of cement wash."[37] Colonel Will Black, the U.S. Corps of Engineers expert on Spanish masonry defenses, visited San Juan to inspect the structures. He opposed using a cement wash and proposed that "everything possible be done to maintain the integrity of the picturesque fortification."[38] A subsequent report by District Engineer Charles McKinstry in 1916 detailed the enormous expense associated with continuous repairs to the city walls and to other historic structures.

After the United States declared war on Germany on April 6, 1917, the War Department accelerated new expenditures to upgrade the coastal defenses at San Juan. In the course of the following month, the army completed new batteries and gun emplacements among the historic fortifications. However, preparations for war suspended the army's efforts to repair and preserve historic structures. In the 1920s, after the conclusion of World War I, the army resumed efforts to stabilize the historic fortifications. In 1924, the U.S. Congress authorized a spending bill that included "$50,000 for the protection, repair, preservation, and maintenance of historical fortifications at San

32. Bearss, *Historic Structures Report*, 54.
33. "Report of the Military Governor of Puerto Rico," page 202, accessed online, https://archive.org/stream/reportofmilitary00puer#page/202/mode/2up/search/canuelo.
34. Bearss, *Historic Structures Report*, 80.
35. Bearss, *Historic Structures Report*, 65.
36. Bearss, *Historic Structures Report*, 59.
37. Bearss, *Historic Structures Report*, 169.
38. Bearss, *Historic Structures Report*, 170.

Juan."[39] During these repairs, large sections of walls were rebuilt; in some instances the walls were completely dismantled and reconstructed on new concrete foundations.

In 1927, the Army Chief Engineer approved a "Preservation of Historical Fortifications" plan that included reconstruction of walls, removing vegetation from the structures and repointing cracks in El Morro. Even though El Cañuelo does not appear in these documents, the army's "Preservation of Historical Fortifications" plan provides a glimpse into the army's "preservation" methods during this period. Under the heading "Joints, Cracks and Crevices" the plan reads,

> Joints in the old masonry where the mortar has disintegrated and fallen out will be thoroughly cleaned and pointed up using mortar consisting of equal parts of clean sand and cement. Cracks and fissures shall be repaired as directed by the contracting officer. Small cracks will be thoroughly cleaned to a depth of 6 inches, if possible, so that a bond by dovetailing or otherwise can be made and pointed up with mortar consisting of equal parts of clean sand and cement. [40]

Local historians and preservationists expressed concerns about the army's treatment of historic structures. Martin Paniagua, dismayed at the Army's apparent insensitivity to local traditional craftsmanship, wrote in the local newspaper, "to substitute the old masonry arrangements from which the construction derives its life, for the modern cement so monstrous in appearance as to make our monumental walls lose their peculiar features of cyclopean construction."[41] He suggested that the Army should make a better effort to preserve the walls in "their original appearance."[42]

The effort required to maintain the fortifications in their "original appearance" continued to exceed the army's available manpower and budget. In 1932 the District Engineer explained the critical difference between the Spanish regime of maintenance and the situation facing the U. S. Army. He wrote to the Chief Engineer that "the Spanish, prior to 1898, had taken "particular care"



Figure 22: "Before El Canuelo was connected to Las Cabras, [January 1935]" (Library of Congress)

in providing for proper drainage of the works… fortifications were kept under constant observation and slight breaks and failure were repaired as soon as they developed. But since 1898 the walls had been allowed to "deteriorate to a considerable extent." To exacerbate their predicament, the U.S. Army appropriated less money for routine maintenance by the middle of the 1930s.

On August 25, 1916, President Woodrow Wilson signed the "Organic Act" that created the National Park Service and gave it responsibility for protecting 35 existing national parks and those created in the future. In 1933, President Franklin D. Roosevelt signed an executive order reorganizing the National Park Service and transferring 56 national monuments and military sites from the Forest Service and War Department to the National Park Service. Some officials in the War Department resisted the transfer, particularly the transfer of active military cemeteries. In August 1933, 57 War Department sites, including military parks, battlefield sites, national monuments, and cemeteries transferred to the National Park Service. Following a trip to Puerto Rico in 1934, Eleanor Roosevelt expressed interest in the creation of national parks and monuments on the island. That year, NPS sent Harold Bryant and George Wright to inspect and prepare a report on that possibility. Their 1935 report criticized the army's impact on the fortification and the general condition of the historic resources. The recommended the transfer of the site to NPS so as to improve preservation and interpretation of the resources that they deemed of national significance. The War Department effectively opposed the transfer of the San Juan Military Reservation to NPS because it was still used as

39. Bearss, *Historic Structures Report*, 194.
40. Bearss, *Historic Structures Report*, 220.
41. Bearss, *Historic Structures Report*, 221.
42. Bearss, *Historic Structures Report*, 222.

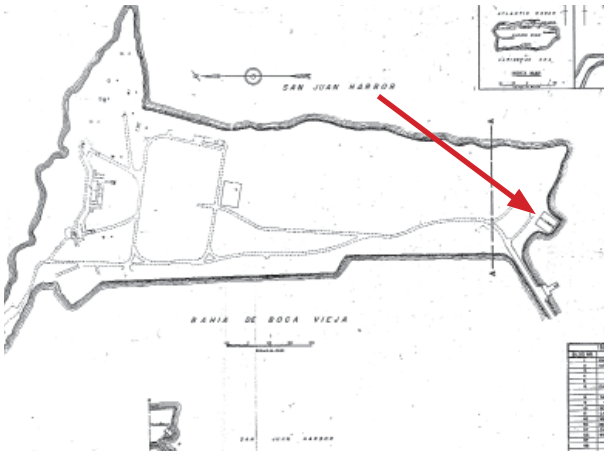


Figure 23: "Fort Amezquita, [1958]" (NPS)



Figure 24: 1887 map overlaid on 2017 aerial



Figure 25: 1958 map overlaid on 2017 aerial

an active military base, needed for the defense of San Juan, and because of the high cost of building replacement facilities.[43] Around this time in the mid-1930s, an unknown photographer captured an image of El Cañuelo. The building had deteriorated since the time of the previous photograph (Figure 14). The roof of the 1841 structure was gone by this time and a large section of the south corner of the building is missing. (Figure 22). This image, dated January 1935, includes the typed caption "The old fort- Cañuela [sic] in the bay, to be remodeled into an aquarium." No further information currently exists on this proposed project.

In 1938, Captain Henry G. Margeson of the 65th Infantry produced measured drawings of El Cañuelo included as Drawing No. NHS-SJ 9665A in the "Fortifications of San Juan P.R. No. 4." Margeson's drawings are the earliest architectural documentation of the fort that have been found to date. It documents the major features present today and provides the most extensive record of the 1841 additions to the terreplein. The 1954 HABS set reproduced these drawings.[44]

From 1938 to 1940, a significant amount of funds became available through the Works Progress Administration, one of President Franklin D. Roosevelt's New Deal programs. At the height of the Works Progress Administration, nearly 2,000 workers participated in projects in San Juan. Over two years, an estimated 3.6 million man-hours were expended at a total cost of $858,819.[45]

The WPA projects were divided into six categories: restoration of the walls, reconstruction of nine damaged or missing sentry boxes, repairs to San Juan Gate and adjacent walls, reconstruction of damaged features at El Morro, restoration of features at San Cristóbal, and general patching of walls and features not covered in other projects.[46]

By June 1940, the WPA program in San Juan had ended. A "*Completion Report: Repairs of Historical Fortifications, Military Reservation*"does not record any work at El Cañuelo.[47] The completed

43. Bearss, *Historic Structures Report*, 255-257.
44. This is probably Henry Beane Margeson (1900-1991) of New Hampshire. Margeson entered the U.S. Military Academy in 1921, receiving a Bachelor of Science in 1925 before enlisting in the infantry. He graduated from the Infantry School Officers' Course in 1929 and the Signal School Communication Officers' Course in 1930. Margeson was promoted to the rank of captain in 1935 and was stationed at El Morro as of 1937. He was stationed at Fort McKinley on Great Diamond Island, Maine, by 1939.
45. Bearss, *Historic Structures Report*, 295.
46. Bearss, *Historic Structures Report*, 260-266.
47. War Department United States Engineer Office, "Completion Report—Repair of Historical Fortifications—Specifications, U.S. Plant and Hired Labor, Nos. F 28-1, F 28-2, F 28-3, F 28-4, F 28-5, F 28-6," June 20, 1940. Copy of document in at SAJU Archives.

work, however, did not impress NPS historical architect Stuart Barnett, who concluded the army's work, "showed almost complete disregard for the importance of such historic structures."

Because of the growing possibility that the war in Europe would threaten the United States, the U.S. Army began a major project to develop a modern coastal defense system at San Juan. Over the next few years, the army constructed a variety of concrete facilities within the Spanish fortifications of El Morro and San Cristóbal. In 1939, the army identified locations for four additional six-inch batteries, including one on Cabras Island, adjacent to El Cañuelo. In 1943, the Army Corps of Engineers completed construction of Battery Reed and Fort Amezquita on Cabras Island. The project included filling the shallow shoals between Cabras and El Cañuelo islands to create a larger landmass for military facilities. It also constructed a causeway between the enlarged island and Toa Baja on the mainland. (Figure 23).

Overlaying maps from 1886 and the 1950s with modern aerials shows how much change has occurred to El Cañuelo Island because of the Corps of Engineers project. (Figure 24); (Figure 25).

Early National Park Service Period 1949-1985

In January 1949, President Harry Truman approved the designation of "the ancient fortifications of San Juan, P.R.," as a national historic site. In February 1949, Secretary of the Interior Julius Krug designated El Morro, San Cristobal, Casa Blanca, and El Cañuelo to be components of the San Juan National Historic Site. On September 4, 1949, the Department of the Army and Department of the Interior signed an agreement providing for the cooperative management of the historic resources at San Juan.[48]

With the 1949 cooperative agreement, the NPS could improve interpretation of the historic site by creating museum exhibits, signs, and historical markers. While final authority of approval of any plan remained with the army, the NPS was able "to prepare, in consultation with the Army, plans for development of additional facilities for visitors, including walks, roadways, and structures necessary for regulated public use of the national



Figure 26: Aerial View San Juan Bay [circa 1954], (Archivo General de Puerto Rico)



Figure 27: "HABS: April 19, 1954 EAST AND NORTH ELEVATIONS", (Library of Congress)



Figure 28: "HABS: April 19, 1954 NORTH ELEVATION," (Library of Congress)

48. Joan Berkowitz, et. al. "Summaries," in *The Fortifications of San Juan National Historic Site, Historic Structures Report, Volume I* (Atlanta: Southeastern Regional Office, National Park Service, 1991), 10.



Figure 29: "HABS: April 19, 1954 DETAIL OF SENTRY BOX CORDON AND MASONRY, NE CORNER," (Library of Congress)



Figure 30: "HABS: April 19, 1954 DETAIL OF KITCHEN AND LATRINE SOUTHWEST CORNER," (Library of Congress)

historic site."[49] Additionally, the Secretary of the Army was supposed to submit plans for maintenance and repairs for the NPS's review and approval. (Figure 26).

While most of their attention focused on the major forts of El Morro and San Cristóbal, the NPS made efforts to repair and maintain El Cañuelo. Beginning in the 1950s, the NPS documented the building and installed site features at the fort to facilitate interpretation and provide visitor services. In 1962, the NPS built a staircase up to the main entrance of the fort and up to the upper level of the fort in an obvious effort to make the building accessible to visitors.

The main fortifications at San Juan continued to suffer serious structural failures that forced the NPS and the army into a series of negotiations about responsibility over their maintenance and repair. In December 1951, a large section of wall of the San Agustin Bastion collapsed due to the failure of the "entire foundation under approximately 130 lineal feet of wall."[50] The NPS sent consulting architect Franz Loesche to San Juan to report on the wall and to prepare treatment recommendations. His recommendations are informative, because some of the treatments appear consistent with work performed at El Cañuelo in the following decades. One of his recommendation was to "build a breakwater parallel to the bastion as protection against the surf, consisting of riprap ½ to 2-1/2 tons, the stones to be flushed with quick setting cement on top." He suggested, "core-drilling along the base of the



Figure 31: "HABS: April 19, 1954 DETAIL OF SENTRY BOX CORDON AND MASONRY, NE CORNER," (Library of Congress)

wall to check ground conditions, preparatory to construction of permanent steel pile bulkhead about 6 to 8 feet from and parallel to wall and fill the subject space with concrete. This bulkhead was required to give permanent protection to the wall footings."[51]

In 1954, NPS sent a crew led by NPS architect Charles W. Lessing and photographer Frederik C. Gjessing to prepare Historic American Buildings Survey (HABS) documentation of El Cañuelo. (Figure 27); (Figure 28); (Figure 29); (Figure 30); (Figure 31); (Figure 32); (Figure 33); (Figure 34). The building was open, though there was no stair or ladder to access the entrance. By this time, most of the vertical features of the 1841 lazaretto

49. Bearss, *Historic Structures Report*, 380.
50. Bearss, *Historic Structures Report*, 390.
51. Bearss, *Historic Structures Report*, 392.



Figure 32: "HABS: April 19, 1954 DETAIL OF ENTRANCE, EAST ELEVATION," (Library of Congress)



Figure 33: "HABS: April 19, 1954 WEST AND SOUTH ELEVATIONS," (Library of Congress)

structure were gone except for ruins of piers and walls. From these ruins, HABS documents confirm the general outline and construction of the lazaretto structure seen in early photographs.

The following year, in 1955, Mario J. Buschiazzo visited El Cañuelo. Buschiazzo was an Argentinian architect who wrote extensively on historic architecture in Spanish America including buildings in San Juan. In the photograph, Buschiazzo inspects the broken south corner of the fort. The concrete and stone apron around



Figure 34: "HABS: April 19, 1954 DETAIL OF ENTRANCE, EAST ELEVATION," (Library of Congress)



Figure 35: "Mario J. Buschiazzo inspecciona gran brecha en la bas del fortin del Cañulo," (University of Puerto Rico)



Figure 36: "Area adyacente al Fortin El Cañuelo en Isla de Cabras," (University of Puerto Rico)

the base of the fort is also clearly visible in the photograph. (Figure 35). A rope tied around the cleaved section suggests that the NPS may have been actively working to repair the damage. In June 1955, photographer Luis Casenave visited the site and captured an image of the top platform of El Cañuelo, showing the condition of the building. (Figure 36).

By the mid-1950s, the army was increasingly turning maintenance responsibilities over the Spanish fortifications to the NPS as they began to decommission and close Fort Brooke. In 1956, NPS completed its first major project in San Juan, the restoration of El Morro Chapel. In 1957, the army reported spending $45,000 to repair the Santa Elena Bastion and committed to spending an additional $90,000 on Santa Elena and San Agustin Bastions the following year. On September 23, 1958, the army announced it was to "transfer El Morro, San Cristobal to U.S. National Park Service." According to the press release, "the historical structures have been maintained and administered by the U.S. Army for nearly sixty years." "In addition to the fortifications and walls to be transferred, the small fort of El Canuelo on Cabras Island will be given over to the exclusive jurisdiction of the National Park Service."[52]

Around this time, during the late-1950s, a photographer captured images of the fort and surrounding landscape. NPS had, between 1954 and the time of this photograph, resurfaced the entire south elevation. The landscape is manicured. There are picnic facilities and interpretive signage present in the open space around the fort. (Figure 37); (Figure 38); (Figure 39). In 1960, the NPS undertook a project to stabilize the foundation under the south corner and the concrete apron. They installed sheet pilings and filled opens spaces with rip-rap and concrete. (Figure 40). In 1962, the NPS installed a staircase to the historic entrance, providing the first documented visitor access to the structure. They secured the entrance

52. Headquarters United States Army Forces Antilles and Military District of Puerto Rico, "Press Release No: 250/58 Army to Transfer El Morro, San Cristobal to U.S. National Park Service," September 23, 1958. Copy of document in SAJU archives.



Figure 37: "View of El Canuelo" (Archivo General de Puerto Rico)



Figure 38: "View of El Canuelo" (Archivo General de Puerto Rico)

with a metal gate and installed protective barriers on the upper platform to present visitors from falling into a "cave-in" in the south corner. (Figure 41); (Figure 42).

In the 1960s, erosion of the landmass surrounding El Cañuelo led the Army Corps of Engineers to propose adding riprap around the base of the fort to protect the structure. (Figure 43).In the early 1970s, Holland and Jones investigated the structure as part of their history study of masonry forts of the National Park Service.[53] In 1976, the

53. F. Ross Holland Jr and Russell Jones, *Special History Study Masonry Forts of the National Park Service*" (Denver: Denver Service Center, 1973), 4.

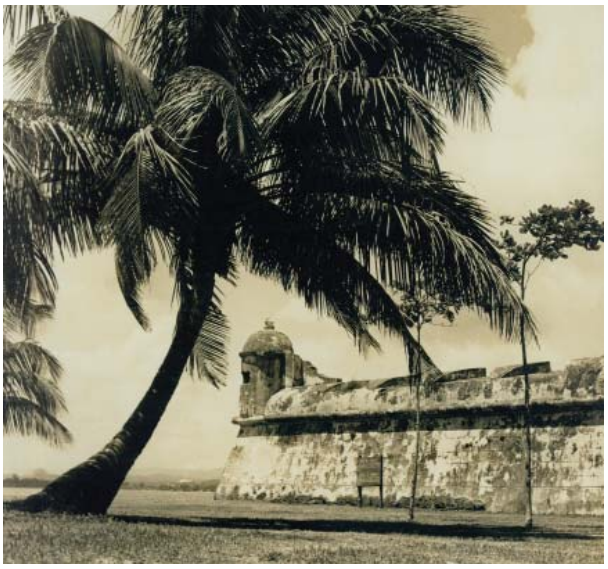


Figure 39: "View of El Canuelo" (Archivo General de Puerto Rico)

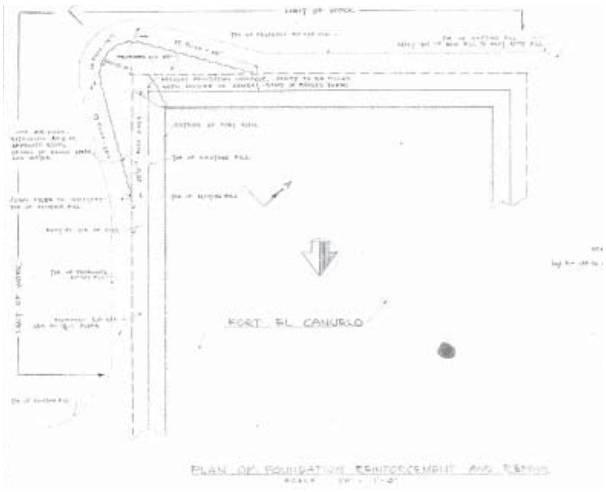


Figure 40: "Restoration of Fort Wall [1960]," (National Park Service)

NPS prepared a "Development Study Package Proposal" for El Cañuelo. The study describes the building in poor condition. It states that a portion of the interior had collapsed blocking the access to the upper level. A large section of the upper level was also caving in, a condition also noted on the 1955 HABS drawings. Additionally, they proposed repair to the exterior walls and to the sentry box. There is no evidence work was ever done; the building was in a similar condition when described in the 1984 draft General Management Plan and when HABS staff revisited the building in 1988.

The NPS developed a General Management Plan for the park in 1984. The plan states,



Figure 41: "View of Stairs at El Cañuelo [circa 1962]," (National Park Service)

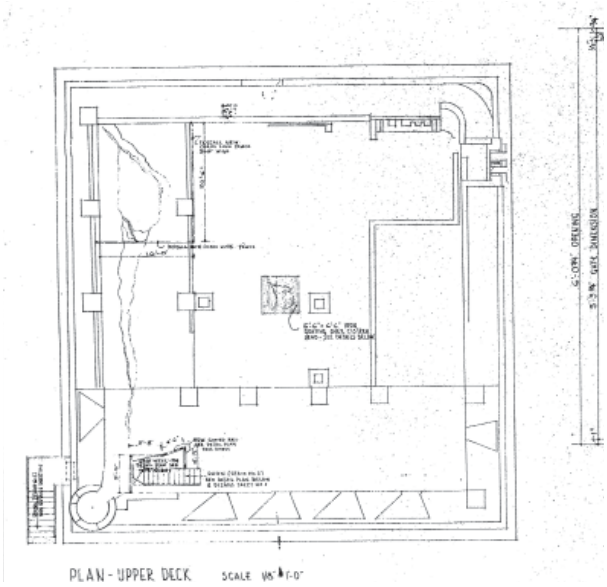


Figure 42: "Stairs and Grate [1962]," (National Park Service)

> The ruins of el Cañuelo… is on 3.4 acres of land owned by the National Park Service and is within the boundary of the national historic site. The area is in the 100-year floodplain. El Cañuelo is in a state of disrepair, and even recent efforts to stabilize the fort and site have fallen short of minimum preservation goals. It is now a safety hazard because people climb the walls and explore the interior. In doing so, they deface the walls by cutting footholds in the stone. Vegetation is growing on the fort's roof, and there is nothing to prevent people who climb onto the roof from falling into the rooms below. … The structure is further deteriorating through natural weathering. A toilet facility that is near the fort and within the historic site boundary does not meet NPS standards.[54]



Figure 43: Photograph showing El Cañuelo [undated]

Proposed actions in the 1984 GMP include a new maintenance program, installation of barricades for safety, vegetation removal, and reestablishing connection with ground level. They also propose the construction of a visitor contact station. Elements of this proposal were accomplished in the subsequent decades, but many recommendations, including one for a visitor contact station, were not implemented.

Recent National Park Service Period 1985-2017

In 1986, researchers with HABS revisited El Cañuelo to resurvey and document the existing conditions of the building. A series of photographs that accompany the HABS documentation are, according to the records of the Library of Congress, dated 1998. During the recent period, extending from the 1986 HABS documentation to the present, the NPS has made repairs and modifications to the structure in an effort to preserve the building and improve accessibility. The major events of this period are the sealing of the upper level of the structure with a 4-inch concrete cap in 1992 and the subsequent reopening of the entrance to provide visitor access to the upper platform in 2012. Throughout the period, and continuing into the present, NPS maintenance staff has performed regular maintenance on the building that includes maintenance of the site grounds, cleaning and repairing the exterior walls, and repairs to individual features of the structure.

54. San Juan National Historic Site, "Draft General Management Plan Environmental Assessment," NPS: San Juan, 1984, page 49. A copy of this document is on file at the Puerto Rico State Historic Preservation Office.

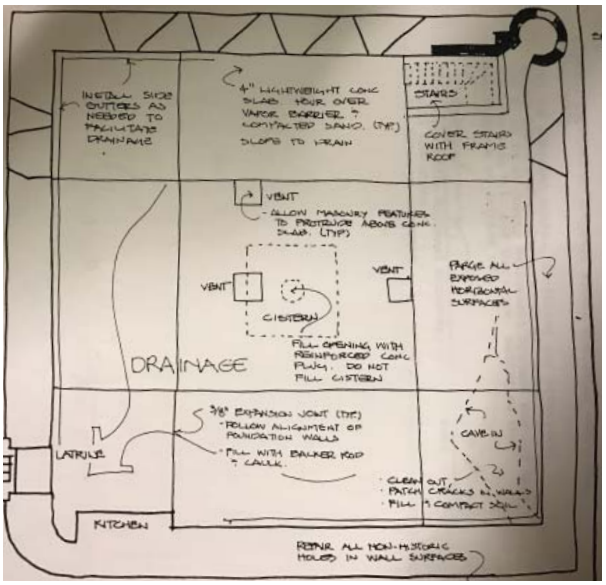


Figure 44: "Sketch of Proposed Work, [circa 1991-1992]" (Puerto Rico State Historic Preservation Office)

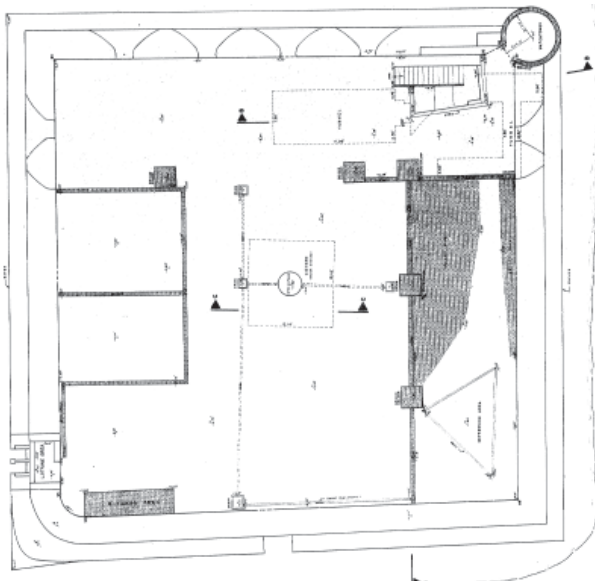


Figure 45: "Fort Amezquita Survey [1991]," (NPS)

HABS staff resurveyed El Cañuelo in 1986. The condition of the fort had not changed dramatically from the earlier, 1954 HABS survey. The 1985 HABS survey shows that the chain link fence the NPS installed in the 1960s was still in place around the cave-in at the south corner. The entrance on the east elevation into the lower level rooms of the fort is sealed, but the opening between the lower rooms and the upper platform is open. It does not appear that either staircase the NPS constructed in the 1960s survived to this time.

In the early 1990s, the NPS implemented several projects to stabilize and preserve the fort.



Figure 46: "HABS PR,7-SAJU,11—10," (Library of Congress)



Figure 47: "HABS PR,7-SAJU,11—11," (Library of Congress)



Figure 48: "HABS PR,7-SAJU,11—10," (Library of Congress)

Hurricane Hugo hit Puerto Rico in 1989, resulting in serious erosion along its shorelines. In the 1992, the NPS installed new rip rap and rock revetments to protect the shoreline at Cabras Island from further erosion. Also in 1992, the NPS poured a 4-inch cap over the entire upper platform of the fort. The intent of the project was to protect the



Figure 49: "HABS PR,7-SAJU,11—13," (Library of Congress)



Figure 50: "HABS PR,7-SAJU,11—14," (Library of Congress)



Figure 51: "HABS PR,7-SAJU,11—15," (Library of Congress)

structure by sealing it from the elements. During this project, the NPS also sealed the lower entrance into the building, effectively closing the structure to visitation. (Figure 44). During this period, prior to implementing the plan to seal the upper platform, the NPS had the building surveyed, giving the last accurate record of the condition of the 1841-era features at the fort. (Figure 45).



Figure 52: "HABS PR,7-SAJU,11—16," (Library of Congress)

HABS photographer Jack Boucher visited El Cañuelo in 1998. His photographs capture the results of much of the work described in the above proposals. (Figure 46); (Figure 47); (Figure 48); (Figure 49); (Figure 50); (Figure 51); (Figure 52).

In the 1990s, the NPS hosted a series of historic preservation symposia where professionals presented papers on numerous topics, including maintenance of historic structures. In 1999, a group of historic preservation experts met in San Juan to provide technical recommendations on the maintenance of the masonry fortifications. Among the "priority concerns" of the report was maintaining proper drainage and monitoring movements of cracks. "Rubble masonry should be inspected to determine the presence of voids, which may have implications for structural stability."[55] The committee recommended removal of vegetation from fortifications and the application of protective renders on vertical elements.

Records indicate that the NPS performed occasional maintenance to the building, having to use ladders to access the upper platform. (Figure 53); (Figure 54).

In 2012, the NPS reopened El Cañuelo to visitation. To improve visitor access and safety, the NPS installed a new staircase to the fort entrance, installed new staircase from lower level to the upper platform, opened a door in the concrete cap, and installed steel railing around the perimeter

55. "Recommendations of the Expert Committee Regarding the San Juan Fortifications, San Juan, Puerto Rico," San Juan, 1999. This document is in the SAJU archives.

of the upper platform. (Figure 55); (Figure 56); (Figure 57).

In 2013, San Juan National Historic Site prepared a Foundation Document that articulates the core mission of the park. The foundation document includes El Cañuelo as a "fundamental resource." Among the threats facing El Cañuelo, the document lists: erosion of walls, vandalism, wear and tear, human waste, iguana burrowing, trash, sea level rise and climate change, vegetation, deterioration of brick masonry, deterioration of sandstone masonry, and impact of natural disasters. The NPS continues to perform regular maintenance on El Cañuelo, even though it is not open to the public on a regular basis.



Figure 53: "1992-2012 Maintenance, North Elevation," (San Juan National Historic Site)



Figure 54: "1992-2012 Maintenance," (San Juan National Historic Site)



Figure 55: "2012 Project," (San Juan National Historic Site)



Figure 56: "2012 Project," (San Juan National Historic Site)



Figure 57: "2012 Project," (San Juan National Historic Site)

I.B Chronology of Development and Use

Military Use of El Cañuelo Island

Drake's Attack

The first documented use of El Cañuelo Island for military purposes was in 1595 during Francis Drake's attack on San Juan. On November 23, 1595, as Francis Drake moved his fleet to anchor off Cabras Island to search for another passage into San Juan Bay, Admiral Pedro Tello de Guzmán sent 28 men to guard the entrance into the Bayamón River. He then had a stockade constructed on El Cañuelo Island, where he stationed 30 infantry. He later reinforced the El Cañuelo garrison with 50 harquebusiers and musketeers. When Drake moved to attack San Juan from the west, passing through the shallow channels near the island, the garrison at El Cañuelo and the garrison on the mainland near the Bayamón River fired upon Drake's troops, forcing their retreat. Drake's attempt to force entrance into San Juan Bay along the shallow channel from Boca Vieja led San Juan's military leaders to re-evaluate the value of the island called El Cañuelo. According to Juan Blanco, "This siege illustrated for them the interrelationship of the ensemble of defenses at the entrance to the channel, bay and harbor as well as those at the eastern tip of the islet. The need for an installation at El Cañuelo shallows where three redoubts would later be built was underlined by this episode."[55]

First Fort Constructed on El Cañuelo

Sancho Ochoa de Castro, who arrived in Puerto Rico in 1602, apparently began construction of a fortification on El Cañuelo Island between 1604 and 1606. He sent the same masons repairing El Morro to the island to construct a wharf and foundations for a fort. According to records, each stone for the foundation weighed between six and ten "quintales."[56]

Gabriel de Roxas y Páramo succeeded de Castro, arriving in San Juan in 1608. De Roxas y Páramo redesigned and finished the fortification on El Cañuelo. This fortress was a round tower constructed of wood and 'cal' y 'canto' (rubble and mortar). It was 4 "pies" thick and capable of holding three to four artillery pieces.[57] According to historian Juan Blanco, after 1609, de Roxas y Páramo reconstructed the fort following a square plan with battlements. This new fort was completed by his successor Felipe de Viamonte y Navarra."[58]

An NPS publication calls this early fort San Juan de la Cruz ("St. John of the Cross"), saying, "During the 1601-10 construction, workmen repaired and expanded [the] easterly defenses. And to the west, across the channel from El Morro, they built a little wooden fort on El Cañuelo Island and called it San Juan de la Cruz. Its firepower would help to control the harbor entrance."[59]

Another history of coastal defenses of San Juan states, "During the years 1608 to 1620 when Gabriel de Roxas and Felipe de Beaumont were governors of Puerto Rico, considerable additions were made to San Juan's defenses. The little island of El Cañuelo at the entrance of the bay, near the mouth of the Bayamón River, was fortified during their terms. This fort's formal name was San Juan de la Cruz, but it came to be known as El Cañuelo after the island. At the time, of course, the island was entirely separate from Cabras Island. El Cañuelo was a square structure, with sentry boxes at each corner and with gun embrasures on all four sides, and a sheltered platform for infantry. Its function was complementary to that of El Morro in covering the channel with long range artillery, that is, long range for its time."[60]

During the invasion of San Juan in 1625, Dutch forces captured the fort on El Cañuelo as part of

55. Blanco, *Fortifications*, 96-98.
56. Blanco, *Fortifications*, 174. A quintal is approximately 100 pounds.
57. Ibid.
58. Ibid.
59. NPS, *The Forts of Old San Juan*, 38.
60. Hoyt, *A History of the Harbor Defenses*, 59.

their effort to cut off supplies from the mainland to the Spanish forces at El Morro. El Cañuelo's location at the mouth of the Bayamón River made it a strategic asset for controlling traffic from the interior of the island. According to one account,

> October 16th, the [Spanish] Governor commissioned Captain Botello to make an attack on El Cañuelo. With two launches and thirty men, the captain made the assault, moving on the fort from the western or Bayamón side of the harbor entrance. The ensuing engagement lasted two hours. In spite of the fact that the Dutch had artillery and were inside a strong little fort, the Puerto Ricans finally captured the position with its garrison of eighteen men, two of whom had been killed. They reduced the fort, as the Spanish account has it, "by putting fire into it.[61]

Following the Dutch invasion in 1625, the Spanish reconstructed damaged fortifications and expanded the system of defenses around San Juan. In September 1626, San Juan officials proposed a new quadrilateral fort on the island of El Cañuelo to replace the wooden one burned during the Dutch attack; though it is unclear that this fort was constructed. El Cañuelo is included in Spanish records as one of the fortifications they actively repaired during this time. According to Juan Blanco, in the years following Drake's departure, up to twelve soldiers were stationed on the island.[62] Records do indicate that there was some structure on the island in 1647, because it is described as in use but in need of repair.[63]

First Masonry Fort at El Cañuelo 1664

In 1658, Governor José Novoa y Moscoso recommended rebuilding a fort on the site of El Cañuelo. During this period, a Spanish military engineer, Jerónimo de Soto, visited multiple sites in the Americas, including San Juan. He is credited with the designs of several forts in the region constructed during this period, however there is no direct evidence that he designed the fort on El Cañuelo. Juan Blanco writes that other "work designed by de Soto resembles similar works built somewhat later and still standing at La Chorrera and Cojimar near Habana, Matanzas near San Agustin as well as San Juan's own Cañuelo."[64] Blanco also draws a connection between El Cañuelo and the "cortadura del taxamar" at the base of San Cristóbal.[65] A paper presented in the *Second International Symposium on Historic Preservation in Puerto Rico and the Caribbean* comments upon the similarities between the sentry box at El Cañuelo and a sentry box at San Cristóbal. It states that these sentry boxes are unique from other remaining sentry boxes among the forts of San Juan. "The earlier sentry boxes from the seventeenth century were simple in appearance, having only a semi-spherical dome over the cylinder of the guard space. Rather than being corbelled out from the corner, as are the later sentry boxes, they merely sat on a circular slab built into the curved corner of the wall. Only two of these seventeenth century boxes remain; one at el Cañuelo (ca. 1660) … and the other on el Espigon (mid seventeenth century), below San Cristóbal."[66] This structure is commonly known today as the "Devil's sentry box" or the "haunted sentry box."

An order from Spain in July 1661 instructed the military governor of Puerto Rico to "cegar," or "blind," the west passage into San Juan Bay.[67] In a May 1663 letter, Captain General Juan Pérez y Guzmán replied that fortifying the west passage into the bay required a fortress capable of sustaining 200 infantry because of its distance from reinforcements. He later reported that a redoubt for six cannons was under construction to guard the rear approach to city. A later letter suggests that this El Cañuelo redoubt was completed by August 1664.[68]

Juan Blanco's describes the information contained in Pérez y Guzmán's reports back to Spain:

> In the report of August 31, 1664 on the work done on the redoubt, Pérez y Guzmán states that it served as an artillery platform for seven pieces: 6 iron 6 and 9 pounders as well as 1 bronze 6 pounder. This was a quadrilateral redoubt built in the middle of the sea of "silleria" and an "obra real", or solid, ashlar construction

61. Hoyt, *A History of the Harbor Defenses*, 65.
62. Blanco, *Fortifications*, 173.
63. Blanco, *Fortifications*, 243.
64. Blanco, *Fortifications*, 178.
65. Blanco, *Fortifications*, 184-186.
66. Blaine Cliver, "El Morro: A Physical History," in Lectures, Second International Symposium on Historic Preservation in Puerto Rico and the Caribbean ed. Milagros Flores Roman (San Juan: NPS, 1991), 63.
67. Blanco, *Fortifications*, 242.
68. Blanco, *Fortifications*, 244.

> with three counterforts per circuit. Each of these curtains could accommodate five pieces of artillery on a terreplein of rough clay and lime residue. The work was surrounded by an "escollera" or stone "calzada" of 10 "tercios de vara" or 3.5 "varas" width with stakes above. It was built on foundations 14 "tercios de vara" wide with a height of 10 "tercios de vara" to the top of the vault and 15 "tercios de vara" to the top of the structures within. It had 21 gunports and 2 garites 2 "varas" wide and 3.5 "varas" high with banquetes .5 varas wide. However, when built the parapets were of "faxina". This fort had a cistern accommodating 100 "pipas" of water and two magazines: one for powder, the other for supplies. It also had an "alojamiento" for the garrison on the terreplein 15 "tercios de vara" wide, 60 "tercios de vara" long and made with pillars of hewn stone located in the center of the terreplein and on the parapets. It was designed for a maximum of 200 and a minimum garrison of 40 men. It maintained, however, a caretaker garrison of only ten men according to later descriptions. The maximum number might be a calculation based on an estimation of the similarity between the dimensions of this quadrilateral redoubt and the organization of a "tercio" as alluded to by Cristóbal de Rojas in his text. The materials for this work were taken to the site on two wooded bridges of 9 "tercios de vara ' wide and 1500 "tercios de vara" in length. The stone used for this work was cut under the direction of Domingo Pelaéz, "official de canteros", and member of the garrison. It is at this time that el Cañuelo was dedicated to San Juan de la Cruz.[69]

According to this document, the foundation walls were approximately 14 feet wide and 10 feet tall. The parapet featured 21 gun embrasures along its four sides, whereas today there are only six, four along the north elevation, one on the west elevation, and one on the east elevation. There were two sentry boxes, whereas today there is only one at the east corner of the building. The interior line of the embrasure walls at the west corner of El Cañuelo is rounded like those in the east corner, suggesting that the second sentry box was in this location. The structure did not have an internal courtyard, but troops were sheltered in a 15 foot by 60 foot long shelter located on the upper platform of the building.

According to an August 21, 1664 letter from Pérez y Guzmán, there were 20 guns mounted at "the Toa Redoubt" at El Cañuelo, "five to a side."[70] Another inventory of artillery from 1683 lists seven weapons at San Juan de la Cruz, including one bronze gun and six iron guns.[71] The earliest found map illustrating this fort is from 1678. It shows a quadrilateral structure on an island flying a Spanish flag. The fort is labeled "Juan de la Cruz." (See Figure 9.)

It is unclear as to when the Spanish began using the name San Juan de la Cruz for the fort. Juan Blanco, quoted above, says that the name refers to 1664 fort. Regarding the significance of the name, he also says, "A similar relationship exists as well between San Juan Gate and the redoubt at el Cañuelo. A syntactical relationship between this gate and this redoubt as a displaced ravelin has already been noted. Here, it is important to take note that San Juan de la Cruz de Jerusalem, like Santiago, were the Patron Saints of two military orders of special dedication among the Spanish. One can conceive of a desire among the Spanish to bless not only the specific site of these defense works and gates but also, and more importantly, the routes of approach which they guarded."[72]

Ongoing Repairs to Fort at El Cañuelo 1665-1785

Most subsequent mentions of the fort on El Cañuelo in Spanish military records refer to its failing condition and need of repair. It appears in Spanish records in 1690, when Alonso Pedraza describes that many of San Juan's fortifications, including San Juan de la Cruz, needed "significant repairs." [73] Among the most frequent issues recorded by Pedraza was cracking in San Juan's fortifications' walls and foundations. According to Blanco, the Governors' records describe repairs made to the fort in 1692. Letters from 1695 and 1698 then suggest that El Cañuelo had fallen into a "state of ruin." By the end of the seventeenth

69. Blanco, *Fortifications*, 244-245; While numerous histories use the name for earlier iterations of forts on El Cañuelo, Blanco's research relies upon primary documents and he attributes the name to the 1664 structure and not earlier.

70. Blanco, *Fortifications*, 277.
71. Blanco, *Fortifications*, 278.
72. Blanco, *Fortifications,* 284.
73. Blanco, *Fortifications*, 250.

century, records indicate that local officials were making constant repairs to many of San Juan's fortifications, but none are recorded at El Cañuelo between 1692 and 1702.[74]

A letter dated April 20, 1702 from Gabriel Gutiérrez de la Riva mentions that "major work" was done on many of the fortifications, including the "redoubts" on San Juan de la Cruz.[75] At some time around 1702, the Spanish installed at El Cañuelo a "caja de pilotaje," a navigation light, to help guide vessels into the channel. It is also noted that during this period that the Spanish constructed a stockade in front of the fort, "before the wall facing the bay as a kind of barbican."[76] A 1764 map of San Juan shows El Cañuelo. It says the "Petit Fort" had 18 cannons. (See Figure 11.)

The fort is included in O'Reilly's inventory of fortifications around San Juan. Under the category of forts in the northern section defending the principal entrance into the bay, O'Reilly writes of placing a battery of eight guns on Cabras Island that "would serve to prevent any attempt of penetration into the bay." O'Reilly appears to be planning for a new battery on Cabras Island that would replace, rather than supplement, El Cañuelo.[77]

Spanish Non-Military Use of Fort El Cañuelo 1785-1898

Spanish Abandon Fort at El Cañuelo 1785-1840

Records indicate that by 1784, the fort was in ruins again and that Puerto Rican officials formally requested permission to abandon the fort in 1785. The May 2, 1787, earthquake damaged structures in Toa Baja in addition to in San Juan. While it seems likely that the earthquake would have affected El Cañuelo, there is no known record of damage to the building.[78]

One history describing Abercromby's invasion of Puerto Rico in April 1797 mentions an artillery battery stationed at El Cañuelo. According to the authors,

> At about nine o'clock in the evening it was observed that the enemy blockade ship and frigates were moving toward Punta Salinas. El Morro and El Cañuelo fired at them but did not sustain their fire because the ships were out of range. . . . Later that night a brigantine anchored near the north side of Cabras Island. El Cañuelo and San Fernando battery, with its thirty six pounders, were ordered to conduct rapid fire to harass the enemy ship. The results were not observed until dawn, when the brigantine moved off out of range as quickly as possible, using both sail and oars.[79]

By mid-century, Spain apparently no longer considered El Cañuelo a strategic asset to San Juan's defense system. While records mention ongoing maintenance to the other fortifications of San Juan, the records do not mention work on El Cañuelo. In 1858, Rafael Clavijo prepared a report that described the condition of San Juan's fortifications.[80] In general, Clavijo described the forts and walls as in a state of abandonment and ruin; however, records do not mention El Cañuelo specifically.[81] The building's condition may have led the Spanish to abandon the fort since previous records continually describe it as a ruin. Its abandonment may also reflect changes in military technology and overall strategy. As navies outfitted their ships with new long-range weaponry, coastal defenses needed to intercept invading forces farther away from the coast. Batteries located along the cliffs of San Juan would be more effective locations for long-range guns than the low-lying island of El Cañuelo.

Lazaretto

Wanda López Bobonis, in her "Preservation Plan for Fort El Cañuelo," reproduces a document from the Archivo General de Puerto Rico showing El Cañuelo modified to serve as a leper hospital or "lazaretto" in 1841.[82] The drawing shows a "U" shaped shelter constructed on the terreplein of the fort. This structure is open on its west side, with an open courtyard framed by the structure's

74. Blanco, *Fortifications,* 251.
75. Blanco, *Fortifications*, 253.
76. Blanco, *Fortifications*, 254.
77. Juan Manuel Zapatero, "Las Fortifications históricas de San Juan de Puerto Rico," *MILITARIA. Revista de Cultura Militar,*(1989): 150.
78. http://www.discoveringpuertorico.com/puerto-rico-earthquakes/.
79. Hoyt, *A History of the Harbor Defenses*, 92.
80. Blanco, *Fortifications*, 754.
81. Blanco, *Fortifications*, 744.
82. Bobonis, *Preservation Plan*, 10.

three wings. This shelter included a roof supported by brick pilasters and brick walls enclosing the north, east, and south sides. Additional features included a kitchen and latrine in the west corner. The original sentry box is visible on the drawing at the east corner; and it may have been at this time that the second sentry box, mentioned in earlier descriptions of the building, was removed. According to Bobonis, the lazaretto was to provide "9 beds for women, 28 beds for men, a kitchen and a latrine."[83] The drawing also shows a latrine perched on the west wall, near the west corner. It also shows a kitchen facility located near the west corner of the fort. (See Figure 17.)

A report from the Captain General of Puerto Rico dated 1861 states there were 36 beds available at the lazaretto, which he referred to as "luxury accommodations." Records contained in the Archivo General Militar de Madrid described repairs to be made to the lazaretto in from August 1864 to January 1865.[84] These records confirm that the building, referred to as "fuerte del Cañuelo," was still in use as a lazaretto. The documents mention the adverse effects that waves were having on the foundation of the structure. It also states that repairs were necessary to keep the building inhabitable. The projects include repairs to the roof, walls and doors. It also mentions reconstructing the structure's kitchen. The project description includes a list of material and mentions a need to manufacture brick for the project.

Two photographs from the early second quarter of the twentieth century show remains of the structure built during this period. In the earlier photograph, the shelter appears to have a flat roof on wood rafters supported by square pilasters. The exterior of the walls and pilasters have a smooth layer of stucco, similar to the render seen on the exterior of the fort's foundation walls, but sections of stucco are missing, exposing the interior brick material. Photographs from the 1950s show the remains of the structure's walls, location of doors, the roof pillars, and brick flooring. These photographs provide additional evidence that the structure's walls and pillars were brick masonry with stucco. The brick floor, which would have been under the northern wing of the structure, was intact into the 1990s. (See Figure 58, Figure 59, Figure 18, Figure 22, and Figure 36.)

Spanish American War 1898

Angel Rivero, a Captain of Artillery who was present during the bombardment, mentions El Cañuelo in his memoir of the Spanish American War. He writes that the Spanish extended a chain across the bay between El Morro and El Cañuelo to block entrance into the harbor. He writes, "The lower battery of the castle of el Morro [sic] had six stoves for heating bullets, and from this same spot started a thick chain, whose other end was tied to el Cañuelo and served to close the port."[85]

United States Agencies Management of El Cañuelo

United States War Department Period 1898-1949

The U.S. Secretary of War Elihu Root on December 15, 1900 issued the declaration, "That Cabras and Cañuelo islands in San Juan Harbor and all lands and buildings on San Juan Island belonging to the United States…[are] to be retained by the War Department for military uses."

The Archivo General de Puerto Rico has a photograph of El Cañuelo taken sometime before 1935, probably in the 1920s or early 1930s.[86] The photograph shows the building's south and east elevations, while still surrounded by water. Water had undercut the foundation along both visible walls. The west corner is missing a section at the water line. A large crack is visible on the west elevation. (The army repaired this fissure at a later date, but is still visible as of 2017.) Several walls and portions of the roof from the 1841 lazaretto were present at this time, as described in a previous section. At the time of this photograph, the top of the latrine structure is broken, exposing its brick interior. The photograph also shows vegetation growing on the terreplein and along the cordon.

83. Bobonis, *Preservation Plan*, 10.

84. A series of documents are available in the digital records of the Archivo General Militar de Madrid Seccion Ultramar del Ministerio de la Guerra. These documents are part of series 5616.02.

85. Angel Rivero, "Crónica de la Guerra hispanoamericana en Puerto Rico" (Madrid: Sucesores de Ryzadeneyra, 1922). The text provided is an approximate translation of the original spanish.

86. The date for photograph date comes by comparing the extant features with a later photograph at the Library of Congress dated 1935.

(See Figure 18 and Figure 58.)

In October 1939, the United States Congress authorized the construction of a large gun battery on Cabras Island. The military named it Reed Battery to honor Brigadier General Henry A Reed; they named the surrounding area Fort Amézquita to honor Juan de Amézquita, a captain in the Spanish Army who gained fame for his valor during the Dutch attack in 1625. To construct the military facility, the Army Corps of Engineers dug an access for construction barges through the coral reef protecting Cabras Island. The Army Corps of Engineers deposited fill dirt in the shallow water between Cabras Island and El Cañuelo to create a single landmass. They connected the enlarged island with a causeway to the tip of Palo Seco. It is possible that the army constructed a rock and masonry apron around the building during this project, because the 1954 HABS documentation describes the apron.

A United States Army history of coastal defenses written in 1943 contains a description of El Cañuelo at that time. It states, "El Cañuelo was not restored in 1938 with the rest of the fortifications and is consequently in sad condition. However, there are remains of gun embrasures and sentry boxes as well as the stone stairway which gave entrance on the southeast side."[87] (See Figure 23.)

Early National Park Service Period 1949-1985

In February 1949, Secretary of the Interior Julius A. Krug designated El Morro, San Cristobal, Casa Blanca, and El Cañuelo as components of the San Juan National Historic Site. On September 4, 1949, the Department of the Army and Department of the Interior signed an agreement over the cooperative management of the historic resources at San Juan. The property handed over to NPS control included the El Cañuelo structure and 3.4 acres of recently-created land surrounding the fort.

NPS has photograph of El Cañuelo that shows the building in 1935. The photograph's caption reads "The old fort – Cañuela [sic] in the bay, to be remodeled into an aquarium." The view of the fort is from a similar direction as the previously described photograph (Figure 18), but this photograph also shows the entire south elevation of the fort. The south corner is missing a large section at the water line; the north corner also has a missing section, as seen in the earlier photograph. The general condition of the building is unchanged from the earlier photograph except the roof structure in the earlier photograph is missing, as are sections of the walls from the 1841 structure. The crack on the west elevation is visible; and waves have undercut the foundation. The exterior wall on the north corner appears to be overhanging the underlying foundation. A second crack is visible on the south elevation. It is filled partially with vegetation. (This crack was later repaired, but is still present as of 2017). (See Figure 22 and Figure 59.)

In 1954, NPS sent a crew led by NPS architects Charles W. Lessing and Frederik C. Gjessing to prepare Historic American Buildings Survey (HABS) documentation of El Cañuelo. Lessing described the condition of the structure at the time,

> The entrance level is approximately 8' above mean low water. It consists of two vaulted chambers with connecting passageways, a cistern and masonry stairs to the upper level. The upper level originally had housing facilities for the troops quartered in the fort. The outer walls are shell walls, constructed as are the foundations, from cut sandstone blocks laid in coursing with rubble and fill. Vaults are constructed from brick. The walls are covered with lime render. There are indications that the structures on the upper level were covered with conventional flat brick roof carried on wood beams and rafters.[88]

When documented by HABS in 1954, a large section of wall at the base of the south corner had broken away from the structure. A note states that "rubble at base of broken section of apron and at foot of NE corner of fort contains fragments of 3' x 3' brick pillars." The concrete apron around the foundation of the fort featured field stone laid in a random pattern and mortared with concrete. The apron exhibited extensive damage in the south corner. According to HABS, the south corner had been refinished prior to the "existing failure of the toe," suggesting that the "toe" may have been repaired once prior to the failure seen in 1954.

87. Hoyt, *A History of the Harbor Defenses*, 125-126.

88. Charles W. Lessing, "The Fort of El Cañuelo," HABS Survey No. PR-52, August 10, 1955, accessed online, http://cdn.loc.gov/master/pnp/habshaer/pr/pr0000/pr0009/supp/pr0009supp.pdf.

(See Figure 27 and Figure 33). A failure at a similar location of the north corner was repaired prior to 1954. (See Figure 28). HABS also documents that some repair and restuccoing had occurred prior to their visit. HABS describes the wall and parapet of the east elevation as "refinished." Figure 32 shows evidence of these repairs. It appears concrete had been applied to stabilize the stone below the door and around the opening into the east wall. HABS describes the stucco of the embrasures and parapet wall of the north elevation as being "of recent date."

The 1954 photographs also show that the top of the latrine structure had been repaired since being photographed in 1935. Figure 33 also shows evidence of a crack on the west wall, between the latrine structure and the west corner. False joint lines applied to the exterior render are more visible in this photograph than in the older photographs. Figure 33 also shows large chips on the south corner, which NPS repaired prior to 1998. A drain is visible protruding out the west wall, which would have drained water from the terreplein. The NPS closed this drain, probably in 1992. This photograph also shows a frame structure several feet from the west elevation near the north corner. The structure has a shed roof and horizontally laid clapboard exterior. It appears to the appropriate size for a small restroom or utility shed. Later documentation mentions a restroom on site. (See Figure 60.)

HABS documents describe the cordon of cut stone as "finished in red stucco, integral coloring." This cordon extends around the entire building except for a portion of the south elevation. HABS also documented the condition of the upper platform that formed the terreplein of the original fort and became the floor for the lazaretto. Floor drains from this platform conveyed water to the exterior on the west elevation or into a 12 foot-by-12 foot cistern located approximately in the center of the structure.

The historic entrance into the fort was open in 1954. HABS photographs show that the stucco of the east elevation was in poor condition at that time. The sentry box in the east corner featured a wide rectangular opening that the NPS restored to a configuration similar to those on other sentry boxes within the national historic site. The photographs also show the breakwater extending off the east corner into the bay had a sheet pile and stones mortared into concrete. (See Figure 61.)

Another HABS photograph taken in 1954 also captures the small shed building near the north corner of the fort. Small palms are growing in the open area north of the fort. There is significant damage to the bottom of the wall, near where the wall meets the ground. Repairs to the embrasure, mentioned in HABS documents, are visible as large concrete patches. The NPS repaired the north corner, shown as broken in 1935, by 1954. (See Figure 62.)

A large cavity had opened in the floor near the south corner before 1954. HABS measures the "sunken area" to be approximately 7 feet deep. Many features remained of the 1841 lazaretto structure, though all the vertical walls seen in the 1935 photograph were gone by this time. The bases of the brick pillars and evidence of the structure's walls were visible and documented. There were also areas paved in brick, laid either in a running bond or herringbone pattern. A photograph showing north and west elevations of the fort taken in 1951 shows an overgrown landscape around the fort and vegetation growing on top of the fort. By 1954, when visited by HABS, the landscape was being maintained and the vegetation on top of the structure had been reduced. (See 1954 HABS drawings in Appendix B; See Figure 30, Figure 36, and Figure 63.)

In June 1955, photographer Luis Casenave visited the site twice. One photograph shows the large section broken off from the south corner. This piece is also visible in 1954 HABS photographs and HABS drawings. It was not visible in the 1935 photograph. This suggests that the army or the NPS repaired the section between 1935 and 1954, only to have it fail again. Or the section was submerged and the army or the NPS hoisted it into place and never attached it. Casenave also took a photograph of the upper platform of El Cañuelo, showing the condition of the building in 1955. The photograph looks south over the portion of the terreplein with the sunken area. Remains of the brick pavement of the 1841 lazaretto are visible in the foreground. The remaining surface is, according to the 1954 HABS drawings, a "lime concrete." Remains of the lazaretto structure include evidence of walls and the bases of brick pillars. Tufts of vegetation grow

from cracks in the pavement. (See Figure 28; and Figures 35 and 36.)

On September 23, 1958, the army announced it was to "transfer El Morro, San Cristobal to U.S. National Park Service." According to the release, "the historical structures have been maintained and administered by the U.S. Army for nearly sixty years." "In addition to the fortifications and walls to be transferred, the small fort of El Canuelo [sic] on Cabras Island will be given over to the exclusive jurisdiction of the National Park Service."[89]

A photograph of El Cañuelo taken between 1954 and 1962 shows that the NPS or army applied a new finish of stucco over the entire east elevation. The original entrance is still open, though a large crack extends from the lower, right-hand-side of the entrance. Patches of vegetation cover large sections of the north elevation. The lower base of the north wall remains damaged. Also visible in the photograph is an interpretive sign mounted in the open space along the north elevation. Beyond the north corner of the building, the shed seen in earlier photographs is missing. It may be out of view of the image, but there does appear to be a concrete slab on the ground, suggesting the NPS had removed the building. (Later NPS documents describe another restroom building on site into the 1980s.) Other photographs from this same period show the NPS had constructed thatched-roof huts on concrete bases as a kind of picnic shelter. A photograph also shows a unique trash receptacle, suggesting that the NPS was actively supporting visitation to El Cañuelo. In 1954, the Puerto Rico Administration of Parks and Recreation proposed the creation of a recreational park to be located on Cabras Island. The park was to include a public beach and picnic area. The combination of NPS interpretation efforts and the development of a local park may account for the increase appearance in site amenities at El Cañuelo. (See Figures 37-39, and Figure 64.)

Sometime between 1955 and 1960, the NPS repaired the broken section of wall, described above, at the base of the south corner of the fort. Either the NPS or the army repaired the corner before engineers with the National Park Service Division of Design and Construction undertook a project in 1960-1961 to stabilize the foundation under the south corner of El Cañuelo. "Rehabilitation of Fort Wall," the project construction drawings show the addition of steel sheet pilings approximately 10 feet below mean low water level and back filling with rip rap. They also filled a cavity "under the southeast corner of the fort" with "a 1:6 mixture of cement and sand in bagged forms." The drawings also show the limits of existing "fill" extending around the perimeter of the base of the fort. (See Figure 40 and Figure 41.)

In February 1962, NPS Eastern Office of Design and Construction prepared construction drawing for the installation of stairs, iron gates, and protective railings at El Cañuelo. The drawings, entitled "Plans Gate and Grate Details" and "Details Star No. 1 and Stair No. 2," show NPS adding a staircase up to the original entrance into the fort on the east elevation, near the east corner. They also installed a wood staircase connecting the interior room on the lower level to the upper platform. The construction plans also call for metal gates to be added to the entrance and for iron grates to cover the cistern opening. They also show a 3-foot tall chain link fence installed around the eroded, sunken area in the south corner described in the 1954 HABS documentation. (See Figure 41 and Figure 42.)

In 1962, Brigadier General H. A. Morris, Division Engineer of the Army of Corps of Engineers, submitted a report to NPS documenting the significant erosion issue at El Cañuelo. There is "instability and recession of the shoreline due to deficiency of supply littoral material and loss of material to offshore waters." He proposed the placement of "protective rubble" around exposed sides.[90] (See Figure 43.)

In the early 1970s, Holland and Jones investigated the structure as part of their history study of masonry forts of the National Park Service. They stated that at "El Canuelo there is serious wearing away of the plaster covering the walls." On the upper level,

> The covering plaster and cement on the upper gun deck has worn away in many places,

89. Headquarters United States Army Forces Antilles and Military District of Puerto Rico, "Press Release No: 250/58 Army to Transfer El Morro, San Cristobal to U.S. National Park Service," September 23, 1958. Copy of document in SAJU archives.

90. Walker, *Narrating Climate Change*, 20.

> permitting water to soak through the earth fill of the walls. This water causes serious internal erosion and deterioration of the walls. To prevent the water from penetrating the walls, the terreplein will have to be sealed with a cement-like covering. The walls are basic to the structures. If their innards are allowed to erode and deteriorate they will eventually collapse and take with them the remainder of the structures.[91]

Recent National Park Service Period 1985-2017

HABS resurveyed El Cañuelo in 1985. The condition of the fort had not changed dramatically from the earlier, 1954 HABS survey. The 1985 HABS survey shows that the chain link fence the NPS installed in the 1960s was still in place around the cave-in at the south corner. The entrance on the east elevation into the lower level rooms of the fort is sealed, but the opening between the lower rooms and the upper platform is open. It does not appear that either staircase shown in NPS drawings in the 1960s survived to this time. (See 1985 HABS drawings in Appendix B.)

In 1991, NPS proposed a project to repair El Cañuelo and protect the fort from further deterioration. The *XXX Form Assessment of Actions Having an Effect on Cultural Resources* states,

> The structure is in fair to poor condition. Holes have been dug in the exterior wall surfaces by vandals trying to climb into the fort. Weathering has also eroded portions of the sentry box, removed stucco from the top of the parapet wall, and exposed sections of the terreplein. Water flow through the interior of the structure has carried away large amounts of soil from the southeast corner of the terreplein and is undermining the southeast corner of the walls.[92]

The condition of the building in 1991, based on this description, had not changed significantly from when it was inspected by HABS in 1985 or when described in the draft general management report in 1984.

The work proposed in 1991 included,

> The "cave-in" in the southeast corner of the port will be filled with clean, dry sand to the level of the terreplein. The terreplein of the fort will be covered with clean, dry sand to a depth of approximately 4" and then topped with a 4", wire-reinforced concrete slab. The slab and sand will be contoured to allow surface flow to existing drainage points in the structure. No sand will be placed in the cistern, the stairway or the lower vaults (magazines). The cistern will be covered with a reinforced concrete cap. The stairway will be covered with a wood frame structure. Expansion joints will be located above the building lines as shown on the attached sketch. Non-historic wall cavities and missing bricks from the sentry box will then be repaired and refinished with matching stucco. For additional details see the attached sketch of the terreplein level. This work will greatly improve the ability of the structure to shed water and will protect the remains of the terreplein and upper level structures from vandalism and erosion by pedestrian traffic.[93]

A handwritten note added onto the form in the files of the Puerto Rico State Historic Preservation Office says that the NPS "Used lightweight concrete on top of a plastic cover to protect historic fabric from overloading." The "concrete cap" portion of the project was completed around 1992. During this project, the NPS also sealed the interior room by installing a wood frame in the lower room to support the concrete slab sealing the upper terreplein. The NPS also closed the exterior entrance into the fort on the east elevation by filling it with concrete blocks. Several remains of the 1841 structure protruded above the concrete cap. NPS staff present during project remembers that they cleared the cistern of debris prior to the pouring of the concrete cap. (See Figure 44.)

It is possible that an existing survey of the fort and surroundings from November 1991 is part of the NPS preparations for the above-described project. The survey, entitled *Fort Amezquita (El Cañuelo)* shows the condition of the fort prior to

91. F. Ross Holland Jr and Russell Jones, *Special History Study Masonry Forts of the National Park Service*" (Denver: Denver Service Center, 1973), 4.

92. Carlos R. Oquendo, *XXX Form Assessment of Actions Having an Effect on Cultural Resources,* July 30, 1991. A copy of this document is on file at the Puerto Rico State Historic Preservation Office: file 10-02-97-01.

93. Ibid.

the installation of the concrete cap covering the features on the upper platform. The features are generally consistent with the conditions described in the 1985 HABS documentation. The large "depression area" where the upper level had caved in is visible. The drawing suggests that the drains on the upper level were operational and conveying water into the historic cistern. (See Figure 45.)

In 1989, Hurricane Hugo struck Puerto Rico resulting in erosion at numerous locations of the park. In 1992, the national historic site proposed a park-wide shoreline stabilization project to stabilize the foundations of the historic fortifications. As part of this project, the NPS placed riprap and rock revetments around ElCañuelo and installed a rock breakwater off shore to protect the fort from wave action.[94] The rocks appear in 1998 HABS photographs. (See Figure 51, Figure 52 and Figure 66.)

Routine maintenance and preservation work on El Cañuelo continued for the next several years. In 1994, the NPS applied a coat of render on portions of northwest elevation (a section near the privy opening) and along the lower section of the southwest elevation.[95]

Around 1997, the NPS made major repairs to the sentry box (garita) in the north corner of the fort.[96] HABS photographer Jack Boucher visited El Cañuelo in 1998. His photographs capture the results of much of the work described in 1991 and the restoration of the sentry box.

Repairs to the sentry box included replacing missing brick and recovering the entire sentry box in a new coat of stucco. The gun port opening on the east side of the sentry box was reconfigured to match the smaller dimensions of the opening on its southeast side. The NPS also installed a circular drain in the east corner of the sentry box that does not appear in earlier photographs or in HABS documentation. The photographs also show the ground around the fort was completely bare of vegetation in 1998. This may be the result of Hurricane Hugo (1989) or Hurricane Georges (1998). NPS repaired the lower section of the north wall, which is in poor condition on previous photographs, prior to 1998. The NPS had also, by 1998, installed new interpretive signage. (See Figure 47, Figure 48, and Figure 65.)

According to the recollections of a current NPS staff person, maintenance staff cleaned the walls of the fort with D/2 Biological Solution, a masonry cleaning product, around 2003-2004. In December 2004 and January 2005, Wanda López Bobonis visited El Cañuelo and prepared a physical conditions report of the structure as part of the historic preservation master thesis, "A Preservation Plan for Fort El Cañuelo, San Juan National Historic Site, Isla de Cabras, Puerto Rico." The two entrances into the lower level of the fort, one from the east elevation and one in the north corner of the terreplein, were not accessible during her visit. Her condition report recorded areas of render loss, deteriorating masonry, and the location of structural cracks in the walls.

In preparation of another campaign to maintain the structure, the NPS submitted Section 106 documentation to the Puerto Rico State Historic Preservation Office in June 2008. The description of project says,

> The interior of Fort San Juan de la Cruz has been closed since 1992. Although preservation work has been performed the structure is in need of stabilization work. The northeast elevation exhibits large areas of loss of the original render, which has left the stone work and joints exposed. There is render loss at the parapet as well as vegetation on top of the cordon and parapet areas. A structural shear crack is visible on the east side of the wall and parapet. The base of the wall is raised from the ground and undercut from the foundations or bedrock. Similarly, the northwest wall shows loss of original lime render, which has left the original stone work and joints exposed and unprotected. Three major structural cracks are visible along this wall. The base of the east corner of the elevation is undercut and detached from the foundation or bedrock. The conditions are similar in the southwest and southeast elevations with noticeable structural cracks in the center of the walls and parapets of both elevations.
>
> The park will remove vegetation on the walls of the fortifications, clean them with D2 antifungal formula, replace damaged bricks, and patch holes and cracks with lime based

94. Walker, *Narrating Climate Change*, 20.
95. Bobonis, *Preservation Plan*, 24.
96. Bobonis, *Preservation Plan*, 7.

> mortar to prevent vegetation growth. In the surrounding areas of the fortification (within park jurisdiction) the park will remove sea grape trees that were planted without authorization from the park. The park will remove existing deteriorated wooded fence and will replace it with stone boulders to prevent illegal parking on the fortification grounds.

NPS PMIS records indicate that between June 2007 and 2008, "28,000 square feet was cleaned and patched of historical wall, firing steps and vertical areas."

In April 2012, the NPS prepared a series of drawings that proposed reopening the entrance into the fort on the east elevation and installing a protective guardrail around the perimeter of the upper platform. These actions were part of the park's effort to reopen the site to the public. The wooden staircase installed during this project was in place as of 2016. It provides access to the original, lower level of the fort on the east elevation. It has stainless steel handrails and stainless steel balusters with[97] metal wire. The safety railing around the perimeter of the upper level is of a similar construction. The posts are set into the concrete cap just inside the embrasure walls. Wire cables pass through the posts and anchor at the corner posts. There are also similar railings protecting remains of the 1841 structure that protrude through the concrete floor. The NPS cut the concrete cap to open an access to the lower level. They constructed a new wooden staircase on top of the historic stone staircase between the upper and lower level. They also installed a wooden door in the eastern wall that, according to staff recollections of the projects, was based on other doors at El Morro and San Cristobal. A photograph from this project shows recent patching of the stucco around the door and embrasure above the entrance into the fort. The national historic site has photographs of work in progress. These photographs show that staff also cleaned the structure, removing vegetation growing along the tops of the walls, and patched the stucco in the lower with the staircase. Also in 2012, according to NPS Staff, they installed crack monitors on the major fissures in the wall.

Other changes recorded at El Cañuelo include the construction of a parking lot adjacent to the access road on Cabras Island. This feature does not appear in 1998 aerials. Other recent additions to the site include the park sign, new interpretive signs and two picnic pavilions in the open space north of the fort that are part of the adjacent park. (See Figure 66 and Figure 67.)

97. Felix Lopez, "Stabilization of Fort San Juan de la Cruz (El Cañuelo) SAJU-08-10" June 18, 2008. A copy of this document is on file at the Puerto Rico State Historic Preservation Office.

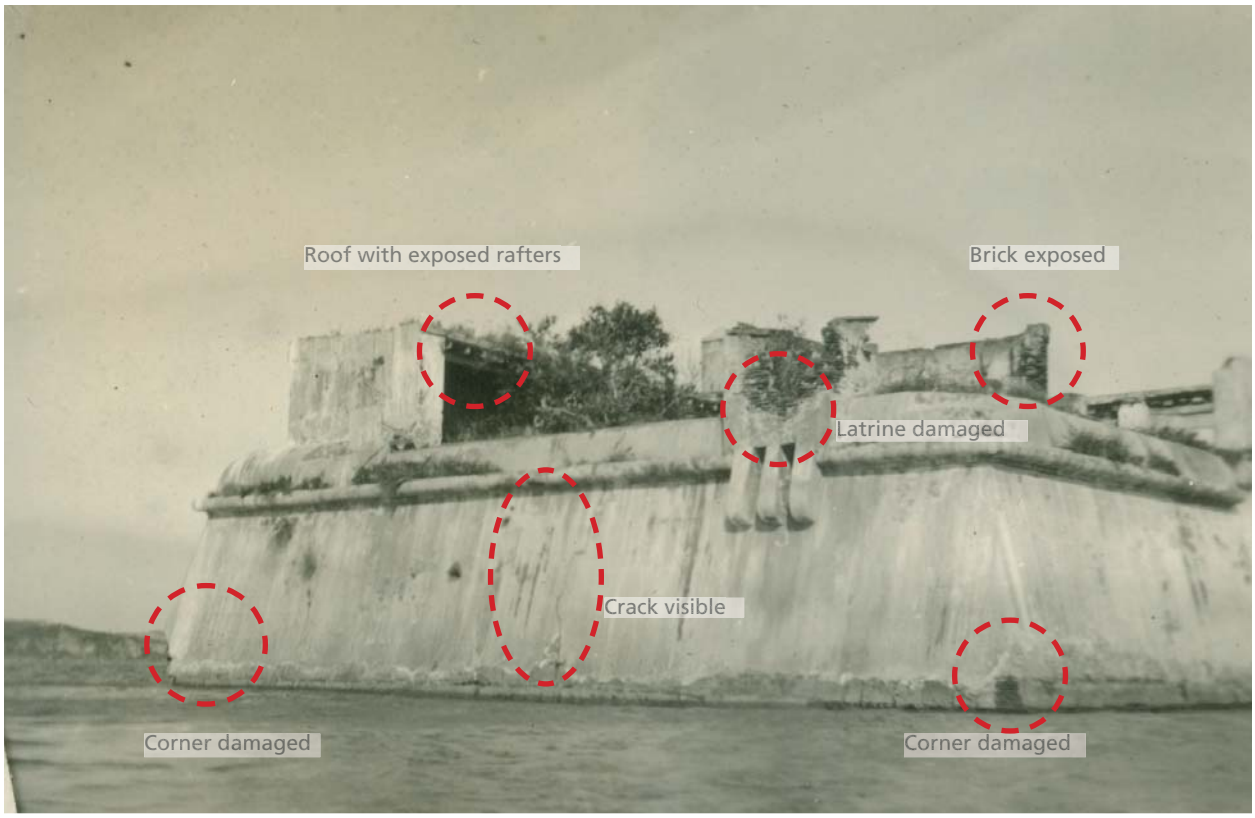


Figure 58: Pre-1935, (Archivo General de Puerto Rico Annotated WLA Studio, 2017)

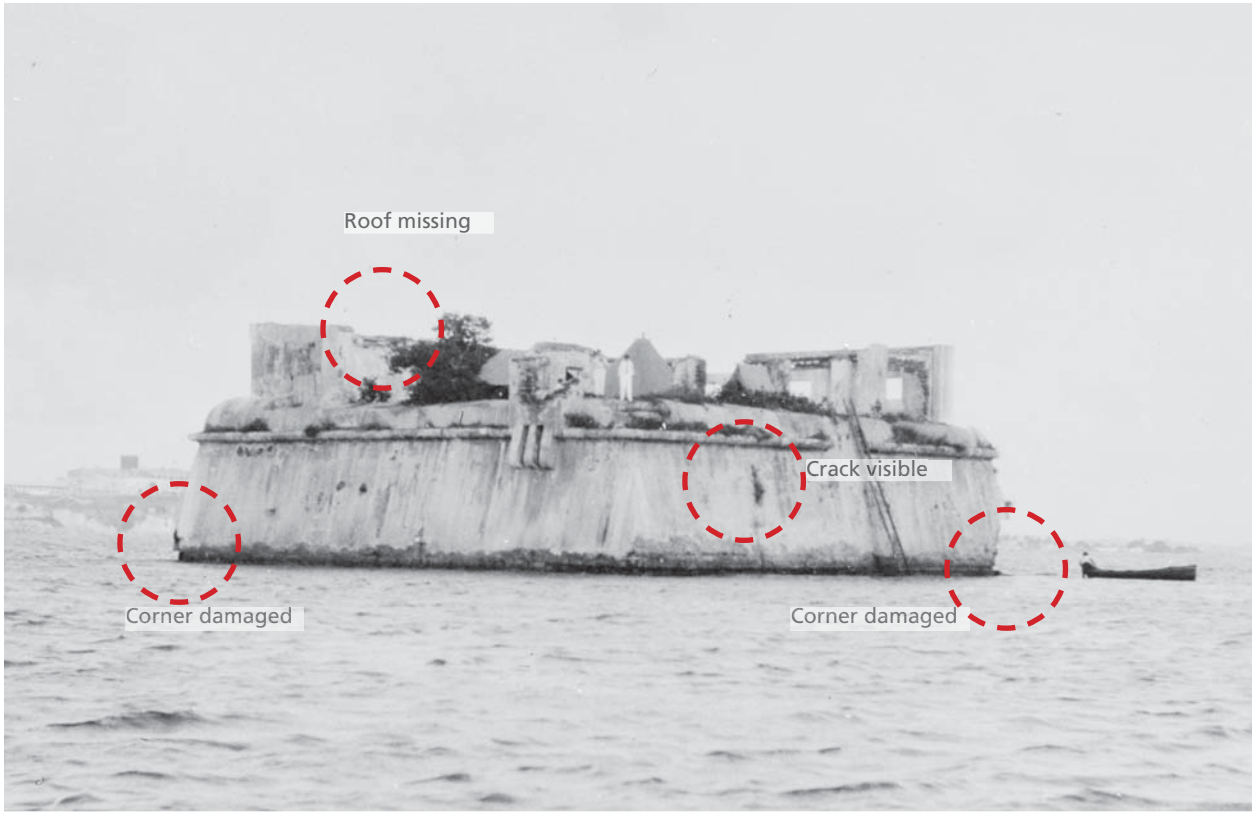


Figure 59: Circa 1935, (Library of Congress, Annotated WLA Studio, 2017)



Figure 60: HABS 1954, (Library of Congress, Annotated WLA Studio, 2017)



Figure 61: HABS 1954, (Library of Congress, Annotated WLA Studio, 2017)

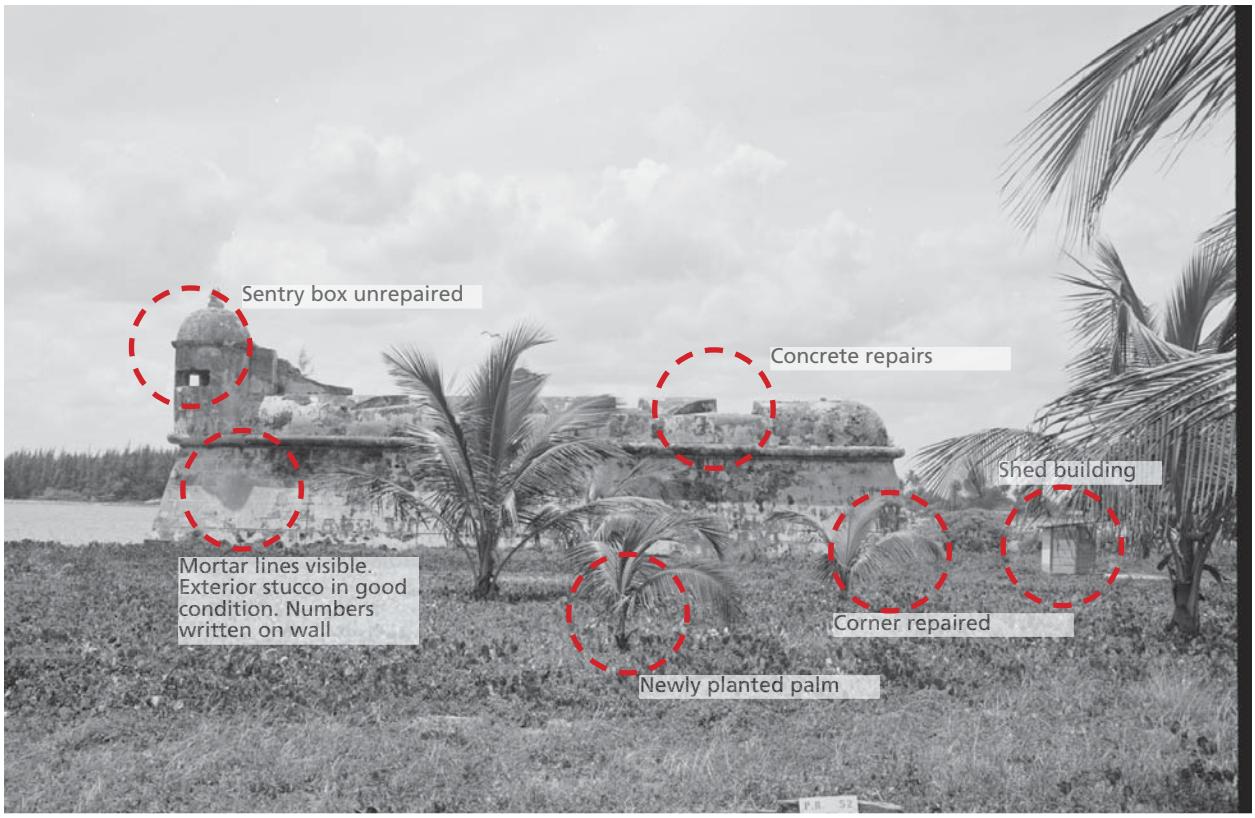


Figure 62: HABS 1954, (Library of Congress, Annotated WLA Studio, 2017)

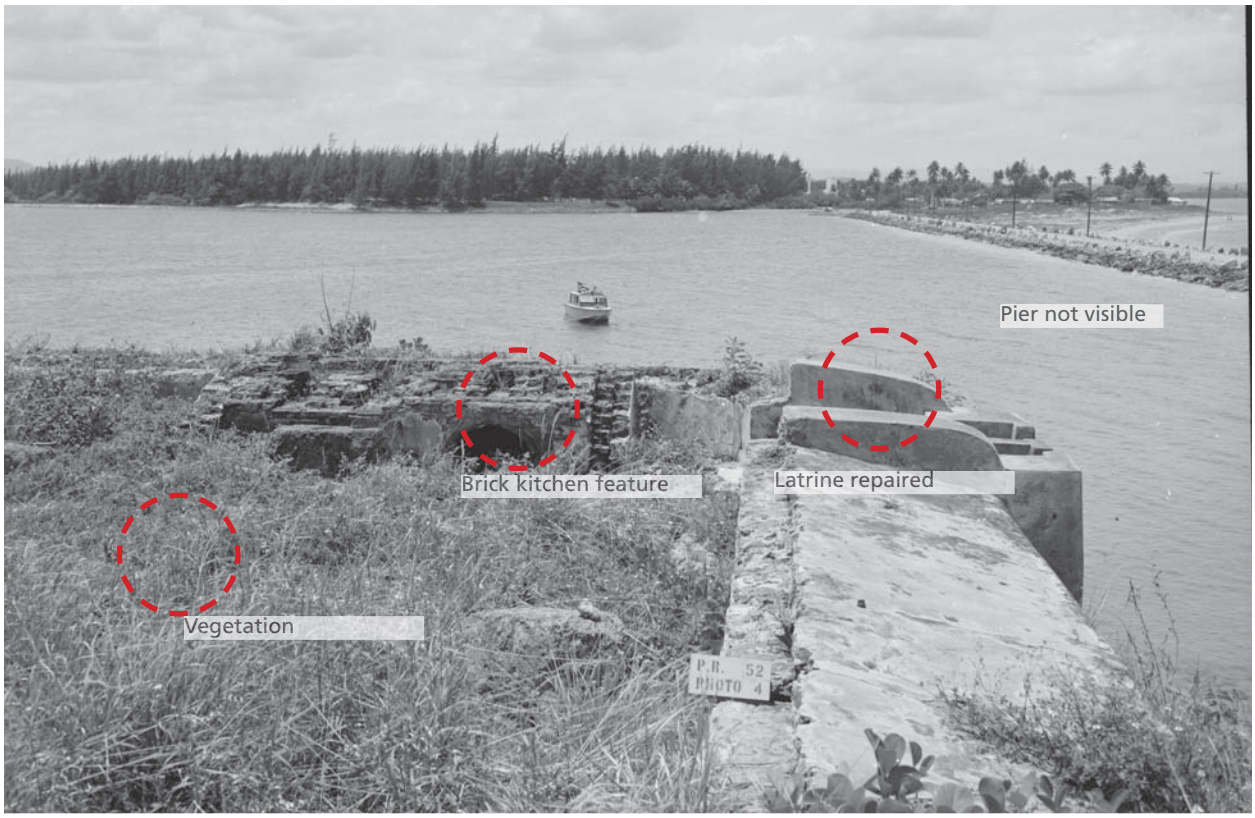


Figure 63: HABS, (Library of Congress, Annotated WLA Studio, 2017)



Figure 64: Circa 1954-1962, (Archivo General de Puerto Rico, Annotated WLA Studio, 2017)

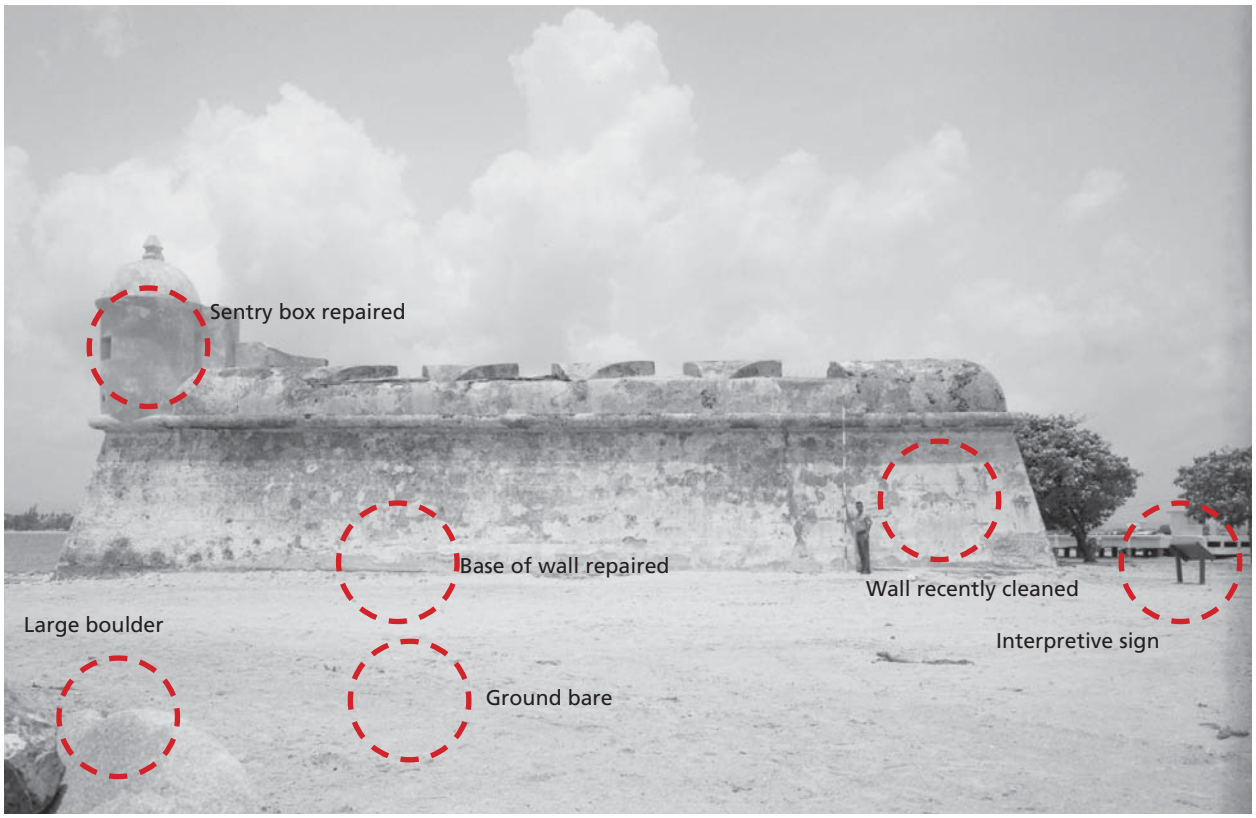


Figure 65: HABS 1998, (Library of Congress, Annotated WLA Studio, 2017)

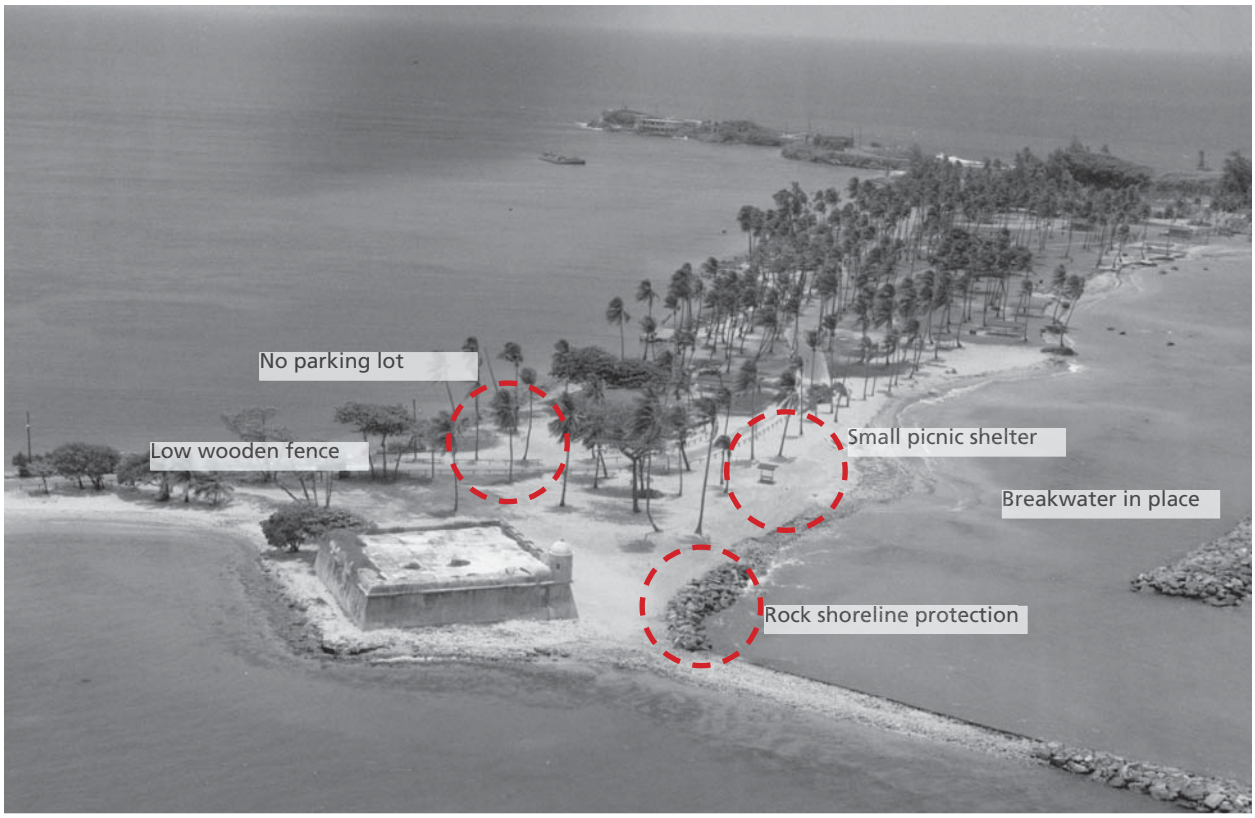


Figure 66: HABS 1998, (Annotated WLA Studio, 2017)



Figure 67: Google Map 2017, (Annotated WLA Studio, 2017)

Timeline

1493: Christopher Columbus encounters island he names San Juan Bautista, now known as Puerto Rico.

1508: Ponce de Leon arrives with soldiers to establish permanent settlement on Puerto Rico Island.

1521: Spanish establish settlement on San Juan Islet.

1579: Ponce de Leon II recommends the construction of a fortification on El Cañuelo

1595: During Francis Drake's raid on San Juan, Tello de Guzmán builds a stockade on El Cañuelo Island and positions men to protect entrance into San Juan Bay.

1598: Lord George Clifford invades Puerto Rico.

1604-1606: Ochoa de Castro constructs a wharf and stone foundations for a fortification at El Cañuelo.

1608-1610: De Roxas y Páramo continues work on El Cañuelo, adding a round wooden tower on a rubble and mortar foundation.

1625: Spanish forces burn tower during effort to recapture fort from Dutch invaders.

1626: Hurricane strikes Puerto Rico damaging buildings and inflicting casualties in San Juan.

1647: de Torres Vargas describes El Cañuelo as a ruin.

1661: Spanish military plans for San Juan include fortifications on El Cañuelo.

1663: Pérez y Guzman reports of plans to construct redoubt at El Cañuelo with six canon.

1664: Pérez y Guzmán reports El Cañuelo Fort completed. Spanish call it Fortín San Juan de la Cruz.

1683: Spanish inventory of artillery records 7 pieces of artillery, including, 1 bronze and 6 iron, at El Cañuelo.

1690: Alonso Pedraza describes El Cañuelo needs repair.

1692: Spanish records of maintenance of fortifications include work at El Cañuelo.

1695 and 1698: Spanish records describe El Cañuelo in state of ruin.

1702: Gabriel Gutiérrez de la Riva records work performed on El Cañuelo.

1702: Spanish add light or navigation system to El Cañuelo and construct stockade on side facing San Juan Bay.

1822: Pedro Tomás de Córdoba describes El Cañuelo as in state of abandonment.

1841: Spanish modify structure to serve as lazaretto.

1864-1865: Spanish records indicate repairs made to lazaretto.

1787: Major earthquake strikes Puerto Rico in May.

1898: Spanish draw chain up across San Juan Bay between El Morro and El Cañuelo during Spanish American War naval bombardment.

1900: United Secretary of War includes El Cañuelo is list of property of to be retained for military use.

1918: Major earthquake strikes Puerto Rico in October.

1928 and 1932: Hurricanes San Felipe (1928) and San Ciprián (1932) strike Puerto Rico.

1943: United States Army enlarge La Cabras Island to include El Cañuelo.

1949: El Cañuelo becomes part of the San Juan National Historic Site, under the administration of the National Park Service.

1949-1954: NPS install site features as part of effort to interpret El Cañuelo.

1954: NPS sends staff to prepare HABS documentation of El Cañuelo.

1955-1960: NPS repairs broken south corner and resurface east elevation.

1960-1961: NPS repairs concrete apron around south foundation of fort.

1962: NPS constructs stairs to entrance on fort.

1983: El Cañuelo, along with other structures within San Juan National Historic Site, designated a UNESCO World Heritage Site.

1986: NPS sends HABS staff to resurvey fort.

1991: NPS proposes Rehabilitation Project, that includes capping with sand and concrete. Closing entrance.

1991: NPS proposes rehabilitation of sentry box. (Possibly not finished until 1997).

1991-1992: NPS closes entrance into fort and seals upper platform with concrete cap.

1992: NPS installs rock breakwater and riprap filled revetment around fort.

1994: NPS applies new render to northwest and southwest elevations.

1998: HABS photographs the building, concluding the 1986 resurvey project.

2003-2004: Walls cleaned with D2.

2008: NPS proposes stabilization work, including cleaning walls, patching cracks, cleaning vegetation, replacing bricks, and improvements to the site's landscape.

2012: NPS reopens entrance into fort. They construct new staircase, railings around upper platform, and cut door into concrete cap.

I.C Physical Description

El Cañuelo: The Site

Las Cabras Island

Las Cabras Island landform constructed in 1943 and containing El Cañuelo is on the west side of San Juan Harbor. The United States Army transitioned 3.4 acres on the southern end of Las Cabras Island that included El Cañuelo to the National Park Service in 1949. North of El Cañuelo, the Puerto Rico National Park Company operates the Isla de Cabras Recreational Park facility with a public beach, bathroom facilities, and picnic facilities. The park is open during the day from Wednesday to Sunday. A gate exists on the southern edge of the island that prevents vehicular access when the recreational facility is closed. There is a short pier extending from the causeway into the bay, just south of El Cañuelo. North of the park, the Police Department of Puerto Rico maintains a firing range and training facility. There are remains of the 1870s Las Cabras lazaretto and remains of the 1940s Battery Reed on the north end of the island.

The contours of the landmass have changed dramatically from its initial construction in 1943. Erosion of the shoreline, caused by wave action and storms, is most extreme on the eastern coast of the island, in the vicinity of El Cañuelo. (Figure 68). Beginning in the 1960s, the United States Corps of Engineers, in conjunction with the National Park Service, constructed a stone revetment extending perpendicular from the shoreline. This features riprap, sheet pile, and stone and mortar revetment. It aligns with the east corner of the El Cañuelo fort to form a jetty, from which people fish today. Around 1990, NPS added a separated breakwater parallel to the eroding coast. This rock feature was intended to absorb the energy from waves, including both naturally occurring and those generated by ships entering the harbor. The lee side of the breakwater contains slow moving water, creating a lagoon-like feature filled with floating debris. (Figure 69).

The lines of these two breakwaters approximately outline the extents of the landmass as constructed in 1943. Erosion has reduced the size of the landmass, as the shoreline retreats inward. Erosion continues to be a serious threat to the landmass, in particular along the east shoreline extending north from El Cañuelo. Because of erosion, the shoreline has developed a steep cut bank. Large sections have collapsed and the bank appears unstable. (Figure 70).



Figure 68: El Cañuelo Breakwaters, November 2016 (WLA Studio)



Figure 69: El Cañuelo Floating Debris in Lagoon, November 2016 (WLA Studio)



Figure 70: El Cañuelo Shoreline Erosion, November 2016 (WLA Studio)



Figure 71: El Cañuelo Access Road, November 2016 (WLA Studio)



Figure 72: El Cañuelo South Elevation, November 2016 (WLA Studio)

A road traverses the NPS parcel, connecting the entrance onto the island from the causeway to the park and firing range beyond El Cañuelo. NPS and the park share a parking lot that is west of the road near where it passes the fort. Large boulders line the road, preventing vehicular access onto the grounds around the fort. NPS installed these boulders in 2012, as part of a site-wide project to open El Cañuelo to visitation. (Figure 71).

In general, the infrastructure installed to facilitate park visitation, including the road and parking lot are in good condition. The overall condition of the landmass is poor, due to the effects of erosion. Despite the breakwaters and revetments, erosion is occurring along the shoreline and along the south and east sides of El Cañuelo.

El Cañuelo Landscape

Water surrounds the south and east sides of the masonry fort. (Figure 72). A stone and concrete apron surround the base of El Cañuelo on the south and east sides. This apron presumably surrounds the other sides, but soil currently covers this feature. The apron is approximately three feet wide with the stones randomly set into mortar. (Figure 73). On the south corner of the building, NPS constructed a steel sheet pile revetment, back-filled with rock, in 1960-1961. (Figure 74).

The site does not have formalized pedestrian circulation. Visitors park in the paved lot and wander around the open space around the fort. A wood staircase, constructed in 2012, provides access into the fort itself. There is no formal vehicular infrastructure apart from the access road passing through the parcel and the parking lot occupying the western edge of the parcel. The road and parking lot, while partially on NPS property are not identifiable as NPS resources, but they appear to be components of the recreational facility adjacent of El Cañuelo.



Figure 73: El Cañuelo Stone and Concrete Apron along South Elevation, November 2016 (WLA Studio)



Figure 74: El Cañuelo Sheet Pile Revetment at South Corner, November 2016 (WLA Studio)



Figure 75: El Cañuelo Picnic Shelters north of Fort, November 2016 (WLA Studio)



Figure 77: El Cañuelo Debris Deposited on Shore, November 2016 (WLA Studio)



Figure 76: El Cañuelo Open Space with Lawn and Trees, November 2016 (WLA Studio)



Figure 78: El Cañuelo Park Sign, November 2016 (WLA Studio)

This is also the case for two picnic shelters north of El Cañuelo. These are not on NPS property, but they function as a shared amenity between El Cañuelo and the recreational facility. (Figure 75).

While water surrounds the south and east elevations beyond the rock revetments and rip rap, open lawn surrounds the north and west sides of El Cañuelo. The grass is in generally good condition, with some invasive species intermixed with the predominate Bermuda grass. Trees grow scattered across the lawn. Coconut palms are the predominate species; some of the palms are large and possible date to the 1950s. NPS has planted several young palm trees, mostly along the edge of the shoreline in the open space north of the fort. There are also several large coccoloba trees growing on the west edge of the lawn area along the edge of the access road. The trees are in good condition. (Figure 76). One palm growing on the edge of the shore is threatened by being undercut by erosion. Waves and high tides deposit debris



Figure 79: El Cañuelo Interpretive Sign, November 2016 (WLA Studio)

along the beach and on land around the fort. (Figure 77).

Other small-scale features on site include four trashcans, four interpretive signs, and one park sign. Two of the trash cans are open plastic barrels. These do not appear to be NPS regulation

features. The remaining two trashcans are more typical of NPS sites, with concrete bases and plastic lids. The park sign is relatively new, likely installed as part of the 2012 upgrades to the site. It features a metal sign mounted on a concrete base. It identifies the site as "San Juan National Historic Site Fort San Juan de la Cruz." (Figure 78). They provide interpretation in both Spanish and English. Themes include "Defending San Juan," "Crossfire," "Imagine Life Here," and "A Never-Ending Challenge," which discusses NPS preservation and maintenance of the fort. (Figure 79). The interpretive signs are fading under the harsh conditions of the climate, but otherwise, the small-scale features are in good condition.



Figure 80: View of El Cañuelo from El Morro (RATIO Architects)



Figure 83: Detail of north elevation showing stucco loss (RATIO Architects)



Figure 81: East and north elevations of El Cañuelo from jetty (RATIO Architects)



Figure 84: Detail of north elevation showing stucco loss and sentry box (RATIO Architects)



Figure 82: North elevation (RATIO Architects)



Figure 85: East and north elevations (RATIO Architects)

El Cañuelo: Building

See Appendix A for drawings of existing and historic condition. See Appendix B for HABS drawings.

Exterior

El Cañuelo is a rectilinear structure approximately 81 feet square at grade level. The building's corners are oriented close to the cardinal directions. The names of the elevations used in this description follow the naming conventions established by the 1954 HABS documentation and used in most subsequent documents. As noted in other sections, the present fort was built on El Cañuelo Island and was surrounding by water on all sides from the 1660s until 1943, when a landfill project connected the building with Cabras Island and a new causeway to Punta Palo Seco. A concrete and stone apron was built along the south and east elevations while earthen fill extends up to the north and west elevations. The present grade is approximately three feet above mean low water. The difference between high and low tides at San Juan is approximately 18 inches.

The building features battered walls rising to a height of approximately 17 feet above present grade. A *cordón* ("stringcourse," here presented as a bullnose cornice) extends around the perimeter of the building approximately 13 feet above present grade. The walls measure approximately 75 feet long at each side at the top of the *cordón* and feature a radiused upper profile forming a parapet enclosure for a space approximately 62 feet square at the terreplein (upper deck). The parapet along the north wall and portions of the returns along the east and west forms a battlement with embrasures. The remainder of the parapet extends only to the height of the sill of the embrasures.

The exterior walls are faced with ashlar stone masonry coated in stucco. The stucco of the lower section of the walls features false mortar joints giving the effect of large, evenly-sized rectangular stones. The stucco of the walls is of a light ochre color, while that of the *cordón* is pink. The parapets above the *cordón* are coated in smooth stucco without false joints. The stucco varies widely in condition, from good to poor to entirely missing. Areas of stucco loss, biological growth, and exposed stone substrates are apparent at all elevations. Stucco patching is more apparent at some elevations than others. The *cordón* shows limited spalling and areas of patching. Areas of stucco loss reveal a grid of holes approximately nine inches in diameter along the outer walls. These holes are filled with mortared brick fragments and concealed by stucco. It is believed that these holes were the result of scaffolding during the fort's original construction. Large structural cracks visible in the exterior walls are treated in more detail in the Structural Analysis section.

The exterior is in fair to poor condition overall. Plants are growing in almost all cracks and pits along the walls, atop the *cordón*, and on the surface of the terreplein. The building's exposed location and infrequent maintenance have contributed to greater deterioration of the exterior than that seen at El Morro and Castillo San Cristóbal, which serve as prime tourist sites in the heart of Old San Juan.

North Elevation (Figures 80-85)

The north elevation presented the fort's primary defensive front, facing El Morro across the entrance to San Juan Bay from the Atlantic Ocean. This elevation is most visible from El Morro and sections of the City Wall north of the San Agustín Bastion. (Figure 80). The sentry box rises from its east corner and the battlement rises approximately five feet above the *cordón* and contains four embrasures. The sentry box is a cylindrical structure approximately 8'-3" in outside diameter. Its walls rise approximately 9'-6" above the *cordón* and are capped by a quarter-round cornice. A window opening with splayed jambs is roughly aligned with the northeast corner of the building. The domed roof of the sentry box is crowned by a four-sided masonry finial. Remnants of a wall on top of the battlement extend from the west side of the sentry box toward the first embrasure. The stucco of the north elevation is in poor condition overall, with extensive loss and damage. Biological growth and staining are more extensive on the north elevation than on other faces of the building, particularly on the exposed stone substrate. A large crack runs the full height of the wall approximately 19 feet from the north corner. This crack shows evidence of prior patching.

East Elevation (Figures 80-81, 85-90)

The east elevation presented a secondary defensive front, facing the interior of San Juan

Bay, and is the elevation most visible from the City Wall between the San Agustín Bastion and La Fortaleza. The sentry box rises from its north corner and its eastern face contains a window opening with splayed jambs facing roughly south. A battlement like that of the north elevation extends approximately 25 feet south from the north corner



Figure 86: Detail of sentry box and northeast corner (RATIO Architects)



Figure 87: Detail of sentry box from southeast (RATIO Architects)



Figure 88: Detail of entry door (RATIO Architects)



Figure 89: Detail of cordón at east elevation (RATIO Architects)



Figure 90: View of grade conditions at east elevation (RATIO Architects)



Figure 91: West and south elevations from dock at Cabras Island gatehouse (RATIO Architects)



Figure 92: View of grade conditions at south elevation (RATIO Architects)



Figure 93: Gap in cordón at south elevation (RATIO Architects)



Figure 94: Detail of stucco loss at south elevation; typical brick infill patch (retaining stucco) to right of center (RATIO Architects)

and contains a single embrasure. The remainder of the parapet is roughly level with the sill of the embrasure.

The fort's entry door is located below the *cordón*, between the embrasure and sentry box. The door opening is roughly 4'-6" above present grade and measures approximately 3'-0" wide by 5'-7" high. No door was present as of 1954. NPS installed a metal gate at the opening in 1962. Sometime before 1986, the gate was removed and the opening was infilled with concrete masonry units. In 2012, the opening was uncovered and a pair of new wood entry doors was fabricated following the design of doors at other forts within the SAJU.

This elevation saw extensive stucco repair and replacement during the 1950s and subsequent repairs after 1998. The east face of the sentry box has seen significant erosion of stucco compared with the north face. The stucco is in fair to poor condition overall, with areas of erosion, cracking, crazing, and mismatched patches. Two large cracks in the east elevation extend the full height and show signs of prior patching.

South Elevation (Figures 91-94)

The south elevation presented a secondary defensive front, facing Punta Palo Seco and the mouth of the Bayamón River. The lower wall contains no openings and the parapet is roughly level with the sill of the embrasures of the other elevations. A 7'-7" wide gap in the *cordón* is roughly centered on this elevation and is believed to have been intended as a point for ladder access and hauling up cargo from boats below to the terreplein. The southeast corner is the fort's most exposed point and has been rebuilt at least twice since the 1930s. The stucco is in fair to poor condition overall, with areas of erosion and stucco loss. Two large cracks extend the full height of the wall and show signs of previous patching.

West Elevation (Figures 95-98)

The west elevation presented a secondary defensive front, guarding the approach to the Bayamón River from the Atlantic Ocean and the Boca Vieja Inlet. A battlement like that of the north elevation extends approximately 21 feet south from the north corner and contains a single embrasure. The remainder of the parapet is roughly level with the sill of the embrasure. Remnants of a latrine extend out over the wall approximately 10 feet north of the south



Figure 95: West elevation (RATIO Architects)

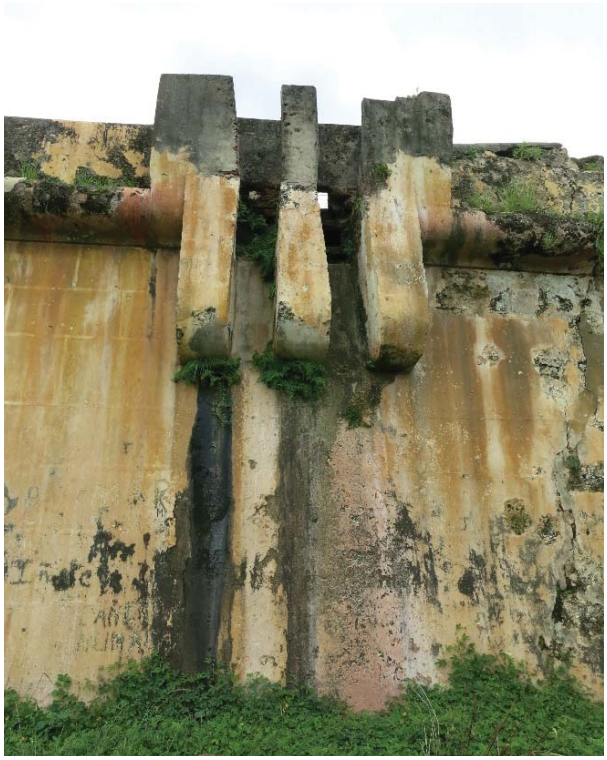


Figure 96: Detail of latrine at west elevation (RATIO Architects)



Figure 97: Typical range of stucco conditions at west elevation (RATIO Architects)



Figure 98: Detail of cracks at west elevation (RATIO Architects)

corner. The parapet is rounded in a series of two layers at the south corner. This feature is reported to have been designed to allow the drawing of sea water, although the presence of the *cordón* and proximity to the latrine would appear to present challenges to this use. The stucco is in fair to poor condition overall, with areas of erosion and stucco loss, although the wall surface appears to be more intact than that of the other elevations. The wall contains three large cracks that extend its full height and show signs of prior patching.

200 Terreplein (Figures 99-101)

The terreplein (also known as the upper deck, gun deck, upper level) is presently an uncovered roof terrace roughly 62 feet square and enclosed by low parapets on four sides. The sentry box rises from the northeast corner and battlements extend along the north elevation and the north ends of the east and west elevations. A low parapet extends around the remainder of the terreplein, with remnants of a kitchen in the west part of the south elevation and a latrine in the south part of the west elevation.

Documentation indicates that parts of the terreplein contained a superstructure of one-



Figure 99: View of terreplein looking northeast (RATIO Architects)



Figure 100: View of terreplein looking southwest (RATIO Architects)



Figure 101: Battlements of west and north walls (RATIO Architects)

story rooms. The configuration of the early superstructure is currently unclear. An 1841 remodeling project appears to have reused some existing masonry columns defining the south side of rooms along the north wall while adding additional columns and rooms along the east and south walls, leaving an open courtyard in the center. This superstructure fell into ruins by the early twentieth century and had mostly collapsed by September 1940. Surviving remnants of the superstructure were removed before 1954. These ruins are partially documented in two early photographs, by drawings from 1938, and by HABS documentation in 1954 and 1986.

HABS documentation from 1954 and 1986 indicates that the terreplein retained a variety of paving treatments. Some areas were paved with lime concrete with crushed brick aggregate. Former rooms along the north and east sides of the terreplein were paved with brick pavers laid in running bond and herringbone patterns. Bands of brick laid in a roller course trimmed areas with lime concrete pavement. These appear to have accentuated the east and south sides of a central courtyard, possibly defining a drainage channel (*drenaje*) between the brick course and the adjacent walls. A matching band along part of the west wall near the latrine defined an open gutter along the west wall. A band of brick laid in a sailor course along the south wall appears to have served as a covering for a subsurface drainage line. A circular opening (3'-0" in diameter) into the cistern was roughly centered on the terreplein. HABS documentation from 1954 indicates a rectilinear area of sunken pavement 2'-3" deep near the center of the west side of the terreplein. This area may reflect the location of a subsurface feature.

A concrete slab or concrete cap, designed in 1991 and installed in 1992, currently covers most of the surface of the terreplein. Several inches of sand were added to separate the slab from the underlying historic pavement and covers were presumably provided at holes including the cistern opening and drain line cleanouts. This slab appears to have been sloped to encourage drainage through outlets in the latrine. Portions of two brick columns extend up through the slab approximately 14 feet west of the east parapet. Gaps between the slab and the parapets, columns, and kitchen ruins are allowing water to run down into the interior of the walls and fill. These gaps are filled with plant material, the roots of which may be contributing to further deterioration and destabilization of the historic masonry. Two one-inch-square holes in the slab are located approximately 11'-6" south of the north parapet. The concrete is in fair to



Figure 102: Detail of stair scuttle door and sentry box (RATIO Architects)



Figure 103: Detail of sentry box (RATIO Architects)



Figure 104: Floor of sentry box (RATIO Architects)



Figure 105: View of El Morro and entry to San Juan Bay from sentry box corner window (RATIO Architects)

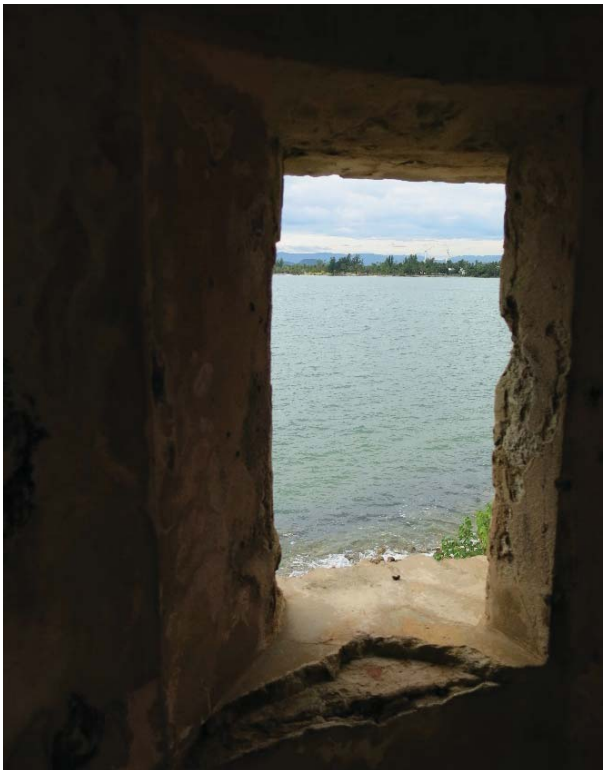


Figure 106: Detail of sentry box south window (RATIO Architects)

good condition overall, appearing to be in stable condition with discoloration from biological growth, but it does not appear to be fulfilling its intended purpose of keeping water out of the building's interior.

Stainless steel cable railings with simple upright posts were installed at the perimeter of the terreplein and around the columns in 2012. The posts are mounted into the concrete slab. The 2012 project also involved the creation of a new hole in the slab over the historic stair and the installation of a two-section steel scuttle door to cover the opening and secure the interior when the building

is not open to the public. Photovoltaic panels are mounted to the interior of the east section of the door and were intended to power interior electric lighting when the scuttle door is open. The scuttle door is in fair to good condition, with some signs of wear to the paint and limited traces of rust.

201 Sentry Box (Garita) (Figures 86-87, 102-106)
The cylindrical sentry box (also known as a garita, sentinel, or bartizan) projects from the northeast corner of the parapet, with its outer walls extending to the edge of the *cordón*. The interior of the sentry box is approximately 5'-8" in diameter and the inner face of the domed roof forms a ceiling with a maximum height of approximately 11'-7". Window openings with splayed jambs are present at the northeast corner (facing east) and along the east side (facing south). A square drain channel is located on the northeast corner. The interior walls and ceiling are coated in stucco like that of the exterior, much of which was installed during a 1998 restoration project. The floor is of lime concrete with areas of wear exposing crushed brick aggregate.

202 Kitchen (Figures 107-109)
The kitchen (*cocina*) was formerly an enclosed room running along roughly 10'-3" of the west part of the south wall. This space is now part of the open terreplein but ruins of the *fogón* or cooking stove/hearth survive along the south wall. The 1841 plan for conversion of the fort into a lazaretto indicated that this feature was to be built along the east wall rather than the south wall of the space. The *fogón* is of brick masonry and is framed by remnants of 12-inch-thick brick walls at the east and west and traces of a six-inch-thick brick wall atop the south parapet. Remnants of the east and west walls survived into the twentieth century but appear to have been lost by 1935. The north wall appears to have been in place in a January 1935 photograph but was gone by 1938.

The *fogón* contains an arched firebox or oven in the western section. This opening was infilled with a concrete patch, presumably at the time of the 1992 concrete slab project. This patch has separated from the adjacent masonry, leaving a wide gap allowing rainwater to pass into the interior. During the team's site visit, a large iguana was observed entering and exiting this gap. The ruins appear to be in largely the same condition documented in a 1954 HABS photograph. Major differences include



Figure 107: Overview of kitchen (202) and latrine (203) (RATIO Architects)



Figure 108: Detail of *fogón* at kitchen (RATIO Architects)



Figure 109: Detail of *fogón* at kitchen (RATIO Architects)

further loss of the east and west wall ruins and erosion of stucco on the face of the *fogón* to either side of the arched opening. The kitchen ruins are in poor condition overall.

HABS documentation from 1954 and 1986 indicates that the floor level of the kitchen was four inches lower than the remainder of the



Figure 110: Latrine (203) (RATIO Architects)



Figure 111: Detail of latrine bench (RATIO Architects)



Figure 112: Detail of south chute of latrine with deck drains below (RATIO Architects)



Figure 113: Detail of east wall showing gap between 1992 concrete slab and walls (RATIO Architects)



Figure 114: Detail of rounded southwest corner between kitchen and latrine (RATIO Architects)



Figure 115: Detail rounded southwest corner from top of parapet (RATIO Architects)

terreplein. Comparison of that photograph with present conditions suggests that the 1992 concrete slab surface is at least 12 inches higher than the historic pavement at the face of the *fogón*. HABS documentation from 1954 indicates that the pavement of the kitchen area was of lime concrete with crushed brick aggregate and that all brick masonry surfaces retained traces of stucco. Extensive plant growth was observed at this area, the brick masonry offering numerous cracks and crevices in which plants can root.

203 Latrine (Figures 107, 110-115)

The latrine (also known as a *letrina*, privy, or garderobe) is located in the south part of the west elevation. The room was built within the depth of the thick parapet wall, with the bench positioned at the west side to allow waste to flow down the battered wall and into the sea below. The floor space of the latrine measures roughly 6'-0" wide north-south and 2'-7" east-west.

The walls are of brick masonry construction and were covered with stucco. A shed roof sloped down to the west. The walls remained in ruins as of 1935 but had collapsed down to their present level by 1938. Two early photographs document the outline of the walls. Drawings from 1938 suggest that a narrow window with splayed sides was present on the north wall of the latrine before its collapse.[98] The remnants of the north, west, and south walls are covered with stucco. The east wall, contiguous with the interior face of the west parapet, is of unprotected brick masonry and is badly deteriorated. Conditions at the upper part of the remaining walls are similar to those documented in a 1954 HABS photo of the area.

The bench was approximately 25" deep and sits over two open chutes. The 1841 plan for converting the building into a lazaretto indicates three circular openings in the bench. A drain along the west side of the terreplein terminated in an outlet in the south chute of the latrine. The present east wall of the bench was rebuilt in the twentieth century with concrete masonry units.

98. A similar opening was documented at House No. 2, the former latrine of Fortín de San Gerónimo, as documented by HABS: Fortifications of San Juan, San Geronimo, Puerta de Tierra, San Juan, Puerto Rico, Survey P.R.49, Sheet 8, 1953.

HABS documentation from 1954 indicates that the latrine's floor level was four inches below that of the terreplein at the door, sloping down to the west. This documentation suggests that the pavement of the latrine was of lime concrete with crushed brick aggregate. The floor is presently covered with concrete installed in 1992. This concrete creates a more pronounced slope, directing water from the terreplein into two square drain openings into the two latrine chutes. Rainwater runoff through these chutes has exacerbated deterioration of the surrounding brick masonry, allowing water to run back into the interior of the building.

Interior

The interior of El Cañuelo contains six known spaces at the lower level. The accessible spaces vary in floor level by approximately three feet. A 1664 description of the fort as originally built indicates that it contained two interior "magazines", one for the storage of gunpowder and one for supplies.[99]

100 Vestibule (Figures 116-118)

The vestibule is located immediately inside the entrance to the fort. HABS documentation lists this space as "entryway" and the 1841 plan for converting the building into a lazaretto labels it *"Entrada al Fuerte"* ("entrance [to] the fort"). The east wall contains a door opening, now fitted with a pair of wood doors installed in 2012. The door opening contains an exterior threshold paved with bricks laid in a herringbone pattern, apparently dating from repair work between 1954 and 1962. The vestibule is a roughly rectilinear space measuring approximately 4'-2" by 8'-4". An asymmetrical brick barrel vault is oriented east-west with a maximum height of approximately 6'-4". The floor and vault slope up to the west. A low opening in the south wall connects to Room 103. The vestibule opens into Room 101 at the west. The wooden stair constructed in 2012 projects from Room 101 into the vestibule. Available documentation indicates that the vault and parts of the walls have seen plaster patching since 1954. The plaster is in fair to poor condition overall, with areas of deterioration and wear apparent.

101 Stair Hall (Figures 116-123)

The stair hall opens from the west side of Room 100 and contains a stair connecting the lower level to the terreplein. The space is roughly 9'-4" wide

99. Blanco, Fortifications, 244-245.



Figure 116: View of Rooms 100 and 101, facing west (RATIO Architects)

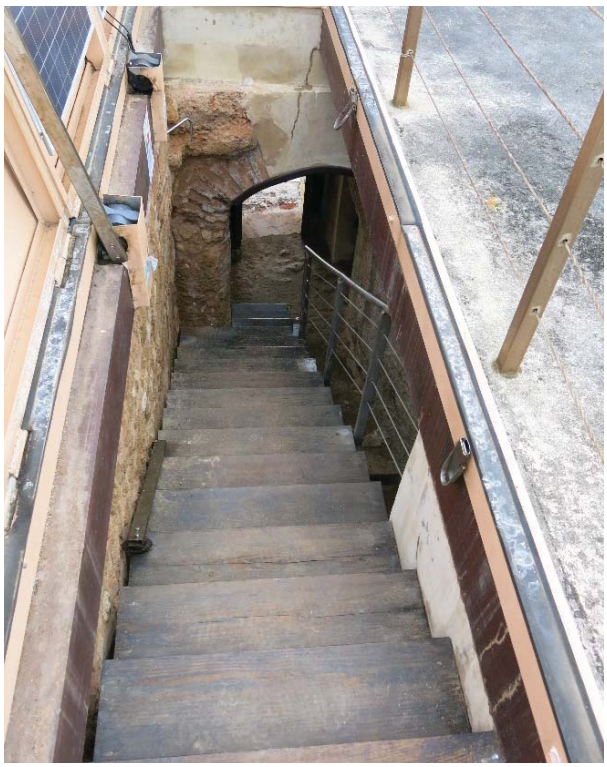


Figure 117: View of Rooms 101 and 100 from terreplein, facing east (RATIO Architects)



Figure 118: Exterior brick threshold at Room 100 (RATIO Architects)



Figure 119: Detail of ruined brick masonry staircase at Room 101, facing northwest (RATIO Architects)



Figure 120: Door to Room 102 at west wall of Room 101 (RATIO Architects)



Figure 121: Ceiling at southwest corner of Room 101 showing 1992 concrete slab and 2012 wood beam (RATIO Architects)



Figure 122: Detail of former beam location at southwest corner of Room 101 (RATIO Architects)



Figure 124: View of Room 102, facing east (RATIO Architects)

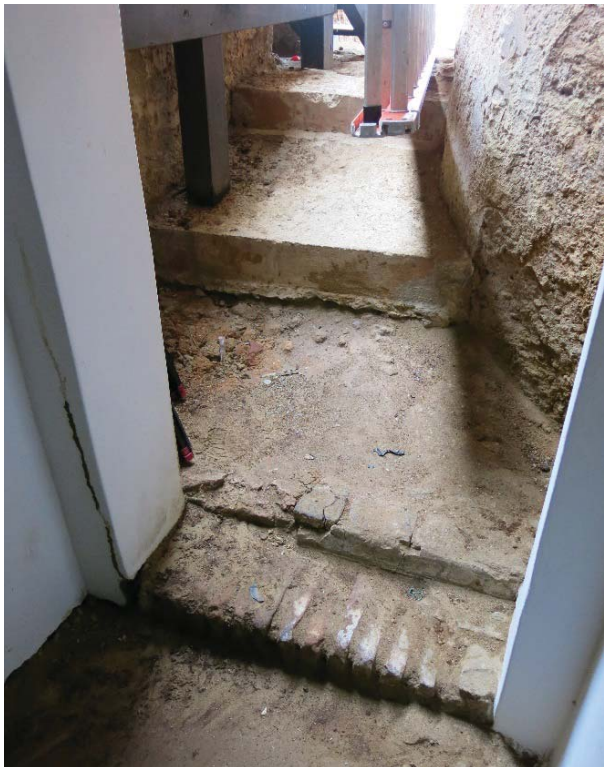


Figure 123: Detail flooring of Rooms 102 (foreground) and 101 (RATIO Architects)

east-west. The south wall curves, splaying out from a width of approximately 5'-3" at the east wall to 8'-0" at the west. The ruins of a brick masonry stair with 11 treads rise along the north wall, including winder steps at the northeast corner. The floor descends in a series of uneven steps from its high point at the base of the stair to the door to Room 102, a depth of approximately 3'-10". Traces of brick pavement are visible along the west wall. The intermediate steps appear to be a mix of stone rubble and lime concrete, the latter appearing to be of comparatively recent date. The lowest steps at the west part of the room shows signs of significant erosion.

The walls are of rubble stone covered with plaster. HABS documentation indicates that the west wall was largely bare masonry as of 1954 while the south wall retained much of its plaster. Stucco repairs to the upper parts of the east and south walls, visible in a 1954 photo, remain in good condition. The west wall clearly exhibits a mix of cut stone, rubble stone, and brick masonry construction. Cut stone voussoirs form a flat arch over the door to

Room 102. The north side of this opening has seen patching since 1954.

The room retains traces of a flat vaulted ceiling at the northeast and southwest corners. The recess at the southwest corner contains voids that appear to have once held wood beams. The remainder of the ceiling is formed by the 1992 concrete slab on the terreplein. When the slab was originally installed, the stair hall was filled with wooden cribbing to support a deck with sand and the concrete slab. In 2012, a wooden beam was installed under part of the slab and the remainder was cut away to accommodate a new wooden stair on top of the ruins of the masonry stair.



Figure 125: View of Room 102 facing west (RATIO Architects)



Figure 126: Detail of termite tube at north wall of Room 102 (RATIO Architects)

102 Vault No. 1 (Figures 123-126)

Located immediately west of Room 101, Vault No. 1 is a rectilinear space measuring roughly 7'-6" by 14'-10". This room is believed to have originally served as a storage vault or magazine. The 1841 plan for converting the building into a lazaretto labels this room *"Repuesto de pólvora subterráneo"* ("subsoil powder repository"). The ceiling is a barrel vault running east-west with a maximum height of approximately 8'-10". The walls and ceiling are covered in plaster that is cleaner and lighter in color than that of other spaces, indicating comparatively recent replastering. The plaster is in fair to good condition overall. Termite tubes were evident along the north and west walls. A cylindrical metal box set into the northeast corner of the ceiling at the entry door appears to have been the junction box for a light fixture, likely added in 1962. The floor is of lime concrete with a brick threshold with traces of lime concrete at the door to Room 101.

103 Passage (Figures 127-132)

Located south of Room 100, this space serves as a passage to Room 104. It is accessed by a low door,



Figure 127: Room 103 looking into Room 100, facing north (RATIO Architects)



Figure 128: Room 103, facing south (RATIO Architects)



Figure 129: Floor of Room 103, facing south (RATIO Architects)



Figure 130: Upper north wall of Room 103 showing recess and pocket at left and graffiti above door (RATIO Architects)



Figure 131: View into pocket in northwest corner of Room 103, facing west (RATIO Architects)



Figure 132: Detail of pocket in east wall of Room 103, facing east (RATIO Architects)

3'-6" high, in the south wall of Room 100. The space does not appear on the 1841 plan for the remodeling of the fort as a lazaretto, suggesting that the opening may have been closed prior to that time or that the space was consider unusable due to the difficulty of access. A low arched opening at the south end of the west wall leads into Room 104. The floor descends roughly 3'-8" in a series of sloped steps from the threshold of the north



Figure 133: Design team and NPS staff in Room 104, facing west (RATIO Architects)



Figure 134: Door from Room 104 to Room 103, facing east (RATIO Architects)

door to the south end. The ceiling is a barrel vault running north-south. The sloped floor increases the maximum height of the vault from roughly 6'-0" at the north to 9'-0" at the south.

A recess approximately six inches deep extends around the north door opening, with a corresponding recess in the west wall. This appears to have once held a substantial wood door, presumably to provide protection from a potential explosion of gunpowder in Room 104. A pocket at the north end of the west wall at the

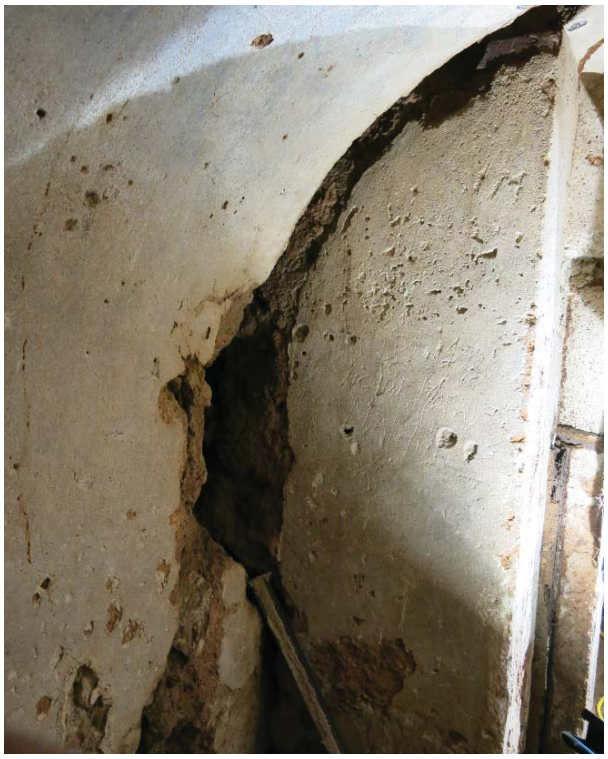


Figure 135: Northeast corner of Room 104 showing large crack (RATIO Architects)



Figure 136: Debris at floor of Room 104, facing northwest (RATIO Architects)



Figure 137: Large crack at south wall of Room 104, facing southwest (RATIO Architects)



Figure 138: View up into crack in ceiling of Room 104 showing debris in crack (RATIO Architects)

head of the recess appears to have held a wooden block that would have supported hinges for the door. A similar pocket at the center of the opening on the east wall appears to have accommodated a bolt to secure the door in place. Two small metal embedments are in place in the north wall above the door.

The walls and ceiling are covered in plaster that remains in fair to poor condition. This plaster does not appear to have been patched during mid-twentieth century repairs, bearing a range of graffiti including the date "1929" and the initials "RBB." The floor appears to be of lime concrete.

104 Vault No. 2 (Figures 133-138)

Located west of Room 103, Vault No. 2 is a rectilinear space measuring approximately 5'-8" by 7'-2". The space is believed to have originally served as a gunpowder magazine. The ceiling is a brick barrel vault running east-west with a maximum height of roughly 7'-0". An arched alcove in the east wall measures roughly 3'-6" wide by 1'-4" deep and contains an arched door opening to Room 103. A wooden guardrail was built in front of the door c. 2012 to prevent visitors from entering Room 104. This guardrail suffered extensive termite damage and its remnants were removed to allow access for the design team in November 2016.

A very large crack extends along the east side of the room and measures approximately 5-1/2" wide. Crack monitors were installed in 2012 and NPS staff report that these have not been monitored. The crack reveals the brick barrel vault structure, rubble fill above the vault, and some fragments of mortared brick masonry that may have fallen into the crack from the terreplein. A pile of masonry debris and droppings below the crack indicates that iguanas and other animals may be accessing the interior by burrowing through the crack. NPS staff report that the room was cleared of debris in 2012.

The walls and ceiling are covered in plaster that ranges from good to poor condition. Many intact areas appear to be in good conditions while others have seen significant plaster damage and loss. This plaster does not appear to have been patched during mid-twentieth century repairs, bearing a range of graffiti including the name "Victor Morales Martinez" The floor appears to be of lime concrete.

105 Cistern

The cistern (*aljibe*) is located at the center of the fort and has been inaccessible since the construction of the concrete slab on the terreplein in 1992. This description is based on prior documentation. The cistern measures roughly 12 feet square and is topped by a barrel vault running north-south. The maximum height of the vault is approximately 11'-0" and lies roughly 3'-0" below the surface of the terreplein. A brick-lined opening 3'-0" in diameter provided access for drawing water. The walls and vault are believed to be of brick masonry covered with plaster. Floor drains in the terreplein and roof drains from its superstructure formerly fed this cistern, providing drinking water to the building during the periods when it was occupied. A drain line running from the cistern feeder cleanout to the west wall appears to have served as an overflow. A 1664 description

Structural Analysis

Description of structural conditions of fort. The inspection was limited to visual observations.

Exterior

Exterior walls – The exterior face of the walls are battered, with the walls measuring 5'-8" thick at the bottom of the Entry Door, and 4'-6" thick at the top of the Entry Door. Based on geometry, this means the base of the walls at the soil line could be over 6'-9" thick. An existing document by Pérez y Guzmán that suggest the walls are even thicker at approximately 14 feet wide and 10 feet tall. The wall surface is stone and mortar, with portions covered in yellow ochre-colored render with white horizontal and vertical lines spaced as to resemble stone blocks. In some areas the stone is exposed. Multiple mortar patches are visible. There is a protruding band, called a cordon, around the building near the top that appears to be masonry rubble, mortared together with the curved surface formed with mortar. The cordon is in relatively good condition, with some spalls and patches in some locations.

North Elevation – The render on this face is mostly eroded down, with the horizontal and vertical lines less clearly visible than on the other walls. The mortar in the head joints at the base of the wall near the east corner has eroded deeply. (Figure 139). There are at least four holes evenly spaced about 10'-0" apart approximately 7'-0" above grade that have been filled with brick pieces. (Figure 140). There is one large crack in the face of the wall that extends full height. It is located approximately 19'-0" from the north corner and is mostly vertical in orientation. See the attached Elevation 1/S2. It has been previously patched, but a new crack has formed that is approximately 1/8" (3.175MM) wide. The previous patching indicates that the crack has either widened over time, or that the patch was inadequate.

East Corner – The sentry box is located on top of the east corner. (Figure 141). The area appears relatively sound. No cracking is visible in the sentry box exterior walls or in the building walls below. There is a rip rap jetty extending from the east corner, so erosion or undermining of the wall should be much less of an issue at this location. However, from the debris around the site, it appears that this area experiences surface water flows during storm events.



Figure 139: North Elevation, closeup of base of wall showing erosion of vertical head joints between stones (Palmer Engineering).

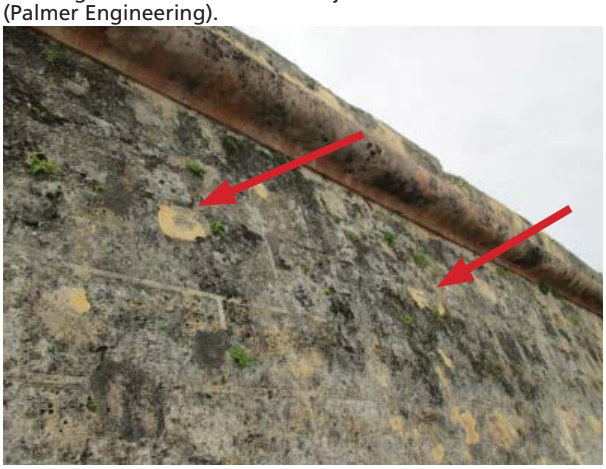


Figure 140: North Elevation, showing several of the holes that have been filled with brick pieces (Palmer Engineering).



Figure 141: East Corner, showing Sentry Box, Entry Door, Exterior Wood Platform and Stair. Note patches above door and to the left of door, as well as debris from storm waves (Palmer Engineering).

East Elevation - The wall surface is stone and mortar covered in render. Near the center portion of the wall, the render is spalling but only in the



Figure 142: Entry Door in East Elevation, showing multiple patches of walls around door. Note missing cable in guardrail (Palmer Engineering).

large rectangles outlined by the white horizontal and vertical lines. At other locations there are multiple mortar patches. The stone cordon has been repaired in several large areas at each end. There are two large cracks in the face of the wall that extend full height, and show evidence of previous patching. See the attached Elevation 2/S3. One crack is approximately 10'-0" from the south corner and is mostly vertical in orientation. At one point, the crack is vertical and runs up the side of one of the white vertical lines. The other is much smaller in width, approximately 1/16" (1.5875MM) wide and it starts at the base of the wall approximately 10'-0" from the east corner and extends diagonally up to reach the bottom right corner of the door opening and continues from the upper left corner of the door diagonally up to the top of the wall. That upper portion is covered with a large patch. (Figure 142). The doorway looks crooked, but appears to have been repaired at some point into that orientation. Small cracks in



Figure 143: East Elevation, showing cracks in render with white efflorescence outines, and close-up of patched cordon and parapet (Palmer Engineering).

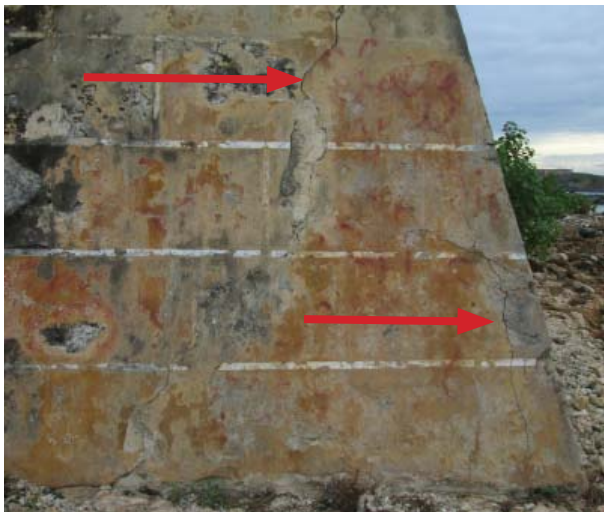


Figure 144: South Corner looking at South Elevation, showing cracks (Palmer Engineering).

the render show signs of efflorescence from water moving outward through the wall and dissolving minerals in the stones and mortar and depositing them on the surface as the water evaporates. (Figure 143).

South Corner – There is documentation that this corner has fallen off and been rebuilt at least two times in the past. Visual inspection shows numerous cracks within a zone approximately 5'-0" closest to the corner. (Figure 144). The breakwater with steel sheet piles and mortared rubble at the base of the wall continues around this corner, with the edge of the water approximately 15'-0" from the corner at high tide. (Figure 145). The cracks at the corner plus the proximity of the water suggest that the lower parts of this corner will break off again at some point. This should not adversely affect the integrity of the building as a whole.



Figure 145: South Corner, viewed from parapet looking down at breakwater and steel sheet piles (Palmer Engineering).



Figure 146: South Elevation, close-up of cordon showing location where cordon was omitted (Palmer Engineering).

South Elevation – The stone cordon has been omitted at the central portion of the south elevation. See (Figure 146). There are two large cracks in the face of the wall that extend full height, and show evidence of previous patching. One crack is approximately 22'-10" from the west corner in a mostly vertical orientation, with the other approximately 28'-0" from the south corner in a vertical orientation. See the attached Elevation 1/S3. (Figure 147). Small cracks in the render show signs of efflorescence from water moving outward through the wall and dissolving minerals in the stones and mortar and depositing them on the surface as the water evaporates. The edge of the water along the South Elevation is approximately 20'-0" from the base of the building at high tide. To protect the building from the adjacent bay, there is a breakwater of stone rip rap along the base of the wall, with the top edge of steel sheet piles visible for the southernmost third and westernmost end of the wall face. For a zone approximately 10'-0" wide closest to the wall, the ground is paved with rubble that has been mortared together. Near



Figure 148: South Elevation looking at South Corner, showing erosion of breakwater (Palmer Engineering).

the central portion of the wall there is an area of erosion that is much closer to the building, at approximately 10'-0" away. (Figure 148). Water elevations will be much higher during storms, with wave action on the building surface a concern.

West Corner - There is documentation that this corner has also fallen off in the past. The repaired corner appears to be in relatively fine condition. The ground has been covered with rubble that has been mortared or concreted into place to reduce further erosion issues. (Figure 149) (Figure 150).



Figure 147: South Elevation, showing mortared crack (Palmer Engineering).



Figure 149: West Corner, looking at West Elevation. Note patched area, as well as mortared stones at grade, with rip rap breakwater beyond (Palmer Engineering).



Figure 150: West Corner, looking at West Elevation (Palmer Engineering).

West Elevation - the majority of the render on this face is intact, but in some areas the stone is exposed. Multiple mortar patches are visible. The stone cordon is in relatively good condition, with some spalls and patches in some locations. There are three large cracks in the face of the wall that extend full height in a mostly vertical orientation, and show evidence of previous patching. One crack is approximately 19'-6" from the north corner, the second is approximately 33'-10" from the west corner, with the third approximately 10'-4" from the west corner. See the attached Elevation 2/S2. The centermost crack includes a hole approximately 10'-0" above the base that extends at least 6" deep into the wall, probably extending full depth. The crack extends full depth of the wall when viewed from the top of the building, where the crack is approximately 4 ½" (114.3MM) wide. (Figure 151). That crack also has three crack monitors centered on the crack. We understand these were placed in 2012,



Figure 151: West elevation at central crack. Note previous mortar patch, with new crack through patch (Palmer Engineering).



Figure 152: West Elevation at top of parapet, at central crack. Note remains of crack monitor (Palmer Engineering).



Figure 153: West elevation at central crack. Note two crack monitors. Note crack widens as it climbs the wall (Palmer Engineering).

but no record of monitoring has been found. One is approximately 15'-0" above the base, one approximately 1'-0" below the top edge of the wall, and the third on the horizontal top surface of the wall. Assuming the monitors were placed with the origins centered, there has been 1 MM horizontal movement apart since they were installed in 2012. (Figure 152) (Figure 153).

North Corner – This corner appears to be in relatively fine condition. Photographs taken in 1936 show a portion of the corner missing close to the waterline. It has apparently been repaired, with no current damage visible.

200 Terreplein (Concrete Cap) - The top surface of the fort is an approximately 4" thick concrete slab cap on top of a plastic vapor barrier and a layer of sand installed in 1992. Welded wire fabric appears to have been laid directly on top of the plastic before the concrete was placed, which



Figure 154: Concrete Slab, from Interior Stair Room. Note termite infestation of wood beam. Note welded wire fabrix located at bottom of slab (Palmer Engineering)..



Figure 155: Scuttle Door in Concrete Slab, edge on top of North exterior wall, showing brick pavers (Palmer Engineering).

is contrary to accepted practice. (Figure 154). However the cap appears intact, with minimal cracking. This concrete has been placed on top of a brick surface. The surface was not visible at the time of inspection, so its condition cannot be verified. A masonry surface was visible at the entry scuttle, but it is not certain if it is the brick surface used elsewhere. (Figure 155).When formed, a wood joint or screed was attached around the perimeter and around the two penetrations near the center of the cap. This piece was removed or has deteriorated, leaving an approximate 1" wide gap between the edge of concrete and the surface. In some locations the gap is filled with dirt and vegetation, in others the sand bed has eroded away and some voids are evident below the cap. (Figure 156) (Figure 157). The surface is sloped to drain at the latrine at the south west corner. Gaps and voids between the cap and the latrine walls are larger and the depth and extents of the voids were deep, caused by erosion from water flow. (Figure



Figure 156: Concrete Slab at Privy, showing gap between concrete and exterior walls. Because the layer of sand and stone beneath has been eroded by water, this gap extends down the wall and under the slab (Palmer Engineering).



Figure 157: Concrete Slab at East Elevation, showing gap (Palmer Engineering).



Figure 158: Concrete Slab at Privy, showing gap between concrete and exterior walls. There is a void below slab at this location that extends down the wall (Palmer Engineering).



Figure 159: Scuttle Door in Concrete Slab. Note arch beyond (Palmer Engineering).



Figure 161: Kitchen, at West Corner, with Privy on the right. Note opening with plug that has shifted out of place (Palmer Engineering).



Figure 160: Sentry Box, soor, note step down from concrete slab (Palmer Engineering).



Figure 162: Privy, looking at top. Exterior is on the right. CMU cells are visible, filled with mortar. Note that intersecting wall is not attached (Palmer Engineering).

158). So, despite the concrete cap, water is able to penetrate into the interior of the fort. The scuttle door in the concrete cap is a steel door with frame made of steel angles with rubber gaskets to provide water seal. Condition is good with minimal rust. Hinge and gas lift operation was not observed at the time of visit. (Figure 159). Wood support frame that supports the door frame shows termite damage.

201 Sentry Box (Garita) – The Sentry Box is appears structurally adequate. Minor cracks are visible in the render on the outside, and previously applied patches are in sound condition. The interior of the dome roof shows no signs of cracks. Portions of render have broken off around the interior of the window and at the door and at the base of the walls. The support below the box appears sound, with only minor cracks none of which should adversely affect its condition. (Figure 160).

202 Kitchen – The remaining bricks that formed the kitchen on top of the walls at the west corner are mortared in place, with a few loose bricks. On



Figure 163: Privy, showing sloped concrete and openings to drain concrete slab (Palmer Engineering).



Figure 164: Privy from West Elevation (Palmer Engineering).

the side of the kitchen wall, an opening is partially visible, with a mortar plug that has shifted out of place and allows water to flow into the opening. (Figure 161).

203 Latrine – The upper portion of the latrine exterior wall appears to not be original, and reconstructed of concrete masonry units covered with a layer of mortar. (Figure 162) (Figure 163). The lower portion is brick covered in render and has been patched as required. The water flow from the concrete cap has been directed to exit at holes in the latrine wall. (Figure 164). The water flow has



Figure 165: Privy from West Elevation. Water from Concrete Top has eroded brick, concrete and stone allowing water to flow back into building (Palmer Engineering).

eroded the walls below the holes and water is able to flow inside the walls. (Figure 165).

Interior

100 Vestibule – The vestibule is a low arched space with stone floor and walls made of mortared stone and brick covered in render. The arch shape was constructed of mortared bricks topped with larger blocks of stone. (Figure 166) (Figure 167) (Figure 168). There is a hole in the wall to the north of the door at the top. (Figure 169). The entry door is a set of wood doors with steel throw bolt. The inside of the door was not reviewed to check for termite damage, but it would be safe to assume that it exhibits damage. The exterior wood platform and stair are slightly weathered, with no signs of termite damage. Wood posts bear on concrete pedestals, while stair stringers are in contact with ground, but appear not to be structurally deficient. One intermediate cable at the railing has come loose.

101 Stair Hall - To the north of the vestibule, the ceiling height is much higher, extending to underside of the concrete cap. The walls are a mixture of exposed mortared stone and brick, with portions covered in render. The interior wood stair



Figure 166: Interior Stair Room looking at Interior Entry Vestibule. Note opening to Ramp to East Magazine on the right. Brown line is a termite tube, not a crack (Palmer Engineering).



Figure 168 Interior Entry Vestible, ceiling (Palmer Engineering).



Figure 167: : Interior Entry Vestibule, wall to the left of Entry Door. Note notches in wall near door, hole at left corner of door, and spalling at individual bricks (Palmer Engineering).



Figure 169: Interior Entry Vestibule, hole in wall at left corner of Entry Door (Palmer Engineering).

butts up to the vertical inside face of the exterior wall. There is evidence of a stone stair below the wood stair. Closer to the door to Room 102, the floor slopes down, and the south wall of the space curves and ends at a corner with the north wall, and the ceiling is lower. Above the small corner area, there is a gap where possibly a wood beam or a layer of wood formwork was located, below a layer of brick set on edge and mortared together. (Figure 170). This is topped by a short knee wall which extends up to the underside of the concrete cap. Portions of the walls are covered with a layer of efflorescence from water being pushed out of the stones. At the wood stair, the frame and wood treads and risers show termite damage. The bottom of wood posts show signs of water wicking up into



Figure 170: Interior Stair Room, low ceiling close to North Magazine. Note curved wall, and impressions in underside of masonry where wood beam or formwork was placed (Palmer Engineering).

the posts. To the north of Room 100, the ceiling height is much higher, extending to underside of the concrete cap. The walls are a mixture of exposed mortared stone and brick, with portions covered in render. The interior wood stair butts up to the vertical inside face of the exterior wall. There is evidence of a stone stair below the interior wood stair. Closer to the door to Room 102, the floor slopes down, and the south wall of the space curves and ends at a corner with the north wall, and the ceiling is lower. Above the small corner area, there is a gap where possibly a wood beam or a layer of wood formwork was located, below a layer of brick set on edge and mortared together. This is topped by a short knee wall which extends up to the underside of the concrete cap. Portions of the walls are covered with a layer of efflorescence from water being pushed out of the stones.

102 Vault No. 1 (North Magazine) – There are two steps down from Room 101 at the door to Room 102. The steps are mortared brick set on edge. The floor is uneven stone. Room 102 is a rectangular room with barrel vaulted ceiling. The walls and ceiling are covered in a white plaster coating, mottled and peeling in spots due to moisture. No cracks are visible in the walls of the room. The door opening in the end wall is rectangular. (Figure 171). From the outside of the room, the opening can be seen to have been made of large stone blocks, assembled to form the lintel over the opening. (Figure 172). The jambs are mortared thin brick and the jamb on the right side appears to have been repaired at some point. (Figure 173).



Figure 171: North Magazine, looking out at opening to Interior Stair Room (Palmer Engineering).



Figure 172: North Magazine, lintel blocks above opening looking into room (Palmer Engineering).



Figure 173: North Magazine, jamb to the right of opening (Palmer Engineering).



Figure 174: Ramp to East Magazine. Note door to East Magazine in the right wall (Palmer Engineering).

103 Passage (Ramp to East Magazine) – There is a low opening with level header in the south wall of the Room 100. There is a small spall in the face of the header. The floor steps down at the opening and the floor ramps downward. The room is a thin rectangle, with a low arched ceiling with stone floor and walls made of mortared stone and brick covered in render. There is a low arched opening in the north wall at the end of the space that leads to the Room 104. (Figure 174).

104 Vault No. 2 (East Magazine) – The floor steps down into the room at the opening. The floor is covered in moist sandy dirt. The room is a rectangular room with a low arched ceiling, the walls covered in render. The arched entry opening is not centered on the arched room. There is a portion of wall protruding into the room from the wall to the north of the entry opening. Between the entry opening and the room, there is a large and pervasive crack that runs the full height of the wall on each side of the opening and across the ceiling. (Figure 175) (Figure 176) (Figure 177) (Figure 178) (Figure 179) (Figure 180) (Figure 181) (Figure 182). The faces of the crack show that the barrel vault was formed with mortared thin brick and the walls are mortared stone. The crack was measured to be approximately 5 1/2" (139.7MM) wide at a point 3'-6" above the floor, and the depth into the wall on each side of the room was at least 51". (Figure 181). The crack continues up above the ceiling at least 12", with the joint filled with rocks and brick rubble. (Figure 182). Crack monitors have been placed across the crack at an angle, one on each side of the opening. At each, two monitors were screwed together due to the width of the crack. Assuming the monitors were placed



Figure 175: East Magazine, base of crack to the left of opening (Palmer Engineering).



Figure 176: East Magazine, upper portion of crack to the left of opening. Note wall protruding into room. Note where render coating on wall has split at crack (Palmer Engineering).



Figure 177: East Magazine, close-up of upper portion of crack to the left of opening. Note remains of crack monitor, and brick and stone inside crack (Palmer Engineering).



Figure 179: East Magazine, upper portion of crack to the right of opening (Palmer Engineering).



Figure 178: East Magazine, crack above opening. Note bricks that form barrel vault. Brown line is a termite tube (Palmer Engineering).



Figure 180: East Magazine, lower portion of crack to the right of opening.

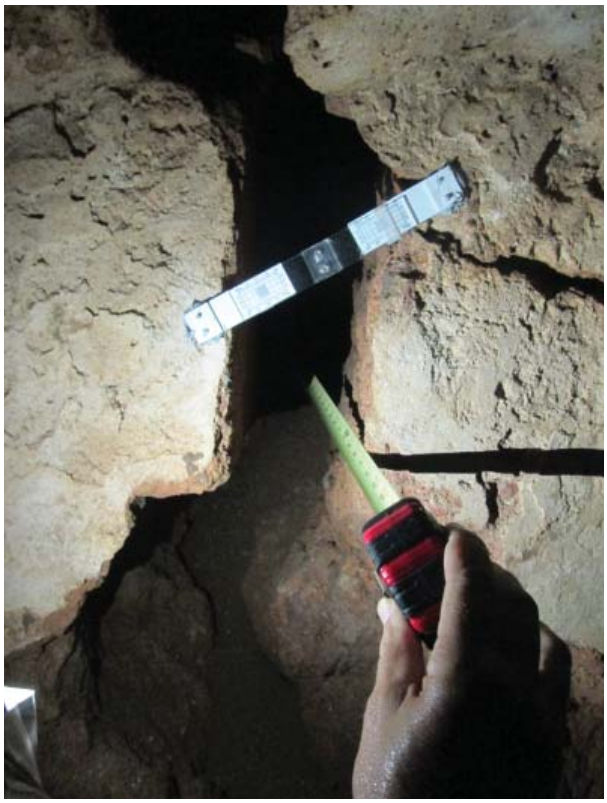


Figure 181: East Magazine, upper portion of crack to the right of opening, with crack monitor.



Figure 182: East Magazine, looking directly up into crack above opening (Palmer Engineering).

with the origins centered, there has been 1" MM horizontal movement apart and 4"MM differential vertical movement since they were installed on an unknown date. The presence of mortar patching in the wall of the nearby Room 101suggested the possibility that the crack extended toward the north to reach Room 101. The HABS drawings from 1954 confirm this suspicion. Those drawings show a crack that extends almost the full length of the building just inside of the East Elevation from the South Corner to Room 101. The crack extends up to the brick paver level, and is much wider close to the South Corner. There are also quantities of approximately 1" diameter iguana droppings on the floors in the space. All other access points to the building interior appear to be well sealed, so this suggests that some of the cracks are extensive enough to allow small animals' passage from the outside to the interior.

Structural Observation

The cracks observed at the site have been occurring for a long time, visible in photos taken in 1936, and shown with mortar patch repairs in photos from 1954 and 1962. The sequence of patching and repatching indicates that the cracks have widened over time. Fractures in the exterior walls seem to be happening in similar locations on each of the four walls, at approximately third points along the wall faces. The cracks are mostly vertical, except the crack at the right side of the East Elevation is diagonal as it passes through the relatively weak door opening. On the South and West Elevations, there is a centrally located crack running vertically up the wall.

Based on our review, we understand that the building walls were constructed of cut sandstone blocks laid in courses to create an exterior battered face and a vertical interior face. The space between those faces is said to be rubble and fill and the rubble has compacted over time. This massive assembly acts as a gravity wall, relying on its mass and geometry to resist the vertical forces placed on it by gravity and the lateral forces placed on it by water on the outside, and buildings and soil on the inside. Sliding forces created by the backfill are transferred to the bearing strata below via friction. The heavy mass increases the coefficient of friction at the rough interface between the rocks and the subsurface material. Overturning forces, applied

as the pressure behind the wall tries to tip the wall over, are resisted by the weight of the wall with the assistance of the thickness of the wall at the base. The battered shape lowers the center of mass of the wall and keeps it toward the center of the wall, creating a stable wall.

The existing cracks and voids are likely exacerbating the deterioration. Superficial cracks and gaps allow water to flow into the building, eroding surfaces and increasing pressure behind the walls. This continues the cycle of cracks becoming wider and produces more cracks, allowing more water to enter further, and so on. The HABS drawings from 1954 show a large void near at the South Corner. Water likely had access to this void, exacerbating its erosion, likely contributing to the failure of that corner.

Possible Contributing Factors to Cracks

- The pressure from the backfill is bowing out the walls.
- The subgrade is failing because to loss of bearing due to erosion.
- The subgrade is failing because of pressure from the backfill onto the subgrade is higher than it can support.
- Earthquakes.
- Any combination of these.

Pressure bowing out the walls –The walls at the corners are restrained from movement by the intersecting walls and so will not move. If the center portions of the wall bow out enough so that the applied tensile forces exceed the tensile strength of the stone and mortar, then a crack occurs. This likely happens at the location where the stiffer portion meets the more flexible portion at the corner of the wall. This crack then allows the flexible portion to continue to move unrestrained by the stiffer adjacent areas.

Figure 183 shows the left hand crack on the East Elevation. The right side of the crack is toward the center of the wall, and the left side is toward the South Corner. The right side of the crack is pushed forward of the left side. This indicates that the relatively flexible central portion of the wall is shifting outward relative to the restrained corner. Figure 184 shows the same condition occurring at the left hand crack on the West Elevation. We were unable to confirm exact relative movement between the two sides of the cracks at the site, however the movement can be very small and still result in cracks. This mechanism produces cracks that are the full depth of the wall. The central cracks on the West and South Elevations could also support this conclusion, as they are wider at the top than the bottom. We did not see that one side of the crack is proud of the other. This mechanism produces cracks that originally are not full depth, as they first form in the outside tension face of the wall. But as movement continues, the crack spreads and extend full depth of the wall. The combination of these two types of cracks suggest the central joints are spreading out as the wall bows out, and the cracks at each side occur as the bowing portion separates from the stiff corner sections.



Figure 183: East Elevation, close-up of left hand crack. Left side is at corner, and right side is toward midsection of wall. Right side is proud or pushed more forward than left side. Note that line runs up the side of a vertical line in the render (Palmer Engineering).

We note that the left side of the North Elevation does not have a crack. This is possibly because the interior voids of Room 100 and Room 101 are flexible enough to interrupt the crack and keep it from extending to the North Wall.



Figure 184: West Elevation, close-up of left hand crack. Left side is at corner, and right side is toward midsection of wall. Right side is proud or pushed more forward than left side (Palmer Engineering).

The crack in the interior walls of Room 104 could confirm this hypothesis, as this crack is wider at the top than the base and much wider than the cracks in the exterior walls. The crack extends well beyond the areas we could access in Room 104, and there is a possibility that it continues to the repaired south wall of Room 100. Based on our observations and our review of previous documentation of the crack it likely extends up for the full height and length of the wall. This is likely one of the contributing factors for the large cave-in at the south corner described in the 1955 HABS drawings. This crack occurs at the inside face of the exterior walls, crossing the intersecting walls of Room 104 at the interface between the exterior wall and the backfill.

We understand that there is documentation that suggests that the backfill that has been placed behind the walls up to the top of the exterior walls is original to the structure with a brick paver layer on top. If that is correct, then we can conclude that the engineers who built the walls accounted for the forces from that back fill in their design. To verify this, we have checked the wall design using RetainPro wall design software using assumed values for subgrade, backfill, and wall dimensions. Using a poorly graded silty sand backfill that applies 45 PSF of lateral pressure/foot of depth, we find that the wall at the base is slightly overstressed in tension. As we move up the wall, the lateral forces placed on the wall decrease and at 2'-6" above the surrounding grade the wall is no longer overstressed in tension.

This calculation is highly dependent on the backfill composition, including the water content. We observed multiple signs of water intrusion into the building, from cracks around the edges of the concrete cap with large voids visible near the latrine, to efflorescence built-up around cracks in the face of the exterior walls, to a thin layer of efflorescence on all surfaces inside the building, and high ambient temperature and extremely high humidity inside.

Due to the rather high water table near the bay, the path for the moisture down through the foundation is limited, and more moisture could actually be wicking up into the building through the foundation. The concrete cap with its layer of plastic prevents water vapor from migrating up through the cap, while still allowing water to enter the building through a gap between the concrete cap and the existing brick walls all around the perimeter. That water flow has caused voids below the edges of the cap and at the latrine area, where the water flow is directed.

A significant amount of water is allowed to enter the building, with limited pathways for it to exit. All of the moisture either remains inside or due to the difference in relative humidity between the inside of the building and the outside is pushed out through the pores and cracks in the exterior walls. This water in the backfill increases the pressure applied to the walls, so that the walls are further overstressed and the bearing pressure applied to the subgrade is greatly increased.

We acknowledge that the cracking has been occurring for quite a long time, long before the concrete cap was installed. Prior to installation of the concrete cap, water flowed into a system of drains that directed water from the roofs to the cistern and the water on the terreplein out of the building through a drain hole in the West

Elevation. Any water that remained soaked down into the building, but could evaporate up through the pavers as well as out through the walls. Water that migrated into the building up from the surrounding bay also could exit this way. The interior of the building probably would have been humid, and the backfill would still have increased pressure on the exterior walls, but the effects would be much less than the building is experiencing currently.

Settlement due to erosion –There is evidence of past damage from erosion, both from direct wave action when the fort was an island and now during storms and high tides. The proximity of the South Corner and South Elevation to the waterline and presence of wave borne debris around the three waterfront sides of the building suggest that this will be a concern in the near future. Sea level rise will further increase the stress on the structure. Depending on the composition of the subgrade - if it is sand or erodible material - the subgrade below the building needs to be confined by soil around it in order to maintain its bearing capacity, and the loss of material around the base of the building is a concern. As the soil weakens, the building loses its support, and settlement cracks occur. If it is rock with a high bearing capacity, with less need to be confined, then this process occurs at a much slower rate. This process could be one of the contributing factors to the reoccurring cracks and wholesale loss of the South Corner in 1954. We understand that the breakwater, steel pile bulkhead, and riprap seen at the site were installed in the 1960s. These appear to need augmentation and repair.

Settlement due to subgrade overstress – We understand that the building was constructed on an existing small natural island protruding out of the bay. This subgrade could be bedrock - which is preferable, or sand - which is less so. Ideally the builders would have dug down to get to a stable subsurface below the sand. Of course they may have relied on the fact that the addition of tons of rock would have compressed the subgrade as the building was erected. If this process was successful, then the building would be stable. If it was not successful, the building would settle differentially, causing cracks between adjacent sections.

If the subgrade is being overstressed due to the pressure from the backfill, the results would be slightly different from the results from the walls bowing out. The backfill presses out on the walls, resulting in an overturning moment that places high downward forces on the outer edges of the wall and subgrade. The forces on the subgrade beneath the interior edges of the wall and interior of the building will be much less. As the subgrade is overstressed, it compacts downward or spreads outward beyond the walls. As the subgrade moves, the walls crack. We see no evidence of soil pushing up around the base of the building, but erosion or vegetation could conceal it. However, the cracks visible in the walls would be diagonal, coming together at the top as portions of wall are undermined, and the cracks would not extend for the full depth of the wall.

This theory was checked using that same RetainPro model of the wall using assumed values for subgrade, backfill, and wall dimensions. Using the weight of the wall itself and applying the lateral pressure from a poorly graded silty sand backfill that applies 45 PSF of lateral pressure/foot of depth, we find that a competent rock subgrade has the capacity to support the applied bearing forces. If the building is placed on sand, or if the backfill pressure increases considerably, then the soil bearing capacity is not adequate.

A geotechnical exploration of the subsurface conditions would be highly beneficial in that it will show the condition of the subgrade and help determine if this as a contributing factor to the cracking. Information about the backfill composition and weight would be a great help in determining the pressure on the walls. Depending on the results of the testing, then the stabilization and remediation recommendations could be changed.

Earthquakes – Puerto Rico sits on the Caribbean Plate south of the Puerto Rico Trench, which is both a transform fault where the Caribbean Plate slides east past the North American Plate sliding west and a subduction zone where the North American plate is being subducted beneath the Caribbean Plate. Puerto Rico experiences numerous earthquakes, most producing moderate shaking with minimal effect on buildings. But there are records of at least four significant earthquakes in the region during the life of the building.

- 1670 earthquake, strength unknown but causing major damage to buildings on the west coast.

- An earthquake on May 2, 1787 with an epicenter north of the island is estimated to be 8.0-8.5 on the Moment Magnitude Scale (M_w). There are records of damage to walls at San Felipe del Morro and San Cristobel.

- November 1867 earthquake estimated to be 7.5 M_w, with epicenter located on the east coast between Puerto Rico and St.Croix, causing major damage to the buildings on the east coast. This event occurred soon after the estimated Category 3 San Narciso hurricane passed over the island from west to east, with its high winds and storm surge.

- October 1918 San Fermín earthquake measured at 7.1 M_w off the northwest coast. Records of damage are concentrated on the west coast of the island.

The building is located in an area with high seismic forces. The Mapped spectral response acceleration parameters are S_s (0.2 sec) = 100%g or 1.000 and S_1 (1.0 sec) = 39.90%g or 0.399. The Design spectral response acceleration parameters are Sds = 0.733 and Sd1 = 0.426. The Site coefficients Fa = 1.100 and Fv = 1.602. These values combine to set the building into Seismic Design Category D. The International Building Code, 2012 Edition, does not allow this type of Ordinary Plain Masonry Shear Bearing Walls to be used in this Seismic Design Category.

The dimensions and construction of the building lend themselves to performing well during an earthquake. The short squat box is a very simple and stable shape. The wide walls are very stiff, especially when loaded in the plane of the walls along their length. For damage in the plane of the wall, we would expect to see full height and depth diagonal cracks, likely two crossing each other in an 'X' shape, especially in the relatively weak areas above and around the Entry Door. A severe earthquake could also result in damage to the Sentry Box where it meets the main building. There are patches in the exterior wall above and around the Entry Door, but it is difficult to relate that damage to earthquakes. During an earthquake, the walls will also be loaded out of the plane of the walls. Where the force is applied toward the building, the backfill will buttress the wall and eliminate movement in that direction, with no damage. Where the force reverses and it is applied away from the building, the short squat nature of the wall and batter at the exterior face act together to reduce outward movement. If movement were to occur due to strong shaking, due to the brittle nature of the building we would expect to see numerous small vertical cracks or spalls in the outer face of the wall concentrated around the central area of the wall at the top where it is thinner and less restrained. Unfortunately, the render and patching makes this difficult to verify.

Despite having survived numerous large earthquakes over its lifespan, we should not expect the building to perform well in a large earthquake. Its brittle construction means that even if an extensive program of large scale reinforcement were performed, there will be significant damage to the exterior walls and Sentry Box. It would be best to focus any reinforcement operations on ways to enhance life safety for occupants.

El Cañuelo: Material Analysis

Introduction

Building Conservation Associates, Inc. (BCA) prepared an analysis of select masonry materials of the Fortín San Juan de la Cruz (El Cañuelo) in San Juan, Puerto Rico. The masonry materials investigated for this study include interior plaster, exterior stuccos, and bedding mortar from the facing stone. The primary goals of the materials analysis are to aid in preparing a construction chronology for the fort, determine if any original or early masonry materials remain, and to discover more information regarding the construction technologies used during the period of use as a Spanish Colonial military installation between 1664 and 1841.

The following report summarizes the findings of the masonry analysis. Following the introductory information regarding the history of the site and the study methodology, the report discusses the findings of the research and the implications for the understanding of the fort's chronology.

For the compositional analysis of the masonry materials, five samples of mortars and stuccos from various elements of the exterior and interior of El Cañuelo were extracted by BCA during a site visit in November 2016 and sent to Highbridge Materials Consulting, Inc. for petrographic and chemical analysis.

All work required for the execution of this study was performed by Kevin Wohlgemuth, BCA Architectural Conservator. Assistance was also provided by Highbridge Materials Consulting, Inc. for the laboratory portion of the masonry analysis.

Background Information[98]

Fortín San Juan de la Cruz, more commonly known as El Cañuelo, sits at the southern tip of the Isla de Cabras, across the Bar Channel from San Juan, Puerto Rico and San Felipe del Morro Fortress (El Morro). It was originally constructed around 1609 as a small, wooden redoubt with a rubble foundation on a small shoal south of the Isla de Cabras. After destruction at the hands of the Dutch in 1625, El Cañuelo was rebuilt as a more durable masonry structure in 1664. After construction, multiple campaigns of repairs were conducted at El Cañuelo. These were recorded as occurring in 1692 and 1702. As this fort was exposed to many harsh natural conditions as well as battles conditions, it is likely that repairs and maintenance were routinely performed and that they were either not recorded or the record has not been located. Although Spanish officials formally requested to abandon the fort in 1785 after being described as a ruin the year before, it appears to play a part in a 1797 attack of San Juan by the British.[99]

In 1841, a proposal to modify El Cañuelo for use as a lazaretto, or quarantine site, was drafted and it appears to have been used for this purpose until 1876, when a more extensive leper colony was constructed on nearby Cabras Island. After 1900, El Cañuelo came under control of the American Military Governor of Puerto Rico and the United States Army. In 1938, a number of military installations in Puerto Rico were restored, although El Cañuelo was called out as not being one of them. The Army Corps of Engineers connected El Cañuelo and Isla de Cabras with a major land works project in 1943, the same year that the fort was described as a ruin. Then, in 1949, the fort is transferred to the National Park Service (NPS) to become part of the San Juan National Historic Site. Under NPS care, El Cañuelo has undergone several preservation and restoration campaigns in an attempt to stabilize and protect the structure.

The construction of the masonry fort at El Cañuelo in 1664 originally used traditional masonry techniques of Spanish Colonial military installations in the region while utilizing materials that were predominantly native to the island of Puerto Rico. It has a rubble and ashlar (*mampostería*) foundation and walls with ashlar "beachrock" facing. There are only three interior spaces: two magazines and a cistern, connected by a series of passageways. During its use as a military installation, all of the military equipment and garrison resided atop the terreplein, in spaces delineated by "pillars of hewn stone."[100] A *cordón*,

98. Archival sources reviewed by BCA are referenced in footnotes throughout the report. All other information included in this section was taken from archival research notes provided by WLA Studio.

99. Blanco, J. "Morphological Structure of Fortifications, 1998, Volume II:127"

100. Blanco, J. "Morphological Structure of Fortifications, 1998, Volume II:127"



Figure 185. View of El Cañuelo, looking south, 2016 (Photograph by BCA).

or stringcourse, surrounds the structure just below the terreplein. It is intentionally broken at the southeast, for ladder access and on the northeast by the latrine. The ramparts and the *cordón* are covered with a stucco finish. The ramparts appear to have an ocher pigmented wash with faux joints while the finish coat of the *cordón* is pigmented red from brick dust. (Figure 185). During its use as a lazaretto, major brick construction was conducted on the upper level, remnants of which remain.

Although the existing structure was abandoned by 1898, repairs and, in particular, restoration campaigns to stabilize the structure have continued into the twenty-first century by the NPS.[101] Because of its long history and the multiple construction, destruction, and modification campaigns through the seventeenth, eighteenth, and nineteenth centuries, it is difficult to impose a rigid chronology upon the extant masonry materials. However, by combining a detailed analysis of the constituents in the masonry materials as documented through BCA's current research with archival research, it may be possible to determine approximate and/or relative chronologies of installation.

Archival Record

The original construction of the masonry redoubt at El Cañuelo can be somewhat inferred from written archival sources that have been researched by WLA Studio.[102] The structural components of the current fort, which are the most likely physical components to date to the seventeenth century, are presently not visible and the materials that can be visually analyzed without destructive probes are likely not as old. While some archival information about the construction of the fort exists, these letters mostly reference the inventory of armaments rather than the specific construction materials such as mortars or stuccos.[103] The rest of the archival record notes various periods in which the fort was active or in states of disrepair, and as noted above, a few instances of repairs. However, since these repairs are not specified, it is not possible to use this information to determine if any of the existing materials were present before these repairs were made or are a part of any of these particular repair campaigns.

The most useful archival information for understanding of the extant masonry materials and their appearance over time, particularly the exterior stucco, are the historic photographs. The earliest of these photographs dates to the 1930s. When taken together and compared, these historic photographs provide a cursory visual repair chronology of the exterior of the fort.

The most comprehensive documentation campaigns at El Cañuelo were conducted by HABS when it was surveyed in 1955 and again in 1986. Condition assessments and photographic documentation from these two surveys serve as the primary record of deterioration and repair, although a few photos from before 1955 and several studies after 1986 also contribute to the archival record.

While this materials analysis does not venture into creating a comprehensive repair chronology, the annotated photographs included below can be used to confirm that exterior rampart, *cordón*, and battlement samples were taken from areas that have not been altered since the historic photos were taken. Unfortunately, since there is little photographic documentation of the interior, this investigative technique cannot be applied to those sample locations.

101. Ownership of the fort was transferred to the National Park Service in 1949.

102. As mentioned above, where statements are not footnoted, the source material was provided in WLA Studio's archival research notes.

103. Zapatero, J.M. "Las fortificaciones históricas de San Juan de Puerto Rico." *Militaria. Revista de Cultura Militar*. N. 1 – 141-175. Edit. Univ. Complutense. Madrid, 1989.

Sample #	Location	Material	Masonry/Substrate
M01	Exterior rampart, northeast elevation	Stucco body	Sandstone/"Beachrock"
M01	Exterior rampart, northeast elevation	Stucco finish	Sandstone/"Beachrock"
M02	Exterior battlement, northwest elevation	Mortar	Sandstone/"Beachrock"
M03a	Exterior latrine, northwest elevation	Mortar	Brick
M03b	Exterior latrine, northwest elevation	Stucco body	Brick
M04a	Exterior *cordón*, southeast elevation	Stucco body (white)	Sandstone/"Beachrock"
M04b	Exterior *cordón*, southeast elevation	Stucco body (pink)	Sandstone/"Beachrock"
M04a	Exterior *cordón*, southeast elevation	Stucco finish	Sandstone/"Beachrock"
M05	Interior wall, passageway	Plaster body	Brick
M05	Interior wall, passageway	Plaster finish	Brick

Table 1. Table of masonry sample locations and materials.

Methodology

Extraction of the masonry samples occurred during a one-day site visit by BCA on November 1, 2016. During the site visit, the fort was physically examined for intact areas from which representative samples of mortars and stuccos could be removed. The locations of these samples were selected based on the potential for original or early extant materials, as well as an intention to compare various materials from different areas of the fort in order to develop relative construction chronologies. The samples were removed using masonry chisels and a hammer.

A total of five representative samples of the various masonry materials were removed from the structure. These included: exterior stucco from the rampart and *cordón*, mortar from the battlement and latrine, and interior stucco from a passageway wall.[104] Sample locations are illustrated in Figure 188, Figure 189, Figure 190, and Figure 191.

These samples were taken back to the laboratory for analysis. Cursory visual examination of the samples was performed by BCA to preliminarily characterize the materials prior to submitting them to Highbridge Materials Consulting, Inc. (Highbridge) for supplemental laboratory analysis. Highbridge performed petrographic examination, chemical analysis (atomic absorption spectroscopy), and, where possible, acid dissolution/sand extraction to separate these components.[105] The goal of this analysis was to identify the binder and aggregate components of each of the masonry materials, as well as the original component ratio. The acid dissolution allowed for the extraction of the aggregate portion of select, representative materials. Although Highbridge's findings are summarized in this report, a draft of their full report (including their methods of examination and data) has also been included in *Appendix C*.

Summary of Findings

Materials Analysis

The results of the laboratory analysis of the masonry materials at El Cañuelo indicate that all of the materials analyzed utilize the same binder—a non-hydraulic, high-calcium lime—regardless of their use (mortar, stucco, plaster) and location on the fort. However, the type of aggregate and pozzolanic additive varies among the samples. This variation in the ingredients of these masonry materials, particularly the use of different pozzolanic additives, suggests that those who historically constructed or repaired the fort may have had a working understanding of the cementitious properties of the materials they selected and that particular additives were included in the mortars and stuccos to achieve a desired durability effect.

One of the most interesting additives documented for the mortars and stuccos is the pozzolan. A pozzolan is a material, usually silicious and/or aluminous, that reacts with calcium oxide (lime) and water to form cementitious compounds, effectively hardening lime-based materials allowing them to behave more like a cement. The degree to which the lime-based material becomes cementitious can be calculated as a "cementation index." The cementation index was defined by E.C. Eckel in 1905 and uses the percentages of silica,

104. Several of the samples contained multiple stratigraphic layers, which were sampled together but analyzed separately.
105. The extracted sand samples will be submitted with the final report.

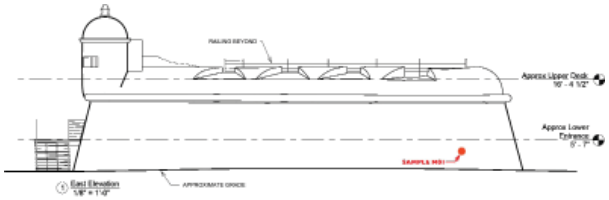


Figure 186. East Elevation of El Cañuelo (Drawing courtesy of RATIO Architects, Inc. Annotated BCA).

alumina, iron oxide, lime, and magnesia in a sample to infer how hydraulic, hard, and durable it will be.[106]

At El Cañuelo, three different pozzolans were found in the masonry materials: volcanic ash (or trass), crushed soft (low-fired) brick and pulverized hard (higher-fired) brick. Mortar samples M02 and M03a, as well as the interior plaster body sample M05a and the exterior stucco sample M03b contain the low-fired brick as a pozzolanic additive. By contrast, the remaining exterior stucco samples contain trass (M01a, M01b, M04a, M04b) or the ground higher-fired brick (M04c) as the pozzolan. The interior plaster finish sample M05b contains no pozzolanic additives.

The masonry materials documented through this analysis can be characterized by the following four material categories: masonry materials with volcanic ash (trass) pozzolans; masonry materials with soft brick pozzolans; masonry materials with harder brick pozzolans; and masonry materials with no pozzolanic additives. A discussion of each type of material follows Table 2 below, which summarizes the results of the laboratory analysis per sample.

Masonry Materials with Volcanic Ash (Trass) Pozzolans

The exterior stucco samples with trass contain this additive in varying quantities. These quantities range between 15% and 19% by weight, resulting in some of the highest cementation indices documented in the current analysis (0.77 for sample M01a and 0.80 for sample M04a).[107] By comparison, the interior plaster finish (sample M05b) with no pozzolanic additive and very low

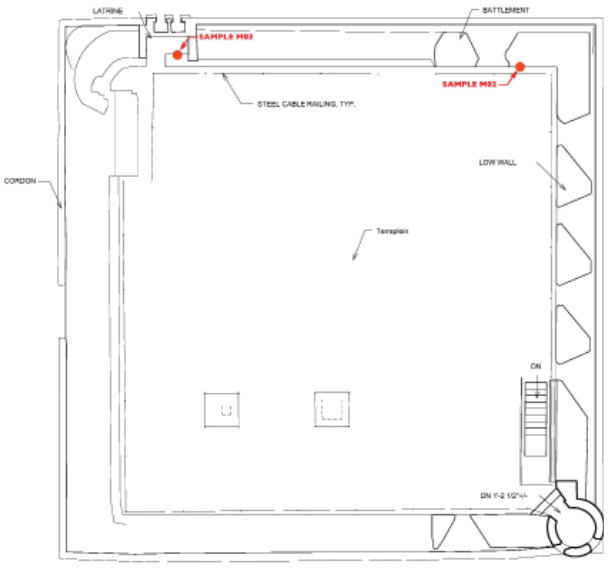


Figure 187. Terreplein Plan of El Cañuelo (Drawing courtesy of RATIO Architects, Inc. Annotated BCA).

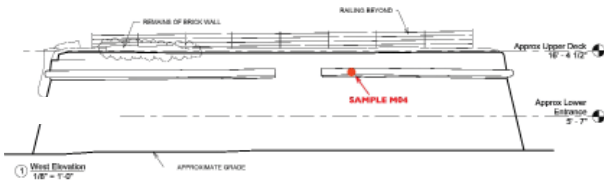


Figure 188. West Elevation of El Cañuelo (Drawing courtesy of RATIO Architects, Inc, Annotated BCA).

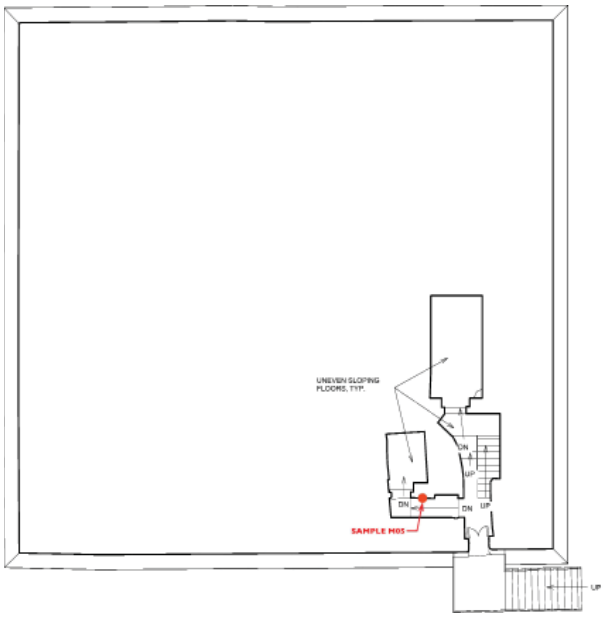


Figure 189. Lower Entrance Section of El Cañuelo (Drawing courtesy of RATIO Architects,Inc. Annotated BCA).

quantities of alumino-silicates has a cementation index of 0.02. With such high cementation indices, these stucco body coats would have been highly durable in the face of the generally harsh sea

106. Eckel, Edwin C. *Cements, Limes, and Plasters*. New York: Robert Drummond, 1905. Print.
107. See elemental percentages in Highbridge draft report in Appendix C.

Sample	Location	Material	Masonry/ Substrate	Pozzolan type	Sand	Lime : Pozzolan	Lime: Sand	Cementation Index
M01a	Exterior rampart	Stucco body[1]	Sandstone	Volcanic ash	Natural sand	1 : 0.22	1 : 0.51	0.77
M01b	Exterior rampart	Stucco finish	Sandstone	Volcanic ash	Natural sand	1 : 0.19	1 : 0.25	0.28
M02	Exterior battlement	Mortar	Sandstone	Soft brick	"Beachrock"	1 : 1.9	1 : 0.69	0.63
M03a	Exterior latrine	Mortar	Brick	Soft brick	None	1 : 2.5	n/a	0.44
M03b	Exterior latrine	Stucco body	Brick	Soft brick	None	1 : 1.5	n/a	0.13
M04a	Exterior *cordón*	Stucco body (white)	Sandstone	Volcanic ash	Natural sand	1 : 0.18	1 : 0.13	0.80
M04b	Exterior *cordón*	Stucco body (pink)	Sandstone	Volcanic ash	Natural sand	1 : 0.26	1 : 0.64	0.22
M04c	Exterior *cordón*	Stucco finish	Sandstone	Harder brick	None	1 : 0.48	n/a	0.88
M05a	Interior wall	Plaster body	Brick	Soft brick	"Beachrock"	1 : 1.9	1 : 0.11	0.23
M05b	Interior wall	Plaster finish	Brick	None	Fine shells	n.d	n.d.	0.02

Table 2. Table of materials analysis results (Highbridge Materials Consulting, Inc.).

conditions, including a continuous presence of moisture, high concentrations of salts, severe wind-driven rains, and battering waves. The finish coat of the rampart (sample M01b), however, with a relatively lower cementation index of 0.28 would have been more of a sacrificial surface material. The proportion of natural sand, which was also present in all of the samples that contained trass, varied significantly between 16% and 48% by weight.

Masonry Materials with Soft Brick Pozzolans

By contrast, the mortar removed from the "beachrock" facing masonry (M02) and the brick masonry (M03a/b), as well as the interior plaster (M05a/b), contained crushed, low-fired brick as pozzolans instead of the trass. While the soft brick fragments provide the mortar and stucco with general cementitious characteristics, like binding strength and some hardness, they have on average a 55% lower cementation index than those that contain the trass. The quantity of low-fired brick additive varies in the samples from 64% (M02) to 85% (M03a) by weight. Given their concealed locations, these materials would not have been exposed to the same potentially damaging natural elements as the trass-containing samples discussed above. So, it is possible that a different pozzolan was used in these locations intentionally. The stark difference between the durability properties of these materials when compared to those that contained the trass additive, as well as the consistency with which they were used in the exposed vs. protected locations, seems to suggest that their use in this way was intentional. It may also be that the lower quality, less durable, and potentially less-expensive materials were selected to be used in the less critical parts of the construction.

It is interesting to note that the mortar and stucco samples from the latrine area (M03a/b) do not contain a natural sand aggregate like the other masonry materials with the soft brick pozzolans. In these samples, the crushed brick is instead functioning as the sole aggregate, contributing a tempering quality to the mortar and stucco in order to reduce shrinkage during curing. The absence of sand in a stucco or mortar is somewhat unusual and has not been documented previously by BCA.

Masonry Materials with Harder Brick Pozzolans

The material with the highest cementation index of the samples examined is the red finish coat at the *cordón* (M04c). This sample contains higher-fired brick inclusions mostly in a brick dust form, which would have had a greater pozzolanic effect on the lime than the low-fired brick materials. This results in a harder, denser stucco coat. Low-fired bricks are generally lighter-weight and less durable than higher-fired bricks, which are denser. Because of this density, they contain more alumino-silicates

to contribute to the pozzolanic reaction. They also break down more slowly, so the pozzolanic reaction can continue longer, creating a stronger, harder cementitious compound.

Masonry Materials with No Pozzolanic Additives
The only sample without any pozzolanic additives is the finish coat of the interior plaster (M05b). This sample also does not contain any aggregate, as is typical for historic plaster finish coats, and is closer to a pure lime plaster with 96.9% calcium oxide (CaO) by weight (the primary compound in lime).

Installation Chronology

Using both the archival and material analysis information, it is possible to hypothesize about the installation chronology for the various masonry materials at El Cañuelo. Since the photographic evidence shows that the samples came from locations that were not significantly damaged or repaired in the 20th century, there are at least some definitive dates before which these materials were installed.

The stone used for the foundation and structural components of the fort likely date to its construction in 1664. Although not specifically stated in any archival sources, the stone, particularly the limestone facing on the ramparts, was possibly locally quarried, perhaps even on Las Cabras. The material analysis included a comparative identification of a fragment of the facing stone, which showed that it was composed of the same material as the "beachrock" aggregate that were present in the mortar sample (M02) and interior stucco body sample (M05). This "beachrock," a variety of calcareous arenite that forms from the *in situ* cementation of beach sand, could be as geologically "new" as a few hundred years and is a common deposit on the northern shore of Puerto Rico.[108]

The bedding mortar for this facing stone would also likely date to the fort's original construction, as it is part of the building's structure. (Figure 188). The sample of mortar that was analyzed indicates that it was made with locally found



Figure 190. "Beachrock" facing stones with lime-brick mortar (Photograph by BCA).



Figure 191. Interior passageway with plaster-coated brick walls (Photograph by BCA).

materials including "beachrock" as the sand component and non-hydraulic, high-calcium lime.[109] This same composition was also used for the possibly contemporaneous interior stucco, albeit with a lower ratio of lime to sand (1:0.69 vs. 1:0.11). (Figure 189). The implication of this ratio difference is that since the mortar has a greater quantity of low-fired brick than the interior stucco, which acts as both a pozzolan and a temper, it is a harder and more durable material (cementation index: 0.63 vs. 0.23). This is appropriate since the mortar has a structural function whereas the interior stucco is neither structural nor requires durability to weathering.

As noted above, the exterior materials are more difficult to date through archival sources due to the frequent and probably often unrecorded repairs during the 234 years in which El Cañuelo was in use as either a Spanish military installation

108. Kaye, Clifford A. "Geology of the San Juan Metropolitan Area Puerto Rico." *Coastal Geology of Puerto Rico, Geological Survey Professional Paper 317-A.* Washington: United States Government Printing Office, 1959. Print.

109. Keyes Williamson, personal communication, February 15, 2017. The crushed brick would also likely have been a local product, although there is no documentation proving so.

or a lazaretto. There are several factors, however, that suggest that the exterior stucco materials do not date to the masonry fort's original 1664 construction and that they likely date to later repairs conducted during the period of use as a military installation (pre-1841), although the possibility remains that they could be restoration materials that date to after the site was transferred to the NPS (post-1949).

First of all, the sand used in the mortars and interior stuccos is different from those used in the exterior stuccos. The mortars and interior stuccos use the same sedimentary calcareous arenite aggregate found in the "beachrock" facing stone substrate and likely come from the same local source. The exterior stuccos, on the other hand, contain a natural sand aggregate that is an igneous andesite with either natural or added volcanic trass. Both of these materials could have been locally sourced and used at nearly any period of time. And although the finish coat of the *cordón* contains high-fired brick fragments, the analysis shows the brick fragments to be softer than bricks manufactured in the 20th century, meaning that they do not belong to modern repairs and were possibly applied at the same time as the lime-trass body coat.

Second, based on the petrographic examination of the exterior rampart stucco sample (M01), there appears to be a very small quantity of a lime-brick mixture in the pores of the facing stone below the current lime-trass stucco. Although it is very little evidence, its presence does suggest that a previous stucco material, possibly more in line with the lime-brick mortars and interior plasters, may have been previously used on the exterior and the extant stucco is a later installation.

Furthermore, conversations between BCA and current NPS staff demonstrate that they are committed to using locally sourced lime and sand for current masonry restoration projects at El Morro.[110] The fact that the NPS identified the stucco at El Cañuelo as a lime-based material in 1955 suggests that their knowledge of the historic materiality of the fort may have allowed this to be the modus operandi for previous repair and restoration projects for the exterior stucco.[111] The archival record notes multiple campaigns for re-stuccoing the exterior surfaces since 1949, the most recent major campaign being undertaken in 1994 with additional patching conducted as late as 2008.[112] Therefore, it is possible that the extant exterior stucco materials, particularly at the rampart, may be modern repairs by the NPS using historically accurate materials.

The use of trass in the exterior stucco at El Cañuelo is also interesting to consider. Its use may represent one of three possibilities.[113] First, the fineness of the trass lends itself to the interpretation that it is a natural inclusion of the sand that was used in these stuccos and therefore its presence may simply be coincidental and the builders may not have known the pozzolanic properties. While the geology of Puerto Rico contains abundant quantities of volcanic materials, further analysis is required to determine if the trass contained in the El Cañuelo construction materials has a local provenience. This interpretation is not likely because of the apparent intent of using stuccos with this particular additive only on the exterior of the fort. Second, it is possible that the trass was either a locally quarried material or a natural inclusion of the sand and it was known that either the trass itself or the sand from this particular location had a pozzolanic effect. In this instance, the intent to use the trass in the exterior stuccos for enhanced durability is clear. Third, the trass may have been an imported product from Europe that was selected for its particular pozzolanic effect. The justification for this interpretation is based on limited optical identification of the trass as rhyolitic whereas the volcanic rocks from San Juan are reported to be andesitic.[114] The interpretation of intentional usage and the geological identification of the trass

110. According to the NPS, the sand is sourced from Isabela in northwest Puerto Rico.

111. Lessing, Charles W. "The Fort of El Cañuelo." *Historic American Building Survey: PR-52*. Washington D.C.: National Park Service, 1955. Print. As a note, some repairs conducted by the National Park Service, notably capping at the terreplein in 1992 and structural crack repairs in 2008, did use incompatible Portland cement materials.

112. From WLA Studio's archival research notes; two of the documented repair campaigns for the exterior stucco note that "matching" or "lime based" materials were used.

113. These three possibilities assume that the exterior stucco was applied at some point during the Spanish military service life of the fort (1664-1875).

114. Kaye, Clifford A. "Geology of the San Juan Metropolitan Area Puerto Rico." *Coastal Geology of Puerto Rico, Geological Survey Professional Paper 317-A.* Washington: United States Government Printing Office, 1959. Print.

favor the third interpretation, although no archival information to support this theory is available.

Conclusions

The analysis performed on the masonry materials of El Cañuelo provides thorough documentation of the materials used historically on the fort. More importantly, however, it provides new and exciting information on Spanish Colonial mortar materials. As such, the authors feel that this research is significant and represents a new contribution to the historic preservation field. The use of pozzolanic additives by people working on the fort originally and subsequently, most likely intentionally, is an important aspect of Spanish Colonial fort construction to document. Understanding these historic materials and their physical characteristics is also important for informing the development of appropriate restoration materials to be used in upcoming repair and restoration efforts by the NPS.

Unfortunately, the results of this materials analysis demonstrate that it is not possible to determine exactly when the extant masonry materials were applied to El Cañuelo. However, some general conclusions can be drawn about the relative chronology of their application.

In terms of historical masonry materials that could date to the fort's period of Spanish Colonial military use, only the structural components including foundation, rubble and ashlar walls, and facing stones can be attributed to the 1664 construction with relative confidence based on archival sources. The lime mortar, as a structural material, could also date to this period.

While it is not possible to date the interior plaster, the fact that it contains low-fired brick pozzolanic inclusions similar to the mortar, suggests that it also has an early installation date.

The exterior stucco materials, including those on the ramparts and *cordón*, are even more difficult to definitively date. However, the evidence supports their installation as part of later repair campaigns during the fort's period of Spanish military use (1664-1841).

Documentation of Repair Chronologies

Sample M01: Sample location of exterior stucco on northeast rampart. Elevation appears to be in an area that has not been altered after 1962. Some adjacent graffiti is present, visible beginning in the 1998 photograph, but the sample was taken below this. (Figure 186, Figure 192, Figure 193, Figure 194, Figure 195, Figure 196).



Figure 194. M01 sample location, pre-1962 (Courtesy of General Archives of Puerto Rico).



Figure 192. M01 sample location, northeast rampart (Photograph by BCA).



Figure 195. M01 sample location, 2008 (Courtesy of Section 106 survey).

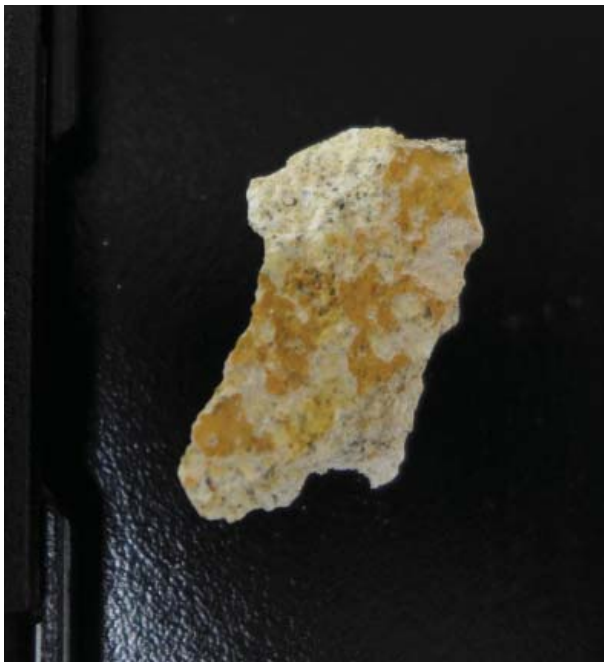


Figure 193. Sample M01, rampart stucco (Photograph by BCA).



Figure 196. M01 sample location, 2016 (Photograph by BCA).

Sample M02: Sample location of facing stone mortar on inside of northwest battlement. Although substantial biological materials have grown in the area of this sample, no significant damage or restoration campaigns have affected the mortar. (Figure 187, Figure 197, Figure 198, Figure 199, Figure 200).



Figure 197. M02 sample location; northwest battlement (Photograph by BCA).



Figure 199. M02 sample location, 2008 (Courtesy of Section 106 survey).



Figure 198. Sample M02, bedding mortar (Photograph by BCA).



Figure 200. M02 sample location, 2016 (Photograph by BCA).

Sample M03a/b: No archival photographs of this sample location have been found. (Figure 187, Figure 201, Figure 202).



Figure 201. M03a sample location; northwest latrine (Photograph by BCA).



Figure 202. Sample M03b, latrine stucco (Photograph by BCA).

Sample M04a/b: Sample location of cordón stucco on southwest elevation. 1930 and 1998 photograph both show biological material at the sample location, which appears to have caused adjacent damage to the cordón. While cleared by 2008, some of the biological materials seems to have reappeared by 2016. However, the biological material does not seem to have affected the specific sample location and no repairs appear to have been made there either. (Figure 188, Figure 203, Figure 204, Figure 205, Figure 206, Figure 207, Figure 208, Figure 209).



Figure 203. M04 sample location; southeast cordón (Photograph by BCA).



Figure 204. Sample M04a, cordón stucco (Photograph by BCA).



Figure 205. M04 sample location, c. 1930 (Courtesy of General Archives of Puerto Rico).



Figure 208. M04 sample location, 2012 (Courtesy of National Park Service, San Juan National Historic Site).



Figure 206. M04 sample location, 1998 (Courtesy of Historic American Building Survey).



Figure 209. M04 sample location, 2016 (Photograph by BCA).



Figure 207. M04 sample location, 2008 (Courtesy of Section 106 survey).

Sample M05a/b: No archival photographs of this sample location have been found. (Figure 189, Figure 210, Figure 211, Figure 212).



Figure 210. M05 sample location; interior passage wall (Photograph by BCA).



Figure 211. Sample M05a, interior stucco body (Photograph by BCA).



Figure 212. Sample M05b, interior stucco finish (Photograph by BCA).

I.D Significance and Integrity

San Juan National Historic Site Purpose and Significance

Purpose

The purpose of San Juan National Historic Site is to preserve the Spanish fortifications, buildings, and the related archeological sites and historic objects for the education, benefit, and inspiration of present and future generations.

Significance

The fortifications in San Juan are the best-preserved element from the Spanish Crown's grand colonial defense system. They are premier examples of military engineering and architectural design. They are one of the finest examples of coastal and land defense systems in the world. Over the centuries of construction and use (1533-1897, Spain, 1898-1961, United States), as new technology developed or a need was identified, the fortifications were changed. Each of these changes was a product of its time and served a particular need in the overall defense mission.[111]

Significance Criteria

The National Register of Historic Places Criteria for Evaluation states:

> The quality of significance in American history, architecture, archeology, engineering, and culture is present in districts, sites, buildings, structures, and objects that possess integrity of location, design, setting, materials, workmanship, feeling, and association, and:
>
> A) That are associated with events that have made a significant contribution to the broad patterns of our history; or
> B) That are associated with the lives of persons significant in our past; or
> C) That embody the distinctive characteristics of a type, period, or method of construction, or that represent the work of a master, or that possess high artistic values, or that represent a significant and distinguishable entity whose components may lack individual distinction; or
> D) That has yielded, or may be likely to yield, information important in prehistory or history.

National Register Significance Evaluation

San Juan National Historic Site was listed on the National Register of Historic Places on October 15, 1966 under the National Historic Preservation Act. Documentation of San Juan National Historic Site was added to the National Register of Historic Places in 1973. El Cañuelo is included as a significant building of the "First Order of Significance." The entire site was listed with a period of significance from 1539 to 1945. The areas of significance include History, Architecture, Engineering, and Military.

San Juan National Historic Site broadly recognizes two periods of significance in its current management of historic resources: Spanish Period from 1533-1897 and United States Period 1898-1961. It was during this first period that El Cañuelo achieved the characteristics that make it eligible for listing on the National Register of Historic Places. This is the primary period of significance.

Character-Defining Features

Character-defining features are those physical features that give a historic building its character and contribute to its historic significance. Character-defining features can include a building's form, materials, craftsmanship, individual features, and setting.

The determination of whether the feature is a contributing feature is based on its existence during the primary period of significance, the Spanish Period (1533-1897). Resources dating to the secondary period of significance, United States Period (1898-1961) are also noted below. Features noted as non-contributing may be more recent additions to the building, some of which may not necessarily detract from the historic character of the building.

El Cañuelo: Site

The outstanding, character-defining feature of the

111. San Juan National Historic Site, "Long Range Interpretive Plan," (San Juan: National Park Service, 2006), 15.

site during this primary period of significance was the island setting. From its earliest construction in 1644 until 1943, the existing fort occupied a low-lying landmass isolated in the shallow waters on the west edge of the Bay of San Juan.

During the secondary period of significance, the United States Army constructed a landmass combining El Cañuelo Island and Las Cabras Island. This landmass connects via a causeway to the mainland. This event occurred in 1943. The contours of this landmass have changed dramatically since 1943. The shoreline of the island, in particular its eastern shore in the vicinity of El Cañuelo, has experienced extreme erosion due to waves and storms. Today, a constructed rock breakwater roughly outlines the original extents of the 1943 landmass.

Between 1949 and 1961, NPS constructed numerous site amenities to facilitate interpretation of the site. These included picnic facilities, restroom facilities, and planted vegetation. Only a few of the planted trees, including four coccoloba trees and a few coconut palms remain from that designed landscape. Subsequent additions to the site include a parking lot west of the access road to the island, new interpretive signs, new picnic pavilions, and new site furnishings.

The view across the bay towards San Juan and El Morro conveys the historic separation from the city that was a characteristic of the setting and feeling during both periods of significance.

Consequentially, the landscape has severely diminished integrity from the primary period and diminished integrity from the secondary period.

It is difficult for a visitor to comprehend the original character of El Cañuelo as an island without interpretation; which NPS provides in the on-site signage. Even so, the outline of the landmass has eroded significantly since its original construction and continues to erode. The addition of the parking lot and modern picnic facilities are modern intrusions that further diminish the integrity of the site from this secondary period.

El Cañuelo: Building

El Cañuelo retains the character-defining features associated with its design and use as a fort (1644-1785) and its later remodeling for use as a lazaretto (1841-c.1877) during the Spanish Period (1533-1897). The building's changing use during this period reflects both developments in defensive technology that rendered the fort obsolete and the Spanish Colonial practice of adapting and building on to existing structures to accommodate productive reuse. The entirety of the building's construction and use occurred during the Spanish Period and it likely suffered deterioration during the two decades of abandonment at the end of this period.

The fort was abandoned and in ruins during the United States Period (1898-1961), suffering from neglect and loss of historic fabric during the first 45 years of this period. A period of accelerated deterioration during the 1930s saw the loss of most of the remaining superstructure. Limited repairs in the mid-twentieth century appear to have removed some remaining sections of Spanish Period features, including remnants of the superstructure, while attempting to stabilize the building as a ruin suitable for interpretation. Repairs during the United States Period were followed by similar piecemeal patching, mothballing (pre-1986, 1992), and tourist access improvements (1962, 2012) over subsequent decades.

Character-defining exterior features include the battered exterior walls with their ashlar face, stucco coating with integral color, false joints, and *cordón*; the battlements with embrasures along the north elevation and portions of the east and west; the sentry box on the northeast corner; the latrine; the kitchen's *fogón*; and paving materials on the terreplein (now concealed by the 1992 concrete slab). The interior appears to retain its original configuration, with character-defining features including barrel-vaulted ceilings, plastered walls, a masonry staircase, and brick paver and lime cement flooring.

Because El Cañuelo saw the entirely of its construction and use during the Spanish Period and only deterioration and limited repairs during the United States Period, the building itself did not acquire new features or significance during the latter period. This is in contrast to the site, where significant development occurred during the secondary period. For this reason, the building's significance is limited to the Spanish Period. Deterioration and limited repairs during the secondary period have diminished the building's

integrity from the primary period. Most of its character-defining features retain a moderate degree of integrity to the period, reflecting the building's long period of abandonment and neglect.

Much of the building's loss of integrity, including deterioration and repair of masonry, stucco, and plaster, is characteristic of most Spanish Period resources in the San Juan National Historic Site and must be considered in context. For example, historic photographs show that the Devil's Sentry Box and the associated San Carlos Ravelin at Castillo San Cristóbal suffered extreme deterioration followed by extensive repairs. Other sections of Castillo San Cristóbal, El Morro, the City Walls, and Fort San Gerónimo de Boquerón have seen significant repairs, restoration, and reconstruction since 1898, with many projects ongoing or repeated in kind since the United States Period. Although it runs counter to conventional notions of integrity, ongoing deterioration and continuous repairs could be seen as character-defining features of the coastal fortifications of the San Juan National Historic Site

Assessment of Integrity

The assessment of integrity involves the evaluation of the existing condition of features that date to the period of significance. The National Register of Historic Places defines seven aspects of integrity: location, design, setting, materials, workmanship, feeling, and association. The National Register Bulletin, *How to Apply the National Register Criteria for Evaluation* states:

Location is the place where the historic property was constructed or the place where the historic event occurred.

Design is the combination of elements that create the form, plan, space, structure, and style of a property.

Setting is the physical environment of a historic property.

Materials are the physical elements that were combined or deposited during a particular period of time and in a particular pattern or configuration to form a historic property.

Workmanship is the physical evidence of the crafts of a particular culture or people during any given period in history or prehistory.

Feeling is a property's expression of the aesthetic or historic sense of a particular period of time.

Association is the direct link between an important historic event or person and a historic property.

A Property must retain the essential physical features that convey its historic significance. The essential physical features of a structure or property are those that demonstrate why a property is historically significant and when it was significant. The National Register Bulletin, *How to Apply the National Register Criteria for Evaluation* defines integrity as "the ability of a property to convey its significance."

Integrity of Location

El Cañuelo retains a high degree of location. The location of the structure has not changed since it was originally constructed in 1664.

Integrity of Design

El Cañuelo retains a high degree of design, despite modifications over the centuries. The form, components, and features are relatively intact from its original construction in 1664, reflecting the structure's original function (during the period 1664-1785) as a fort. The lazaretto additions built on the terreplein in the 1840s lack integrity of design, surviving only as fragmentary ruins.

Integrity of Setting

El Cañuelo exhibits a moderate degree of integrity of setting. In the 1940s, the United States military constructed a land mass around the fort, which was originally an isolated island sitting in the middle of the bay. About half of the building is still surrounded by water. The remaining elevations look over a maintained lawn with trees. More recent changes include the addition of a parking lot and public park within the viewshed of the fort. However, the most significant view from the fort is across the bay towards El Morro. This view is very similar to what it would have been during the period of significance.

Integrity of Materials and Workmanship

El Cañuelo retains a high degree of materials and

workmanship. Some features from the period of significance are missing or have been altered, but the majority of original materials remain. Non-original materials include new doors, stairs, and render.

Integrity of Feeling

El Cañuelo retains a high degree of integrity of feeling. The fort conveys its character and use as a Spanish colonial coastal fortification.

Integrity of Association

El Cañuelo retains a high degree of association with Spanish colonization and the construction of defenses to protect San Juan, Puerto Rico.

II Treatment and Use

San Juan National Historic Site Preservation Philosophy

The 1985 San Juan National Historic Site General Management Plan states:

> The fortifications of San Juan must be viewed as a historic district that has evolved over time, beginning with the earliest construction of La Fortaleza in 1533, following with the construction of El Morro in 1540, and extending up to the transference of a major portion of the site to the Department of the Interior in 1961. This evolution of all the major components (El Morro, San Cristóbal, El Cañuelo, the walls and bastions, and the San Cristóbal outworks), including the structural modifications that have been undertaken, contributes significantly to the overall story of the fortifications of Old San Juan. Over the centuries of construction and use, the fortifications have remained one of the finest examples of coastal and land defense systems in the world. As new technology was developed or a need was identified, the fortifications were changed. Each of these changes was a product of its time, and each served a particular need in the overall defense mission. Therefore, the final result of these changes should be preserved so that the whole story can be told to the millions of visitors who come each year. The changes that have taken place are evidence of the history and development of the fortifications and their environment, and they are significant in their own right.
>
> To restore all or portions of San Juan [National Historic Site] to a particular period or periods would be a costly and questionable undertaking. Restoration may impair or destroy the original fabric, and despite research, the replacement of missing fabric or elements must be based on conjecture. Past experience at San Juan and at other historic sites has demonstrated that comprehensive or substantial modifications, extensive restoration treatments, or ill-advised large-scale reconstruction projects have harmed more resources than they have preserved. In addition, the expense of such actions has been considerable.
>
> Therefore, the National Park Service will preserve the San Juan fortifications in their existing form, retaining as closely as possible their appearance between 1949 and 1961, the period during which the facilities were last used for military purposes. This preservation philosophy is consistent with sound cultural resource management standards, and it fully meets the NPS mandate to perpetuate in an unimpaired condition the cultural resources within the national park system. The adoption of this preservation philosophy has the following implications.
>
> - Missing historic fabric will not be reconstructed except when it is determined through the preservation maintenance program… that reconstruction is necessary to ensure the structural stability of the fortifications.
>
> - No physical alterations will be undertaken to provide for adaptive use of the casemates or other interior spaces, or to provide handicapped visitor access of for visitor safety, if it is determined that such actions will impair the significant architectural features or structural system of the fortifications.
>
> - Interior spaces will generally not be restored unless it is absolutely necessary to help convey an interpretive theme.

Alternatives for Treatment and Use

NPS considers four major treatment options for historic structures: Preservation, Rehabilitation, Restoration, and Reconstruction. NPS defines the four treatments as:

Preservation is defined as the act or process of applying measures necessary to sustain the existing form, integrity, and materials of an historic property. Work, including preliminary measures to protect and stabilize the property, generally focuses upon the ongoing maintenance and repair of historic materials and features rather than extensive replacement and new construction. New exterior additions are not within the scope of this treatment; however, the limited and sensitive upgrading of mechanical, electrical, and plumbing systems and other code-required work to make properties functional is appropriate within a preservation project.

Rehabilitation is defined as the act or process of making possible a compatible use for a property through repair, alterations, and additions while preserving those portions or features, which convey its historical, cultural, or architectural values

Restoration is defined as the act or process of accurately depicting the form, features, and character of a property as it appeared at a particular period of time by means of the removal of features from other periods in its history and reconstruction of missing features from the restoration period. The limited and sensitive upgrading of mechanical, electrical, and plumbing systems and other code-required work to make properties functional is appropriate within a restoration project.

Reconstruction is defined as the act or process of depicting, by means of new construction, the form, features, and detailing of a non-surviving site, landscape, building, structure, or object for the purpose of replicating its appearance at a specific period of time and in its historic location.

Requirements for Treatment and Use

NPS has policies that direct the implementation of treatment recommendations and use of historic structures at the National Parks. Key laws, regulations, and functional requirements that apply to the following treatment recommendations include:

National Park Service Cultural Resources Management Guideline (Director's Order 28) that requires planning for the protection of cultural resources on NPS property.

Section 106 of the National Historic Preservation Act that mandates that federal agencies take into account the effects of their actions of properties listed or eligible for listing on the National Register of Historic Places.

The Secretary of the Interior's Standards for the Treatment of Historic Properties with Guidelines for the Treatment of Cultural Landscapes.

Americans with Disabilities Act (ADA)

International Building Code (IBC)

International Existing Building Code (IEBC)

The IEBC contains this statement on Historic Buildings:

> The provisions of this code relating to construction, repair, alteration, addition, restoration and movement of structures, and change of occupancy shall not be mandatory for historic buildings where such buildings are judged by the building official to not constitute a distinct life safety hazard.

When undertaking repairs to El Cañuelo, the NPS should strive to comply with model building code standards. NPS Denver Service Center for design and construction uses the International Building Code as its standard.

Ultimate Treatment and Use

The following treatment recommendations were developed in accordance with The Secretary of the Interior's Standards for Preservation (37 CFR 68) and the Guidelines for Implementing Preservation.

As discussed in the Structural Analysis section of the Part I. C-Physical Description, there are unresolved questions that complicate the consideration of treatment recommendations. Additional data on the subsurface conditions would potentially show if failure in the subgrade, such as settlement, is contributing to the

cracking of the walls. Similarly, additional data on the composition of the backfill and the water content of the backfill would help determine if lateral forces placed on the interior of the walls is causing the cracking. Further analysis is critical for understanding the causes of the cracking in the wall. Completing these actions are necessary to determine proper treatments and repairs. These steps are outlined in the following Recommendations for Additional Research.

It is the consensus of the project team that the infiltration of water through the concrete cap has a negative impact on the structure. One of the priorities of the following treatment recommendations is to prevent water flow into the back fill.

Another factor complicating treatment recommendations is the lack of documentary and physical evidence that would support the reconstruction or restoration of missing features. If additional research discovered sufficient documentation to permit an accurate reconstruction of the missing lazaretto structure, it would assist in interpreting another layer in the structure's history. More importantly, the lazaretto structure would also provide the benefit of having a roof over much of the fort's terreplein, thereby protecting it from the negative effects associated with rainfall. The arguments against reconstructing the lazaretto include lack of information, cost, the fact that the primary use of the structure was as a military resource, and the added weight of the superstructure.

For these reasons, preservation, which involves sustaining the building in its existing form, is the most appropriate treatment for El Cañuelo. Preservation is appropriate because it provides for immediate stabilization of the building. Preservation provides a public benefit by continuing to preserve El Cañuelo and its association with the military history of Spanish colonialization of Puerto Rico. Preservation also provides for the retention of features remaining from the lazaretto, allowing the NPS to continue to present multiple eras of the structure's history. Preservation is also the most cost effective of the treatment options and the only treatment option supported by historical documentation. A preservation treatment would not preclude removal of the 1992 concrete cap.

Rehabilitation is the appropriate treatment for the landscape associated with El Cañuelo because of the National Park Service mission to provide interpretation and visitor access. Rehabilitation will also allow for the addition of material around the foundation of the fort to protect it from the destructive forces of wave action and rising sea levels.

The Secretary of the Interior's Standards for Preservation

1. A property will be used as it was historically, or be given a new use that maximizes the retention of distinctive materials, features, spaces, and spatial relationships. Where a treatment and use have not been identified, a property will be protected and, if necessary, stabilized until additional work may be undertaken.
2. The historic character of a property will be retained and preserved. The replacement of intact or repairable historic materials or alteration of features, spaces and spatial relationships that characterize a property will be avoided.
3. Each property will be recognized as a physical record of its time, place, and use. Work needed to stabilize, consolidate, and conserve existing historic materials and features will be physically and visually compatible, identifiable upon close inspection and properly documented for future research.
4. Changes to a property that have acquired historic significance in their own right will be retained and preserved.
5. Distinctive materials, features, finishes and construction techniques or examples of craftsmanship that characterize a property will be preserved.
6. The existing condition of historic features will be evaluated to determine the appropriate level of intervention needed. Where the severity of deterioration requires repair or limited replacement of a distinctive feature, the new material will match the old in composition, design, color, and texture.
7. Chemical or physical treatments, if appropriate, will be undertaken using the gentlest means possible. Treatments that cause damage to historic materials will not

be used.

8. Archeological resources will be protected and preserved in place. If such resources must be disturbed, mitigation measures will be undertaken

The Secretary of the Interior's Standards for Rehabilitation

1. A property shall be used for its historic purpose or be placed in a new use that requires minimal change to the defining characteristics of the building and its site and environments.
2. The historic character of a property shall be retained and preserved. The removal of historic materials or alteration of features and spaces that characterize a property shall be avoided.
3. Each property shall be recognized as a physical record of its time, place, and use. Changes that create a false sense of historical development, such as adding conjectural features or architectural elements from other buildings, shall not be undertaken.
4. Most properties change over time; those changes that have acquired historic significance in their own right shall be retained or preserved.
5. Distinctive materials, features, finishes and construction techniques or examples of craftsmanship that characterize a property will be preserved.
6. Deteriorated historic features shall be repaired rather than replaced. Where the severity of deterioration requires replacement of a distinctive feature, the new feature shall match the old in design, color, texture, and other visual qualities and, where possible, materials. Replacement of missing features shall be substantiated by documentary, physical, or pictorial evidence.
7. Chemical or physical treatments, such as sandblasting, that cause damage to historic materials shall not be used. The surface cleaning of structures, if appropriate, shall be undertaken using the gentlest means possible.
8. Significant archeological resources affected by a project shall be protected and preserved. If such resources must be disturbed, mitigation measures shall be undertaken.
9. New additions, exterior alterations, or related new construction shall not destroy historic materials that characterize the property. The new work shall be differentiated from the old and shall be compatible with the massing, size, scale, and architectural features to protect the historic integrity of the property and its environment.
10. New additions and adjacent or related new construction shall be undertaken in such a manner that if removed in the future, the essential form and integrity of the historic property and its environment would be unimpaired.

Prioritization of Treatment Recommendations

Two levels of treatment have been developed for the stabilization and preservation of El Cañuelo: **Immediate** temporary stabilization and **Long-Term** restoration for active interpretation. These treatments build in intensity and cost and could be completed in sequence. The temporary stabilization would not preclude work proposed in the long-term treatment.

The existing concrete cap, installed in 1992, is causing two simultaneous negative effects on the structure: it is failing to prevent moisture infiltration as intended while also preventing water evaporation from the structure's interior fill material. These effects have caused saturation of the structure's interior fill material, increasing the forces pushing out on the exterior walls. These treatments are designed to address the ongoing water infiltration and saturation issues that currently threaten the integrity of El Cañuelo.

Level 1 - Immediate

This level of treatment should be regarded as temporary stabilization, doing the minimum repair work necessary to slow the ongoing deterioration of the structure until funding for the long-term repairs can be secured. This stabilization treatment includes minimal repairs of the building shell and temporary treatments to facilitate moisture migration out of the structure's interior fill. This temporary stabilization treatment should be anticipated to last three to five years, assuming

adequate maintenance and barring natural disasters, but should not be expected to last longer.

1. Remove all plant growth from walls, ramparts and cordon, and terreplein surfaces. Clean all stone masonry surfaces with D/2 Biological Solution or another appropriate cleaner. Test patches should be prepared to evaluate the effects of any cleaner before use on the entire structure. Refer to Appendix D for material product information and safety data for D/2 Biological Solution.
2. Clean existing joint at perimeter of concrete cap on terreplein and stone masonry rampart using hand tools taking care not to damage stone masonry surfaces. Fill large gaps and voids with sand. Install closed-cell foam backer rod into the joint and fill remainder of joint with a polyurethane sealant to form a flexible, watertight seal. Tool sealant to create positive drainage away from masonry ramparts. Refer to Appendix D for material product information and safety data for closed-cell foam backer rod and polyurethane sealant. Refer to Appendix E for detail sketch.
3. Clean open joints and cracks in masonry walls, and ramparts, cordon, and sentry box (garita) surfaces using hand tools taking care not to damage underlying stone and brick masonry surfaces. Prior to repointing, fill large gaps and voids with sand. Repoint open joints and cracks in masonry walls and rampart surfaces with Repair Mix #1, refer to Repair Mortar, Stucco, and Plaster Mixes below for composition, paying the particular attention to the interior and exterior stucco surfaces of the sentry box and the wall below the latrine.
4. Install movement gauges over the major cracks in masonry walls and rampart and cordón surfaces and establish a cyclical monitoring program. Record gauge readings and dates in a table or database. Refer to Appendix D for product information.
    - Most cracks can be monitored using gauges that record movement in X and Y directions, including the Avonguard "Standard Tell-Tell," Crackmon "4020A Crack Monitor," Avonguard "Plus Tell-Tell," and Crackmon "XL 150450A." The crack monitor for each location shall be selected based on the size of the crack to be monitored.
    - Locations where cracks need to be monitored for out of plane movement in the Z direction should be monitored using the Avonguard "Displacement Tell-Tell" or the Crackmon "3D XYZ-Axis Crack Monitor."
    - To monitor the large crack in Room 104:
        - Fabricate two sheets of acrylic and epoxy and bolt onto each end of the selected crack monitor.
        - Attach the sheets to the masonry wall on either side of the crack with epoxy and screws.
5. Repair/replace existing access hatch on concrete cap on terreplein and ensure proper operation. Refer to Appendix D for product information.
6. In select locations, core drill vertically through the existing concrete cap, vapor barrier, and compacted sand down to the historic terreplein surfaces, including the area above the cistern. Install low-profile passive or solar-powered vents, set on curbs, over drill holes to facilitate moisture vapor transmission from terreplein surface and interior mass. Care should be taken to minimize damage to historic terreplein surfaces during drilling operations. Refer to Appendix D for Product Information and Appendix E for detail sketch.
7. Install a termite "barrier" and a termite baiting system.
    - Treat the ground along the base of the masonry walls surfaces by injecting a liquid termite "barrier." Barrier termite treatments are designed to prevent termites from entering a structure. These treatments will also prevent termites inside the structure from getting to the soil to get the moisture needed to

survive. Nonrepellent products are undetectable by termites. The termites cannot see, smell, taste or avoid them. However, currently available chemical barrier pesticides are very short lived, in some cases, no more than 5-8 years and, considering that termites can tunnel through small untreated gaps in the soil as thin as a pencil lead, the use of a chemical barrier treatment should be augmented by baits designed for termites. The structure's proximity to water needs to be considered when treating with insecticides, many of which are toxic to aquatic life. NPS should consult with a local pest control experienced applying insecticides prior to application. A local pest control expert should be able to identify an insecticide appropriate for use in this location.

- There are various baiting systems for termites on the market. Termite baits can be set directly into the ground base around the base of the masonry walls surfaces which the termites will find, feed on and die. Termite baits alone could be used if there is concern about injecting the soil termiticides into the soil in close proximity to the bay. Refer to Appendix D for material product information and safety data.

8. Because use of insecticide may be limited because of its setting, it is recommended that all wooden features be removed and replaced with pressure-treated wood rated for ground contact.
9. Consider ground-penetrating radar (GPR) to look for voids and features within the walls and interior fill.[163]

Level 2 - Long-Term

Because El Cañuelo did not remain in military use as long as the other forts in the San Juan National Historic Site, it lacks later contributing alterations—notably those dating from the 1840s through the 1940s—and could potentially be restored to an earlier appearance to provide a distinct dimension of interpretation not currently present within the San Juan National Historic Site. This is a unique opportunity within the San Juan National Historic Site and could generate greater interest in the site in spite of its distance from other sites in Old San Juan. However, further investigation of the building's evolution would be necessary before a specific restoration period and treatment could be determined. This would likely include archaeological investigation of the terreplein, ground-penetrating radar studies of the interior fill, and examination of the cistern.

The Level 2 preservation treatments should be designed to address all current concerns, including removal of the concrete cap and repair of the historic drainage system, while permitting the building to be open for interpretation. These treatments would be designed for public access and allow the structure to operate with regular maintenance for approximately 20 years before any major rehabilitation work would be anticipated, barring natural disasters.

Testing and planning for the implementation of these treatments should begin immediately. Implementation should occur as soon as possible.

1. Install energy-absorbing rip-rap around the perimeter of the stone apron at base of the masonry walls surfaces. The height of the rip-rap to be determined based on analysis of the mean high spring tide, storm surge, and wave heights. Smaller core stones should be placed as a base and to act as a filter layer then covered with the larger armor stones. Consider the installation of steel sheet piles at the edge as an option to help stabilize the armor stones. Consider consultation with a local civil or marine engineer experienced in local bank protection.
2. Improve walking surface atop rip-rap surface around fort's foundation by mortaring the stones in place or installing a concrete or wood walkway on top.
3. Remove the existing access hatch and stairway. Remove the existing post and cable railing and the concrete cap, vapor barrier, and compacted sand down to the

163. A proposal to conduct GPR investigation was submitted to NPS as a part of this project but this work was not accepted.

historic terreplein surfaces.

4. Once the terreplein surface is exposed, the NPS should have a thorough condition assessment of the exposed surface to inform future work. (See following Recommendation #5.)
5. Our intention is that once the terreplein surface is exposed, large pieces of rubble should be removed, both to allow surface repair but also to allow large voids to be filled with a compactible material to create a walkable surface using materials and procedures developed for other resources within the San Juan National Historic Site. Install new post and cable railing around the stair hatch opening and a matching railing or a cover at the restored cistern opening. Repair historic terreplein drainage system and cistern overflow drain to manage rainwater.
6. Construct new stair leading from the entry on the East Elevation to the stabilized terreplein surface level and install new operable hatch for security.
7. Install a full stucco coating as a waterproofing system for the horizontal surfaces of the stone masonry ramparts and cordón to prevent water from penetrating between the outer and inner faces of the masonry walls. The stucco coating of the ramparts and cordón should use Repair Mix #2 or #3. Refer to Repair Mortar, Stucco, and Plaster Mixes below.
8. Fill remaining losses (cracks and voids) in all masonry walls and rampart and cordón surfaces using appropriate coating mixes established by additional material investigation and analysis.
9. Pack large crack in Room 104 with sand. Finish patch surface with Repair Mix #5; refer to Repair Mortar, Stucco, and Plaster Mixes below for composition.
10. Clean and preserve existing plaster wall and ceiling surfaces within Rooms 100, 101, 102, 103, and 104. Patch cracks, fill voids and refinish deteriorated plaster wall and ceiling surfaces with Repair Mix #5; refer to Repair Mortar, Stucco, and Plaster Mixes below for composition.

Repair Mortar, Stucco, and Plaster Mixes

Provided below are BCA's recommendations for replication mixes to be used for repair of the historic mortars and stuccos at El Cañuelo. These recommendations are based on field and laboratory observations by BCA and the petrographic and chemical analysis of mortar and stucco samples, conducted in February 2017 by Highbridge Materials Consulting (HMC). The repair mixes take into consideration the results of the analysis, modern standards for lime-based mortars and stuccos, as well as performance and aesthetic factors. These replication mixes utilize historically appropriate materials that are in line with the preservation philosophy to preserve and stabilize the fort, as it exists today.

The analysis by HMC showed that all of the mortar and stucco samples contain high-calcium lime with various materials acting as aggregates, pozzolans, and pigmenting agents. Based on this, BCA recommends that a similar high-calcium lime binder be used for all of the repair mortars and stuccos. It is understood that SAJU prepares their own lime putty for repair projects.[164] As long as this lime putty is derived from a quicklime containing 0%-5% magnesium carbonate,[165] it is appropriate for use as a high-calcium lime binder for the repair of the mortars and stuccos at El Cañuelo. Although BCA's recommended repair mortar and stucco mixes are based on high-calcium lime putty, a natural hydraulic lime (NHL) could also be considered instead of the high-calcium lime. NHLs have characteristics similar to those of pure lime mortars (lime putty) including permeability, moderate compressive strength, and good flexural strength, but they cure relatively quickly and can cure in the presence of moisture, reducing potentially problematic shrinkage issues. These characteristics would be beneficial at a site like El Cañuelo. If the use of hydraulic lime-based repair materials is of interest to the NPS, then BCA can provide recommended mixes based on this alternate binder, since the overall ingredient ratios would be different than what is included below.

164. Lopez, Felix. Personal interview. 2 November 2016.
165. National Lime Association. "FAQs: Terminology & Specifications." National Lime Association, http://lime.org/about-us/faqs/. Accessed 17 May 2017.

The replacement sands and pozzolans should match the particle size, distribution, and color of these materials in the original samples as closely as possible.[166] This information is included in the full materials analysis report from HMC, which has been included as an appendix to this report. The replacement sands should also conform to the requirements of ASTM C144 Standard Specification for Aggregate for Masonry Mortar.

The recommended components alone should yield appropriately colored and textured replication mortars and stuccos; they should not require supplementary pigmentation or additives. However, BCA recommends the creation of samples by the NPS or selected contractor in order to confirm visual and textural matches to the existing materials. These repair materials are recommended only for use to restore or repair the specified existing materials. BCA cannot assure their effectiveness or performance for other applications.

Repair Mix #1: Exterior Sandstone Mortar, Exterior Brick Mortar, Exterior Brick Stucco, and Interior Plaster Base Coat

The two mortar samples, from the exterior sandstone and the exterior brick, as well as the stucco from the exterior brick and the plaster base coat at the interior can all utilize the same repair mix. These four materials were all identified during the analysis as containing a high- calcium lime binder with crudely disaggregated soft brick acting as aggregate, pozzolan, and pigmenting agent. Each contains approximately the same ratio of binder to brick aggregate.

For this repair mortar and stucco mix, the following materials should be used at the specified ratio (by volume):

Binder: 1 part high-calcium lime binder

Aggregate/Pozzolanic Additive: 2 parts low-fired brick fragments (conforming to the size and distribution of the original material as documented in sections 6.1, 6.2, and 7.5 of the HMC full report)

Repair Mix #2: Rampart Stucco Body Coat and Cordón Stucco Body Coat

The stucco bodies at the rampart and cordón can both utilize the same repair mix. These two materials were identified during the analysis as containing a high-calcium lime binder with natural sand aggregate and a volcanic ash (trass) pozzolanic additive. They both contain approximately the same ratio of binder to sand to trass. For this repair stucco mix, the following materials should be used at the specified ratio (by volume):

Binder: 1 part high-calcium lime

Aggregate: 1/2 part natural sand (conforming to the size and distribution as documented in sections 6.5 and 7.2 of the HMC full report, as well as ASTM C144)

Pozzolanic Additive: 1/5 part volcanic trass

NOTE: When such a small amount of aggregate is utilized in a lime-based mortar, particularly with lime putty, the material runs the risk of developing shrinkage cracks while curing. This material may require more attention or a different application method, including the filling of shrinkage cracks. It is also possible that the inclusion of the pozzolanic additive may aid in speeding the curing rate and therefore reducing the degree of shrinkage cracking.

Repair Mix #3: Rampart Stucco Finish Coat

The historic stucco finish at the exterior rampart has a slightly different ratio of lime to sand to pozzolan than the stucco bodies of the rampart and cordón. The sand is present in a smaller percentage, leading to a smoother texture of the finish coat. To achieve a similarly smooth finish coat in a repair mix, a lower percentage of sand can be used.

As with the previous mix, when such a small amount of aggregate is utilized in a lime-based mortar, particularly with lime putty, care should be taken to avoid shrinkage cracks while curing. The final aesthetic of the existing rampart stucco includes an ocher finish with pencil joints to replicate the ashlar masonry construction. As no analysis of the finishes has been conducted, it is not possible at this time to recommend materials to

166. Reactivity can vary in pozzolans such as trass. Trass is commercially available from Natural Pigments (https://www.naturalpigments.com) and Kremer Pigments (http://shop.kremerpigments.com/en/).

replicate this finish or to determine if this was the original finish scheme.

For this repair stucco mix, the following materials should be used at the specified ratio (by volume):

Binder: 1 part high-calcium lime

Aggregate: 1/4 part natural sand (conforming to the size and distribution as documented in sections 6.5 and 7.2 of the HMC full report, as well as ASTM C144)

Pozzolanic Additive: 1/5 part volcanic trass

Repair Mix #4: Cordón Stucco Finish Coat

The stucco finish at the exterior cordón was identified during the analysis as containing a high- calcium lime binder with crushed brick acting as aggregate, pozzolan, and pigmenting agent. The brick in this sample was harder and more finely crushed (≤1 mm in size) than that utilized for the mortars, brick stuccos, and interior stucco body (see above, Repair Mix #1). While this brick is higher fired than the brick described above, it is still not as high-fired as 20th century equivalent bricks.

The finish coat has a compact and very smooth texture. Along with the repair mix below, it is recommended to use a method of application that achieves a similarly smooth texture.

Neither pigment nor a painted finish is to be utilized to achieve the color and texture of the cordón finish.

For this repair stucco mix, the following materials should be used at the specified ratio:

Binder: 1 part high-calcium lime

Aggregate/Pozzolanic Additive: 1/2 part higher-fired crushed brick fragments (conforming to the size and distribution as documented in sections 6.4 and 7.6 of the HMC full report)

Repair Mix #5: Interior Plaster Finish Coat

The plaster finish at the interior was identified as containing a high-calcium lime binder with a small addition of sand aggregate that includes bioclastic shells.

As stated above, due to the small amount of sand in this recommended mix, attention should be paid during the curing process to prevent shrinkage cracks from forming. In addition, because this finish does not contain a pozzolanic additive, it is more likely to develop such shrinkage cracks.

For this repair plaster mix, the following materials should be used:

Binder: 1 part high-calcium lime

Aggregate: Small addition of fine, bioclastic shell sand (conforming to the size and distribution documented in section 6.3 and 7.3 of the full materials analysis report by HMC, as well as ASTM C144)

Future Research/Additional Investigations

National Register Update

1. San Juan National Historic Site was nominated for and listed on the National Register of Historic Places in 1973. The document is brief and utilizes antiquated nomenclature for assessing the historic significance of features, i.e. “First Order of Significance.” The description of El Cañuelo is very brief, only three paragraphs. While the information is accurate, additional documentation, using the information in this report, would significantly improve the nomination.

Condition Assessment

2. As mentioned above, when the concrete cap is removed a condition assessment of the surface is recommended. By removing the concrete cap, the NPS will have access to the terreplein surface and potentially the interior of the fort fill, which may influence future rehabilitation decisions.

Structural Issues

1. Subsurface explorations: Investigate the subgrade foundation to identify any instability issues. Conduct subsurface explorations to evaluate the soil conditions around and below the structure to identify potential for settlement or to predict the behavior of the structure based on

the underlying existing soils. Additional data on the subsurface conditions would potentially show if failure in the subgrade, such as settlement, is contributing to the cracking of the walls. Borings would be required, at a minimum at the four corners of the fort.

2. Internal Backfill explorations: Similarly, additional data on the composition of the backfill and the water content of the backfill would help determine if lateral forces placed on the interior of the walls is causing the cracking. Horizontal or vertical boring into this fill could potentially provide information on the composition and water content. Vertical borings through the concrete cap would minimize adverse impact on the historic fabric of the exterior walls.
    - The project team considered recommending the creation of weep holes to allow for the drainage of trapped moisture inside the building. If elevated moisture levels are found, core drill horizontally in select locations located towards the base of the masonry walls through the exterior stone wall facing to the rubble fill. This will facilitate moisture transmission (both liquid and vapor) from the interior mass. Drill holes should be located in existing mortar joints. The thickness of the exterior stonewall facing is unknown (estimates range from 6'-9" to up to 14'-0") and may require larger diameter cores. As a less invasive option, shorter cores that would be smaller in diameter and installed to a depth just through the first exterior face of the wall may be considered with the understanding that these depths may be less effective than full depth cores.
3. Continued movement analysis: If the cyclical monitoring program of the movement gauges indicates continued movement, consideration should be given to additional, more invasive stabilization methods. Possible solutions could involve the installation of through tie-rods or corner reinforcement, or removing a certain amount of the interior mass fill and replacing it with a lighter weight fill material to reduce the outward forces on the exterior walls.

Material Investigations

1. Raw material comparison: The results of the materials analysis presented herein can be compared to raw, local samples of lime, "beachrock," and natural sand to confirm the theories regarding these materials, particularly the provenance of the pozzolanic trass additive. The analysis of these samples should include trace element identification for comparison.
2. Earlier exterior stucco investigation: Additional investigation of the interface between the facing rampart stones and the stucco should be conducted in order to more concretely identify the material observed by the petrographic analysis in the pores of the stone. An analysis of this material could determine if the material was a previous stucco coat and how it compares to the potentially historic mortar and interior stucco.
3. Brick investigation: The different brick materials identified in the masonry materials as part of this analysis should be compared to the bricks used to construct the fort in order to determine whether the bricks used as pozzolanic additions are the same material. This could further aid in dating the masonry materials.
4. Comparative material investigation: Additional comparative investigation could be conducted with the materials at the other 17th century Spanish Colonial military installations in San Juan including San Felipe del Morro, Castillo de San Cristóbal, and San Gerónimo del Boquerón. The shared design elements of these forts likely would have extended to the specific materials, and more extensive archival information may be present for the larger forts such as El Morro that could illuminate the construction at El Cañuelo.
5. Finishes investigation: Although a finish analysis of the exterior stucco was not completed as part of this materials analysis, a few general notes may be stated

that could aid in the possible chronological appropriation of the material and a more in-depth finishes study should illuminate this further. The warm ocher color of the finish on the rampart stucco and deep, brick red on the cordón appear to have been a common feature for Spanish Colonial forts in San Juan. Investigations at both El Morro[167] and San Cristóbal[168] both note the presence of this polychrome finish. Since much of the photographic record, up to and including the 1998 HABS documentation, is in black and white, it is not possible to use this for evidence of finish alterations, although the potential for dating this material and its substrate could come from a comparative instrumental analysis of these finishes. The recommended finishes analysis should include the pencil joints on the exterior stucco to determine how these were employed and whether or not this decoration is part of the original design of the fort.

6. Archival repair chronology: As previously noted in I.C Physical Description Chapter, the photographs that exist from the 1930s to the present can serve as source material for a repair chronology and can, at least, identify locations of potentially historic materials. This information can then inform a second round of materials analyses of more targeted samples. The Documentation of Repair Chronologies (Figure 194 to Figure 212) shows an example of how this could be implemented.

Resilience to Natural Hazards

El Cañuelo's location on the edge of San Juan Bay makes it particularly susceptible to threats associated with climate change. The most dramatic climate change-relate threats include rising sea levels and increased tropical storm intensity. Rising temperature and changes in precipitation patterns pose a similar risk to the long-term sustainability of the fort. The nature of the structure's construction and setting make it vulnerable to each of these climate change trends. The building is a masonry structure exposed to the elements. The original architectural features that historically drained water from the surface of the building are non-functioning today. The infiltration of water into the interior of the building is likely causing structural damage to the fort. The fort originally occupied an island. By building a landmass around the structure and connecting it to adjacent Las Cabras Island and mainland, the United States Army radically altered natural hydrologic patterns. Erosion, as the waters attempt to carve a way through the artificial landmass, will be an ongoing challenge at El Cañuelo.

National Park Service cultural resources including historic buildings "are fixed in place or derive much of their significance from the place within which they were created. Many are non-living, and all are unique. As a result, the capacity of cultural resources to adapt to changing environments is limited."[169]

As stated in the Director's Policy Memorandum 14-02, "NPS cultural resource management must keep in mind that (1) cultural resources are primary sources of data regarding human interactions with climate change; and (2) changing climates affect the preservation and maintenance of cultural resources."[170]

Patrick Gonzalez prepared for NPS a report summarizing the "Climate Change Trends for Park Planning at San Juan National Historic Site, Puerto Rico" in December 2012.[171] The report examines the historical trends of temperature and precipitation.

Among the historical trends facing the National Historic Site are mean annual temperature increase and precipitation decrease. The three future

167. Cliver, E. Blaine. "El Morro: A Physical History" Lectures: Second International Symposium on Historic Preservation in Puerto Rico and the Carribbean. Ed. Milagros Flores Roman. San Juan: National Park Service, San Juan National Historic Site, 1991. Print.
168. Wells, Jeremy C., "History and Characterization of Mortars in Spanish New World Fortifications: A Case Study on El Castillo de San Cristóbal, San Juan, Puerto Rico" (2004). Theses (Historic Preservation). 62.
169. National Park Service, "Cultural Resources and Climate Change," (n.p., 2016), accessed December 9, 2016, https://www.nps.gov/subjects/climatechange/upload/06-CCRP-Cultural-Resource-Brief-FEB-2016.pdf.
170. John B. Jarvis, February 10, 2014, 2.
171. Gonzalez, Patrick, "Climate Change Trends for Park Planning at San Juan National Historic Site, Puerto Rico," NPS, 2012.

climate scenarios projected that the 21st century temperature in San Juan will increase 2.5 times the amount of warming experienced in the 20th century. The majority of models also projected a decrease in annual precipitation and increase in periods with minimal rain (<1 mm). The projections, however, indicate an increase in the "frequency of extreme precipitation events."

Maria Caffrey with NPS prepared the report "Sea Level Trends for Planning at San Juan National Historic Site" in 2012.[172] Historic sea levels along the Puerto Rico coast are rising at the same rate as the global sea level. This report also refers to an Intergovernmental Panel on Climate Change report that suggests that storm intensity is predicted to increase resulting in increased storm surges.

Impact on El Cañuelo

An increase in temperature can lead to the "increased crystallization of efflorescent salts due to increased evaporation rates, leading to increased rates of structural cracking deterioration."[173] Higher relative humidity, resulting from higher temperatures, would increase the moisture absorption rates for brick and porous stone. This increased moisture absorption would result in the decrease of crystallization and dissolution of salts within the stone materials and masonry. The increased moisture would also increase the rates of growth of vegetation on masonry surfaces and increase the rate of rot for wooden features.[174]

A decrease in precipitation may be expected to increase the levels of salt deposits that collect on the surfaces of masonry and porous stone. These salt deposits would then be infiltrated into the porous stone during a rain event. This cycle would cause spalling and fractures in the material.

An increase in heavy rain events would stress the structure's ability to shed water, allowing water to find cracks and crevices into the interior of the structure. The infiltration of water into the interior will result in increased pressure on the masonry walls and result in subsidence/shrink swell soils. The extreme rain events will result in accelerated decay of masonry due to increased extremes of wetting and drying. The extreme cycle of wetting and drying will also increase the deposition and the eventual infiltration of salts into the porous material of the structure.

San Juan has experienced numerous natural disasters, including both earthquakes and hurricanes. Hurricanes represent a complex threat to El Cañuelo because of the negative effects of high wind, heavy precipitation, and storm surge. Threats associated with extreme weather events include damage from wind, rain, and wind-born debris. Storm surge associated with extreme weather events can cause structural damage or collapse from blunt force or undermining the structure's foundation. While not directly associated with an extreme weather event, rising sea levels pose a specific threat to El Cañuelo because of its location. Coastal erosion is currently a problem that will only worsen with rising sea levels. The combination of erosion and rising water table can compromise the foundation and threaten the building.

Implications – Adapting to Natural Hazards and Increased Climate Variability

According to NPS documents, impacts to buildings and structures related to temperature and drought extremes include: deterioration, conflagration, and desiccation.[175] A loss of resource integrity may occur over time from conditions related to natural hazards, increased climate variability and their impacts. Typically, documentation is one of the first mitigation techniques undertaken in response to deterioration. This document, which includes narrative, photographs, measured drawings, and recommendations, fulfills this first step in the mitigation process.

This structure does show signs of previous deterioration and recommendations for repair are included in this document. The treatment recommendations, while focusing on preventing water from infiltrating the building, also address resilience to natural hazards.

172. Caffrey, Maria, "Sea Level Trends for Planning at San Juan National Historic Site," NPS, 2012.
173. Rockman, Cultural Resource Climate Change Strategy, 20.
174. Ibid.
175. Marcy Rockman, "An NPS Framework for Addressing Climate Change with Cultural Resources," The George Wright Forum 32, no. 1 (2015), accessed December 9, 2016, http://www.georgewright.org/321rockman.pdf.

The treatment recommendations address drainage issues and repair to cracks, which will help counteract the effects of heavy rainfall associated with extreme weather events. The application of a protective coating of stucco on horizontal surfaces of the ramparts and cordón will protect the masonry surfaces from the effects of increased temperature, periods of drought, and heavy rains associated with extreme rain events.

The treatment recommendations include augmentation of the riprap and steel pile bulkhead around El Cañuelo. This is likely the most effective protective measure against storm surge as it will absorb some of the energy of the waves in a major weather event.

Page intentionally left blank.

Bibliography
References

Bearss, Edwin. *Historic Structure Report: Historical Data Section.* Denver: Denver Service Center, National Park Service, 1984.

Bense, Judith A. *Presidios of the North American Spanish Borderlands*. Historical Archaeology, vol. 38, No. 3. The Society for Historical Archaeology, 2005.

Berkowitz, Joan, et. al. *The Fortifications of San Juan National Historic Site, Historic Structures Report, Volume I-III.* Atlanta: Southeastern Regional Office, National Park Service, 1991.

Blanco, Juan. "A Study of the Morphological Structure of the System of Fortifications of San Juan de Puerto Rico with a Special Emphasis on the Development of the 'Frente de Tierra de San Cristobal." Copyrighted by author, 1988. This report is at the research library at National Park Service Southeastern Regional Office.

Bobonis, Wanda López. "A Preservation Plan for Fort El Cañuelo, San Juan National Historic Site, Isla de Cabras, Puerto Rico." Master's thesis, University of Pennsylvania, 2005.

Bonet, Walter A Cardona. *Islotes de Borinquen*. San Juan: Comité Historia de los Pueblos, 1985.

Cliver, Blaine. "El Morro: A Physical History." In *Lectures, Second International Symposium on Historic Preservation in Puerto Rico and the Caribbean,* ed. Milagros Flores Roman. San Juan: NPS, 1991.

Charola, A. Elena, Fernando M.A. Henriques, Luis Torres Montes, Jeanne Marie Teutonico, Luz Angela Useche. "Recommendations of the Expert Committee Regarding the San Juan Fortifications, San Juan, Puerto Rico." San Juan, 1999. This document is in the SAJU archives.

Cobos-Guerra, Fernando. "Technical and systemic keys and context of Hispanic fortifications on Western Mediterranean coast." In *Defensive Architecture of the Mediterranean XV to XVII Centuries,* ed. Rodriquez-Navarro. (Accessed online 2/27/2017: http://dx.doi.org/10.4995/FORTMED2015.2015.1803).

Hartzel, Charles. *Register of Porto Rico for 1903*. San Juan, Puerto Rico: Louis E Tuzo and Company, 1903.

Holland, F. Ross and Russell Jones. *Special History Study Masonry Forts of the National Park Service*. Denver: Denver Service Center, 1973.

Hoyt, Edward, ed. *A History of the Harbor Defenses of San Juan, P.R., under Spain 1509-1898: including a brief history of artillery and a guide to the ancient fortifications*. San Juan: United States Army Puerto Rico Coast Artillery Command, 1943.

Lessing, Charles W. "The Fort of El Cañuelo," HABS Survey No. PR-52, August 10, 1955. (Accessed online, http://cdn.loc.gov/master/pnp/habshaer/pr/pr0000/pr0009/supp/pr0009supp.pdf).

López, Andriana María Garriga. “Colonial Palimpsest: the biopolitical history of Isla de Cabras leper colony and the problematics of the memorialization of suffering.” Final seminar paper: Columbia University, 2003.

Lopez, Felix. “Stabilization of Fort San Juan de la Cruz (El Cañuelo) SAJU-08-10.” San Juan, 2008. (A copy of this document is on file at the Puerto Rico State Historic Preservation Office.)

National Park Service. *The Forts of Old San Juan, Official National Park Handbook. San Juan National Historic Site*. Washington, D.C.: NPS, nd.

National Park Service, *Spanish Exploration and Settlement: The National Survey of Historic Sites and Buildings*. Washington, D.C.: NPS, 1959.

Oquendo, Carlos R. “XXX Form Assessment of Actions Having an Effect on Cultural Resources,” San Juan, 1991. (A copy of this document is on file at the Puerto Rico State Historic Preservation Office.)

“Report of the Military Governor of Puerto Rico.” (Accessed online, https://archive.org/stream/reportofmilitary00puer#page/202/mode/2up/search/canuelo.

Rivero, Angel. *Crónica de la Guerra hispanoamericana en Puerto Rico.* Madrid: Sucesores de Ryzadeneyra, 1922.

San Juan National Historic Site, “Draft General Management Plan Environmental Assessment,” San Juan: NPS, 1984. (A copy of this document is on file at the Puerto Rico State Historic Preservation Office.)

Walker, Leslie Paul. “Narrating Climate Change at San Juan National Historic Site.” Masters thesis, University of South Florida, 2015.

War Department, United States Engineer Office. “Completion Report—Repair of Historical Fortifications—Specifications, U.S. Plant and Hired Labor, Nos. F 28-1, F 28-2, F 28-3, F 28-4, F 28-5, F 28-6,” June 20, 1940. Copy of document in at SAJU Archives.

Weltzin, Rosanna. “The Forts of Old San Juan: Guardians of the Caribbean. Teaching with Historic Places.” Washington D.C.: National Park Service, 2000.

United States Army Forces Antilles and Military District of Puerto Rico, Headquarters. “Press Release No: 250/58 Army to Transfer El Morro, San Cristobal to U.S. National Park Service,” September 23, 1958. (Copy of document in SAJU archives.)

Zapatero, Juan Manuel “Las fortificaciones históricas de San Juan de Puerto Rico,” *MILITARIA. Revista de Cultura Militar* (1989): 141-175.

El Cañuelo

San Juan National Historic Site

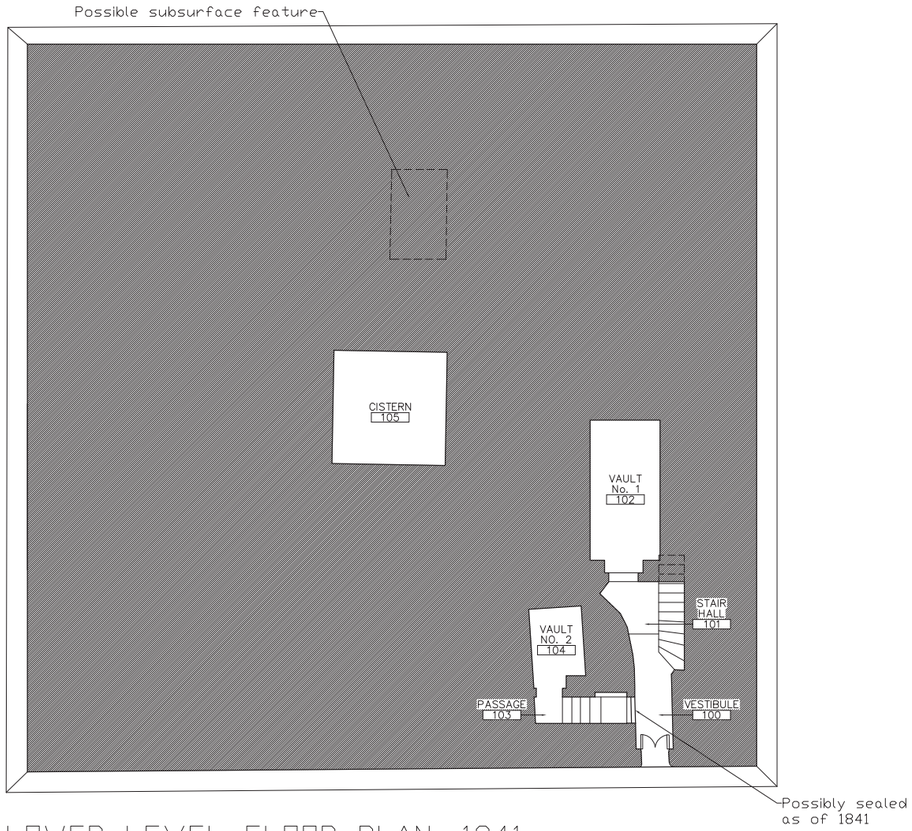
Historic Structure Report Appendices

May 2018
Prepared by:
WLA Studio
RATIO
Palmer Engineering
Building Conservation Associates, Inc.

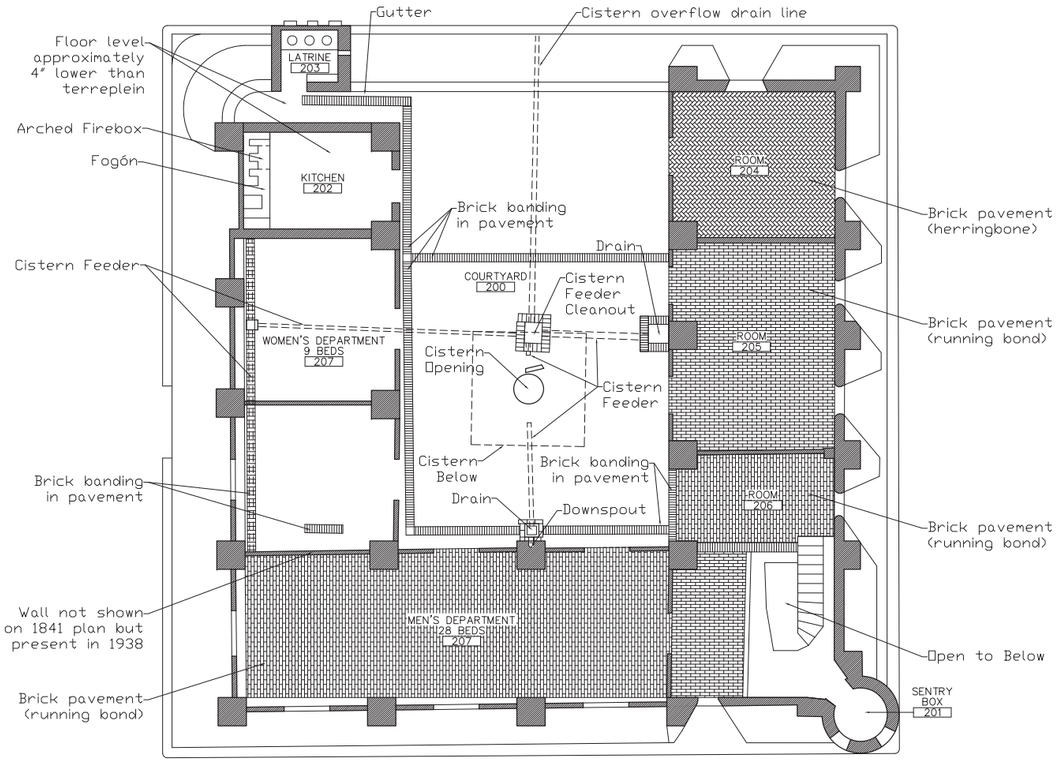
Under the direction of
National Park Service
Southeast Regional Office
Cultural Resources, Partnerships, & Science Division

Page intentionally left blank.

Appendix A:
Existing Condition Plans
Historic Condition Plans
Structural Analysis Plans
Treatment Details



LOWER LEVEL FLOOR PLAN, 1841



TERREPLEIN FLOOR PLAN, 1841

0 5 10 15 20 25
SCALE IN FEET

0 5 10 15 20 25
SCALE IN FEET

References:
Refer to Figures 17, 18, 22, and 36 in Part 1.A, Historical Background.
Refer to Appendix B for HABS drawings.

RATIO DESIGN
PALMER ENGINEERING COMPANY
WLA STUDIO

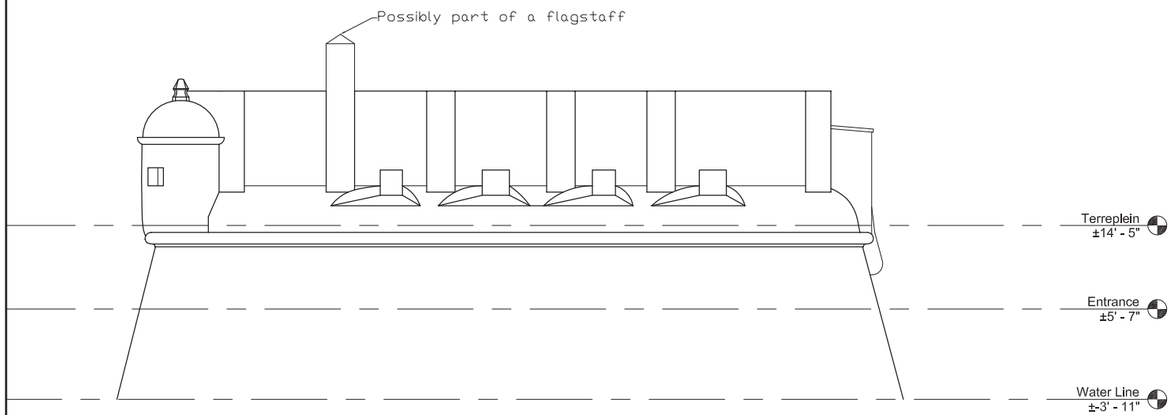
EL CANUELO FORTIFICATION
SAN JUAN NATIONAL HISTORIC SITE
UNITED STATES, DEPARTMENT OF THE INTERIOR
NATIONAL PARK SERVICE, SOUTHEAST REGION

DATE
05.02.2018

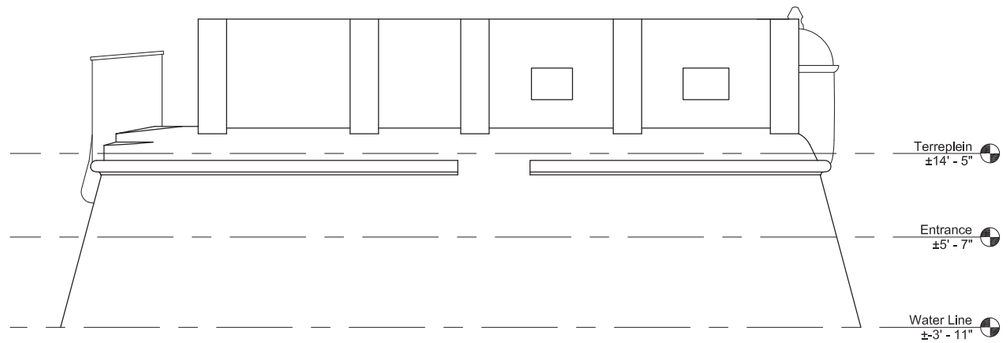
RECORDED BY:
BR

SCALE:
see graphic scale

A1

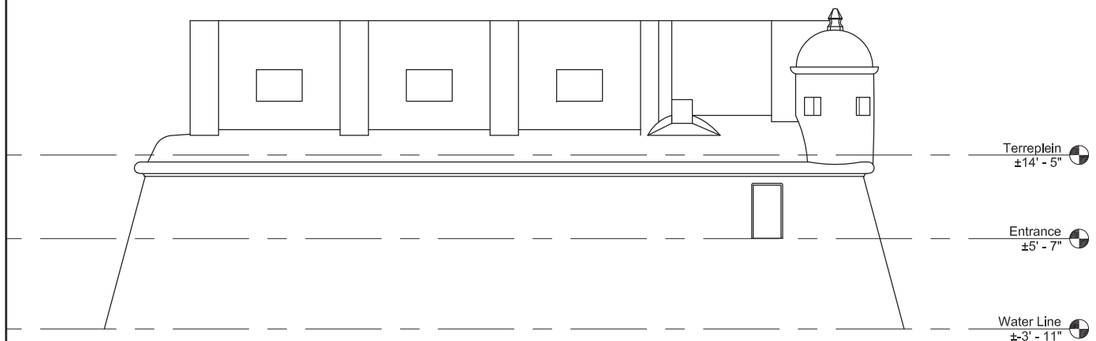


NORTH ELEVATION, 1841

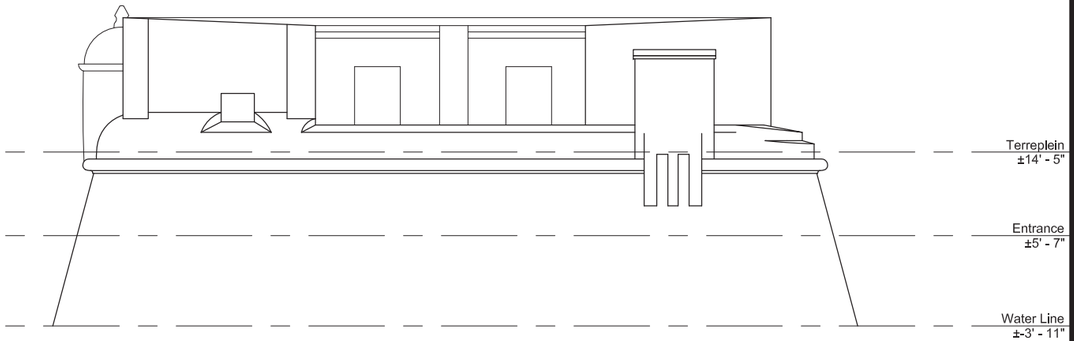


SOUTH ELEVATION, 1841

0 5 10 15 20 25
SCALE IN FEET



EAST ELEVATION, 1841



WEST ELEVATION, 1841

References:
Refer to Figures 17, 18, 22, and 36 in Part 1.A, Historical Background.
Refer to Appendix B for HABS drawings.

RATIO DESIGN
PALMER ENGINEERING COMPANY
WLA STUDIO

EL CANUELO FORTIFICATION

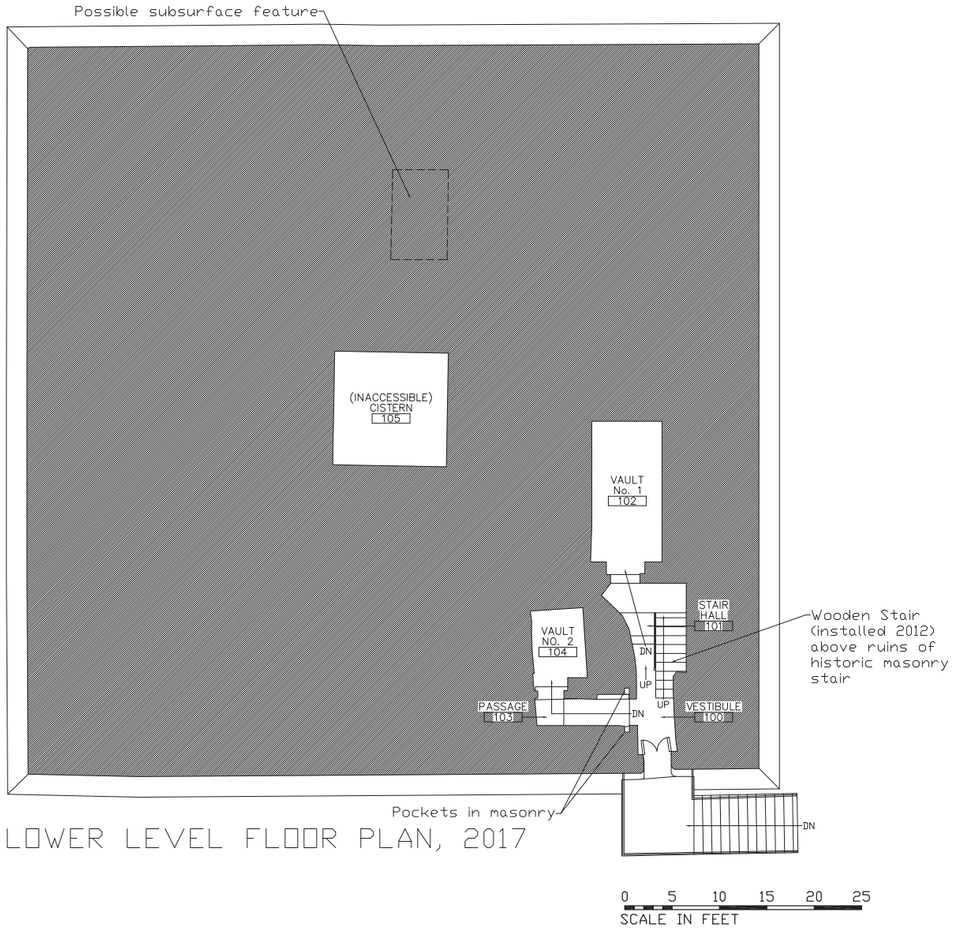
SAN JUAN NATIONAL HISTORIC SITE
UNITED STATES, DEPARTMENT OF THE INTERIOR
NATIONAL PARK SERVICE, SOUTHEAST REGION

DATE
05.02.2018

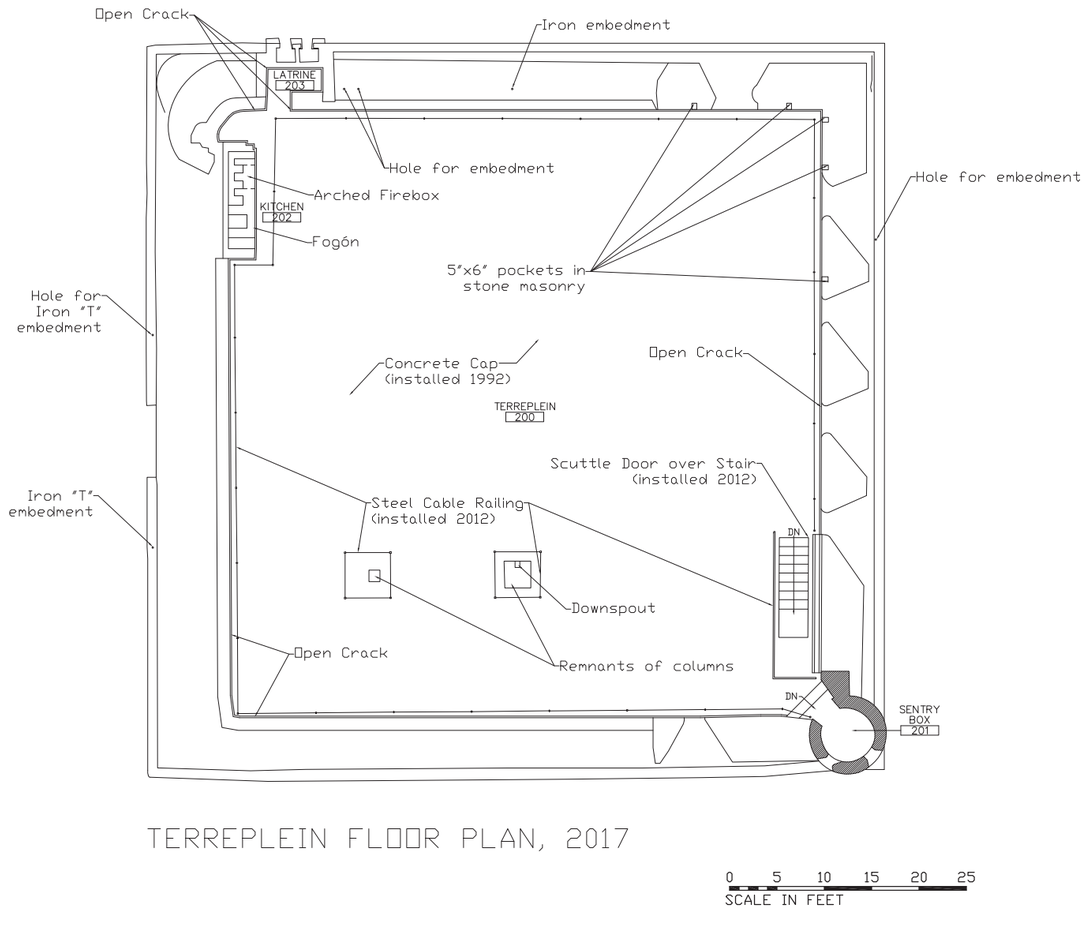
RECORDED BY:
BR

SCALE:
see graphic scale

A2



LOWER LEVEL FLOOR PLAN, 2017



TERREPLEIN FLOOR PLAN, 2017

RATIO DESIGN
PALMER ENGINEERING COMPANY
WLA STUDIO

EL CANUELO FORTIFICATION

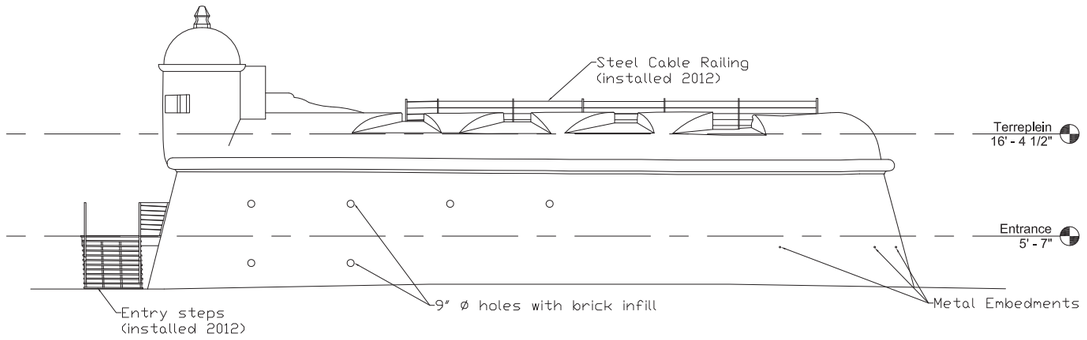
SAN JUAN NATIONAL HISTORIC SITE
UNITED STATES, DEPARTMENT OF THE INTERIOR
NATIONAL PARK SERVICE, SOUTHEAST REGION

DATE
05.02.2018

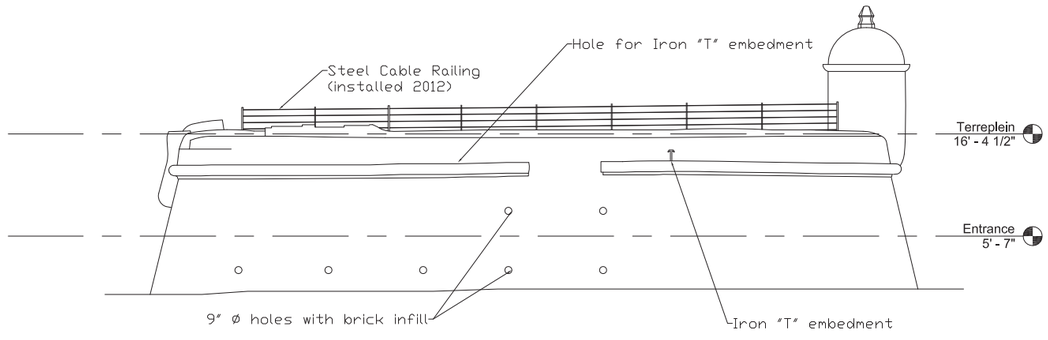
RECORDED BY:
BR

SCALE:
See Graphic Scale

A3

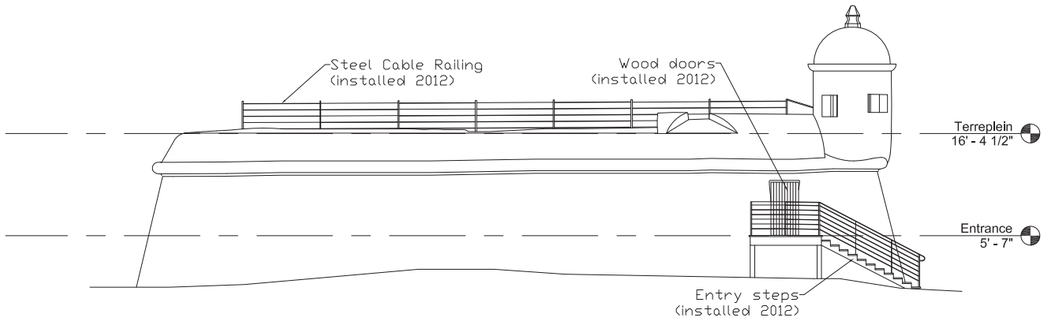


NORTH ELEVATION, 2017

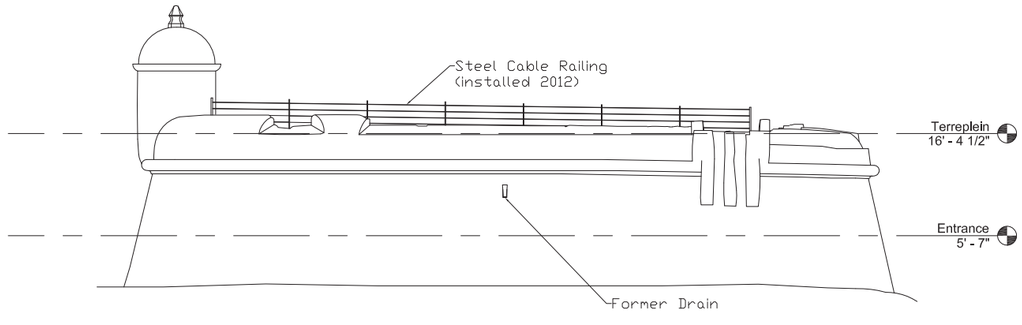


SOUTH ELEVATION, 2017

0 5 10 15 20 25
SCALE IN FEET



EAST ELEVATION, 2017



WEST ELEVATION, 2017

RATIO DESIGN
PALMER ENGINEERING COMPANY
WLA STUDIO

EL CANUELO FORTIFICATION

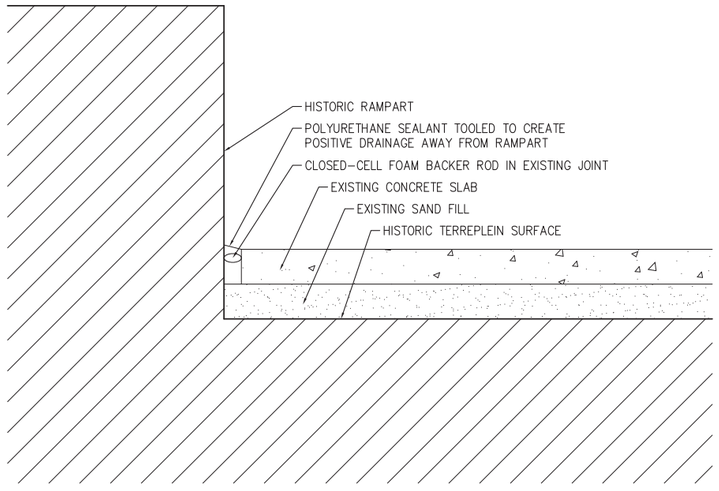
SAN JUAN NATIONAL HISTORIC SITE
UNITED STATES, DEPARTMENT OF THE INTERIOR
NATIONAL PARK SERVICE, SOUTHEAST REGION

DATE
05.02.2018

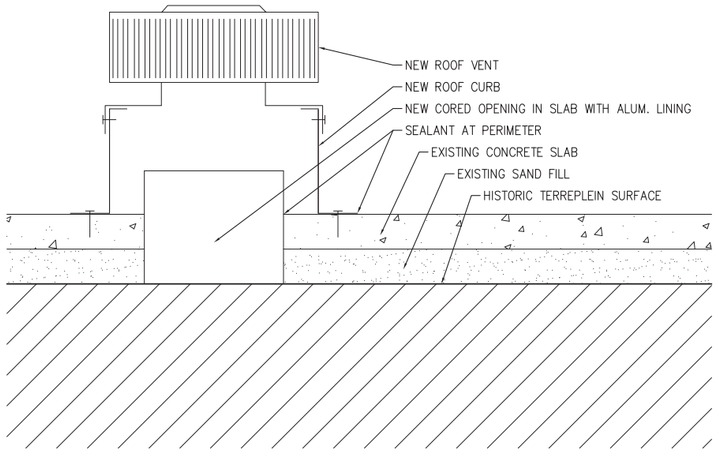
RECORDED BY:
BR

SCALE:
see graphic scale

A4



DETAIL OF PERIMETER JOINT



DETAIL OF ROOF VENT

RATIO DESIGN
PALMER ENGINEERING COMPANY
WLA STUDIO

EL CANUELO FORTIFICATION

SAN JUAN NATIONAL HISTORIC SITE
UNITED STATES, DEPARTMENT OF THE INTERIOR
NATIONAL PARK SERVICE, SOUTHEAST REGION

DATE
05.02.2018

RECORDED BY:
BR

SCALE:
NTS

TREATMENT DETAILS

A5

81'-6 3/8"±

WEST ELEVATION

EX02 2

WEST CORNER

SLOPE DOWN

SLOPE DOWN

NORTH CORNER

STONE BLOCKS, MORTARED. COVERED IN RENDER

APPROXIMATE WATER LINE

MORTARED RUBBLE AT GRADE

BARREL VAULTED CEILING, PLASTERED. SIGNS OF WATER INFILTRATION, EFFLORESCENCE, SOME SPALLING OF PLASTER. STONE FLOOR. NO CRACKS VISIBLE

ASSUMED LOCATION OF CISTERN

81'-0"±

SOUTH ELEVATION EX02 4

NORTH ELEVATION 1 EX02

SOUTH ELEVATION EX02 4

76'-10 5/8"±

LARGE STONE BLOCK LINTEL ABOVE OPENING

WWF AND PLASTIC VAPOR BARRIER VISIBLE FROM BELOW

LOW CEILING, POSSIBLY FORMED WITH WOOD UNEVEN SLOPING FLOORS, TYP

TERMITE INFESTED WOOD STAIR. STONE STAIR BELOW

4'-3" MIN

CRACK IN WALL ABOVE OPENING

A A

B B

DN UP

MORTAR IN WALL SUGGESTS THAT CRACK EXTENDED TO THIS FACE. NO NEW CRACKING IN MORTAR

CRACK IN WALL WITH APPROX 5 1/2" (140 MM)

DN DN UP

SOUTH CORNER

SLOPE DOWN

EAST CORNER

UP

MORTARED RUBBLE AT GRADE

3 EX02 EAST ELEVATION

RIP RAP

CORRUGATED STEEL SHEET PILE WALL, TOPS PROTRUDING ABOVE RIP RAP

CRACK AT INTERSECTION OF WALLS PROTRUSION

CORNER OF WALL

ENTRY OPENING

CRACK

OUTLINE IN WALL

DETAIL A-A DETAIL B-B

PLAN — AT ELEVATION OF LOWER ENTRANCE — 1 / S1

SCALE: 1/16" = 1'-0"

77'-10 1/2"±

WEST ELEVATION

EX02 2

BRICK FILLED SLOTS IN PARAPET

SLOTS IN PARAPET

TWO SMALL PIECES OF METAL PROTRUDING FROM PARAPET, POSSIBLY FROM INTERSECTING WALLS

WALLS NOT CONNECTED TO SLOT

DEEP VOIDS BELOW SLAB AT GAP

NORTH CORNER

WEST CORNER

STEEL CABLE RAILING,TYP

SLOPE DOWN

HOLE IN WALL, MORTAR PLUG SHIFTED OUT OF PLACE

4" THICK CONCRETE SLAB WITH WWF AND PLASTIC VAPOR BARRIER AT BOTTOM OF SLAB, ON TOP OF 4" THICK SAND LAYER ON TOP OF RUBBLE

1"Ø HOLES IN CONCRETE

SLOPE DOWN

SLOPE DOWN

LOW WALL

1 EX02 NORTH ELEVATION

DN

BRICK SUPPORTS, 1 1/2" GAP AROUND PERIMETER

DN

EAST CORNER

SOUTH CORNER

1 1/2" MIN WIDE GAP AROUND PERIMETER OF CONCRETE CAP. NAILS AND PLASTIC VAPOR BARRIER VISIBLE.

EVIDENCE OF CONCRETE/MORTAR COAT ADDED BEFORE OR AT THE TIME OF CONCRETE CAP INSTALLATION

22" FROM TOP OF CONCRETE TO TOP OF BRICK PAVERS VISIBLE AT STAIR

3 EX02 EAST ELEVATION

PLAN — AT ELEVATION OF UPPER DECK — 2 / S1

SCALE: 1/16" = 1'-0"

RATIO DESIGN
PALMER ENGINEERING COMPANY
WLA STUDIO

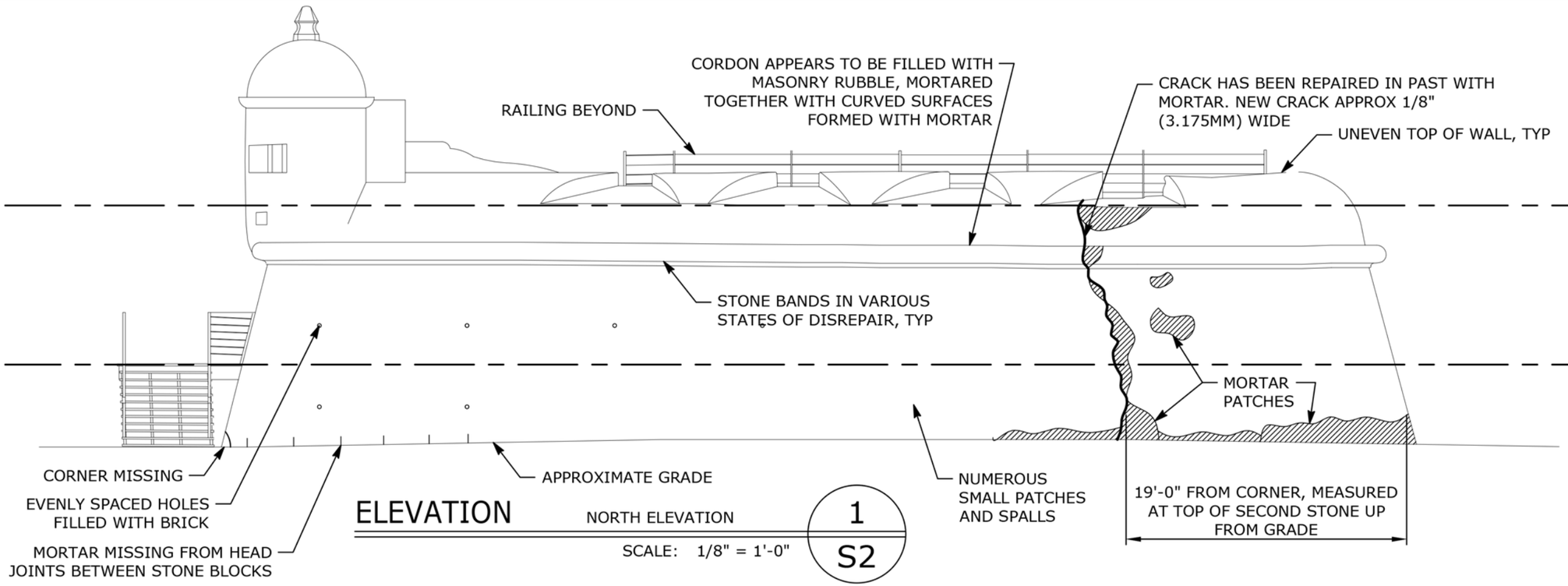
EL CANUELO FORTIFICATION
SAN JUAN NATIONAL HISTORIC SITE
UNITED STATES, DEPARTMENT OF THE INTERIOR
NATIONAL PARK SERVICE, SOUTHEAST REGION

DATE
05.02.2018

RECORDED BY:
AB

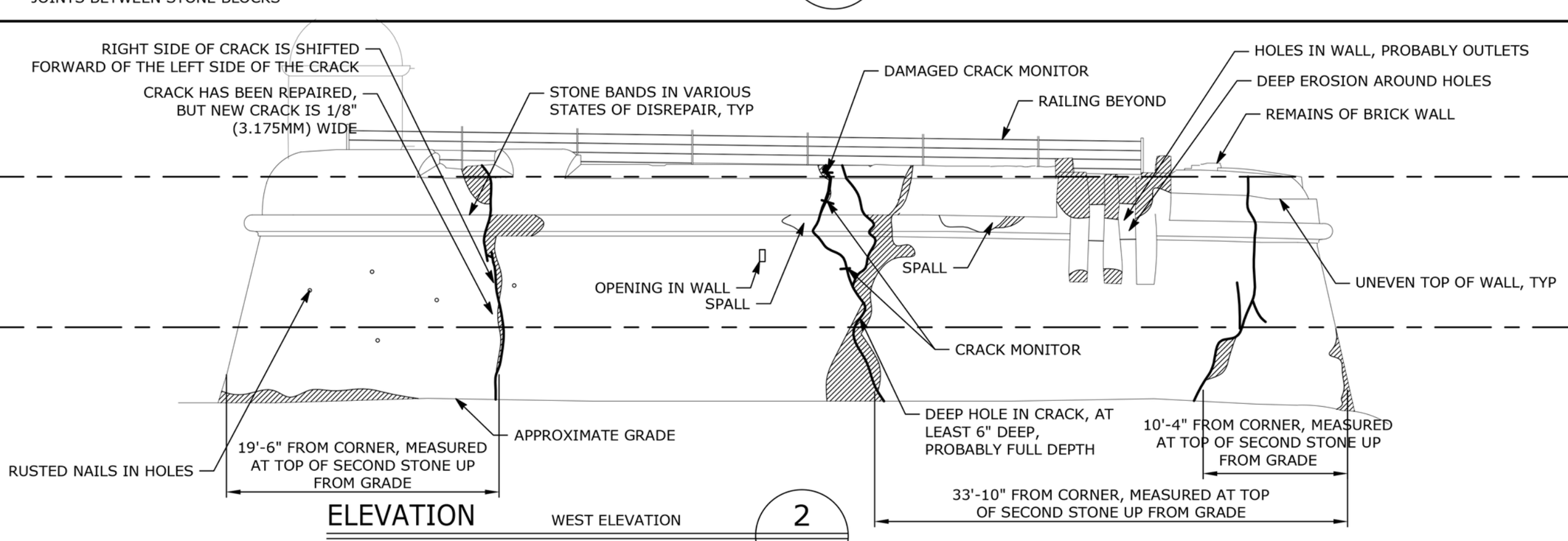
SCALE:
1/16"= 1'-0"

S1



ELEVATION — NORTH ELEVATION — 1 / S2

SCALE: 1/8" = 1'-0"



ELEVATION — WEST ELEVATION — 2 / S2

SCALE: 1/8" = 1'-0"

RATIO DESIGN
PALMER ENGINEERING COMPANY
WLA STUDIO

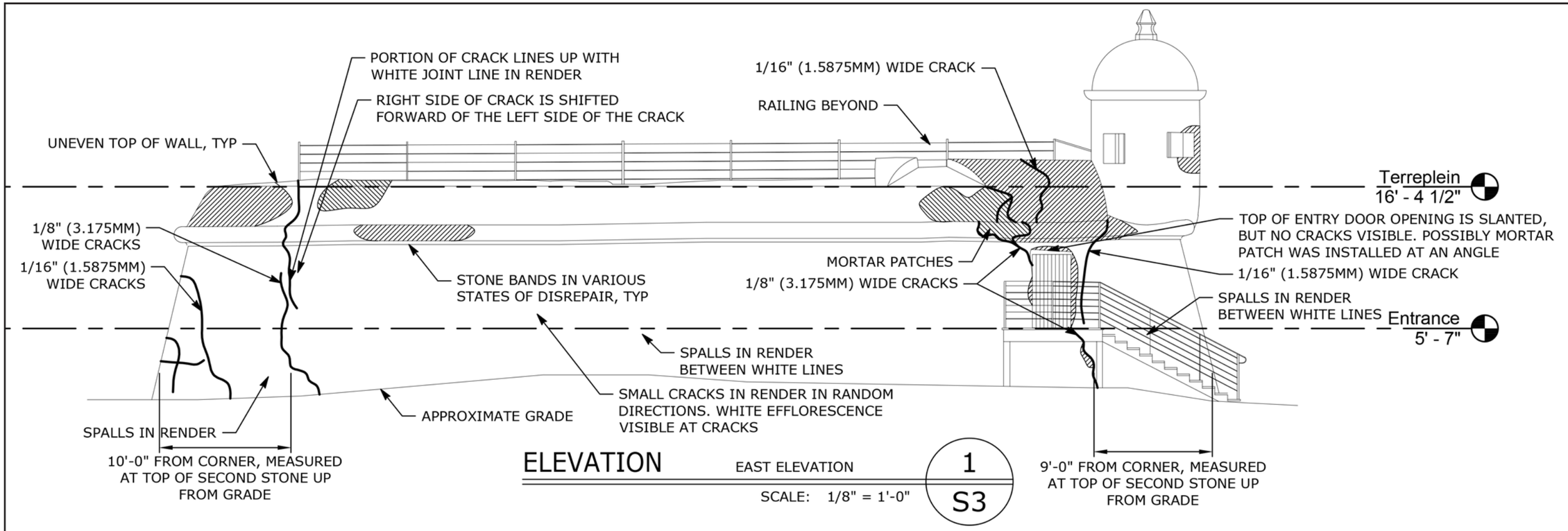
EL CANUELO FORTIFICATION
SAN JUAN NATIONAL HISTORIC SITE
UNITED STATES, DEPARTMENT OF THE INTERIOR
NATIONAL PARK SERVICE, SOUTHEAST REGION

DATE
05.02.2018

RECORDED BY:
AB

SCALE:
1/8" = 1'-0"

S2

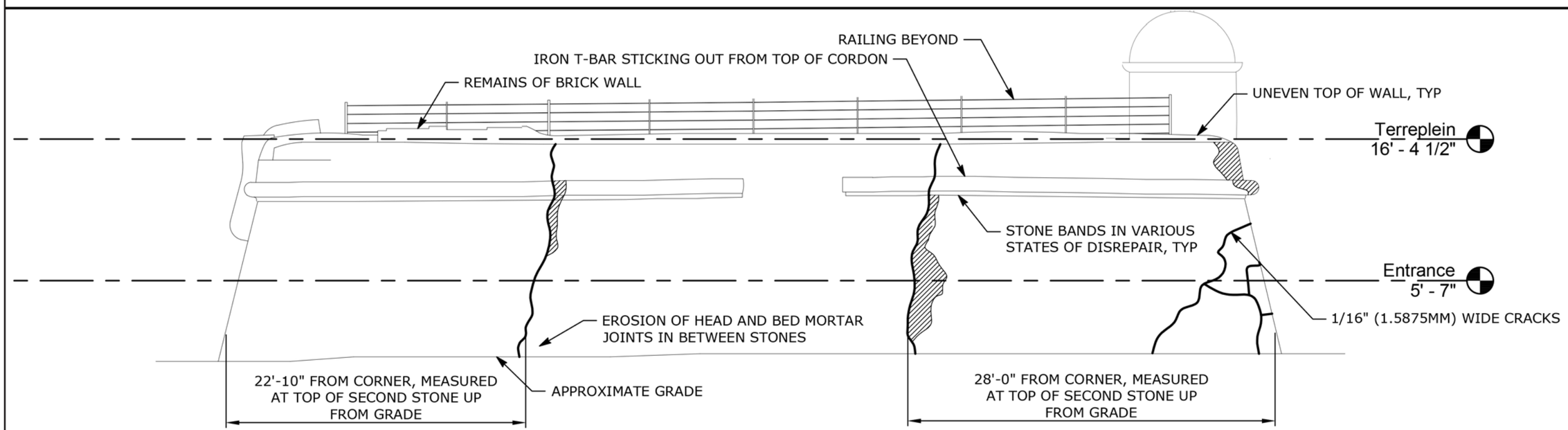


ELEVATION

EAST ELEVATION

SCALE: 1/8" = 1'-0"

1 / S3



ELEVATION

SOUTH ELEVATION

SCALE: 1/8" = 1'-0"

2 / S3

RATIO DESIGN
PALMER ENGINEERING COMPANY
WLA STUDIO

EL CANUELO FORTIFICATION
SAN JUAN NATIONAL HISTORIC SITE
UNITED STATES, DEPARTMENT OF THE INTERIOR
NATIONAL PARK SERVICE, SOUTHEAST REGION

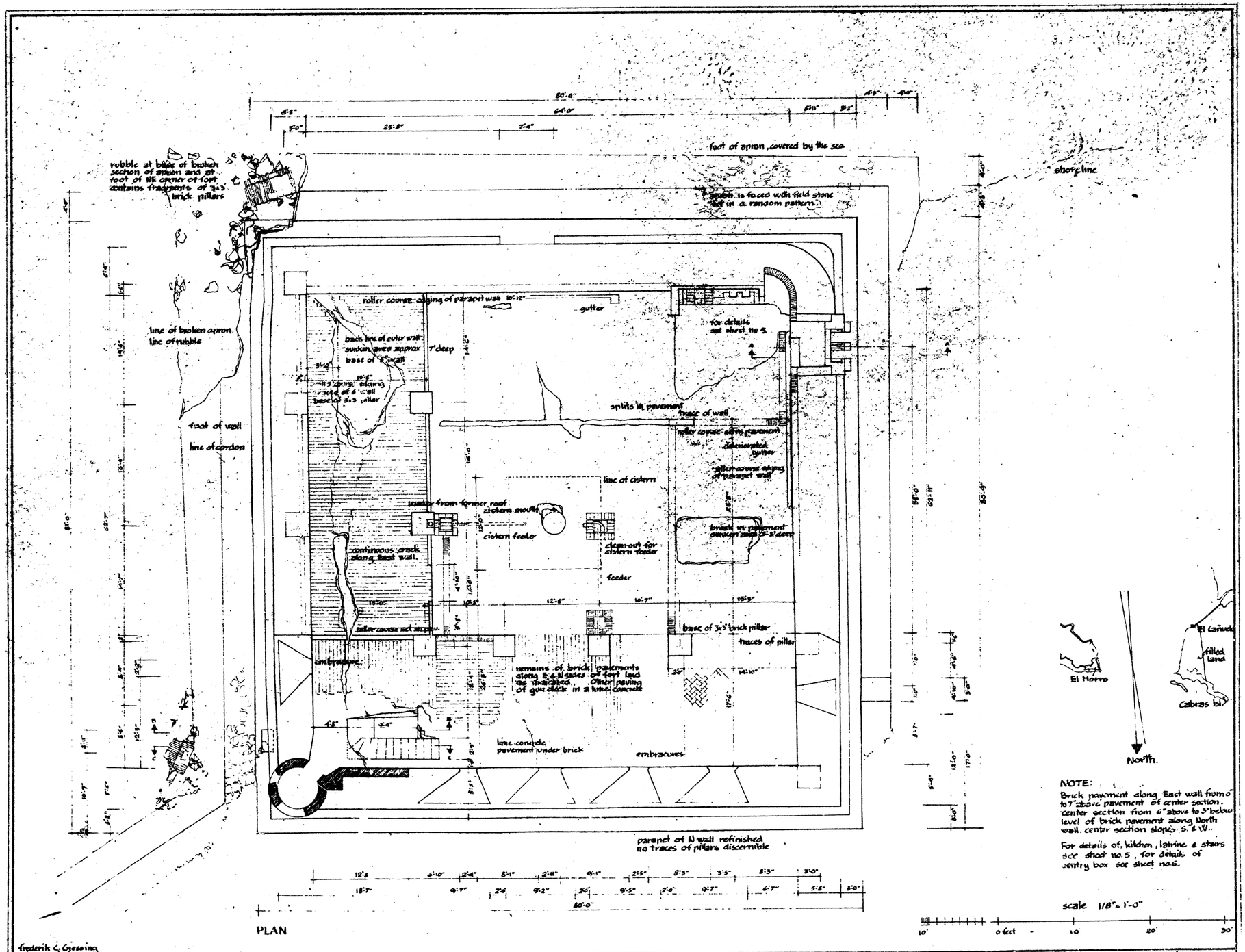
DATE
05.02.2018

RECORDED BY:
AB

SCALE:
1/8" = 1'-0"

S3

Appendix B:
HABS Drawings
1841 Lazaretto Drawing



Frederik C. Gjessing

U.S. DEPARTMENT OF THE INTERIOR OFFICE OF NATIONAL PARKS, BUILDINGS, AND RESERVATIONS BRANCH OF PLANS AND DESIGN	NAME OF STRUCTURE FORTIFICATIONS OF SAN JUAN, EL CANUELO CABRAS ISLAND, SAN JUAN PUERTO RICO	SURVEY NO. HA-3-PR-52	HISTORIC AMERICAN BUILDINGS SURVEY SHEET 2 OF 6 SHEETS	INDEX NO.

393/80035

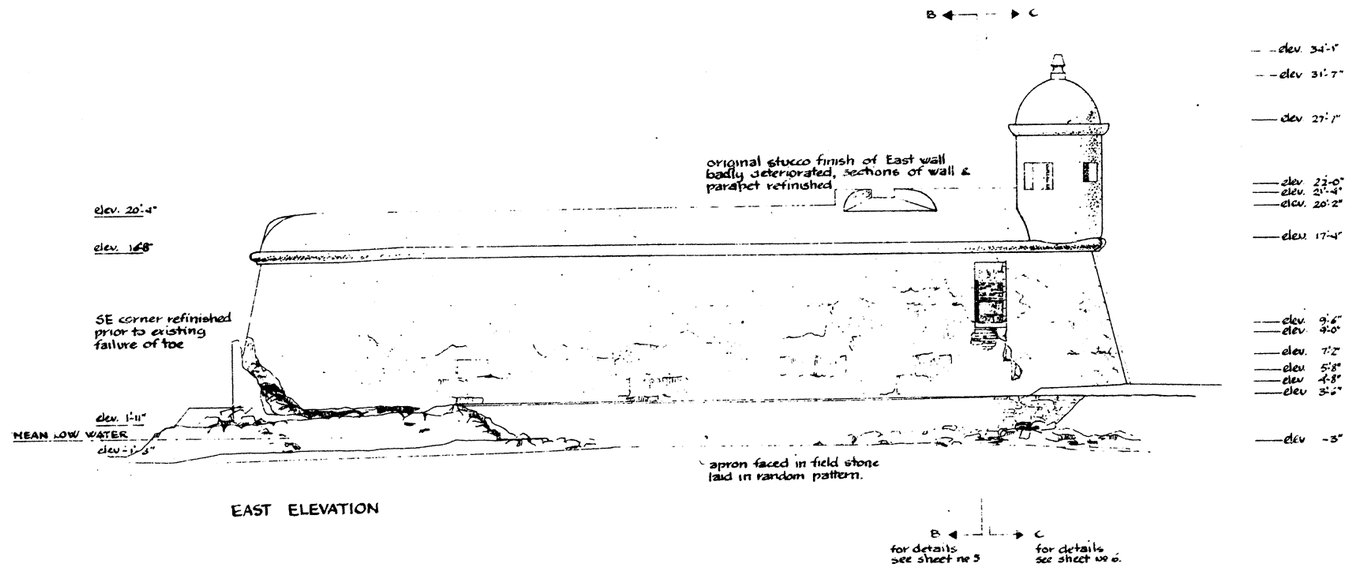
EL CANUELO FORTIFICATION
SAN JUAN NATIONAL HISTORIC SITE
UNITED STATES, DEPARTMENT OF THE INTERIOR
NATIONAL PARK SERVICE, SOUTHEAST REGION

RATIO DESIGN
PALMER ENGINEERING COMPANY
WLA STUDIO

1952 HABS DRAWINGS

SCALE:
see graphic scale

HABS
1



frederik C Gjessing

U.S. DEPARTMENT OF THE INTERIOR OFFICE OF NATIONAL PARKS, BUILDINGS, AND RESERVATIONS BRANCH OF PLANS AND DESIGN	NAME OF STRUCTURE FORTIFICATIONS OF SAN JUAN, EL CAÑUELO CABRAS ISLAND, SAN JUAN PUERTO RICO	SURVEY NO. HABS-PR 52	HISTORIC AMERICAN BUILDINGS SURVEY SHEET 3 OF 6 SHEETS	INDEX NO.

393/80035

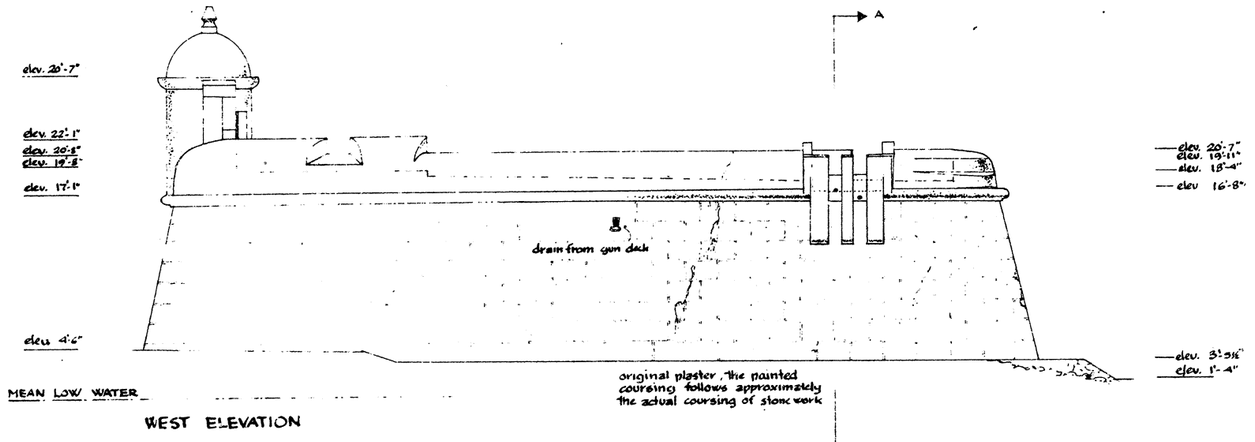
EL CANUELO FORTIFICATION
SAN JUAN NATIONAL HISTORIC SITE
UNITED STATES, DEPARTMENT OF THE INTERIOR
NATIONAL PARK SERVICE, SOUTHEAST REGION

RATIO DESIGN
PALMER ENGINEERING COMPANY
WLA STUDIO

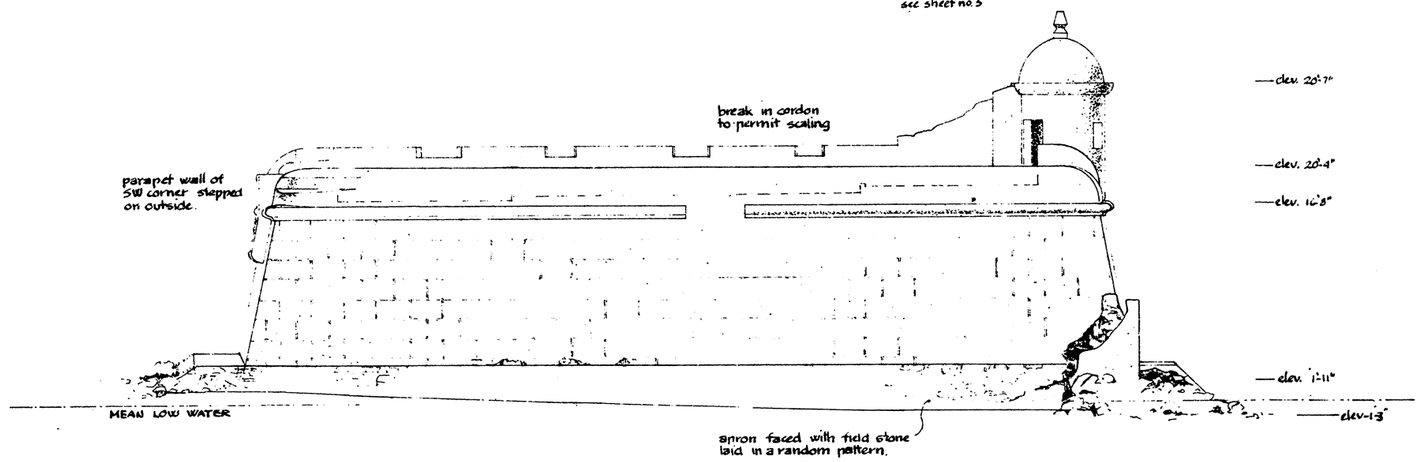
1952 HABS DRAWINGS

SCALE:
see graphic scale

HABS
2



WEST ELEVATION



SOUTH ELEVATION

NOTE:
Elevations shown are in feet above mean low water.

scale 1/8"=1'-0"

10' 0 feet 10' 20' 30'

frederik c. Giessing

U.S. DEPARTMENT OF THE INTERIOR OFFICE OF NATIONAL PARKS, BUILDINGS, AND RESERVATIONS BRANCH OF PLANS AND DESIGN	NAME OF STRUCTURE FORTIFICATIONS OF SAN JUAN, EL CAÑUELO CABRAS ISLAND, SAN JUAN PUERTO RICO	SURVEY NO. HABS-PR 52	HISTORIC AMERICAN BUILDINGS SURVEY SHEET 4 OF 6 SHEETS	INDEX NO.

393/80035

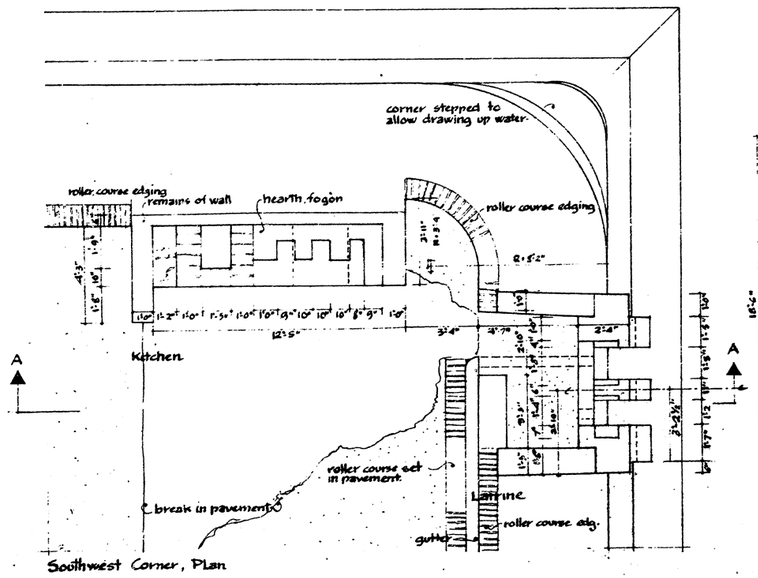
EL CANUELO FORTIFICATION
SAN JUAN NATIONAL HISTORIC SITE
UNITED STATES, DEPARTMENT OF THE INTERIOR
NATIONAL PARK SERVICE, SOUTHEAST REGION

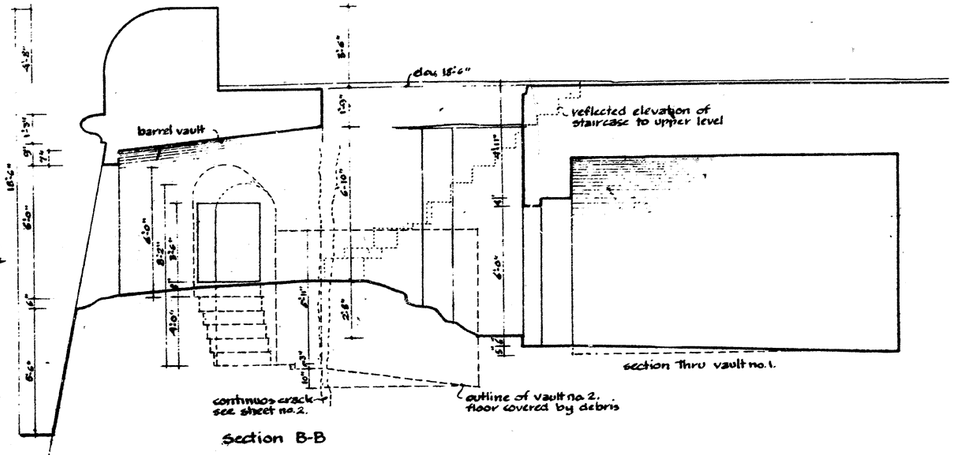
RATIO DESIGN
PALMER ENGINEERING COMPANY
WLA STUDIO

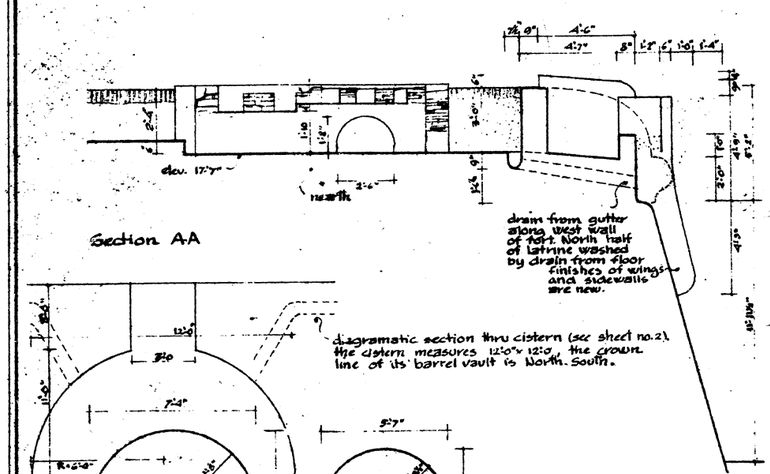
1952 HABS DRAWINGS

SCALE:
see graphic scale

HABS
3





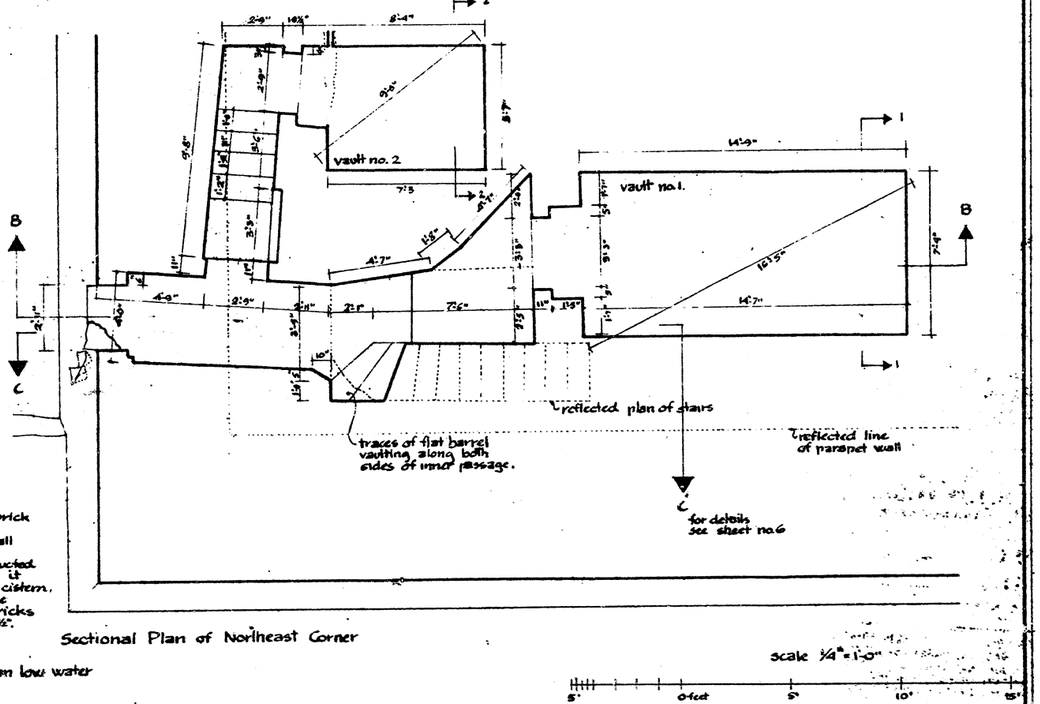


diagramatic section thru cistern (see sheet no. 2). the cistern measures 12'0"x 12'0" the crown line of its barrel vault is North-South.

NOTE

remains of pavement in kitchen area are a lime concrete with a crushed brick aggregate.
except for exposed brick edging all wall surfaces were covered by stucco.
all vaults are barrel vaults, and constructed in brick, except for vault no. 1, where it could not be determined, and for the cistern, the construction is one brick deep, in the cistern the arch construction is two bricks deep. the brick employed is 13"x 5½"x 2½".

Elevations shown are in feet above mean low water



frederik C. Gjessing

U.S. DEPARTMENT OF THE INTERIOR OFFICE OF NATIONAL PARKS, BUILDINGS, AND RESERVATIONS BRANCH OF PLANS AND DESIGN	NAME OF STRUCTURE FORTIFICATIONS OF SAN JUAN, EL CAÑUELO CABRAS ISLAND, SAN JUAN PUERTO RICO	SURVEY NO. HABS-PR 52	HISTORIC AMERICAN BUILDINGS SURVEY SHEET 5 OF 6 SHEETS	INDEX NO.

EL CANUELO FORTIFICATION
SAN JUAN NATIONAL HISTORIC SITE
UNITED STATES, DEPARTMENT OF THE INTERIOR
NATIONAL PARK SERVICE, SOUTHEAST REGION

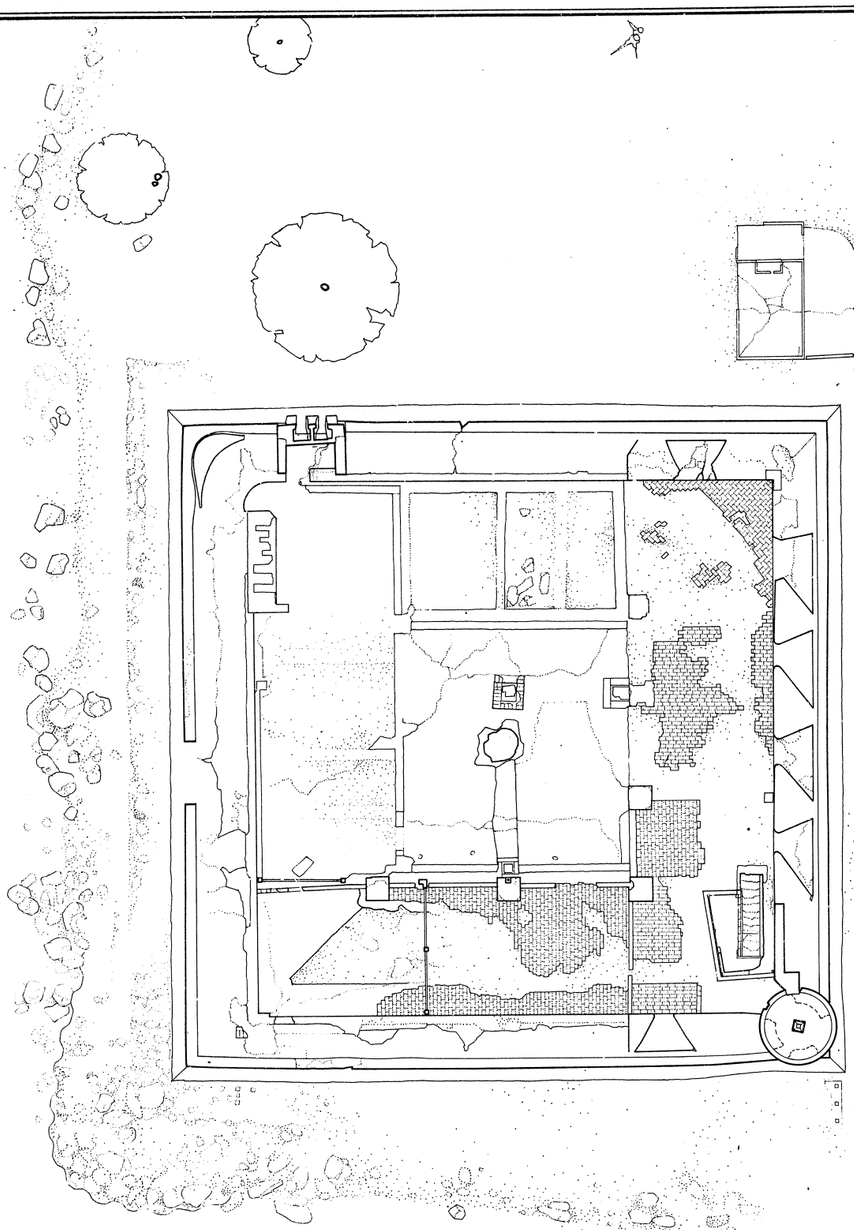
RATIO DESIGN
PALMER ENGINEERING COMPANY
WLA STUDIO

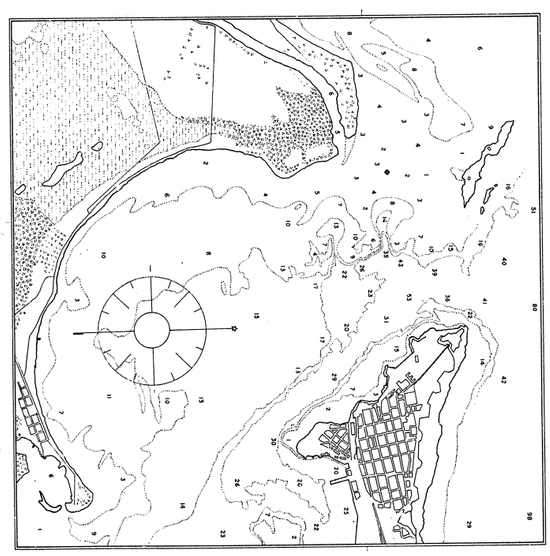
1952 HABS DRAWINGS

SCALE:
see graphic scale

HABS
4

Filmed MAY 2003 @ 29x





DRAWN BY: ERIC FRASER NIEMY

SAN JUAN NATIONAL HISTORIC SITE PROJECT - 1986

NATIONAL PARK SERVICE
UNITED STATES DEPARTMENT OF THE INTERIOR

NAME AND LOCATION OF STRUCTURE

ADDENDUM TO **FORTIN DE SAN JUAN DE LA CRUZ, EL CAÑUELO**
ISLA DE CABRAS SAN JUAN NATIONAL HISTORIC SITE TOA BAJA PUERTO RICO

SURVEY NO. PR-52

HISTORIC AMERICAN BUILDINGS SURVEY
SHEET OF SHEETS

LIBRARY OF CONGRESS PHOTO NUMBER

IF REPRODUCED, PLEASE CREDIT: HISTORIC AMERICAN BUILDINGS SURVEY, NATIONAL PARK SERVICE. NAME OF DELINEATOR, DATE OF THE DRAWING

393/80033 1 OF 5

HABS 5

SCALE: see graphic scale

1988 HABS DRAWINGS

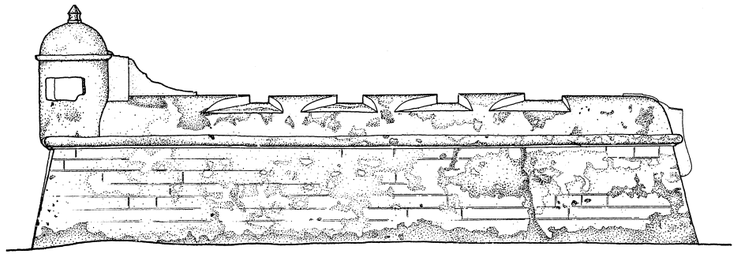
EL CANUELO FORTIFICATION

SAN JUAN NATIONAL HISTORIC SITE

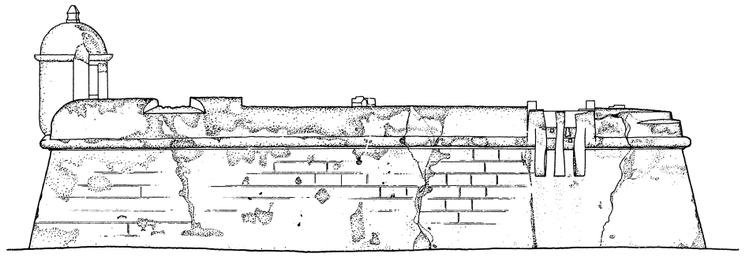
UNITED STATES, DEPARTMENT OF THE INTERIOR

NATIONAL PARK SERVICE, SOUTHEAST REGION

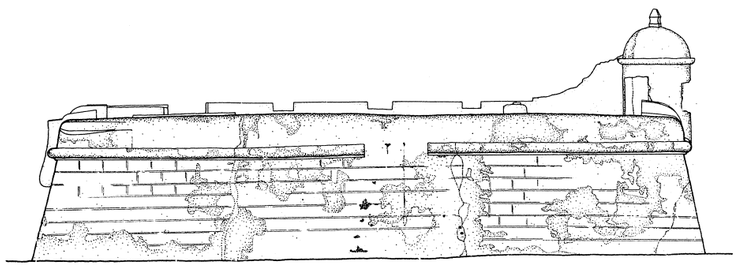
RATIO DESIGN
PALMER ENGINEERING COMPANY
WLA STUDIO



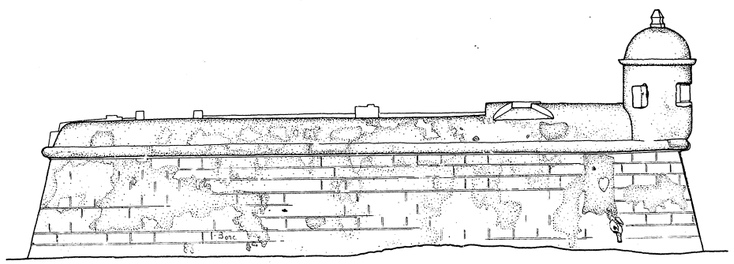
NORTH ELEVATION A-A



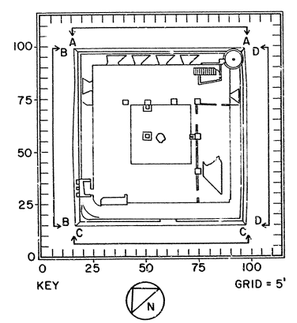
WEST ELEVATION B-B



SOUTH ELEVATION C-C



EAST ELEVATION D-D



BUILDING ELEVATIONS

FEET 1/8" = 1'-0" 0 5 10 15 20 25

METERS 1:96 0 1 2 3 4 5

NAME AND LOCATION OF STRUCTURE
FORTIN DE SAN JUAN DE LA CRUZ, EL CAÑUELO
ADDENDUM TO SAN JUAN NATIONAL HISTORIC SITE
ISLA DE CABRAS TOA BAJA PUERTO RICO

SURVEY NO. PR-52

HISTORIC AMERICAN BUILDINGS SURVEY
SHEET OF SHEETS

LIBRARY OF CONGRESS CATALOG NUMBER

IF REPRODUCED, PLEASE CREDIT HISTORIC AMERICAN BUILDINGS SURVEY, NATIONAL PARK SERVICE, NAME OF DELINEATOR, DATE OF THE DRAWING

DRAWN BY: ORLANDO BADILLO
SAN JUAN NATIONAL HISTORIC SITE PROJECT - 1986
NATIONAL PARK SERVICE
UNITED STATES DEPARTMENT OF THE INTERIOR

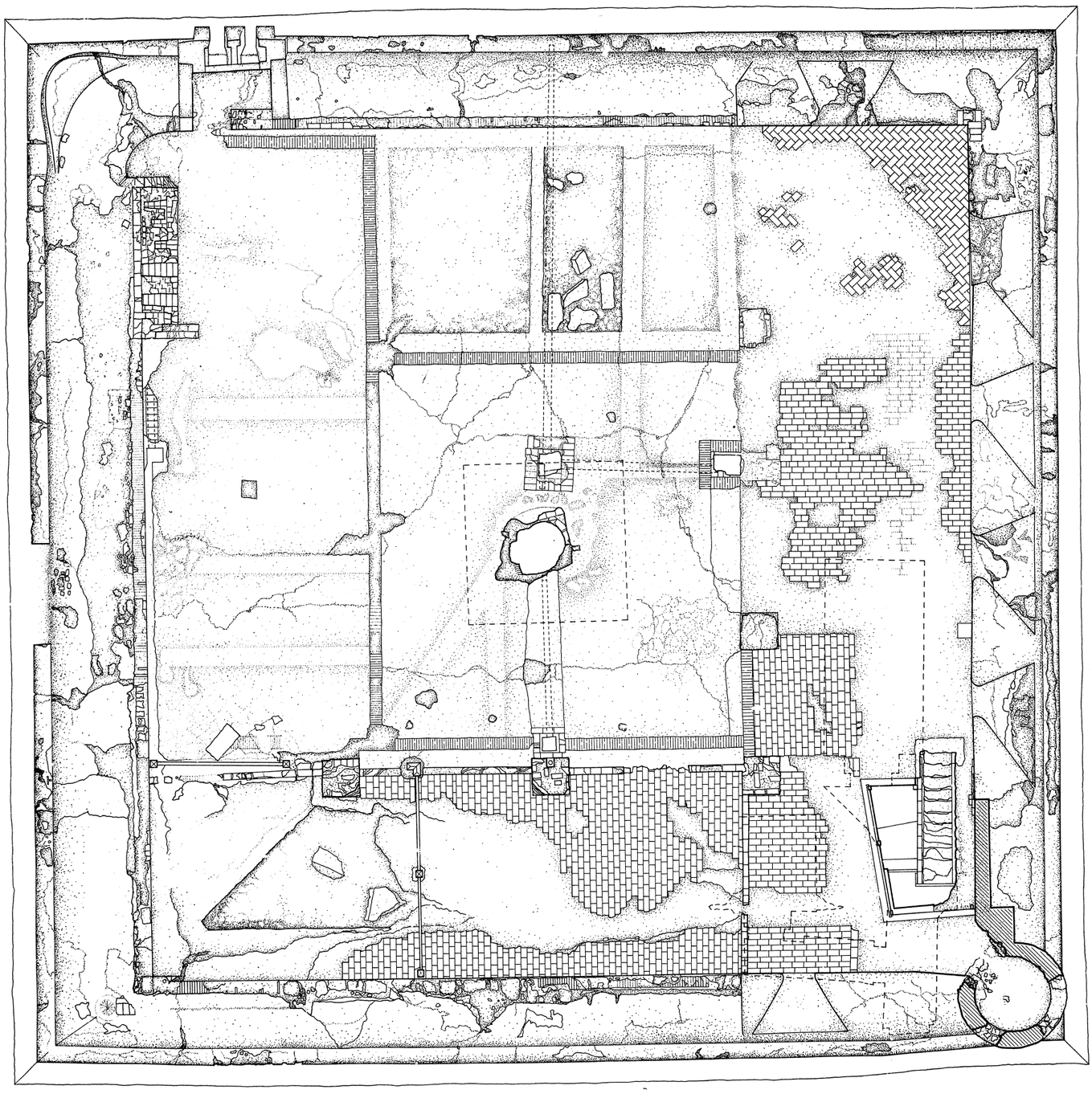
EL CANUELO FORTIFICATION
SAN JUAN NATIONAL HISTORIC SITE
UNITED STATES, DEPARTMENT OF THE INTERIOR
NATIONAL PARK SERVICE, SOUTHEAST REGION

RATIO DESIGN
PALMER ENGINEERING COMPANY
WLA STUDIO

1986 HABS DRAWINGS

SCALE:
see graphic scale

HABS
6



N

FEET 1/4" = 1'-0"
METERS 1:48

FLOOR PLAN

DRAWN BY: T. L. BAILEY

SAN JUAN NATIONAL HISTORIC SITE PROJECT - 1986
NATIONAL PARK SERVICE
UNITED STATES DEPARTMENT OF THE INTERIOR

NAME AND LOCATION OF STRUCTURE
ADDENDUM TO FORTIN DE SAN JUAN DE LA CRUZ, EL CAÑUELO
ISLA DE CABRAS SAN JUAN NATIONAL HISTORIC SITE TOA BAJA PUERTO RICO

SURVEY NO. PR-52

HISTORIC AMERICAN BUILDINGS SURVEY
SHEET OF SHEETS

LIBRARY OF CONGRESS PHOTO NUMBER

IF REPRODUCED, PLEASE CREDIT HISTORIC AMERICAN BUILDINGS SURVEY, NATIONAL PARK SERVICE, NAME OF DELINEATOR, DATE OF THE DRAWING

393/80033 2 of 5

HABS 7

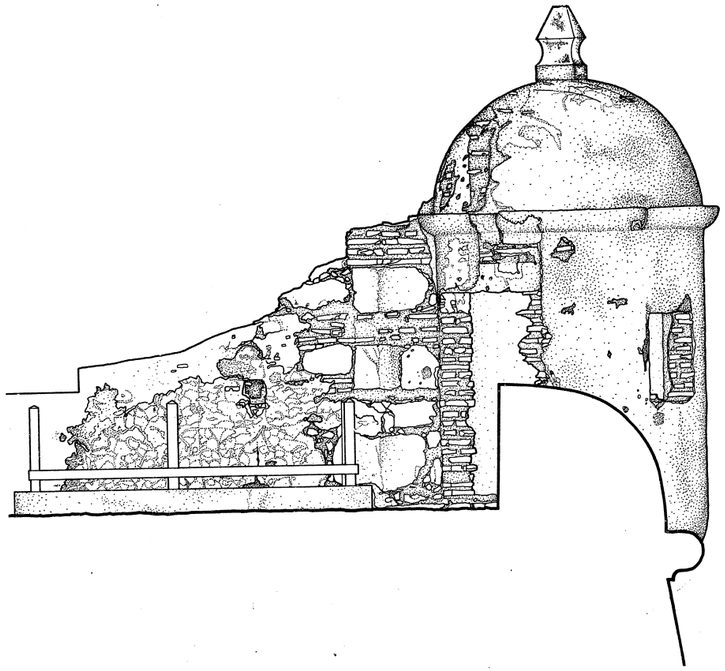
1986 HABS DRAWINGS

SCALE: see graphic scale

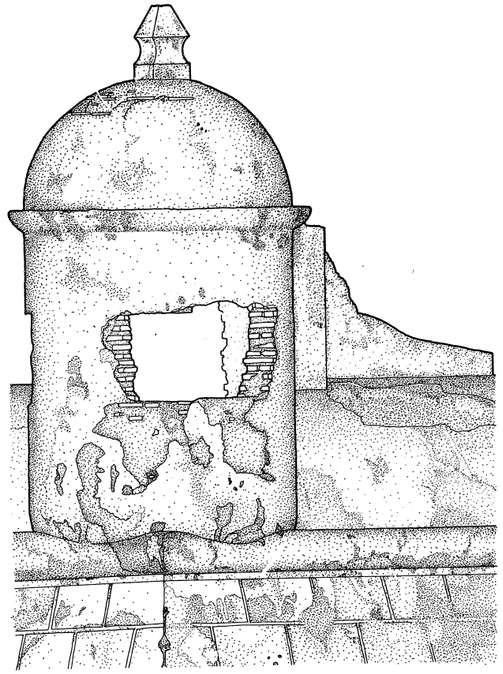
EL CANUELO FORTIFICATION
SAN JUAN NATIONAL HISTORIC SITE
UNITED STATES, DEPARTMENT OF THE INTERIOR
NATIONAL PARK SERVICE, SOUTHEAST REGION

RATIO DESIGN
PALMER ENGINEERING COMPANY
WLA STUDIO

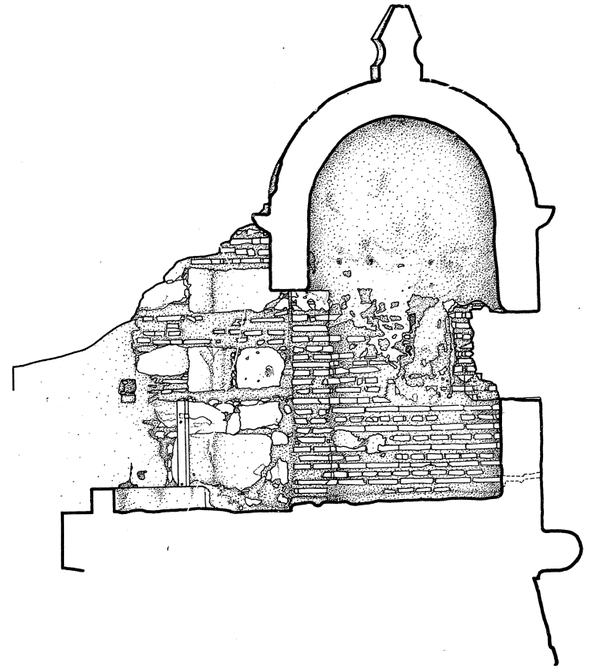
TRIM LINE



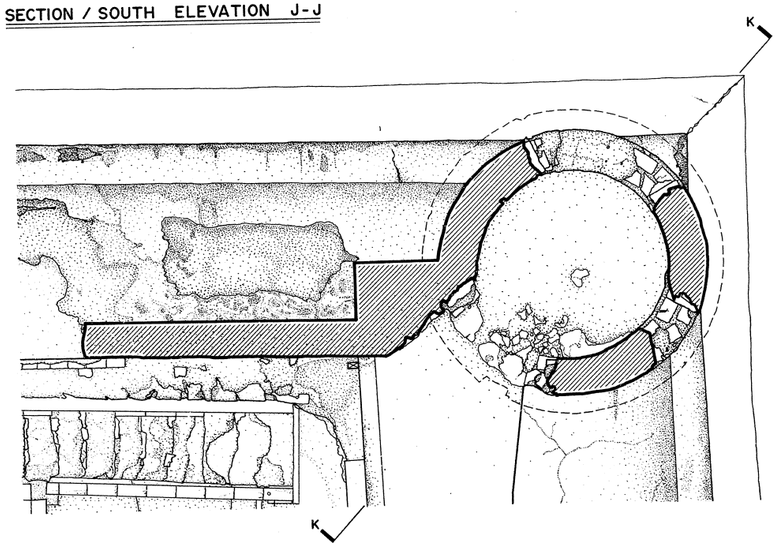
SECTION / SOUTH ELEVATION J-J



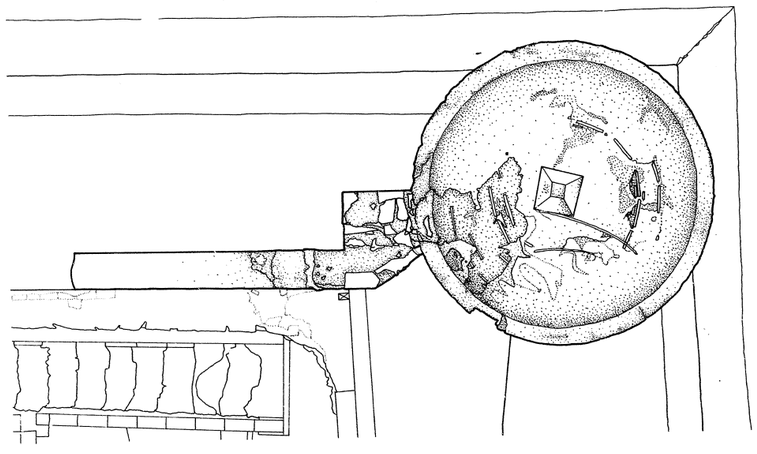
SENTINEL POINT ELEVATION



SECTION K-K



FLOOR PLAN

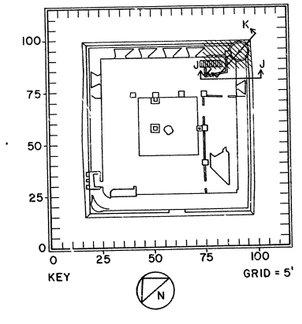


ROOF PLAN

SENTRY BOX DETAILS

FEET 1/2" = 1'-0" 0 1 2 3 4 5

CENTIMETERS 1:24 0 50 100 150



NAME AND LOCATION OF STRUCTURE: **SAN JUAN DE LA CRUZ, EL CAÑUELO** TOA BAJA PUERTO RICO

SURVEY NO. PR-52

HISTORIC AMERICAN BUILDINGS SURVEY SHEET OF SHEETS

SAN JUAN NATIONAL HISTORIC SITE

HISTORIC AMERICAN BUILDINGS SURVEY, NATIONAL PARK SERVICE. NAME OF DELINEATOR, DATE OF THE DRAWING

IF REPRODUCED, PLEASE CREDIT: HISTORIC AMERICAN BUILDINGS SURVEY

FORTIN DE SAN JUAN ADDENDUM TO ISLA DE CABRAS SAN JUAN NATIONAL HISTORIC SITE

DRAWN BY: JORGE L. SEIN

SAN JUAN NATIONAL HISTORIC SITE PROJECT - 1986

NATIONAL PARK SERVICE

UNITED STATES DEPARTMENT OF THE INTERIOR

393/80033 5 of 9

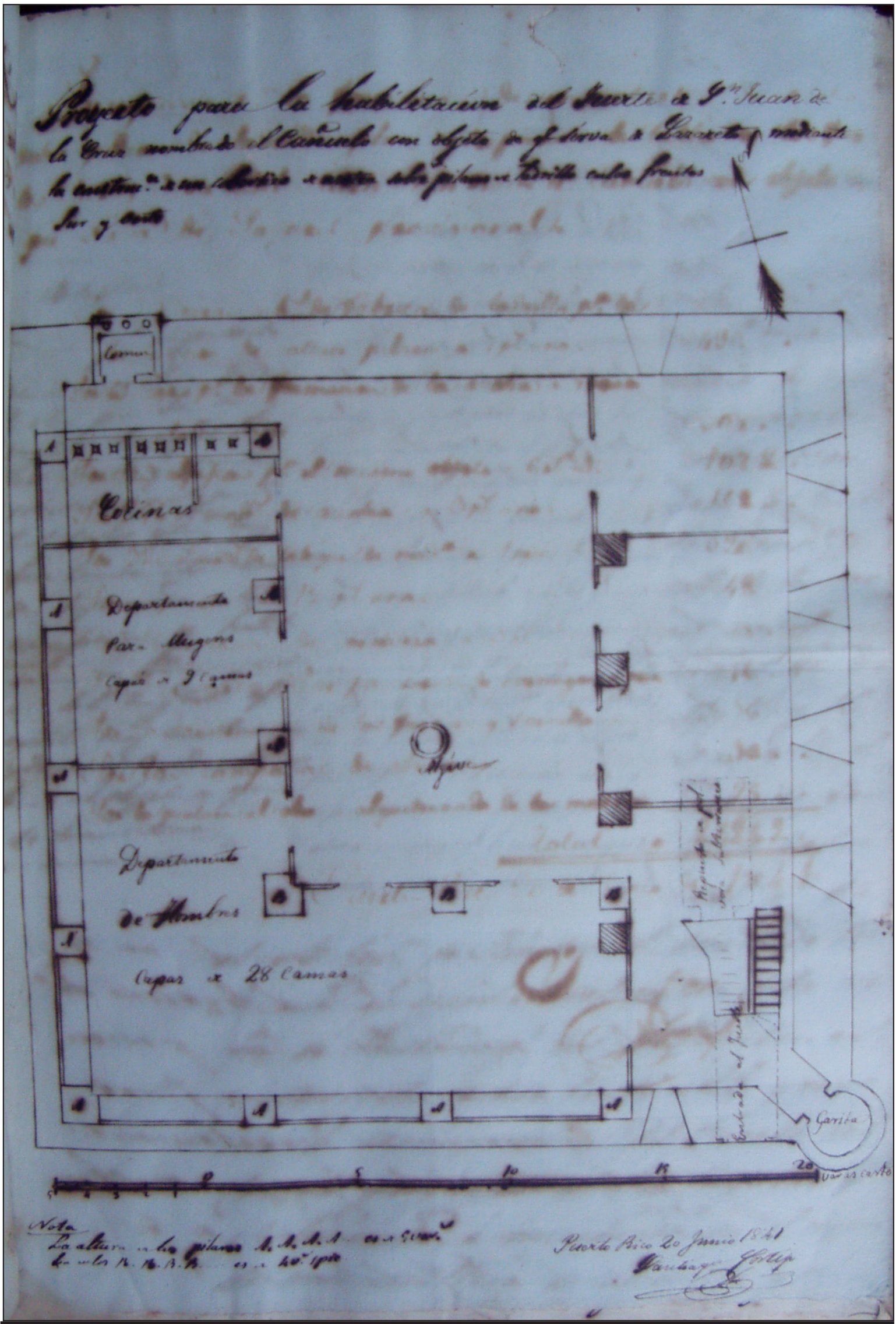
EL CANUELO FORTIFICATION
SAN JUAN NATIONAL HISTORIC SITE
UNITED STATES, DEPARTMENT OF THE INTERIOR
NATIONAL PARK SERVICE, SOUTHEAST REGION

RATIO DESIGN
PALMER ENGINEERING COMPANY
WLA STUDIO

1986 HABS DRAWINGS

SCALE:
see graphic scale

HABS
8



References: Image provided by Wanda Boboris. Original in Puerto Rico Archives.	SCALE: see graphic scale	1841 DRAWING		EL CANUELO FORTIFICATION SAN JUAN NATIONAL HISTORIC SITE UNITED STATES, DEPARTMENT OF THE INTERIOR NATIONAL PARK SERVICE, SOUTHEAST REGION	RATIO DESIGN PALMER ENGINEERING COMPANY WLA STUDIO

Appendix C: Material Analysis Report

HIGHBRIDGE
MATERIALS CONSULTING, INC.

404 Irvington Street
Pleasantville, NY 10570
Phone: (914) 502-0100
Fax: (914) 502-0099
www.highbridgematerials.com

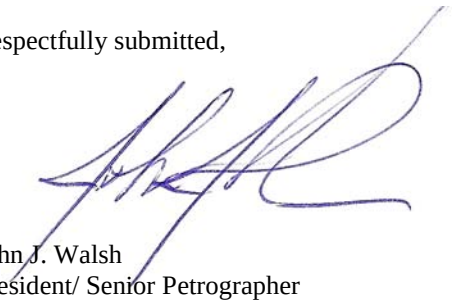
MATERIALS ANALYSIS REPORT

Client:	Building Conservation Associates, Inc.	**Client ID:**	BUIL005
Project:	El Cañuelo	**Report #:**	SL1095-01
Location:	Isla de Cabra, Puerto Rico	**Date Received:**	11/11/16
Sample Type:	Mortar, render, and plaster	**Report Date:**	03/03/17
Delivered by:	Client (D. Krotzer)	**Petrographer:**	J. Walsh
		Chemist:	H. Hartshorn
		Analyst:	S. Sauer
		Page 1 of 93	

Report Summary

- Seven samples containing ten distinct materials are analyzed for this report. These include mortars, renders, and plasters from El Cañuelo in San Juan, Puerto Rico.
- The samples all represent a single materials tradition where lime-based binders are modified with pozzolanic additives. Crushed brick and volcanic ash are both identified. The latter is restricted to the exterior wall and it is possible that this represents an early replacement of the surface cladding. Sands are usually sparse if present at all. Beachrock grains, fine-grained natural sands, and shell fragments are all identified as aggregates.

Respectfully submitted,



John J. Walsh
President/ Senior Petrographer
Highbridge Materials Consulting, Inc.



Heather Hartshorn
Staff Scientist/ Chemist
Highbridge Materials Consulting, Inc.

Table of Contents

1. Introduction 4
Table 1.a: Summary of Sample Identifications and Locations 4
2. Methods of Examination 5
3. Standard of Care 5
4. Confidentiality 5
5. Executive Summary 6
Table 5.a: Summary of Material Compositions 7
6. Characterization of Mixture Types 8
6.1 - Lime-Crushed Brick Mixtures (Samples M03a and M03b) 8
Table 6.1a: Estimated Combined Binder Chemistry (Lime-Brick Mixes) 9
Table 6.1b: Calculated Components (Lime-Brick Mixes) 10
6.2 - Lime-Crushed Brick Mixtures with Beachrock Sand (Samples M02 and M05 Body Coat) 11
Table 6.2a: Estimated Lime Chemistry (Lime inclusion) 12
Table 6.2b: Estimated Combined Binder Chemistry (Lime-Brick Mixes with Beachrock Sand) 13
Table 6.2c: Calculated Components (Lime-Brick Mixes with Beachrock Sand) 13
6.3 - Lime Plaster Finish (Sample M05) 14
Table 6.3a: Estimated Binder Chemistry 14
6.4 - Lime-Brick Dust Finish Coat (Sample M04a) 15
Table 6.4a: Estimated Combined Binder Chemistry (Lime-Brick Render Finish) 16
6.5 - Sanded Mixtures of Lime and Natural Volcanic Pozzolan (Samples M01 and M04) 16
Table 6.5a: Estimated Binder Chemistry (Lime-Natural Volcanic Pozzolan Mixes) 18
Table 6.5b: Estimated Binder Chemistry (Lime-Natural Volcanic Pozzolan Mixes) 19
7. Materials 20
7.1 - Calcareous Arenite (Beachrock) 20
7.2 - Natural Sand 21
Table 7.2a: Sand Gradation Profiles - Cumulative Percent Passing 22
7.3 - Shell Sand 22
7.4 - Lime Binder 23
Table 7.4a: Abundance and Size of Undispersed Lime Grains 23
Table 7.4b: Summary of Minor Textural Features Identified in the Lime Binder 24
Table 7.4c: Estimated Lime Chemistry (Lime inclusion) 25
7.5 - Low-Fired Brick 25
Table 7.5a: Description of Temper Constituents in Soft-Fired Brick Inclusions 26
Table 7.5b: Cumulative Passing Percentages of Material Assumed to Represent Brick Temper and Fired Clay 27
7.6 - Higher-Fired Brick (Sample M04 Finish Coat) 28
7.7 - Volcanic Glasses (Trass) 29
7.8 - Pigment 29

8. Open Questions and Possible Courses for Future Evaluation 30
8.1 - Soft-Fired Brick 30
8.2 - Lime Composition and Sources 30
8.3 - Beachrock 30
8.4 - Volcanic Ash 30
8.5 - Exterior Render Stratigraphy 31
8.6 - Salt Contamination 31
8.7 - Performance Evaluations of Candidate Pozzolans for Use in Repair Mixes 31
9. Sieve Analysis of Sand or Other Extracted Inclusions 32
Table 9.a: Extracted Sand and Inclusions Data (Lime-Crushed Brick Mixtures) 33
Table 9.b: Extracted Sand and Inclusions Data (Lime-Crushed Brick Mixtures with Beachrock Sand) 34
Table 9.c: Extracted Sand and Inclusions Data (Lime-Brick Dust Finish Coat) 35
Table 9.d: Extracted Inclusions Data (Sanded Mixtures of Lime and Natural Pozzolan) 36
10. Chemical Analysis 37
Table 10.a: Chemical Analysis Results (Fraction Passing No. 100 Sieve) 37
Table 10.b: Chemical Analysis Results (Fraction Retained on No. 100 Sieve) 38
Table 10.c: Normalized Weight Percent Totals (Combined Fractions) 38
Table 10.d: Chemical Analysis Results (all samples including those reported in Table 10.c) 39
Table 10.e: Estimated Binder Chemistry 39
Table 10.f: Calculated Components (Lime-Crushed Brick Mixtures) 40
Table 10.g: Calculated Components (Lime-Crushed Brick Mixtures with Beachrock Sand) 40
Table 10.h: Calculated Components (Lime-Brick Dust Finish Coat) 41
Table 10.i: Calculated Components (Sanded Mixtures of Lime and Natural Pozzolan) 41
Appendix I: Visual Description of Samples as Received 42
Appendix II: Photographs and Photomicrographs 46

1. Introduction

On November 11, 2016, Highbridge received seven mortar, render, and plaster samples containing a total of ten distinguishable materials. These were received from Ms. Dorothy Krotzer of Building Conservation Associates, Inc.. According to Ms. Krotzer, these samples were taken from Fortín San Juan de la Cruz (a.k.a. El Cañuelo) in San Juan, Puerto Rico. Ms. Krotzer reports that the fort was originally constructed in 1664. She describes the exterior walls of the fort as rubble masonry with a load-bearing sandstone ashlar veneer that is covered with a multi-layer render and painted finish. According to the client, interior walls are also rendered. The samples were taken from multiple locations and represent a variety of materials. The client has identified the samples and provided the details about locations as follows. Highbridge has also noted the materials contained within each sample.

Table 1.a: Summary of Sample Identifications and Locations

Client ID	Location	Materials Included
M01	Exterior, northeast elevation	Render body coat and finish layer
M02	Northwest elevation at cap level	Mortar
M03a	Northwest elevation at roof level	Mortar
M03b	Northwest elevation at roof level	Render body coat
M04a	Exterior, southwest elevation at cordon	Render body coat and finish layer
M04b	Exterior, southwest elevation at cordon	Render body coat
M05	Interior, corridor wall	Plaster brown coat and finish layer

Following a discussion with the client, Highbridge has agreed to perform a compositional analysis wherever possible on all of the materials included in the samples with the exception of paints or color washes. This testing includes petrographic and chemical analysis to identify constituents, evaluate overall condition, and estimate component proportions. Where it is possible to separate certain aggregate or other non-binder components from the sample, these materials were extracted and a sieve analysis performed. The extracted and graded samples are returned to the client.

2. Methods of Examination

The petrographic examination is conducted in accordance with the standard practices contained within ASTM C1324. Data collection is performed or supervised by a degreed geologist who by nature of his/her education is qualified to operate the analytical equipment employed. Analysis and interpretation is performed or directed by a supervising petrographer who satisfies the qualifications as specified in Section 4 of ASTM C856.

Chemical analysis is conducted according to the procedures outlined in ASTM C1324. Water and carbon dioxide weight percentages are not determined due to the sample preparation and analysis methods chosen in order to more completely isolate the binder from the other mortar components. Aggregate weight percentages are determined gravimetrically. Oxide weight percentages are determined by inductively coupled plasma optical emission spectroscopy (ICP-OES). The methods are modified when accounting for dolomitic lime. Rather than approximating lime through DTA with possible errors due to carbonated lime, dolomitic lime is instead calculated directly from the chemical analysis by simultaneous equations based on typical dolomitic lime chemistry.

3. Standard of Care

Highbridge has performed its services in conformance with the care and skill ordinarily exercised by reputable members of the profession practicing under similar conditions at the same time. Interpretations and results are based strictly on samples provided and/or examined.

4. Confidentiality Statement

This report presents the results of laboratory testing requested by the client to satisfy specific project requirements. As such, the client has the right to use this report as necessary in any commercial matters related to the referenced project. Any reproduction of this report must be done in full. In offering a more thorough analysis, it may have been necessary for Highbridge to describe proprietary laboratory methodologies or present opinions, concepts, or original research that represent the intellectual property of Highbridge Materials Consulting and its successors. These intellectual property rights are not transferred in part or in full to any other party. Presentation of any or all of the data or interpretations for purposes other than those necessary to satisfy the goals of the investigation are not permitted without the express written consent of the author. The findings may not be used for purposes outside those originally intended. Unauthorized uses include but are not limited to internet or electronic presentation for marketing purposes, presentation of findings at professional venues, or submission of scholarly articles.

5. Executive Summary

The several mortar, render, and plaster samples examined from El Cañuelo on Isla de Cabra, Puerto Rico represent a single materials tradition divided into two distinctly different manifestations. The overall tradition predates the use of hydraulic limes and cements as a means of providing durability and water-resistance initiated during the Industrial Revolution, and includes the incorporation of pozzolans to react with lime. Pozzolans are poorly crystalline or otherwise chemically unstable forms of silica and alumina that are capable of reacting with building lime in a relatively short time to create hydraulic products that increase overall strength and density. The two types of pozzolan used at El Cañuelo include crushed clay brick and volcanic ash. Only a thin lime plaster finish with some crushed shell aggregate in Sample M05 does not include any pozzolan at all.

The first group of samples includes a high-calcium lime mixed with a soft-fired brick. This includes mortar samples M02 and M03a, render sample M03b, and the plaster brown coat of Sample M05. The brick is a low quality product that readily disintegrates into its constituent parts. In fact, it appears that the brick was crudely disaggregated rather than crushed before being incorporated into each mix. The coarseness is greater in Samples M03a and M03b where unbroken particles are as large as a centimeter in diameter. Because at least 85% of the brick is a quartz sand temper, the disaggregated brick acts as much as an aggregate as it does a pozzolan if not more so. In fact, the sandy brick granules are present at 1.5 to 2.5 parts for every unit volume of lime (equated to a dry hydrate basis). Samples M02 and M05 also contain a light addition of coarse sandstone particles. These are identified as the same beachrock constituting the masonry substrate and may simply represent intentional inclusions of debris derived from the stone-cutting.

The brick in these four sample layers behaves as an effective pigment and all of the mixtures have a rich and mostly uniform pastel orange color. The pozzolanic activity generated by the crushed brick is not very consistent as suggested by the variable cementation indices calculated from the chemical analysis (Table 5.a). In part, these may be the result of differences in the level of disaggregation but this is not a wholly satisfying interpretation. Variability in the intrinsic chemical quality is more likely responsible. In any case, the pozzolanic effect is only really apparent in the chemical analysis and not in the qualitative characteristics apparent macroscopically in the samples themselves. All layers are quite soft and highly water permeable. All four materials are capable of being disaggregated with modest finger pressure.

The second group of samples includes lightly sanded, high-calcium lime mixtures that have gained strength through reaction with a very fine-grained volcanic glass or ash. The increased cohesion and strength are more macroscopically apparent in these samples. The materials containing ash include the exterior wall render samples M01, M04a, and M04b, though a different type of finish is present over the body coat of M04a. The sand is fine-grained and very sparsely distributed in these samples. The layer with the highest sand content has a binder to sand ratio of 1 : 0.64 with the lime calculated as a dry hydrate (Table 5.a). The fines that include the volcanic ash represent about 20% of the total lime volume. This fine volcanic glass appears to be rhyolitic in composition. Technically, it cannot be proven that the ash was an intentional addition. Even if intentional, it is not apparent whether the ash was an impurity of the sand, a separate local deposit of concentrated ash or volcanic earth, or an imported European trass. In any case, the ash has produced a more notable strengthening of the matrix. While all of the uniformly white or light-colored mixtures have a moderately soft paste and a high permeability, the materials are more cohesive than those containing the soft-fired brick. This is also noted in higher cementation indices on average that are calculated from the chemical analysis. Variations in the amount of solubilized silica that controls this index are interpreted to be the result of variations in the carbonation reaction. Carbonation tends to inhibit or arrest the pozzolanic reaction since it consumes the calcium hydroxide that is necessary to react with the pozzolan.

Sample M01 represents the vertical field of the outer wall. In this sample, the white body coat is overlain by a pale yellow finish coat of a few millimeters thickness. This outer layer is essentially identical in composition to the body coat with the exception of a minor dosage of mineral pigment. However, this layer might not have been the final presentation face as a much brighter color wash with a similar yellow hue is applied over the finish coat. Photographs provided by the client indicate faux white joints scribed into the render as well. Neither the color wash or the faux joints were examined as part of this study. Sample M04a and M04b represent a protruding string course near the top of the wall. In this case, the body coat is covered with a hard-troweled finish layer containing lime and crushed brick. The brick serves as a pigment as well as a pozzolan, and the method of finish has concentrated the colorant along the presentation face. No additional color washes are detected or thought to be necessary. The brick is also found to be a harder-fired variety than that detected in the other samples and contributes much more strength and density due to a very effective pozzolanic reaction.

Table 5.a: Summary of Material Compositions

Sample	Material	Masonry/Substrate	Pozzolan type	Sand	Lime : Pozzolan	Lime : Sand	Cementation Index
M01	Render body	Sandstone	Volcanic ash	Natural sand	1 : 0.22	1 : 0.51	0.77
M01	Render finish	Sandstone	Volcanic ash	Natural sand	1 : 0.19	1 : 0.25	0.28
M02	Mortar	Sandstone	Soft brick	Beachrock	1 : 1.9	1 : 0.69	0.63
M03a	Mortar	Brick	Soft brick	None	1 : 2.5	n/a	0.44
M03b	Render body	Brick	Soft brick	None	1 : 1.5	n/a	0.13
M04a	Render body (white)	Sandstone	Volcanic ash	Natural sand	1 : 0.18	1 : 0.13	0.80
M04b	Render body (pink)	Sandstone	Volcanic ash	Natural sand	1 : 0.26	1 : 0.64	0.22
M04a	Render finish	Sandstone	Harder brick	None	1 : 0.48	n/a	0.88
M05	Plaster brown coat	Brick	Soft brick	Beachrock	1 : 1.9	1 : 0.11	0.23
M05	Plaster finish	Brick	None	Fine shells	n.d.	n.d.	0.02

It is possible that the two general categories of materials all represent original or at least contemporaneous construction. If this were true, it might suggest that the builders favored a harder and somewhat more water-resistant render for the exterior wall coating and allowed lower quality and potentially less-expensive materials to be used in less critical parts of the construction. However, it is also possible that the currently installed exterior render is a later repair. There is some very minor evidence consistent with this interpretation in that residues of lime-brick render are contained within the masonry pores below the lime-ash renders. Though speculative, it is possible that the same lime-brick mixtures found in Samples M02, M03a, M03b, and M05 were used to clad the building exterior. If true, a completely different aesthetic may have been intended for the building.

6. Characterization of Mixture Types

Five general mixture compositions are distinguished through the laboratory analysis. These include lime-brick mixtures, lime-brick mixtures with beachrock grains, one lime plaster, one lime-brick finish with a different brick type, and sanded lime-pozzolan mixtures with volcanic ash. Each of the sections below provides detail on the microstructural and compositional characteristics of each of these mixes along with some commentary on quality and condition wherever appropriate. Due to the fact that some of the constituent materials are used in more than one of the mix types, it was decided that details regarding the individual constituents were better deferred to a separate section (Section 7).

6.1 - Lime-Crushed Brick Mixtures (Samples M03a and M03b)

Sample M03a is reported to be a brick bedding mortar and M03b an exterior surface render that was taken in close proximity (Fig. 1). Both are monolithic in composition though M03a shares a contact with a trace piece of white lime mortar. The latter may represent an unassociated repair. Both samples are a pastel orange color and have a dull, grainy texture. Sample M03b contains rounded red-colored brick fragments up to about a centimeter in diameter. These are present in moderate concentration and are visually obvious on freshly exposed surfaces of the render. A few millimeter-scale lime particles are also apparent but are not a major influence on the aesthetics. This variegated texture is not as immediately obvious in the small pieces provided for Sample M03a, but the same coarse-grained brick fragments are identified petrographically for this sample. Both samples have a cured binder that is soft and highly permeable. Though cohesive, the matrix in both samples can be effectively disaggregated with low to moderate finger pressure.

The two samples are essentially identical in composition and consist of lime-based mortars with a crushed brick pozzolan. The coarseness of the brick causes it to behave as an aggregate as well. As described in Section 7.5, the brick is a soft-fired product that is highly friable and contains at least 85% of a quartz sand temper sized mostly between the No. 30 and No. 100 sieves. Both samples have a microstructure that is defined by a fairly dense distribution of brick fragments evenly distributed throughout a homogeneous, fully carbonated lime paste (Fig. 2). The two mixtures were not especially well consolidated and the air content is as high as 12-18% in some areas. Nevertheless, the material appears compact at the visual scale.

The brick grains are densely distributed throughout the matrix. Because the brick is so friable, much of it had broken down into its constituent parts before or during mixing. However, there are no cracked or crushed temper particles and this indicates that the original workers did not use great force to break the brick. It appears that a light beating with simple hand tools may have been all that was required to reduce the brick to its current size. Petrographically, the quartz temper could be mistaken for a simple sand except that virtually every grain has a thin lining of fired clay adhered to its surface (Fig. 3). The clay body is also broken down into fine particles and powder. At some scale, the fine powder is more like a binder component than an aggregate component. At the other end, a moderate number of brick particles had survived the original mixing and remain as discrete grains up to about a centimeter in size (Fig. 1). As discussed in Section 7.5, it was not possible to preserve the existing particle gradation after decomposing the lime binder with acid. The coarser intact brick fragments all broke down into their constituent parts (Fig. 4). Still, the gradation profiles reported in Table 7.5b should be considered a reasonably faithful representation of the finer end of the original particle size distribution. The actual distribution is coarser and broader.

The lime is interpreted to be a high-calcium, nonhydraulic product probably burned from a sedimentary limestone. Admittedly, the interpretation of the chemistry is based on the measurement of a single lime grain extracted from Sample M02 and the soluble chemistry of the lime plaster finish in Sample M05. However, these two samples are likely contemporaneous with Samples M03a and M03b. The soluble chemistry of these two samples is normalized to 100% and reported in Table 6.1a.

Table 6.1a: Estimated Combined Binder Chemistry (Lime-Brick Mixes)

Sample ID	**M03a**	**M03b**
Material type	**Mortar**	**Render Body Coat**
Component (wgt. %)		
SiO_2	9.2	2.4
CaO	78.6	89.9
MgO	1.8	2.0
Al_2O_3	8.1	4.1
Fe_2O_3	1.2	0.6
Other	1.0	1.0
CaO/MgO ratio	**43.2**	**45.8**
Hydraulicity index	**0.22**	**0.07**
Cementation index	**0.44**	**0.13**

The soluble chemistry represents the combination of the lime binder with the products created by the brick pozzolanic reaction. Any soluble salts that may have deposited within the mortars may also be represented in this chemistry. First, it is noted that the CaO contents are still relatively high and clearly much greater than the MgO contents. Since the lime is certainly not dolomitic, the MgO may have come from magnesium salts in the seawater. This may also be supported by the fact that the interior plaster samples have CaO/MgO ratios that are generally about two to three times higher than the exterior mortars and renders (Table 10.e). The other elements including SiO_2 and Al_2O_3 are solubilized constituents of the brick that have produced some hydraulic product on reaction with the lime. To evaluate the magnitude of this reaction, hydraulicity and cementation indices are calculated from the chemical data. The interpretation of these indices are discussed by Eckel (1905). These are somewhat crude indicators and are generally meant to evaluate single binders rather than the hardened products of two reacted binders. Nevertheless, there is some notable difference between the two samples. The mortar has a hydraulicity index of 0.22 and cementation index of 0.44. These would be considered equivalent in hydraulicity to a feebly to moderately hydraulic lime. In contrast, the render body has a hydraulicity index of 0.07 and a cementation index of 0.13. Though this suggests more hydraulicity than the lime alone, the indices are lower than most weakly hydraulic limes.

The difference in reactivity is unresolved in this study. It is certainly possible that the brick does not produce a consistent pozzolan. In discussions with the client, it has become apparent that the brick used in the wall construction is more indurate than the crushed brick used in the mortar. It is possible that poor quality bricks were set aside after firing and reserved for crushing. If this were true, there might not be any expectation of consistency. Alternatively, it would be expected that reactivity would be a function of the specific surface or average grain size of the crushed brick. Brick crushed more finely would present a greater surface area for reaction and should yield higher chemical indices. It is difficult to evaluate this possibility since Sample M03a contains only a limited number of small pieces. However, this sample appears to have fewer centimeter-scale brick fragments than does Sample M03b.

Despite these apparent chemical differences, there does not appear to be any appreciable difference in qualitative hardness or permeability between the two samples. Both are relatively soft and can be broken up by hand. Neither are consistent in quality with a modern hydraulic lime of moderate strength (e.g. NHL 3.5). It may be that the production of hydraulic product is more localized and inefficient in the lime-brick mix than it might be in a hydraulic lime containing distributed calcium silicates and calcium aluminates.

The chemical analysis was also used to estimate the original component proportions. The mix designs are especially simple for these two samples as they contain only two components. Calculating the lime as the equivalent of a modern dry hydrate, the lime to brick ratio is estimated at 1 : 2.5 for Sample M03a and 1 : 1.5 for Sample M03b. This is a somewhat crude estimate since it equates all of the brick with a natural sand and uses a similar bulk density in the calculation. Of course, a portion of the crushed brick behaves more like binder. Even assuming the brick/sand equivalency is valid, the reported values overestimate the "aggregate" to some degree. Nevertheless, the main point to take away from these arguments is that the distribution of brick particles within the lime matrix produces a composite that is similar in texture to a properly sanded lime mortar if not slightly oversanded.

It should also be noted that though the lime was obviously incorporated in the form of a putty, the binder is reported here as a dry hydrate. The calculation of the lime as a dry hydrate is convenient because it does not have to take into account the mix water used in a lime putty. If a recalculation of the proportions is desired, it can be assumed that a volume of dry hydrate will lose approximately 40-50% of its volume when water is added to produce a putty of stiff consistency. One could simply double the "aggregate" volume to yield an equivalent ratio relative to a putty. All this said, Table 6.1b (and 10.f) also report the estimated weights of the raw materials. This is considered the most accurate of all since they represent direct measurements of material mass and are not dependent on assumptions of original bulk density.

Table 6.1b: Calculated Components (Lime-Brick Mixes)

Sample ID	**M03a**	**M03b**
Material type	**Mortar**	**Render Body Coat**
Component		
Lime expressed as dry hydrate (wgt. %)	16	25
Brick (wgt. %)	84	75
Lime : brick ratio (by volume with lime as a dry hydrate)	1 : 2.5	1 : 1.5
Lime : brick ratio (by volume with lime as a putty)	1 : 5.1	1 : 3.0

Notes:
1. The lime weight is calculated by mathematically converting the measured CaO to its respective hydroxide by molecular weight conversion and reporting it in the form of a dry lime hydrate. The brick weight is taken directly from the insoluble residue in addition to the remaining four measured oxides. The lime and brick weights are normalized to 100% to return the materials to a dry weight basis. Volumetric ratios are calculated assuming bulk densities for dry lime hydrate and brick of 40 lbs./ft.^{3} and 80 lbs./ft.^{3} respectively. Another calculation is provided assuming the lime in putty form. This assumes a unit of dry lime hydrate will lose approximately half its volume when mixed to the consistency of a stiff paste. The brick volume then increases for the same weight of lime.

The two lime-brick samples exhibit some secondary service effects, none of which appear to have significantly compromised the materials. Traces of secondary salts are noted in both samples (Fig. 5). The petrographic properties of these include colorless crystals that have low optical relief. Some are isotropic and some have low first order birefringence. Based on the optical properties, these are probably mixtures of halite and gypsum. Other salts could be present and simply not detectable at the scale of the light microscope. It is not unusual for salt-rich samples to yield little to no petrographic evidence if the salts are distributed throughout the micropores of the binder. In this case, the petrographically visible salts are present in air-voids and along the broken surfaces of Sample M03a. In Sample M03b, the salts are mostly restricted to the outer surface of the render and just a little beyond. A few other minor mineralizations are detected in Sample M03b. In some places, an exceptionally thin veneer of carbonate spar lines air-voids in a zone at the outermost few millimeters of the render. There are also a few coarser brick fragments that display some internal microcracking. The cracks in one of these observed petrographically contain linings of a different salt that is not positively identified. Since it is restricted to the brick, it may have derived from this component.

Both samples contain some biogrowth along originally exposed or broken surfaces. In Sample M03b, carbonated lime grains located near the surface of the render contain microbial boring channels usually filled with green biota (Fig. 6). The channels are vermicular in shape, generally perpendicular to the outer render surface, and have diameters measured in microns. The author has no expertise in microbiology but assumes that these are algal borings of some kind. Interestingly, the channels only seem to occur in undispersed lime particles and not the surrounding lime matrix. It appears that the lime grains provide a more favorable environment for the microbes.

6.2 - Lime-Crushed Brick Mixtures with Beachrock Sand (Samples M02 and M05 Body Coat)
Sample M02 is a sandstone masonry mortar from the exterior wall. Sample M05 is an interior plaster with a reddish-colored body coat and a thinner white finish layer (Fig. 7). The mortar and the body coat of the plaster both have a pastel orange color and a dull, grainy texture similar to that of the lime-crushed brick mixtures. In this case, coarser brick fragments are not visually apparent. Some coarser lime particles are noted on fresh surfaces of Sample M02. This sample also contains adhered fragments of orange-colored beachrock. Some of the coarser pieces are likely to be fragments of the substrate masonry. However, at some finer sizes it is difficult to tell whether the fragments are adherent substrate or actual inclusions. As with the lime-crushed brick samples, these samples have a cured binder that is soft and highly permeable. The materials are mostly cohesive but the matrix can often be disaggregated with low to moderate finger pressure. This is sometimes difficult to tell in Sample M02 when the pieces are dusty and underlain by a much harder fragment of beachrock.

These two samples are essentially the same as the lime-crushed brick materials. It is suspected that they represent the same construction vintage though it is always possible for materials use and technological traditions to have some temporal persistence, especially in pre-industrial construction. The only difference with these two samples is the addition of a minor amount of beachrock sand (Fig. 8). As described in Section 7.1, the beachrock is a porous stone consisting of narrowly-graded beach sand that is cemented in place with calcium carbonate. It is suspected that this particular beachrock is a very recent geological formation that may be locally available as thin pavements along the shoreline. Based on the larger fragments adhered to the exterior wall samples M01 and M02, it appears that the beachrock was used as a building stone. Discussions with Mr. Wohlgemuth regarding the appearance of the substrate stone suggests that this is likely.

The beachrock grains perform as a minor aggregate addition in both samples (Fig. 8). These may have been intentionally added to improve volume stability or they may have been added just to get rid of jobsite debris. What is not clear is whether this relatively pure sand was available as a sediment or if the beachrock was broken down by the original workers to produce a sand-sized material. Assuming that the beachrock was used to construct the wall, it is possible that the fragments identified in the samples are the waste derived from dressing the rock for masonry use.

There is some overlap in sizes between the beachrock sand and the crushed brick pozzolan (Fig. 9). However, in the gradation profile produced by the laboratory from disaggregated samples (see Table 9.b), the No. 30 sieve (i.e. 600 µm) separates these two components relatively well (Fig. 10). Due to their friability, most coarser brick grains are broken down into individual temper grains and powder from the clay matrix. Most of the temper passes the No. 30 mesh. Very few beachrock grains are finer than this sieve. For the body coat of Sample M05, beachrock grains are found up to the No. 4 sieve. These coarser grains are observed petrographically but the "sand" extraction procedure only recovered particles up to the No. 16 sieve. For Sample M02, the "sand" recovery contains beachrock grains evenly distributed between the No. 4 and No. 30 sieves. Grains that are even coarser are found in hand sample but it is not clear if these are actually fragments from the masonry substrate. Overall, the beachrock sand addition is interpreted to have a somewhat limited particle size distribution between the No. 4 and No. 30 sieves.

With exceptionally minor differences described in Section 7.5, the crushed brick used in Samples M02 and M05 is the same as that found in Samples M03a and M03b. As discussed earlier, the brick is a soft-fired product with a densely distributed, quartz-rich sand temper narrowly graded between the No. 30 and No. 100 sieves (Fig. 10). The friable material is readily disaggregated into its constituent parts without the need to apply a force sufficient to crush the temper. When incorporated into the mortars, the clay-coated sand grains became distributed throughout the lime matrix to create a dense sanded texture while the fired clay intermixed with the lime binder (Fig. 11). The brick is more disaggregated in these two samples relative to the M03 samples. Unbroken grains are only found to about 1.5 and 3 millimeters in diameter for Samples M02 and M05 respectively. The larger-scale mixing and consolidation properties of the mortar as a whole are not as well observed in these two samples due to the limited amount of material available for thin section analysis. Nevertheless, the temper from the brick is more or less evenly distributed throughout the lime binder with much sparser occurrences of the beachrock particles (Fig. 8). These samples appear to be a bit more completely consolidated than the other two samples. Some areas in the brown coat of Sample M05 contain randomly-oriented lenticular microvoids with total air contents perhaps as high as 8%. Where not fragmental, Sample M02 contains fine subspherical voids less than 0.25 mm at less than 5% by volume.

The lime in both samples is interpreted to be a high-calcium, non-hydraulic product probably burned from a sedimentary limestone. Petrographic arguments are discussed in Section 7.4. The chemical interpretation is based on a pure lime particle about 5 millimeters in diameter that was extracted from Sample M02. The composition of this particle is summarized in Table 6.2a. At over 98% CaO, the lime would have been a fast-slaking and highly workable fat lime. It is assumed that the lime in Sample M05 would have been similar in composition. In fact, the finish coat that directly overlies the body coat lacks any pozzolanic contributors and the lime in this layer has a CaO content estimated at nearly 97%.

Table 6.2a: Estimated Lime Chemistry (Lime inclusion)
Chemical analysis was performed on a coarse lime inclusion removed from Sample M02. Its chemistry is presented below.

Sample ID	**M02**
Component (wgt. %)	
SiO_2	0.2
CaO	98.2
MgO	0.3
Al_2O_3	0.3
Fe_2O_3	0.1
Other	1.0
CaO/MgO ratio	**322.5**
Hydraulicity index	**0.00**
Cementation index	**0.01**

As discussed for the lime-crushed brick materials, the soluble chemistry of the bulk sample represents the combination of the lime binder with the products created by the pozzolanic reaction (Table 6.2b). Any soluble salts contaminating the materials may also be represented in this chemistry. As discussed before, it is suspected that most of the MgO may be attributed to magnesium sulfate salts common in seawater. It is noted that the MgO content is higher in the exterior mortar sample than it is in the interior plaster sample. The SiO_2 and Al_2O_3 are not generally present in soluble salts and are instead interpreted to represent that portion of the brick that has engaged in pozzolanic reaction with the lime to produce hydrated silicates and aluminates of calcium. The hydraulicity and cementation indices are mathematical tools used to evaluate the potential hydraulicity of single binders (Eckel, 1905). They are calculated and used here in a relatively crude way to compare the amount of pozzolanic reaction that may have occurred. For the body coat, the hydraulicity and cementation indices are calculated at 0.12 and 0.23 respectively. Based on arguments made by Eckel, this might be considered chemically similar to a feebly hydraulic lime. In contrast, Sample M02 has indices of 0.29 and 0.63 more consistent with a moderately hydraulic lime.

A similar broad range in the solubilized brick components was found in the other lime-brick mortars (M03a and M03b) and it was stated earlier that the reason for variations in the apparent reactivity remains uncertain. Possibilities include variability in the quality of the source brick or differences in the specific surface of the crushed grains. The latter does not seem to be a satisfying solution to the problem since there is not a clear correlation between hydraulic quality and the top size of the crushed brick fragments. Perhaps more importantly, there again does not appear to be a notable difference in the qualitative hardness or friability between any of the four mixtures. All samples are relatively soft and can be disaggregated by hand. None are consistent in quality with a modern hydraulic lime of moderate strength (e.g. NHL 3.5). It was suggested earlier that the production of hydraulic product could be more localized and inefficient in the lime-brick mix than it might be in a hydraulic lime containing distributed calcium silicates and calcium aluminates.

Table 6.2b: Estimated Combined Binder Chemistry (Lime-Brick Mixes with Beachrock Sand)

Sample ID	**M02**	**M05**
Material type	**Mortar**	**Plaster Body Coat**
Component (wgt. %)		
SiO_2	13.6	5.1
CaO	74.6	87.0
MgO	1.2	0.9
Al_2O_3	8.4	5.3
Fe_2O_3	1.1	0.7
Other	1.0	1.0
CaO/MgO ratio	**59.8**	**95.3**
Hydraulicity index	**0.29**	**0.12**
Cementation index	**0.63**	**0.23**

The chemical analysis was also used to estimate the original component proportions (Table 6.2c and 10.g). Calculating the lime as the equivalent of a modern dry hydrate, the lime to brick ratio is estimated at approximately 1 : 2 by volume for both samples. Not knowing the original bulk density of the crushed brick reduces the accuracy of the volumetric estimate though the weight ratios are reasonably well understood. Still, the values indicate a composite mortar that is similar in texture to a properly sanded lime mortar when the brick fragments are treated as an aggregate. The chemical arguments are also supported by the petrographic observations. The brick temper is as densely packed as a natural sand would be in a common lime-sand mortar with about the same proportioning.

In the body coat for Sample M05, the beachrock sand is estimated at only a tenth of a part for each equivalent volume of dry hydrated lime. This quantity is calculated to be about seven times higher in Sample M02. However, it is suspected that some of this material may be adhered fragments of the masonry substrate rather than intentional inclusions in the mortar (Fig. 12). It is possible that the actual addition is much closer to that of Sample M05. In either case, it is clear that the beachrock is a fairly minor volumetric component that is subordinate to the crushed brick addition.

In all cases, the lime is first considered as a dry hydrate even though it was clearly prepared as a putty. This is simply a more convenient calculation that does not suffer as much from the inaccuracies introduced by unknown amounts of mix water in a lime putty. Nevertheless, any variability in the bulk density of any of the components will affect the accuracy of the estimated volume proportions. For that reason, the weight percentages for each constituent are also reported and these should be considered the most accurate.

Table 6.2c: Calculated Components (Lime-Brick Mixes with Beachrock Sand)

Sample ID	**M02**	**M05**
Material type	**Mortar**	**Plaster Body Coat**
Component		
Lime expressed as dry hydrate (wgt. %)	16	20
Brick (wgt. %)	64	76
Beachrock (wgt. %)	20	3.8
Lime : brick : beachrock ratio (by volume with lime as a dry hydrate)	1 : 1.9 : 0.69	1 : 1.9 : 0.11
Lime : brick : beachrock ratio (by volume with lime as a putty)	1 : 3.9 : 1.4	1 : 3.8 : 0.22

These two particular samples exhibit very little evidence for deleterious service effects. Both materials are fully carbonated but this is a normal and desirable consequence of long-term curing. Some gypsum is detected in the Sample M05 body coat but this appears to be in pieces that are closer to the finish layer. As discussed in Section 6.3, a significant amount of gypsum has precipitated along the surfaces of the lime plaster finish coat. Of course the absence of microscopically detectable salt deposits does not necessarily indicate that salts are absent. It is quite common for soluble salts to be present within the submicroscopic pores of the lime binder and other mortar components. In these cases, the extremely fine-grained salts are often finer than the resolution of the light microscope. Specific types of chemical and mineralogical analyses are better suited to the evaluation of salt contamination and these were not a part of the project scope.

6.3 - Lime Plaster Finish (Sample M05)

Sample M05 is an interior plaster over brick masonry that contains a lime-pozzolan body coat mixture overlain by a lime plaster finish coat of approximately several millimeters in thickness (Fig. 13). The body coat was described in the last section. Most sample pieces do not contain the contact surface between the two materials. The exposed surface of the finish is coated with secondary gypsum but the underlying face is compact, planar, and sandy-textured. The fresh mortar is uniform in appearance with a dull white color. The cured binder is soft and highly permeable. The plaster as a whole remains cohesive but some of the apparent strength may be provided by the continuous gypsum crust.

The mixture is identified as a common lime plaster with a sparse aggregate of bioclastic sand (Fig. 14). No pozzolanic materials or pigments are detected in this layer. The variety of small shell fragments have sizes ranging from about the No. 30 to the No. 4 sieves. The lime is a nonhydraulic, high-calcium variety (Table 6.3a). Though well-slaked and now fully carbonated, there is a high concentration of diffuse lime particles throughout the cured matrix. Nevertheless, the highly microporous matrix is well consolidated with an air content estimated at 3-4% by volume. This does not include any pore spaces remaining within the dispersed shell fragments. It was not possible to accurately estimate the lime to sand ratio for this particular layer. However, it is clear from the sparse shell distribution observed petrographically that the sand content would have been rather low.

Table 6.3a: Estimated Binder Chemistry

Sample ID	**M05**
Material type	**Plaster Finish**
Component (wgt. %)	
SiO_2	0.3
CaO	96.9
MgO	0.7
Al_2O_3	0.9
Fe_2O_3	0.2
Other	1.0
CaO/MgO ratio	**140.6**
Hydraulicity index	**0.01**
Cementation index	**0.02**

All of the finish layer pieces are surrounded by gypsum crusts that range in thickness from 10s of µm to about 750 µm (Fig. 15). These are often found on both sides of a sample piece indicating that parts of the plaster finish were disbonded from the body coat substrate. The crystals themselves usually have a bladed morphology. Sizes vary greatly from submicroscopic to blades with length of approximately 300 µm and width up to 50 µm. The gypsum is not often observed to intrude the lime binder except along microscopic shrinkage cracks in the paste. Given the fragmental condition of the plaster, no other statements regarding the condition may be offered.

6.4 - Lime-Brick Dust Finish Coat (Sample M04a)

Of the exterior render materials, only one contains crushed brick as a pozzolan. It is convenient to discuss this sample in advance of the other exterior mixtures. According to the client, there is a protruding string course along the exterior wall. Sample M04a was taken from this architectural element and contains whitish body coat mixes overlain by a dense and compact finish coat layer of just under two millimeters in thickness (Fig. 16). This finish is the subject of this section. The layer is tabular with highly smooth and planar surfaces both at the contact with the substrate and at the exposed face. The exposed face is compact and exceptionally smooth with a texture not unlike modern steel-trowel finishes. It is assumed that a similar type of process would have been used to create this effect. The surface color is a mostly uniform brick red and this is likely the result of the "floating" of fine brick dust to the outer face during the finish procedure. In fresh cross section, the color is a lighter pink and there is a fine variegation produced by red and white particulates of brick and lime (Fig. 17). The finish material is rather hard and indurate and the cured binder is not noticeably water permeable.

The finish layer is identified as a mixture of non-hydraulic, high calcium lime with a crushed brick pozzolan. Calculated on a dry hydrate basis, the lime and brick were added at approximately equal proportions by weight (Table 10.h). By volume, this might be close to a lime : brick ratio of about 1 : 0.5 but the accuracy of this is highly dependent on the bulk density of the two constituents. The cured binder matrix is homogeneously developed with a relatively low capillary porosity consistent with an appreciable pozzolanic reaction (Fig. 17). Overall, the mixture is well blended but moderately coarse-textured with an abundance of undispersed lime grains up to about 0.5 millimeters in diameter and brick grains up to 1 millimeter in size (Fig. 18). This texture is hidden by the finish which has brought fine brick dust to the surface and homogenized the visual appearance. The trowel-type finish had also compacted and consolidated the layer quite well and the total air content is much less than 1% by volume.

The lime is a high-calcium rather than a dolomitic product and is likely similar to the lime used elsewhere on the building. As discussed in Section 7.6, the brick in this layer is a more clay-rich material burned at higher temperature and is clearly different from the soft-fired brick fragments found in several of the other samples. The fragments in this sample are clearly crushed rather than disaggregated and a larger particle found in the underlying body coat is glassy and indurate (Figs. 19 and 20). Though a higher quality brick, the qualities are still not quite equivalent to those of a more modern twentieth century brick.

The soluble chemistry of the combined and reacted binder is presented in Table 6.4a. The hydraulicity and cementation indices are of particular interest and are calculated at 0.40 and 0.88 respectively. Though a comparison to natural hydraulic lime is not quite accurate, historical limes having these types of indices would be expected to fall within the eminently hydraulic category (Eckel, 1905) and produce comparatively strong and indurate mortars. In fact, the finish coat is relatively hard and dense and has clearly undergone a significant pozzolanic reaction greater than those in the other lime-brick mixtures. In this case, the chemical indices are a good predictor of performance. The low permeability of the finish coat is also evident through the near absence of carbonation throughout the layer. The low permeability of the hydraulic binder matrix has likely inhibited the infiltration of atmospheric carbon dioxide. Of course, the inhibited carbonation has also increased the potential for a protracted curing period. There is a positive feedback between the pozzolanic reaction and the density of the matrix.

Table 6.4a: Estimated Combined Binder Chemistry (Lime-Brick Render Finish)

Sample ID	**M04a**
Material type	**Render Finish**
Component (wgt. %)	
SiO_2	18.4
CaO	67.7
MgO	2.3
Al_2O_3	8.4
Fe_2O_3	2.3
Other	1.0
CaO/MgO ratio	**29.9**
Hydraulicity index	**0.40**
Cementation index	**0.88**

Some secondary cracking and mineral deposition is identified in the finish coat. A discussion of these features is deferred to the next section after describing the remainder of the render composition.

6.5 - Sanded Mixtures of Lime and Natural Volcanic Pozzolan (Samples M01 and M04)

The remaining samples represent render layers sampled from the exterior wall (Figs. 21 and 22). It is understood that most of the wall is constructed of sandstone masonry. Based on the samples received, the masonry is covered with a body coat of white lime-based render containing a natural pozzolan. Three of these body coat mixtures are examined for Samples M01, M04a, and M04b. Sample M01 is taken from the vertical masonry field and Sample M04a and M04b from a protruding string course near the top of the elevation. The author has not visited the site personally but the two samples along with several photographs supplied by the client suggest a stone ashlar deceit and a polychrome finish. The vertical render represented by Sample M01 is an ochre color. The underlying body coat is covered by a thin pale yellow finish coat that is essentially the substrate mixture with a minor quantity of yellow pigment. A deeper yellow color wash is applied over this finish layer. The wash was not examined for this study. The photographs also indicate thin lines scored into the render to emulate white mortar joints between ashlar stone blocks. The string course represented by Sample M04 is pigmented a deep red color by the addition of a crushed brick pozzolan. In this case, the finely troweled finish layer appears to be the intended presentation surface without any overlying washes or paints.

With the exception of the red finish layer (described in Section 6.4), all materials contain a high-calcium, non-hydraulic lime and a sparse addition of natural sand aggregate. A notable pozzolanic reaction was produced by a very fine-grained volcanic ash. Visually, the materials are uniform in appearance with a nearly white color (Figs. 21 and 22). A portion of the body coat in Sample M04a and most of the material in Sample M04b has a faintly more pinkish hue. The finish coat in Sample M01 is pale yellow in color. The cured binder in each sample is moderately soft and highly water permeable. However, all renders are slightly harder than any of the lime-brick mixtures that include the soft-fired brick. Furthermore, the materials are nonfriable and highly indurate. All exhibit the qualitative properties of a hydraulic mortar in contrast to the lime-brick mortars that are all readily disaggregated by hand.

The timing of the exterior surface application is not completely clear. However, it is possible that all of the examined material may represent a later refinishing of the wall. First, it is almost certain that all parts of Sample M01 and M04 are contemporaneous. The three body coat renders contain virtually identical constituents and are clearly of the same vintage. Wherever finish coats are identified, these are found to have been placed over fresh, unweathered body coats. This suggests a single campaign for the entire render thickness at the two locations. In fact, the finish coat in Sample M01 contains the same components as the body coat. Second, the sands and pozzolans are completely different than those identified in the other examined samples. Even where brick is used as a pozzolan in the finish coat of Sample M04, the brick is an entirely different variety and indicative of a better quality of production. Of course, it could be argued that a higher degree of water-resistance and durability was desired for the exterior render. An intent such as this would make it plausible for all mortars and renders to be original to the construction even if disparate in composition.

Still, a third piece of evidence is found at the interface between the white body coat render and adhered fragments of beachrock in Sample M01 (Fig. 23). The surface of the beachrock is highly irregular and embayed at the microscopic level as a result of its granularity and incomplete cementation. A material that predates the white render is found within the subsurface pores of the beachrock but not along the plane of the stone at the interface with the body coat. The earlier embedded material is a lime-based mixture with crushed brick dust. Though only traces of this material are observed in thin section, it appears very similar to the lime-crushed brick mortar and renders of Samples M02, M03a, M03b, and M05. It is possible that the lime-brick renders were also used on the exterior of the building but had been stripped and replaced at some later date. This would explain the residues within the surface pores. However, the lime-brick mixture is also used as a construction mortar for the substrate sandstone (e.g., Sample M02). It is also possible that the traces are just residues of the bedding mix that became embedded into the stone during construction. This might be a more likely possibility if the Sample M01 location overlies a masonry joint. Of course, all of this discussion assumes that the attached beachrock represents fragments of the underlying sandstone masonry.

With all this said, the remaining render materials are unique and clearly distinguished from the other samples examined. The only similarity is the use of a high-calcium lime. However, it is not possible to clearly demonstrate that different lime sources were used. This is due to the absence of a unique microtextural character and the inability to detect major chemical differences because of an inseparable pozzolan signal. A fine-grained sand is sparsely distributed throughout the lime-rich matrix in each layer (Fig. 24). The sand is more thoroughly described in Section 7.2. In short, the material is light buff in color with a "salt-and-pepper" quality (Fig. 25). The components include a mixture of volcanic rock grains, bioclastic particles, and quartz. The aggregate is fine-grained with most material passing a No. 30 mesh (Fig. 26). Most of the sand is retained over the No. 100 sieve except for the white body coat in Sample M04a where a substantial portion passes this mesh.

The sparsely distributed sand grains are well coated with lime binder and each layer appears to be well consolidated based on the small sample pieces examined (Fig. 24). The highest air content is found in the body coat of Sample M01. Even here, the air volume is estimated at only 4-6% and the voids are generally less than 0.5 millimeter in diameter. The capillarity porosity of the binder appears to have some relationship with the degree of carbonation in each sample (Fig. 27). This is attributed to the interplay between the densifying nature of the pozzolanic reaction and the arresting qualities of the carbonation reaction. Pozzolans react with uncarbonated lime to produce hydrated calcium silicates and hydrated calcium aluminates. These reactions occur in the hardened state causing the reaction products to fill the locally available pore spaces. In the case of cured lime binder, these are the submicroscopic capillary pores that are left behind after the evaporation of excess mix water. These reactions continue with time so that a render will continue to become more dense as long as the reactants are not consumed.

In Sample M04a, the entire thickness of finish coat and underlying white body coat have remained virtually uncarbonated. Though the body coat is permeable on average, there are dense patches throughout the binder matrix due to the continued reaction between the pozzolan and the highly alkaline lime. In fact, the finish coat has a uniformly low capillarity and this has likely assisted in inhibiting the transport of atmospheric carbon dioxide into the substrate. However, there are portions of the body coat that have a more pinkish hue including most of Sample M04b and small strips of the body coat in Sample M04a. These pieces are fully carbonated and the pink hue is a result of this secondary reaction. In these sample pieces, the

capillary porosity is uniformly high and it is suspected that the suspension of further pozzolanic reaction has "locked in" an earlier curing condition. It is not known why these pinkish layers may have had greater access to carbon dioxide. The client's photographs depict areas where the outer finish is eroded away. Perhaps the carbonated body coats were taken from these areas. Sample M01 is a bit more like Sample M04b though the carbonation is not as thoroughly developed. Based on a cross section taken parallel to the face of the wall, there may be some gradient of carbonation within the pale yellow finish coat as well. However, a perpendicular cross section was not possible.

In addition to the lime and sand, there are very fine-grained components distributed throughout the binder most of which are not visible petrographically but are only revealed once the lime is decomposed in acid. Only in the finish coat of Sample M01 do these fine particulates represent a pigment addition. In this layer, there is a sparse distribution of ultrafine-grained orange-toned flecks that are likely some type of iron oxide/hydroxide such as limonite or goethite (Fig. 28). In the extracted residues, they impart a slightly more yellowish tone to the pale brown pozzolanic material. In hand sample, they result in the faint pale yellow tone that just barely distinguishes the body coat from the finish coat.

The remaining fines comprise a pale brown dust that contains a mixture of glass, silt, and clay (Fig. 26). As discussed in Section 7.7, the glass is interpreted to represent a fine volcanic ash. The silt and clay may be fines from the natural sand, an impurity of the ash, or both. Of the few components present in these four render layers, only this siliceous glass is capable of producing the significant degree of hydraulicity indicated by the quantity of solubilized SiO_2 and Al_2O_3 present in the binder (Table 6.5a). Referring again to the hydraulicity and cementation indices, the body coat of Sample M01 and the white uncarbonated body coat of Sample M04a have values of about 0.3 and 0.8 respectively. These are second in apparent reactivity only to the dense lime-brick dust finish coat in Sample M04a interpreted to be contemporaneous with these renders and not necessarily of common vintage to the other materials studied. The pozzolanic reaction developed in these two samples is roughly equivalent in hydraulic potential to a strong natural hydraulic lime. The chemistry of the finish coat in Sample M01 and the pink-colored body coat in Sample M04b also indicates a strengthening reaction but to an appreciably lower degree. Again, the carbonation of these layers is interpreted to have arrested the pozzolanic reaction by depleting the calcium hydroxide required to create hydraulic product. But despite any variability in the measured chemistries, this group of renders displays a more indurate character than the other materials examined for this study. This indicates the use of a more effective pozzolan on the whole.

Table 6.5a: Estimated Binder Chemistry (Lime-Natural Volcanic Pozzolan Mixes)

Sample ID	**M01**	**M01**	**M04a**	**M04b**
Material Type	**Render Body Coat**	**Render Finish**	**Render Body Coat (White)**	**Render Body Coat (Pink)**
Component (wgt. %)				
SiO_2	18.4	5.8	19.6	4.3
CaO	72.8	80.9	72.7	85.3
MgO	1.7	4.2	1.5	2.0
Al_2O_3	5.2	6.4	4.2	6.2
Fe_2O_3	1.0	1.7	1.0	1.2
Other	1.0	1.0	1.0	1.0
CaO/MgO ratio	**43.4**	**19.2**	**49.1**	**43.1**
Hydraulicity index	**0.32**	**0.15**	**0.33**	**0.12**
Cementation index	**0.77**	**0.28**	**0.80**	**0.22**

The source of the pozzolan is not resolved by this study and three possibilities are hypothesized. The ash could simply be a part of the clay fraction of the natural sand that was not rinsed away prior to use. If this were the case, the pozzolanic qualities may or may not have been known to the builders. The ash also could have been a local product quarried specifically for its pozzolanic properties. Finally, the material could represent an imported European trass. The possibility that the ash is part of the sand is favored by the fine size of the particulates. None are detectable at the resolution of the light microscope. While volcanic ash can be very fine, trass is usually just coarse enough to be detected petrographically unless largely consumed by many years of continued reaction. It would have been thought that some coarser residual material could be identified in the carbonated matrix of Sample M04b, but this is not the case even while twice as much fine residue is extracted from the cured binder after acid digestion. Contrasting this argument is the apparent rhyolitic composition of the ash based on its optical properties. Most of the volcanics in the San Juan area are reported to be andesitic in composition (Kaye, 1959a). This is also true of the volcanic rock particles contained within the sand. The roughly estimated composition of the ash is certainly inconsistent with the rest of the aggregate and it may also be uncharacteristic of most deposits in the region surrounding the site. This would tend to argue for an imported product.

As with the other samples, the chemical analysis was also used to estimate the original component proportions. Calculating the lime as the equivalent of a dry hydrate, the volume of lime is always greater than that of the sand, in one case as high as a factor of 7.5 (Table 6.5b and 10.i). The sanding is exceptionally lean and this is consistent with the sparse distribution of particles observed petrographically. The fines containing the volcanic ash represent about a fourth or fifth of the volume of the lime. As described in previous sections, there are always errors expected in these estimates due to uncertainties in original bulk densities of the raw materials. Simplifying the lime as a hydrate is one way of managing the error. However, the most accurate estimates are based on weight proportions and these are also presented in the tables.

Table 6.5b: Estimated Binder Chemistry (Lime-Natural Volcanic Pozzolan Mixes)

Sample ID	**M01**	**M01**	**M04a**	**M04b**
Material type	**Render Body Coat**	**Render Finish**	**Render Body Coat (White)**	**Render Body Coat (Pink)**
Component				
Lime expressed as dry hydrate (wgt. %)	42	56	64	37
Volcanic fines (wgt. %)	15	17	19	16
Sand (wgt. %)	43	27	16	48
Lime : volcanic fines : sand ratio (by volume with lime as a dry hydrate)	1 : 0.22 : 0.51	1 : 0.19 : 0.25	1 : 0.18 : 0.13	1 : 0.26 : 0.64
Lime : volcanic fines : sand ratio (by volume with lime as a putty)	1 : 0.44 : 1.0	1 : 0.37 : 0.49	1 : 0.36 : 0.25	1 : 0.52 : 1.3

Given the suspected age of the materials, there is relatively little service distress detected petrographically in either sample area. The finish layer in Sample M01 contains several parallel but staggered microcracks spaced approximately one millimeter apart (Fig. 29). All of these are healed with calcium carbonate. Traces of secondary calcium carbonate are also detected within the lime matrix of the body coat. A somewhat elevated MgO content in the finish layer (Table 10.e) is suggestive of some salt infiltration. However, no salts are visible at the scale of the light microscope and there is no evidence for binder degradation. Sample M04 also contains surface-perpendicular microcracks spaced at a submillimeter scale. Some of these penetrate the finish layer and extend into the body coat. A few surface-parallel cracks are also detected in the body coat. All cracks are exceptionally thin. In areas that are not carbonated, gypsum and ettringite are identified as secondary deposits within the cracks (Fig. 30). These salts are also present within air-voids. Within the carbonated body coat pieces, microsparry calcite lines the cracks.

7. Materials

A number of distinctive materials are characterized in the samples provided for analysis. Three different aggregate types are identified including beachrock particles, fine-grained natural sand, and fine shell fragments. The only binder present is a high-calcium lime. No hydraulic cements or other distinctly modern products are identified. However, pozzolanic additions are an important component of all but one sample. These include a low-fired red clay brick, a more highly fired clay brick, and fine volcanic ash. The low-fired brick also behaves as an aggregate as a result of its abundant quartz sand temper. Both brick types are also strong coloring agents. Other than the brick, there is only one example of a mineral pigment. This section focuses strictly on the characteristics of these individual constituents.

7.1 - Calcareous Arenite (Beachrock)

A type of calcareous sandstone is identified in three of the samples. In the body coat of render sample M01, there are chunks of the sandstone attached to the lime mortar (Fig. 31). The author is not familiar with the site but Mr. Kevin Wohlgemuth of BCA confirms that the stone masonry substrate has a similar appearance. In this case, the fragments are likely pieces of adhered substrate. In Sample M02 (a mortar sample) and the body coat of Sample M05 (an interior plaster), the sandstone is found as a coarse sand mixed throughout the lime matrix. Along with the crushed brick in the finer size fractions, this relatively sparse proportioning of sandstone grains is assumed to represent an aggregate addition.

The sandstone is a homogeneous, orange-toned, granular rock. Well sorted sand particles are bound by a calcium carbonate cement that does not completely fill the original interstitial void space between the grains (Fig. 32). The rock is classified as a calcareous arenite but does not conveniently satisfy any of the more common classification schemes for sandstone or limestone. The source rock is probably best described as a "beachrock" and this is the simpler term that will be used throughout this report. Beachrock is a stone that forms from the in situ cementation of beach sand. Though the author does not have firsthand experience with the stratigraphy of the San Juan region, it is understood from the geological literature that very recent beachrock deposits are fairly common along the northern shore line of Puerto Rico (Kaye, 1959b). These may be the source of the arenite sand. Whether this is also the source of the masonry stone would have to be evaluated on site.

The sand particles within the beachrock consist of bioclastic grains, quartz, and a minor assemblage of other trace silicates (Fig. 33). The bioclastic particles are generally rounded to subrounded in shape and have aspect ratios that range from equant to mildly subequant. The bioclasts are essentially the abraded remains of shelled invertebrates. A few oolites are detected in Sample M05 including one particle with a core of plagioclase feldspar. The quartz grains are equidimensional and mostly subangular in shape. The other silicates are similarly-shaped and mostly include feldspar. The feldspar is often fresh and complete. However, some grains are skeletal and probably volcanic in origin, and others are corroded due to secondary alteration. Other trace grains include epidote and epidotite, amphibole, zircon, and volcanic rock grains. The epidote and epidotite are interpreted to represent the alteration products of the local volcanic rocks. The volcanic grains themselves are sometimes corroded due to secondary decomposition. Sedimentary chert and fine-grained quartz arenite are only detected in Sample M05.

Most grain sizes range from about 150-500 µm (i.e. fine to medium sand as defined by the Wentworth classification). Within this range, the beachrock tends to be a little coarser on average in Sample M01 and finer in Sample M05. The beachrock in Sample M02 is the coarsest of the three and has some particles with grains ranging from 500-1000 µm (i.e. coarse sand). Despite the size distribution, the sand tends to be very well sorted within any one beachrock fragment and usually lies within a single size interval.

The sand grains are all bound by a cement of fine-grained sparry calcite (Fig. 32). Traces of aragonite needles are detected in the pores of Sample M01 but these are rare. The cement does not usually fill the interstitial space between sand grains though the closure tends to be more complete around the finer sand grains. This is not surprising given the smaller interstitial diameter between the fine sand particles. Otherwise, irregularly-shaped pores of several hundred µm in size are common throughout the stone. It is assumed that these pores are mostly interconnected and cause the stone to have a notable permeability.

7.2 - Natural Sand

A natural sand aggregate is identified only in Sample M01 (exterior render) and the body coat of Sample M04 (exterior string course render). A filler of shell fragments serves as an aggregate addition in the finish coat of Sample M05 (interior plaster). As described earlier, beachrock grains serve as a sparse coarse sand addition in Sample M02 (sandstone masonry mortar) and the body coat of Sample M05 (interior plaster). It could also be argued that the crushed brick pozzolan functions in part as an aggregate and this is found in Samples M02 (stone masonry mortar), M03a (brick mortar), M03b (brick masonry render), M04 (exterior render finish), and M05 (interior plaster body coat). This section focuses on the natural sand materials. The qualities of the other aggregate types are described elsewhere.

The sand in Sample M01 is a fine-grained natural aggregate. The material extracted from the mortar is semi-opaque and mildly variegated in appearance. The average color is a light buff (Munsell code approximately 10YR 7/1.5). However, the sand has a "salt-and-pepper" quality due to the mixture of darker gray, nearly white, and light buff grains (Fig. 25). The aggregate contains a mixture of volcanic grains, bioclasts, and quartz, and these correspond to the variously colored particles (Fig. 34). The volcanic rocks are rich in plagioclase feldspar and are likely some type of andesite. Based on the geological literature (Kaye, 1959a), andesitic volcanics are relatively common in the local stratigraphy. The feldspar phenocrysts and sometimes the groundmass are highly corroded and porous due to secondary alteration. A small amount of sericitization and epidotization is also noted. The former is a reaction that produces white clays and mica. The latter produces the mineral epidote.

The extracted material also contains an abundance of fines that have a uniform pale brown color distinctly different from that of the sand. It is possible for these to represent unwashed clays or other fine sediments present in the sand deposit. However, microscopic examination of the material passing a No. 325 sieve indicates a notable proportion of volcanic glass with a rhyolitic rather than an andesitic character. The chemical analysis also shows that the white lime mortars contain some type of hydraulic component. It is possible that the fines represent a separate and intentional trass addition and this is discussed at greater length in Section 7.7. This interpretation may only be partially correct, in which case a portion of this fraction should be considered an unwashed constituent of the sand.

The sand grains in Sample M01 are equidimensional in aspect and variable in shape. However, the particles likely average within the subangular range. The aggregate gradation profile is best assessed from the body coat of the render. The results for the finish coat are considered less accurate due to the small sample size, sparseness of the sand addition, and the use of acid to decompose the matrix. A summary of the profiles are presented in Table 7.2a below. The sand is fine-grained with most material passing the No. 30 sieve. The particle size distribution is somewhat narrow with about 90% of the sand retained between the No. 30 and No. 100 sieves (two standard sieve intervals). Though not included in Table 7.2a, the fines passing a No. 325 sieve constitute about 7.5% of the extracted material. This would represent a fairly sizable quantity of unwashed fines if the trass interpretation were incorrect. In either case, the gradation profile would not comply with modern permissible limits for exterior plaster sand as specified by ASTM C897. Of course, this standard is written explicitly for portland cement-based mixtures.

The sands in the two body coats of Sample M04 appear generally similar to the aggregate in Sample M01. The body coats were tentatively separated into a white variety and a pink variety with more of the latter available for a sand extraction. However, it is believed that the only difference between these two coats is the degree of carbonation. Any apparent differences in the sand may be attributable to the small sample size and the sparseness of the aggregate addition. In any case, the sands appear similar to those of Sample M01. Both are mildly variegated with a "salt-and-pepper" appearance due to white, gray, and buff particles (Fig. 25). However, there are also some reddish grains in both coats and pale green grains in the white coat. Both sands have an average light buff color (Munsell code approximately 10YR 7/2.5 for the pink coat and 2Y 6/2 for the white coat). The mineralogy is essentially the same as that identified in Sample M01 though clinopyroxene particles are a subtle but significant addition in the M04 coats (Fig. 35). The pyroxene must derive from the volcanic rocks. Both coats also contain traces of sedimentary wacke that was not identified in Sample M01. These subtle differences suggest that the Sample M04 sands may have been sourced from another horizon within the same general deposit. Both coats of Sample M04 also contain an abundance of the pale brown fines. These are also found to contain the volcanic glasses suspected to function as a natural pozzolan. Interestingly, there is a negative correlation between the percentage of residual fines and measured hydraulicity. The white uncarbonated coat contains fewer residual fines but exhibits a higher degree of reaction.

The sand in Sample M04 has similar physical characteristics to that in Sample M01. The grains are equidimensional and variable in shape but tend to be a little more angular on average. The sands are similarly fine-grained with most if not all material passing the No. 30 sieve (see Table 7.2a). The peak abundance is again found between the No. 50 and No. 100 sieves. However, there is appreciably more passing the No. 100 mesh in this sample. The profile for the pink body coat is probably more accurate than that of the white body coat. There was more material available for the latter and less opportunity for partial dissolution of carbonate grains due to the exclusion of acids for most of the preparation.

Table 7.2a: Sand Gradation Profiles - Cumulative Percent Passing

The mortars and renders were mechanically disaggregated and separated across a No. 100 sieve. The coarser retention was cleaned to remove any residual lime. The finer material passing the sieve was digested to decompose the lime binder. For the finish coat in Sample M01 and the white body coat in Sample M04, the entire sample was digested in dilute acid. Since carbonate bioclasts are also present in these coats, it should be assumed that these were partially dissolved and that the reported profiles contain a modest error. Otherwise, the gradation profiles for the other two samples are estimated to represent the aggregate addition in each render coat. After all portions of the insoluble residues were recombined, the material passing the No. 325 sieve was examined microscopically and determined to contain fine volcanic glass in addition to quartz and clays. Though possibly an oversimplification, the whole of this sieve interval is interpreted to represent a separate trass addition rather than unwashed fines. This fraction was not included in the gradation analysis below.

Sample ID	**M01**	**M01**	**M04a**	**M04b**
Material type	**Render body coat**	**Render finish**	**Render body coat (white)**	**Render body coat (pink)**
No. 4	100.0	100.0	100.0	100.0
No. 8	100.0	100.0	100.0	100.0
No. 16	100.0	100.0	100.0	98.8
No. 30	98.0	87.5	100.0	95.1
No. 50	66.0	62.5	72.7	63.4
No. 100	8.0	12.5	27.3	13.4
No. 200	2.0	0.0	9.1	3.7
Pan	0.0	0.0	0.0	0.0
Fineness modulus	**1.28**	**1.38**	**1.00**	**1.29**

7.3 - Shell Sand

Sample M05 is an interior plaster that has a thin white finish coat. This layer contains a very sparse sand addition consisting predominantly of bioclastic grains and fewer beachrock and quartz particles (Fig. 36). The bioclasts often include open-textured shells with unfilled voids. The amount of sample was quite limited and there was no attempt made to recover a sample of the aggregate. It should be assumed that the grains would have the typical white and semi-opaque appearance of marine shells. It is difficult to judge the full range of shapes but these are clearly variable. The shells exhibit a maximum size of approximately 3 millimeters and all grains are estimated to pass the No. 4 sieve. Very little material is found below the No. 30 mesh (i.e. 0.6 millimeters).

7.4 - Lime Binder

All of the samples examined for this report contain a non-hydraulic high-calcium lime as the primary binder. Almost all of them are modified by the addition of a pozzolan. Some of these include crushed brick that was certainly used as an intentional pozzolanic additive. Others include a fine reactive volcanic glass that may have been intentional but also could have been an impurity present in an unwashed sand. Of the ten mortar and render layers, eight exhibit the consistently high capillary porosity typical of lime-rich mortars. This despite any pozzolanic reactions that may have occurred. The exceptions include the two of three materials that exhibit the highest degree of hydraulicity. These are both from render sample M04a including the uncarbonated portion of the body coat containing what is interpreted to be a trass addition and the finish layer containing a moderately-fired crushed brick. The finish layer in Sample M04a has a consistently low capillary porosity and is notably harder and less permeable than all of the other materials (Fig. 17). The body coat has areas of high porosity interspersed with denser clots (Fig. 24). The increased density in both is attributed to the longer time available for pozzolanic reaction. Carbonation of the paste in the other samples would be expected to effectively shut down the pozzolanic reaction due to the consumption of calcium hydroxide, a principal reactant in the pozzolanic reaction. This would lock in the microporosity structure at the time the reaction ceased.

Lime-based mortars, particularly those will low sand contents, often exhibit a pattern of discontinuous polygonal microcracks attributable to early drying shrinkage. The only samples for which this type of cracking is identified are Sample M03b and the brown coat of Sample M05, and even here only sporadically (Fig. 37). The lack of typical shrinkage features is probably due to the volume stabilizing influence of the pozzolan. The renders containing finish coats exhibit microcracks perpendicular to the finished face of the application and these are likely later features resulting from cyclic volume changes. Samples M01 and M04a displays extremely fine microcracks at a submillimeter scale (Fig. 29). Those in M04a extend into the uncarbonated portions of the body coat. Sample M05 contains similarly distributed microcracks in the finish coat except that these have a greater opening width. The contact between the finish and body coat is not well represented in this sample and it is not known if these cracks would have extended more deeply into the plaster.

Undispersed lime grains are detected in all samples to some degree (Fig. 38). Table 7.4a summarizes differences in concentration and size range of these grains. The grains are not usually more than a millimeter or two in diameter and do not produce a lot of visual texture from a normal viewing distance. The sample with the greatest content of unblended lime is the lime plaster finish coat of Sample M05 and this is hardly visible in hand sample due to the white color of the matrix itself. Petrographically, most of the lime particulates are diffuse and exhibit relatively few relict textures from the original source material. Nonetheless, there is an absence of the types of textures that would almost always be identifiable in a lime burned from a shell source.

Table 7.4a: Abundance and Size of Undispersed Lime Grains

Sample ID	Abundance of undispersed grains	Size distribution
M01 Body Coat	Moderately high	Variously sized grains up to approximately 2 mm.
M01 Finish Coat	Moderately high	Up to approximately 0.5 mm.
M02	Variable abundance from piece to piece but the visual appearance suggests that most fragments have a moderately high content.	Two pieces in thin section are found to several mm in size. However, most are much less than 1 mm.
M03a	Moderately high	Variously sized grains up to approximately 2 mm.
M03b Body Coat	Moderately high	Variously sized grains up to approximately 3 mm.
M04a - White Body Coat	Lime grains are difficult to distinguish due to the isotropism of the uncarbonated lime paste. A few areas exhibit hints of mosaic texture likely indicating the presence of diffuse undispersed grains.	Only a few discrete grains are identified in the 0.5 mm to 1 mm range and these happen to be fully carbonated in contrast to the uncarbonated matrix.
M04b - Pink Body Coat	High	Variously sized grains up to a little over 1 mm.
M04a Finish Coat	Moderate abundance of grains up to about 0.5 mm maximum.	Up to about 0.5 mm maximum.
M05 Body Coat	Very low abundance of detectable grains.	
M05 Finish Coat	Very high	Variously sized grains up to approximately 2 mm.

Though the evidence is extremely sparse, the lime in all samples is interpreted to have been burned from a sedimentary rock source. There are several limestone formations in the local San Juan stratigraphy but the author does not know which would be good candidates for lime production. All samples contain a relatively low proportion of grains that exhibit a faint "mosaic" texture (Fig. 38). This is usually created by the thermal disaggregation of calcite crystals in the original lime rock. The fine to medium size of the mosaic polygons likely provides some information regarding the grain size of the original source. While interesting, this type of evidence is never sufficient to make a positive statement regarding the source material. Beyond the mosaic texture, a minor number of other textural relicts and siliceous impurities are detected petrographically. These are summarized in Table 7.4b. They include a few occurrences of quartz silt within undispersed lime particles (Fig. 39) and isolated grains of quartz within the matrix that have experienced thermal cracking and incipient fusion (Fig. 40). Though similar textures could be found in certain kinds of brick, there is an absence of any appreciable thermal effects in any of the quartz temper clearly associated with the crushed brick pozzolan identified in several of the samples. Other than the mosaic textures and minor quartz inclusions, there is only a single grain in Sample M03b that contains a patterned texture consistent with some type of invertebrate fossil (Fig. 41). Again, all of this is scant evidence for a sedimentary limestone source.

Table 7.4b: Summary of Minor Textural Features Identified in the Lime Binder

All lime grains exhibit some minor occurrences of a faint mosaic texture likely coinciding with the original crystal boundaries in the source rock. These are observed even where no other textural features are discernible. The table below summarizes some of the additional relict textures and impurities identified petrographically for the various samples. In some cases these are associated with the original lime rock. In others, they are representative of the mortar preparation.

Sample ID	Discrete textures identified within lime particles
M01 Body Coat	None detected.
M01 Finish Coat	None detected.
M02	One grain with trace quartz silt inclusions. Only one or two grains with uncarbonated cores.
M03a	Only two instances of burned quartz in thin section, one in a lime grain and one as an approximately 0.5 mm diameter particle exhibiting incipient fusion.
M03b Body Coat	There are a number of lime grains that exhibit some internal texture. One coarser lime lump contains a number of diffuse smaller lumps possibly indicating some retempering or knocking up of the lime. At least a few particles of coarser fused quartz are found as isolated particles. A few lime grains contain sparse quartz sediment. One lime grain exhibits a faint fossiliferous texture.
M04a - White Body Coat	None detected. It should be noted that few lime grains are distinguishable in thin section.
M04b - Pink Body Coat	None detected.
M04a Finish Coat	None detected.
M05 Body Coat	None detected. It should be noted that few lime grains are distinguishable in thin section.
M05 Finish Coat	Some coarser lime grains contain many smaller lumps within possibly indicating some retempering of the lime putty.

Sample M02 contained a single coarse lime grain of about 5 millimeters in diameter. This was large enough to extract and perform a chemical analysis on without any interference from sand or pozzolan. The results of this analysis are presented in Table 7.4c. The lime has a CaO content over 98% by weight on a nonvolatile basis. This suggests a very low content of impurities consistent with the petrographic observations. It also suggests a product that would have been considered a fast-slaking and highly workable fat lime. The only other sample for which a relatively accurate chemistry could be established for the lime was the finish coat for the interior plaster (Sample M05). This is estimated to have a CaO content of nearly 97% by weight. In all of the other samples, the acid-soluble chemistry represents a contribution from the lime as well as any pozzolans and possibly some salts (Table 10.e). Nevertheless, none have a dolomitic chemistry and any increased MgO signal is probably attributable to contamination from magnesium sulfate in seawater.

Table 7.4c Estimated Lime Chemistry (Lime inclusion)
Chemical analysis was performed on a coarse lime inclusion removed from Sample M02. Its chemistry is presented below.

Sample ID	**M02**
Component (wgt. %)	
SiO_2	0.2
CaO	98.2
MgO	0.3
Al_2O_3	0.3
Fe_2O_3	0.1
Other	1.0
CaO/MgO ratio	**322.5**
Hydraulicity index	**0.00**
Cementation index	**0.01**

7.5 - Low-Fired Brick

Crushed brick was used as a pozzolan in several of the mortar and render samples. These include Samples M02 (sandstone masonry mortar), M03a (brick bedding mortar), M03b (render body coat over brick masonry), M04 (render finish coat over string course), and M05 (interior plaster "brown" coat over brick masonry). The crushed brick in Sample M04 is clearly different than the others and is discussed in the next section. This section discusses the brick used in the other four samples. Several pieces of evidence indicate that this brick was a low-fired product. These include a friable matrix with an orange-toned color, absence of thermal effects in the temper, no high-temperature aluminosilicate phases, and a clay matrix that retains a high crystallinity.

It was possible to characterize the microstructure of the original brick product since the brick was not crushed to a powder or screened prior to its blending in the lime paste. This characterization is easier in Samples M03a and M03b where brick fragments are found up to about a centimeter in size (Fig. 1). Nonetheless, some coarser-scale texture is also identifiable petrographically in Sample M05 even if there is not a statistically significant amount of material available for analysis.

All of the softer brick is identified as an orange-red, friable product containing a narrowly-graded natural sand temper embedded in a homogeneous clay matrix (Fig. 42). The temper distribution is fairly dense and close-packed in Samples M03a and M03b but a bit sparser in Sample M05. In either case, the brick has a microtexture comparable to that of a clay-rich sandstone. In some cases, the clay is well-consolidated around the sandy temper. Grains with this more compact character are more common in Samples M03b and M05. However, brick fragments with less complete consolidation are also relatively common. In these particles, consolidation voids on the order of several 100s of μm occur in the interstitial space between clay-coated sand particles. These voids were created during the original forming of the brick rather than during the firing. Where consolidation voids are present, these may be as abundant as 20-30% by volume. The voids are more regular in shape and distribution in the M03 samples and a bit more sporadically distributed and irregular in shape in Sample M05.

The temper is a natural sand having equidimensional particles that are mostly subangular to angular in shape. Quartz is the predominant mineral constituent and feldspar is present in minor to lesser quantity (Fig. 43). A summary of the other minor and trace constituents is presented in Table 7.5a. Though not especially abundant, the mineral epidote along with rock fragments consisting largely of epidote (i.e. epidotite) are notable among the accessory grains. These are interpreted to represent the alteration products of volcanic rocks some of which are also identified in less altered condition. For the most part, any differences in the identified assemblage of minor grains is just as likely a function of sampling statistics as they may be an indication of subtle differences between the source sediments for the temper. However, there is a sufficient quantity of quartz arenite in Sample M03a that its absence in the other samples does suggest some very minor variability in the temper source.

Table 7.5a: Description of Temper Constituents in Soft-Fired Brick Inclusions

All of the brick inclusions include monocrystalline quartz and minor polycrystalline quartz as the predominant constituent of the temper. The table below describes the various lesser, minor, and trace phases detected petrographically. Note that the absence of a particular trace may be due to the statistics of sampling.

Sample ID	Description of subordinate mineral and rock grains
M02	Minor feldspar and epidote/epidotite. Minor to trace opaque grains. Traces include chert, amphibole, zircon, volcanic grains, and "beachrock"
M03a	Minor to lesser feldspar. Minor to trace epidote/epidotite. At least one brick fragment in thin section contains minor to lesser quartz arenite. A few isolated arenite grains may be present elsewhere in thin section. Volcanic grains are minor. Traces include chert, zircon, opaque grains, and maybe granite.
M03b	Minor feldspar. Trace to minor epidote. Trace amphibole, chert, granite, zircon, opaque grains, and bioclasts.
M05	Minor feldspar. Trace to minor epidote/epidotite. Trace amphibole, volcanic grains, and opaques.

Any remaining brick fragments in the mortars and renders are exceptionally friable. As such, the process of mechanically disaggregating the samples to remove and digest the lime binder resulted in the brick grains being reduced to their constituent temper particles. For Samples M03a and M03b, all residual material remaining after the decomposition of the lime is approximately equivalent to the original particle size distribution of the raw materials used in producing the bricks (Fig. 4). This material was graded and its size profile is presented in Table 7.5b (and Table 9.a). It is notable that the temper gradation is almost identical between these two samples despite the fact that these mortar and render samples were taken from two different locations. It suggests that the bricks used as a pozzolan at these two locations had raw materials that were carefully proportioned before molding and firing. Similar procedures were used to disaggregate Samples M02 and M05. However, these samples also contain beachrock fragments in the coarser sand-sized fraction (Fig. 10). In Table 7.5b, all material retained on a No. 30 sieve is assumed to represent this additional component and is mathematically removed from the gradation profile. Since there must be some minor size overlap between the beachrock sand and the brick temper, the reported size distributions are not as accurate as those for the other two samples. Nevertheless, the temper size ranges are still quite similar in all four samples.

The results of the gradation illustrate that nearly 90% of the temper is sized between the No. 30 and No. 100 sieves (i.e. between 600 and 150 μm). This assumes that the material passing the No. 325 mesh is all clay matrix. Quartz temper coarser than a No. 50 sieve will often exhibit thermal cracking, fusion rims, and margins adjacent to clay matrix that contains quench phases. None of these features are detected in the temper of any sample and this is one feature that indicates a low firing temperature. The narrow particle size distribution suggests that the source of the temper could have been a beach sand. Of course, it is also possible that a more broadly graded sediment could have been screened for use as a temper. It should be possible to evaluate local sand sources and compare these to the temper identified for this study.

Table 7.5b: Cumulative Passing Percentages of Material Assumed to Represent Brick Temper and Fired Clay

For all four samples containing the soft-fired brick pozzolan, the mortars and renders were mechanically disaggregated and separated across a No. 100 sieve. The coarser retention was cleaned to remove any residual lime binder. The finer material passing the sieve was digested to decompose the lime binder. Any acid-insoluble material was returned to the coarser retention. All of the retained material was passed through a sieve stack using sizes typically used for mineral aggregates. For Samples M02 and M05, the material retained above a No. 30 consists mostly of beachrock sand rather than brick pozzolan. This material was not included in the gradation profile. Some of the material passing the No. 30 sieve in these two samples likely consists of sand from the beachrock but the inclusion of this material in the gradation profile is considered a negligible error. The particle size distributions reported below are interpreted to represent the original size profile of the temper and clay in the brick before firing.

Sample ID	M02	M03a	M03b	M05
No. 16	100.0	100.0	100.0	100.0
No. 30	100.0	98.4	98.6	100.0
No. 50	56.4	64.6	65.4	57.5
No. 100	22.1	21.1	21.1	19.6
No. 200	17.9	14.1	14.2	15.4
No. 325	14.5	11.4	11.4	12.1
Pan	0.0	0.0	0.0	0.0

Based on the gradation analysis, the brick has a fired clay content estimated at between 10-15% by weight. The pre-fired weight percentage was likely a little higher due to the combined water that would have been removed through dehydroxylation on firing. In all samples, the fired clay is quite homogeneous under plane polarized light (Fig. 44). There seems to be some variability from sample to sample. For instance, Sample M03a appears to have more grains where the interstitial clay matrix contains a higher proportion of fine quartz sand below the No. 200 sieve. Sample M05 seems to have more grains with sparser temper and higher clay contents. However, the particle gradation presented in Table 7.5b suggests these differences are a function of a small sample size relative to the occurrence of brick particles greater than a few millimeters in diameter. Overall, the clay is present as a relatively pure phase between discrete temper particles and contains few if any particulates. No high temperature phases such as mullite are identified and no glass phases are observed. The matrix is a uniform orange-red color. No submicroscopic porosity is detectable at the scale of the light microscope within the fired clay body itself. This does not include the coarser consolidation pores created during molding. The fired clay lacks the lenticular void structures often observed in higher-fired brick with lower temper additions.

All of the matrix exhibits a coarse residual birefringence under cross polarized light indicating a relatively high degree of relict crystallinity in the clay (Fig. 45). This is one of the more robust indicators of firing temperature as crystallinity diminishes with increasing temperature. Some variability is noted in the morphology of the crystalline material. In Samples M02 and M03a, most of the birefringent material observed petrographically is plate-like in shape. In Sample M03b, there are greater occurrences of coarse patchy material. Sample M05 contains some particles where the crystal plates are arranged in even coarser sheaths.

7.6 - Higher-Fired Brick (Sample M04 Finish Coat)

The crushed brick used in the Sample M04 finish coat is clearly different than the others and is interpreted to represent a higher-fired product. Though this might indicate a later installation, the material appears more typical of pre-twentieth century manufacture. For the softer bricks, the material extracted out of the lime binder has a size distribution that essentially represents the original gradation of raw materials used to manufacture the brick. This is because the brick is friable and easily disaggregated into its constituent parts. In contrast, the brick in the finish coat of Sample M04 is much more cohesive. The size distribution of this material is representative of the crushing process alone (Fig. 19). Virtually all of the material extracted from the finish coat itself is finer than a No. 16 sieve.

Most of the textural evidence for the original brick is based on the fine crushed fragments identified petrographically in a relatively thin surface layer. Based on these observations, the brick has a much more compact clay-rich matrix than the brick in the other samples and the temper content is relatively low (Fig. 46). Most pieces are too small to permit a description of the macroscopic texture and appearance of the original brick. However, a single fragment of about 0.5 centimeter diameter was found in the underlying body coat (Fig. 20). This piece is nonfriable, uniformly dark red in color, dense, and impermeable. The freshly exposed interior of the fragment has a relatively vitreous luster.

The temper is a relatively fine-grained natural sand with most particles up to a maximum size of approximately 300 µm. Grains are mostly equidimensional and subangular in shape. Coarser particles consist of quartz with lesser or minor feldspar (Fig. 46). Minor polycrystalline quartz aggregates may represent some type of devitrified volcanic rock. In fact, some are associated with epidote. A few isolated bioclastic particles are identified in the matrix but none exhibit a clear association with fired clay. It is suspected that these are just sand contaminants from the underlying render body. Epidote and clinopyroxene are minor constituents in the finer sizes below the No. 100 sieve. Amphibole is also identified as a trace constituent and it has turned from green to red due to firing. Despite some color changes, no thermal cracking is identified in any particle. However, most of the temper is below the size expected to exhibit cracking at moderate temperatures.

Most of the fired clay body is uniformly dark red under plane polarized light. However, there are a few particles observed petrographically that have a low iron content and are lighter in color. No submicroscopic porosity is detectable at the scale of the light microscope within the fired clay body itself. However, sporadic occurrences of fine lenticular voids are noted and these are sometimes randomly oriented in the particles in which they are found. The matrix exhibits a variable degree of residual birefringence under cross polarized light indicating a modest degree of relict crystallinity in the fired clay. This suggests a moderate firing temperature that is also supported by the absence of higher temperature phases such as mullite or fused glass.

7.7 - Volcanic Glasses (Trass)

Four of the examined samples are lightly sanded lime mortars with no brick dust additions. These include the body and finish coats of Sample M01 (exterior stone masonry render) and the two examined body coats for Sample M04 (exterior string course render). In all four cases, a fairly significant quantity of fines was extracted after disaggregating the mortar and decomposing the lime binder (Fig. 26). Microscopic examination of these fines indicates a major proportion of volcanic glass along with bits of fine quartz silt and clay. It is suspected that the glass represents a separate and intentional trass addition rather than an unwashed constituent of the sand. The other crystalline constituents could represent fines from the sand or they could be impurities associated with the trass.

The primary evidence for a trass addition is the extraction of an appreciable quantity of fines passing the No. 325 sieve in these four samples (i.e. less than 45 µm). The color of the powder is a pale brown and this is distinctly different than the appearance of the sand in the coarser size fractions (Fig. 47). In all cases, the fine fraction was mounted in various refractive index oils and examined using polarized light microscopy. Many of the constituent grains appear as angular particles with grain sizes ranging from a few µm to as much as about 25 µm (Fig. 48). These are colorless in plane light and mostly clear. All of these particles are isotropic and have low refractive indices in the range of approximately 1.47. The optical properties are consistent with a glass that has a rhyolitic or high-silica composition.

For some reason, the volcanic glass particles are not detectable in thin section. Certainly the particles finer than approximately 10 µm would be anticipated to almost disappear within the lime paste given their low refractive index and lack of birefringence. Nevertheless, it would have been expected for the coarser particles to be detectable under close and deliberate scrutiny. The reason for the apparent disparity between the grain mount microscopy and thin section petrography is not clear. Still, the impact of the glass addition is quite obvious in the chemical analysis where a modest to high degree of hydraulicity is noted in all samples for which the fine glass is identified.

Trass is a natural pozzolan derived from ash beds or earth rich in volcanic ash. The stratigraphy of the San Juan region contains several volcanic horizons. Though the author has not studied the area personally, it is certainly feasible that there could be unconsolidated ash beds or volcanic-rich earth that could yield a sufficiently reactive pozzolan. However, to the author's knowledge, Puerto Rico is not widely known to have been a producing region for trass. Instead, regions in Italy and the Rhine Valley were well-renowned for their volcanic ash and the Dutch were known to have exported some of these products to the New World during the colonial period. The author has little knowledge regarding trade between the Spanish and Dutch during the seventeenth and eighteenth centuries and cannot speak confidently on the likelihood of an imported product. However, it is notable that the glasses appear to be rhyolitic in composition rather than andesitic. Admittedly, this is based on the refractive index of the glass rather than a careful chemical analysis of a concentrated trass sample. Nevertheless, the approximate composition of the glass does not appear to be consistent with the local rock types reported in the literature and identified in the coarser sand grains.

7.8 - Pigment

The crushed brick identified in Samples M02, M03a, M03b, M04a, and M05 acts as a highly effective pigment even if the primary function of the material is a pozzolanic additive. Only the finish layer in Sample M01 contains evidence for the addition of a pigment used solely for aesthetic purposes. Petrographically, the pigment is detected as sparsely distributed, ultrafine-grained, particulates (Fig. 28). These are likely based on some type of iron oxide-hydroxide. The addition results in a pale yellow color at the macroscopic scale and this yellowish tint is observed in fines extracted from the lime binder by acid digestion.

References
1. Baragona, Tony. "Re: Hi and a question!" Received by Heather Hartshorn, 17 Jan. 2017.
2. Eckel, Edwin C. *Cements, Limes, and Plasters.* New York: Robert Drummond, 1905. Print.
3. Kaye, Clifford A. "Geology of the San Juan Metropolitan Area Puerto Rico" *Coastal Geology of Puerto Rico, Geological Survey Professional Paper 317-A.* Washington: United States Government Printing Office, 1959. Print.
4. Kaye, Clifford A. "Shoreline Features and Quaternary Shoreline Changes Puerto Rico" *Coastal Geology of Puerto Rico, Geological Survey Professional Paper 317-B.* Washington: United States Government Printing Office, 1959. Print.

8. Open Questions and Possible Courses for Future Evaluation

Though the sampling was small and the testing scope limited, the compositional analysis alone revealed a wealth of information regarding the material traditions and building technologies in use during the construction of El Cañuelo. Still, the analysis has raised as many questions as it has answered. The client has asked that Highbridge include a short summary section that may help organize future directions for study. Some of these suggestions are simply academic and might serve as projects for graduate students or interns, while others might be critical for any repair or rehabilitation efforts.

8.1 - Soft-Fired Brick

The soft-fired brick used as a pozzolan is exceptionally soft and friable. The material was clearly disaggregated rather than crushed before inclusion in the mortars and renders. It would be interesting to know whether this was the normal condition of this brick source or if defective or lower quality bricks were set aside for use as a pozzolan. A visual survey of the building might reveal whether the same general type of brick was used in the construction. This should be probed to assess whether the brick is as friable as the crushed brick used as a pozzolan. Areas clearly damaged by water or salt should be avoided for this evaluation. Petrographic examination might be necessary to confirm a similar provenance if this is not immediately apparent from a visual analysis.

Since the clay can be readily separated from this particular brick, the material might be a good candidate for provenance studies using trace element chemistry. This would represent an involved study requiring a large number of analyses for statistical significance. The database could be used to compare with known or suspected clay pits or with other constructions of similar vintage. The temper can be similarly studied. In this case, mineralogical composition and particle size distribution of suspected sand sources would be a more appropriate comparator.

8.2 - Lime Composition and Sources

The author is not aware whether there are any written references or local lore regarding sources for lime burning during the seventeenth century. This type of information is usually only available locally if available at all. It would be interesting for this to be researched. Testing for verification would also be useful. Unfortunately, the small samples sizes left little opportunity to accurately determine original lime compositions. If further study is undertaken, samples could be selected to maximize the potential for evaluating the lime alone. This would include careful sampling of undispersed lime grains in the existing mortars. Determining the composition of large lime lumps avoids the chemical interferences from the pozzolanic additives. In addition to the major oxide composition, trace element chemical analysis could also be performed. If potential quarry sources can be identified, stone from these locations can be studied petrographically and chemically and compared to the materials on site.

8.3 - Beachrock

It is suspected that some of the aggregate present in Samples M02 and M05 is the same material used for the masonry construction. Furthermore, it is suspected that this material was quarried from shoreline exposures of beachrock reported to be quite common along the north shore of Puerto Rico. It would be useful to reconnoiter the region for potential sources of this stone. It would be important to know the thickness of the wall stone as this could limit the number of candidate outcroppings. Beachrock pavements can be relatively thin and some exposures might not have sufficient thickness to have supplied the masonry.

8.4 - Volcanic Ash

Very little is understood about the volcanic ash used as a pozzolan in the exterior renders. In fact, it cannot be stated conclusively that the addition was intentional. As with the lime, local history may provide clues to probable sources and traditions. A literature search would be necessary before attempting any actual field reconnaissance given the complexity of the problem. Local geologists may be better aware of any candidate sources of more silicic ash. Of course additional petrographic examination of local sands and volcanic deposits could assist in narrowing potential sources. However, this would not be an efficient exercise without more informed targeting of potential study areas.

8.5 - Exterior Render Stratigraphy
For one of the exterior wall samples, the petrographic examination revealed residues of lime-crushed brick mortar adhered to the substrate stone below the white lime-pozzolan render. It was suggested in this report that this could represent residues of an original surface render suggesting that the existing finishes are later repairs. Admittedly, it is also possible that the residue is simply an overrun of another mortar that was being used contemporaneously. For example, a similar lime-brick mortar is identified as a stone masonry bedding mortar in Sample M02. This question obviously has a bearing on the interpretation of the building and its finishes. Further evidence would need to be sought through a careful survey of the exterior wall. The author is not aware if there are many existing windows into the substrate or if destructive probes would be necessary.

A strategy for evaluating this question would have to be developed on site. Features to look for might include the degree to which mortar joints containing any red-colored mixtures are raked out along bed joints and head joints. Patches of residual lime-brick render under the white body coat would obviously be important to identify as would small pockets of red-colored render in any deeper embayments within the wall stone. Once observations are made, samples could be taken for additional microscopic analysis if desired. These would need to be carefully oriented and secured in order to preserve the evidence and not introduce any contaminants.

8.6 - Salt Contamination
This report focuses only on the composition of materials used in the construction. Clearly, marine salts have interacted with the materials over the years. Determining the types of salts present and their influence on any observed deterioration can be important for an understanding of the building performance. This can also help inform any future interventions by identifying any materials that might interact with planned treatments. The subject is too involved to make any specific recommendations without having studied the site.

8.7 - Performance Evaluations of Candidate Pozzolans for Use in Repair Mixes
It is assumed that there might be a desire to include the material traditions in the interpretation of the site. As such, these mortar and render materials could be candidates for "replication in-kind". However, great care must be used when attempting to recreate historical material traditions with modern materials. It is always advisable to plan a series of performance evaluations on all candidate materials. The subject it too large for this summary. However, some factors to consider would include the following:

- The degree of reactivity of any particular candidate pozzolan based on its chemistry, mineralogy, and fineness.
- The properties achieved when mixed at various proportions and water contents with any given lime source. Plastic properties might include water retentivity, plasticity, and ability to be "knocked up". Physical properties might include compressive strength and modulus of elasticity. Important hygrothermal properties would include capillary uptake rates and water vapor transmissivity.
- The durability of potential repair mixes relative to one another or to an established control. Resistance to various salts would be an important feature to consider.

9. Sieve Analysis of Sand or Other Extracted Inclusions

For samples that did not contain any significant acid-soluble material in the inclusions, the analysis is performed by digesting the sample in an acid sufficient to dissolve the binder. For samples where there was a notable abundance of carbonate material in the inclusions, the sample was disaggregated in a mortar and pestle and passed over the No. 100 mesh. The material retained on the sieve is further washed to remove any adherent binder residue. The material passing the No. 100 sieve is interpreted to contain no significant soluble aggregate component and is subject to acid digestion for the chemical analysis. The recovered insoluble residue from the chemical analysis is added back to the washed material retained on the No. 100 sieve to represent the inclusion gradations presented below for these samples.

The inclusion gradations presented below represent different components for each of the mix types. These are described further for each of the tables presented below. A qualitative description of these components is given in the discussions above, and the recovered samples are returned to the client. The sample size is significantly smaller than would be required to perform a sieve analysis on fresh aggregate materials as per ASTM C136 and some small errors should be expected.

Table 9.a: Extracted Sand and Inclusions Data (Lime-Crushed Brick Mixtures)

The material extracted from these samples represents the brick addition. However, the brick is soft and friable and the quantified grain sizes are more equivalent to the temper in the brick rather than the size of the brick particles themselves. In fact, coarse brick fragments up to the centimeter scale are observed in both samples but none of these have been recovered intact from the analysis. Additionally, the material passing the No. 325 sieve represents mostly the fired clay portion of the brick. Though presented as part of the raw data, this material is excluded from the cumulative passing and retained percentages.

Sample ID	**M03a**	**M03b**
Material type	**Mortar**	**Body coat**
Sample weight (g)	**5.20**	**19.82**
Extracted material	**Raw Data - Weight Retained (g)**	
No. 4	0.00	0.00
No. 8	0.00	0.00
No. 16	0.00	0.00
No. 30	0.06	0.18
No. 50	1.25	4.20
No. 100	1.61	5.60
No. 200	0.26	0.88
No. 325	0.10	0.35
Pan	0.42	1.44

	Cumulative Passing (wgt. %)	
Sample ID	**M03a**	**M03b**
Material type	**Mortar**	**Body coat**
No. 4	100.0	100.0
No. 8	100.0	100.0
No. 16	100.0	100.0
No. 30	98.2	98.4
No. 50	60.1	60.9
No. 100	11.0	11.0
No. 200	3.0	3.1
Pan	0.0	0.0

	Cumulative Retained (wgt. %)	
Sample ID	**M03a**	**M03b**
Material type	**Mortar**	**Body coat**
No. 4	0.0	0.0
No. 8	0.0	0.0
No. 16	0.0	0.0
No. 30	1.8	1.6
No. 50	39.9	39.1
No. 100	89.0	89.0
No. 200	97.0	96.9
Pan	100.0	100.0
Fineness Modulus	**1.31**	**1.30**

Notes:
1. Both of these samples were extracted via acid digestion.

Table 9.b: Extracted Sand and Inclusions Data (Lime-Crushed Brick Mixtures with Beachrock Sand)

The material extracted from these samples represents a combination of the brick beachrock sand additions. Most of the material above the No. 30 sieve consists of beachrock while the majority of the material passing the No. 30 mesh is derived from the brick. The brick is mostly present as broken up dust rather than coarser fragments, and as such the presented gradation is considered to be mostly representative of the distribution of sand and brick particles throughout the samples. The material passing the No. 325 sieve represents mostly the fired clay component of the brick. This fraction is included in the raw data table but excluded from the cumulative passing and retained percentages since it is not expected to contribute to the effective aggregate distribution.

Sample ID	**M02**	**M05**
Material type	**Mortar**	**Body coat**
Sample weight (g)	6.49	3.53
Extracted material	**Raw Data - Weight Retained (g)**	
No. 4	0.00	0.00
No. 8	0.29	0.00
No. 16	0.31	0.00
No. 30	0.49	0.11
No. 50	1.44	0.91
No. 100	1.13	0.81
No. 200	0.14	0.09
No. 325	0.11	0.07
Pan	0.48	0.26

	Cumulative Passing (wgt. %)	
Sample ID	**M02**	**M05**
Material type	**Mortar**	**Body coat**
No. 4	100.0	100.0
No. 8	92.6	100.0
No. 16	84.7	100.0
No. 30	72.1	94.5
No. 50	35.3	48.7
No. 100	6.4	8.0
No. 200	2.8	3.5
Pan	0.0	0.0

	Cumulative Retained (wgt. %)	
Sample ID	**M02**	**M05**
Material type	**Mortar**	**Body coat**
No. 4	0.0	0.0
No. 8	7.4	0.0
No. 16	15.3	0.0
No. 30	27.9	5.5
No. 50	64.7	51.3
No. 100	93.6	92.0
No. 200	97.2	96.5
Pan	100.0	100.0
Fineness Modulus	**2.09**	**1.49**

Notes:
1. Both of these samples were extracted via the mechanical disaggregation method described above.

Table 9.c: Extracted Sand and Inclusions Data (Lime-Brick Dust Finish Coat)

The material extracted from this sample represents the brick addition. The brick is reasonable hard, and did not break down further upon extraction. As such, the presented gradation is considered to be mostly representative of the distribution of brick particles throughout the sample. The material passing the No. 325 sieve represents mostly the fired clay component of the brick. This fraction is included in the raw data table but excluded from the cumulative passing and retained percentages since it is not expected to contribute to the effective aggregate distribution.

Sample ID	**M04a**
Material Type	**Finish**
Sample weight (g)	1.46
Extracted material	**Raw Data - Weight Retained (g)**
No. 4	0.00
No. 8	0.00
No. 16	0.00
No. 30	0.00
No. 50	0.02
No. 100	0.05
No. 200	0.02
No. 325	0.01
Pan	0.12

	Cumulative Passing (wgt. %)
Sample ID	**M04a**
Material Type	**Finish**
No. 4	100.0
No. 8	100.0
No. 16	100.0
No. 30	100.0
No. 50	80.0
No. 100	30.0
No. 200	10.0
Pan	0.0

	Cumulative Retained (wgt. %)
Sample ID	**M04a**
Material Type	**Finish**
No. 4	0.0
No. 8	0.0
No. 16	0.0
No. 30	0.0
No. 50	20.0
No. 100	70.0
No. 200	90.0
Pan	100.0
Fineness Modulus	**0.90**

Notes:
1. The sample was extracted via acid digestion.

Table 9.d: Extracted Inclusions Data (Sanded Mixtures of Lime and Natural Pozzolan)

The material extracted from this sample represents the sand addition as well as any insoluble part of the pozzolan addition. The material passing the No. 325 sieve is composed mostly of fines from the pozzolanic addition. In the finish from Sample M01, some pigment is also found in this finest fraction. The fraction passing the No. 325 mesh is presented in the raw data table for each sample. However, it is excluded from the cumulative and retained percentages, which are considered to be representative of the gradation of the sand alone.

Sample ID	**M01**		**M04a**	**M04b**
Material type	**Body coat**	**Finish**	**White body coat**	**Pink body coat**
Sample weight (g)	1.86	0.43	1.23	2.75
Extracted material	**Raw Data - Weight Retained (g)**			
No. 4	0.00	0.00	0.00	0.00
No. 8	0.00	0.00	0.00	0.00
No. 16	0.00	0.00	0.00	0.01
No. 30	0.01	0.01	0.00	0.03
No. 50	0.16	0.02	0.03	0.26
No. 100	0.29	0.04	0.05	0.41
No. 200	0.03	0.01	0.02	0.08
No. 325	0.01	0.00	0.01	0.03
Pan	0.04	0.03	0.01	0.19

	Cumulative Passing (wgt. %)			
Sample ID	**M01**		**M04a**	**M04b**
Material type	**Body coat**	**Finish**	**White body coat**	**Pink body coat**
No. 4	100.0	100.0	100.0	100.0
No. 8	100.0	100.0	100.0	100.0
No. 16	100.0	100.0	100.0	98.8
No. 30	98.0	87.5	100.0	95.1
No. 50	66.0	62.5	72.7	63.4
No. 100	8.0	12.5	27.3	13.4
No. 200	2.0	0.0	9.1	3.7
Pan	0.0	0.0	0.0	0.0

	Cumulative Retained (wgt. %)			
Sample ID	**M01**		**M04a**	**M04b**
Material type	**Body coat**	**Finish**	**White body coat**	**Pink body coat**
No. 4	0.0	0.0	0.0	0.0
No. 8	0.0	0.0	0.0	0.0
No. 16	0.0	0.0	0.0	1.2
No. 30	2.0	12.5	0.0	4.9
No. 50	34.0	37.5	27.3	36.6
No. 100	92.0	87.5	72.7	86.6
No. 200	98.0	100.0	90.9	96.3
Pan	100.0	100.0	100.0	100.0
Fineness Modulus	**1.28**	**1.38**	**1.00**	**1.29**

Notes:
1. The body coat from Sample M01 and pink body coat from Sample M04b were extracted via the mechanical disaggregation method described above.
2. The finish from Sample M01 and the white body coat from Sample M04a were extracted via acid digestion. However, further investigation of the white body coat from Sample M04a revealed that some carbonate material was present in the sand. As such, the extracted material for this sample may have a skewed gradation analysis. It is likely that the actual particle size distribution is closer to that of the pink body coat in Sample M04b.

10. Chemical Analysis

For some of the samples, a typical chemical analysis procedure was not performed since there is a notable calcareous component in the aggregate that is expected to interfere with the chemical analysis upon digestion. In order to most accurately measure the binder chemistry, the samples were mechanically disaggregated and passed over a No. 100 sieve to produce a concentrated sample of the binder and minimize any interferences from the sand. The results of the chemical analysis of only these finer fractions are presented in Table 10.a below. The fractions retained on the No. 100 sieve are rinsed with water and further disaggregated to remove the majority of any remaining adherent binder. The washed material represents the coarse fraction of the sand, and the results of this chemical analysis are presented in Table 10.b below.

In order to assess the composition of the samples as a whole, the components measured in the fraction passing the No. 100 sieve are proportionalized to the difference between the total sample weight and the weight of the sand retained on the No. 100 sieve. These results are presented in Table 10.c and are repeated in Table 10.d with the remaining samples that were analysis through more typical methods. Though the described methods are successful in isolating the binder chemistry, the resulting calculations could slightly overestimate the sand content due to the minor amount of binder that remains adhered to the sand in the fraction retained on the No. 100 sieve.

Table 10.a: Chemical Analysis Results (Fraction Passing No. 100 Sieve)

The results presented in this table represent the chemistry of material passing the No. 100 sieve after mechanical disaggregation. Note that there are insoluble residue results indicating some fine insoluble material remains behind in this portion of each of the samples. These residues are proportionalized and added back to the residues remaining on a No. 100 sieve after mechanical disaggregation.

Mix Type	**Lime-crushed brick mixtures with beachrock sand**		**Sanded mixtures of lime and natural pozzolan**	
Sample ID	**M02**	**M05**	**M01**	**M04b**
Material Type	**Mortar**	**Body coat**	**Body coat**	**Pink body coat**
Component (wgt. %)				
SiO_2	5.16	1.78	10.11	1.94
CaO	28.34	30.50	40.05	38.56
MgO	0.47	0.32	0.92	0.89
Al_2O_3	3.18	1.85	2.86	2.81
Fe_2O_3	0.43	0.25	0.55	0.56
Insoluble residue	34.89	36.71	14.21	20.48
LOI to 110°C	n.d.	n.d.	n.d.	n.d.
LOI 110°C-550°C	n.d.	n.d.	n.d.	n.d.
LOI 550°C-950°C	n.d.	n.d.	n.d.	n.d.
Measured Total	**72.47**	**71.40**	**68.71**	**65.25**

Notes:
1. Some components are marked "n.d." to indicate that these were not determined. Losses on ignition were not determined due to the limited quantity of sample provided for analysis.

Table 10.b: Chemical Analysis Results (Fraction Retained on No. 100 Sieve)

Mix Type	**Lime-crushed brick mixtures with beachrock sand**		**Sanded mixtures of lime and natural pozzolan**	
Sample ID	**M02**	**M05**	**M01**	**M04b**
Material Type	**Mortar**	**Body coat**	**Body coat**	**Pink body coat**
Total sample wgt. (g)	6.4923	3.5306	1.8602	2.7494
Wgt. of fraction retained on No. 325 sieve after cleaning (g)	3.7787	1.8475	0.6719	1.2542
Sand retained on No. 325 sieve as wgt. % of total sample	58.2028	52.3282	36.1198	45.6172

Table 10.c: Normalized Weight Percent Totals (Combined Fractions)

This table represents the combined data from the chemical analysis of the fraction passing the No. 100 sieve and the remaining residue retained on the No. 100 sieve. The coarser fraction was rinsed with water and further disaggregated to remove remaining adherent binder. Based on the resulting insoluble residue of this fraction, the measured components of the finer fraction were proportionalized to include the weight of the binder discarded from the coarser fraction during rinsing.

Mix Type	**Lime-crushed brick mixtures with beachrock sand**		**Sanded mixtures of lime and natural pozzolan**	
Sample ID	**M02**	**M05**	**M01**	**M04b**
Material Type	**Mortar**	**Body coat**	**Body coat**	**Pink body coat**
Component (wgt. %)				
SiO_2	2.01	0.76	7.50	1.37
CaO	11.04	13.07	29.72	27.35
MgO	0.18	0.14	0.69	0.63
Al_2O_3	1.24	0.79	2.12	2.00
Fe_2O_3	0.17	0.11	0.41	0.40
Insoluble residue	70.46	66.78	43.48	57.17
LOI to 110°C	n.d.	n.d.	n.d.	n.d.
LOI 110°C-550°C	n.d.	n.d.	n.d.	n.d.
LOI 550°C-950°C	n.d.	n.d.	n.d.	n.d.
Calculated Total	**85.10**	**81.64**	**83.92**	**88.92**

Table 10.d: Chemical Analysis Results (all samples including those reported in Table 10.c)

Mix Type	Lime-crushed brick mixtures		Lime-crushed brick mixtures with beachrock sand		Lime plaster finish	Lime-brick dust finish	Sanded mixtures of lime and natural pozzolan			
Sample ID	**M03a**	**M03b**	**M02**	**M05**	**M05**	**M04a**	**M01**	**M01**	**M04a**	**M04b**
Material Type	**Mortar**	**Body coat**	**Mortar**	**Body coat**	**Finish**	**Finish**	**Body coat**	**Finish**	**White body coat**	**Pink body coat**
Component (wgt. %)										
SiO_2	1.36	0.45	2.01	0.76	0.14	8.09	7.50	2.31	10.14	1.37
CaO	11.58	16.87	11.04	13.07	46.57	29.74	29.72	32.23	38.14	27.35
MgO	0.27	0.37	0.18	0.14	0.30	1.00	0.69	1.68	0.77	0.63
Al_2O_3	1.19	0.77	1.24	0.79	0.38	3.68	2.12	2.54	2.19	2.00
Fe_2O_3	0.18	0.12	0.17	0.11	0.10	1.00	0.41	0.66	0.51	0.40
SO_3	n.d.	n.d.	n.d.	n.d.	6.55	n.d	n.d.	n.d .	0.57	n.d.
Total insoluble residue	74.64	65.62	70.46	66.78	4.24	24.30	43.48	28.76	13.84	57.17
LOI to 110°C	n.d.	n.d.	n.d.	n.d.	n.d	n.d	n.d.	n.d.	n.d.	n.d.
LOI 110°C-550°C	n.d.	n.d.	n.d.	n.d.	n.d	n.d	n.d.	n.d.	n.d.	n.d.
LOI 550°C-950°C	n.d.	n.d.	n.d.	n.d.	n.d	n.d	n.d.	n.d.	n.d.	n.d.
Measured Totals	**89.22**	**84.20**	**85.10**	**81.64**	**58.29**	**67.81**	**83.92**	**68.17**	**66.18**	**88.92**

Notes:
1. Some components are marked "n.d." to indicate that these were not determined. Losses on ignition were not determined due to the limited quantity of sample provided for analysis. SO_3 was only determined for samples where a significant sulfate content was suspected based on the identification of gypsum in the petrographic examination.
2. For Samples M03a, M03b, and the finish coat of M05 as well as the white body coat and the finish layer of Sample M04a, the chemical analysis is performed directly on the sample. The digestion procedure was modified in order to ensure complete dissolution of the binder and to avoid leaching silica from the other components. The acid digestion was performed at room temperature and the base digestion was excluded. Insoluble residue is taken directly from the digestion used to extract the soluble oxides and not performed as a separate procedure.
3. For the remaining samples, the chemical analysis is performed according to the methods described at the beginning of Section 10.

Table 10.e: Estimated Binder Chemistry

Mix Type	Lime-crushed brick mixtures		Lime-crushed brick mixtures with beachrock sand		Lime plaster finish	Lime-brick dust finish	Sanded mixtures of lime and natural pozzolan			
Sample ID	**M03a**	**M03b**	**M02**	**M05**	**M05**	**M04a**	**M01**	**M01**	**M04a**	**M04b**
Material Type	**Mortar**	**Body coat**	**Mortar**	**Body coat**	**Finish**	**Finish**	**Body coat**	**Finish**	**White body coat**	**Pink body coat**
Component (wgt. %)										
SiO_2	9.2	2.4	13.6	5.1	0.3	18.4	18.4	5.8	19.6	4.3
CaO	78.6	89.9	74.6	87.0	96.9	67.7	72.8	80.9	72.7	85.3
MgO	1.8	2.0	1.2	0.9	0.7	2.3	1.7	4.2	1.5	2.0
Al_2O_3	8.1	4.1	8.4	5.3	0.9	8.4	5.2	6.4	4.2	6.2
Fe_2O_3	1.2	0.6	1.1	0.7	0.2	2.3	1.0	1.7	1.0	1.2
Other	1.0	1.0	1.0	1.0	1.0	1.0	1.0	1.0	1.0	1.0
CaO/MgO ratio	**43.2**	**45.8**	**59.8**	**95.3**	**140.6**	**29.9**	**43.4**	**19.2**	**49.1**	**43.1**
Hydraulicity index	**0.22**	**0.07**	**0.29**	**0.12**	**0.01**	**0.40**	**0.32**	**0.15**	**0.33**	**0.12**
Cementation index	**0.44**	**0.13**	**0.63**	**0.23**	**0.02**	**0.88**	**0.77**	**0.28**	**0.80**	**0.22**

Notes:
1. The binder chemistry is estimated on a non-volatile basis assuming the five measured oxides represent 99% of the total. The hydraulicity index is calculated by dividing the sum of silica and alumina by the measured calcium oxide. The cementation index is calculated by dividing the “hydraulic elements” by the “lime elements” after multiplying each by coefficients normalizing them to their molecular rather than weight contribution.

Table 10.f: Calculated Components (Lime-Crushed Brick Mixtures)

Mix Type	**Lime-crushed brick mixtures**	
Sample ID	**M03a**	**M03b**
Material Type	**Mortar**	**Body coat**
Component		
Lime expressed as dry hydrate (wgt. %)	16	25
Volcanic fines (wgt. %)	Not detected	Not detected
Brick (wgt. %)	84	75
Beachrock (wgt. %)	Not detected	Not detected
Sand (wgt. %)	Not detected	Not detected
Lime : brick ratio (by volume with lime as a dry hydrate)	1 : 2.5	1 : 1.5
Lime : brick ratio (by volume with lime as a putty)	1 : 5.1	1 : 3.0

Notes:
1. The lime weight is calculated by mathematically converting the measured CaO to its respective hydroxide by molecular weight conversion and reporting it in the form of a dry lime hydrate. The brick weight is calculated from the addition of the remaining four measured oxides and the insoluble residue. The lime and brick weights are normalized to 100% to return the materials to a dry weight basis. Volumetric ratios are calculated assuming bulk densities for dry lime hydrate and brick of 40 lbs./ft.^{3} and 80 lbs./ft.^{3} respectively. Another calculation is provided assuming the lime in putty form. This assumes a unit of dry lime hydrate will lose approximately half its volume when mixed to the consistency of a stiff paste. The brick volume then increases for the same weight of lime.

Table 10.g: Calculated Components (Lime-Crushed Brick Mixtures with Beachrock Sand)

Mix Type	**Lime-crushed brick mixtures with beachrock sand**	
Sample ID	**M02**	**M05**
Material Type	**Mortar**	**Body coat**
Component		
Lime expressed as dry hydrate (wgt. %)	16	20
Volcanic fines (wgt. %)	Not detected	Not detected
Brick (wgt. %)	64	76
Beachrock (wgt. %)	20	3.8
Sand (wgt. %)	Not detected	Not detected
Lime : brick : beachrock ratio (by volume with lime as a dry hydrate)	1 : 1.9 : 0.69	1 : 1.9 : 0.11
Lime : brick : beachrock ratio (by volume with lime as a putty)	1 : 3.9 : 1.4	1 : 3.8 : 0.22

Notes:
1. The lime weight is calculated by mathematically converting the measured CaO to its respective hydroxide by molecular weight conversion and reporting it in the form of a dry lime hydrate. The insoluble residue contains both brick and beachrock. The beachrock component is mostly retained on the No. 30 sieve while the brick component mostly passes the No. 30 sieve. The insoluble residue is proportionalized into these two components based on this separation by grain size. The total brick component is represented by calculated portion of the insoluble residue plus the four remaining measured oxides. The beachrock is taken directly from the other portion of the insoluble residue. The lime, brick, and beachrock are normalized to 100% to return the materials to a dry weight basis. Volumetric ratios are calculated assuming bulk densities for dry lime hydrate, brick, and beachrock of 40 lbs./ft.^{3}, 80 lbs./ft.^{3}, and 70 lbs./ft.^{3} respectively. Another calculation is provided assuming the lime in putty form. This assumes a unit of dry lime hydrate will lose approximately half its volume when mixed to the consistency of a stiff paste. The other component volumes then increase for the same weight of lime.

Table 10.h: Calculated Components (Lime-Brick Dust Finish Coat)

Mix Type	**Lime-brick dust finish**
Sample ID	**M04a**
Material Type	**Finish**
Component	
Lime expressed as dry hydrate (wgt. %)	51
Volcanic fines (wgt. %)	Not detected
Brick (wgt. %)	49
Beachrock (wgt. %)	Not detected
Sand (wgt. %)	Not detected
Lime : brick ratio (by volume with lime as a dry hydrate)	1 : 0.48
Lime : brick ratio (by volume with lime as a putty)	1 : 0.97

Notes:
1. The lime weight is calculated by mathematically converting the measured CaO to its respective hydroxide by molecular weight conversion and reporting it in the form of a dry lime hydrate. The brick weight is calculated from the addition of the remaining four measured oxides and the insoluble residue. The lime and brick weights are normalized to 100% to return the materials to a dry weight basis. Volumetric ratios are calculated assuming bulk densities for dry lime hydrate and brick of 40 lbs./ft.^{3} and 80 lbs./ft.^{3} respectively. Another calculation is provided assuming the lime in putty form. This assumes a unit of dry lime hydrate will lose approximately half its volume when mixed to the consistency of a stiff paste. The brick volume then increases for the same weight of lime.

Table 10.i: Calculated Components (Sanded Mixtures of Lime and Natural Pozzolan)

Mix Type	**Sanded mixtures of lime and natural pozzolan**			
Sample ID	**M01**	**M01**	**M04a**	**M04b**
Material type	**Body coat**	**Finish**	**White body coat**	**Pink body coat**
Component				
Lime expressed as dry hydrate (wgt. %)	42	56	64	37
Volcanic fines (wgt. %)	15	17	19	16
Brick (wgt. %)	Not detected	Not detected	Not detected	Not detected
Beachrock (wgt. %)	Not detected	Not detected	Not detected	Not detected
Sand (wgt. %)	43	27	16	48
Lime : volcanic fines : sand ratio (by volume with lime as a dry hydrate)	1 : 0.22 : 0.51	1 : 0.19 : 0.25	1 : 0.18 : 0.13	1 : 0.26 : 0.64
Lime : volcanic fines : sand ratio (by volume with lime as a putty)	1 : 0.44 : 1.0	1 : 0.37 : 0.49	1 : 0.36 : 0.25	1 : 0.52 : 1.3

Notes:
1. For the white body coat in Sample M04a, a proportion of the measured CaO is attributed to gypsum based on the determined SO_3 content. For all of the samples, the lime weight is calculated by mathematically converting the measured CaO (or corrected CaO for Sample M04a) to its respective hydroxide by molecular weight conversion and reporting it in the form of a dry lime hydrate. The insoluble residue contains both sand and volcanic fines. The material passing a No. 325 sieve in the sand extraction procedure is used to adjust the insoluble residue proportionally so that a maximum volcanic fines content can be deducted from this value. The subtracted fines are added to the other four measured oxides to represent the maximum volcanic fines component. The sand is taken from the remaining insoluble residue component. The lime, volcanic fines, and sand weights are normalized to 100% to return the materials to a dry weight basis. Volumetric ratios are calculated assuming bulk densities for dry lime hydrate, volcanic fines, and damp, loose sand of 40 lbs./ft.^{3}, 65 lbs./ft.^{3}, and 80 lbs./ft.^{3} respectively. Another calculation is provided assuming the lime in putty form. This assumes a unit of dry lime hydrate will lose approximately half its volume when mixed to the consistency of a stiff paste. The other component volumes then increase for the same weight of lime.
2. The assumed bulk density for the volcanic fines is based on an average of values provided for natural pozzolans by Mr. Tony Baragona, who has reportedly determined the density of these materials in accordance with ASTM D1895B.

Appendix I: Visual Description of Samples as Received

Sample ID	**M01 (Body coat)**
Description	The entire sample consists of approximately half a dozen small render pieces with multiple smaller fragments and a low abundance loose powder weighing a total of 25 grams. The individual pieces contain multiple materials including the sandstone substrate, the render that has both a body coat and a finish coat, and a thin coating. The render is the focus of this examination, and the characteristics of the body coat only are described in this table. This body coat has between approximately 0.5" and 0.75" of depth represented between the underlying stone substrate and the finish coat. The finish coat of the render is described separately. Neither the sandstone nor the color wash are evaluated as part of this investigation.
Surfaces	None of the surfaces of the body coat are exposed. The body coat appears to be well compacted into the irregularly shaped sandstone substrate. The body coat appears to have had a roughly planar outer surface and the finish coat is intimately placed over this surface. The two materials are well adhered with no notable gaps, voids, separations, or cracks.
Hardness / Friability	The paste is moderately soft, yet the mortar is cohesive and nonfriable.
Appearance	Freshly exposed surfaces have a dull luster and are nearly white in color (Munsell code approximately 10YR 8.5/0.5).
Other Details	No cracks are visible in hand sample. The body coat in one of the sample pieces contains air-voids that are lined with white, needle-like crystals. There is a moderately low abundance of millimeter-scale white lime grains, a moderately low abundance of submillimeter red-orange to reddish brown inclusions, and trace black inclusions. There is also one millimeter-scale inclusion of paste that is the same color as the finish coat. Fresh surfaces of the body coat are rapidly water absorptive.

Sample ID	**M01 (Finish)**
Description	The entire sample consists of approximately half a dozen small render pieces with multiple smaller fragments and a low abundance loose powder weighing a total of 25 grams. The individual pieces contain multiple materials including the sandstone substrate, the render that has both a body coat and a finish coat, and a thin coating. The render is the focus of this examination, and the characteristics of the finish coat only are described in this table. This finish coat is approximately 1/8" thick as represented in the sample. The body coat of the render is described separately. Neither the sandstone nor the color wash are evaluated as part of this investigation.
Surfaces	The outer surfaces are smooth, planar, and covered with a white and dark orange coating. Portions of the outer surface appear to be worn back in negative relief, and these areas have a somewhat irregular surface that is covered with dark gray to black soiling. The rear surface of the finish is not exposed, but this material appears to have been intimately compacted over the roughly planar surface of the body coat. The two materials are well adhered with no notable gaps, voids, separations, or cracks.
Hardness / Friability	The paste is moderately soft, yet the mortar is cohesive and nonfriable.
Appearance	Freshly exposed surfaces have a dull luster and are very pale yellow in color (Munsell code approximately 10YR 8/2).
Other Details	No cracks, efflorescence, or mineral deposits are visible in hand sample. There is a high abundance of millimeter-scale white lime grains and a low abundance of submillimeter red-orange to reddish brown inclusions. The sample also contains a low abundance of black, reflective, angular inclusions less than one millimeter in diameter. Fresh surfaces are rapidly water absorptive while the outer surfaces that are covered with either a coating or soiling are somewhat slowly absorptive.

Sample ID	**M02 (Mortar)**
Description	The sample consists of multiple small mortar pieces and a moderate abundance loose powder weighing a total of 50 grams. Some of the mortar pieces also contain adherent pieces of the stone masonry. The orientation of the pieces is not evident, and no joint thickness or represented depth can be discerned. However, the largest piece is 0.5″ x 0.75″ x 1″.
Surfaces	No tooled surfaces are detected. Some pieces contain surfaces that are potentially formed. These are irregular yet compact, sandy-textured, and covered with biological growth and potentially some mineralizations. All other surfaces are mostly compact and dusty to sandy-textured.
Hardness / Friability	The paste is soft, and the mortar is nonfriable. However, the mortar pieces can easily be disaggregated with light to moderate finger pressure.
Appearance	Freshly exposed surfaces have a dull luster and are red-orange in color (Munsell code approximately 7.5YR 6/6.5).
Other Details	Cracking cannot be fully assessed due to the small size of the sample pieces. It is possible that some kind of continuous mineral deposit is covering the formed surfaces, but this is difficult to discern due to the presence of biological growth. The sample contains a moderately high abundance of white inclusions ranging in size from less than one millimeter up to approximately five millimeters in diameter. Some of these pieces represent the beachrock component of the mortar and exhibit notable millimeter-scale pitting. Fresh surfaces are rapidly water absorptive while the potentially formed surfaces are only slowly absorptive.

Sample ID	**M03a (Mortar)**
Description	The sample consists of multiple small mortar pieces and a moderately high abundance loose powder weighing a total of 27 grams. The orientation of the pieces is not evident, and no joint thickness or represented depth can be discerned. However, the largest piece is 0.5″ x 0.75″ x 1″.
Surfaces	No tooled surfaces are detected. Some pieces contain surfaces that are potentially represent bed surfaces. These are irregularly formed, sandy-textured, and compact. A moderately high proportion of these potential bed surfaces are covered with dark gray soiling. All other surfaces are irregular, compact, and mostly sandy-textured.
Hardness / Friability	The paste is soft. The mortar is nonfriable but can be easily disaggregated under low to moderate finger pressure.
Appearance	Freshly exposed surfaces have a moderately dull luster and are pink in color (Munsell code approximately 6.5YR 6.5/4).
Other Details	Cracking cannot be fully assessed due to the small size of the sample pieces. No mineral deposits of efflorescences are visible in hand sample. There is a moderate abundance of white binder inclusions mostly less than one millimeter but some are up to two millimeters in diameter. The sample also contains a moderate abundance of millimeter to centimeter-scale red, friable brick inclusions as well as a low abundance of associated fine brick dust much less than one millimeter in diameter. Fresh surfaces are rapidly water absorptive while the potential bed surfaces vary between moderately to rapidly absorptive.

Sample ID	**M03b (Body coat)**
Description	The sample consists of one large piece of render, several small render fragments, and a minor abundance loose powder weighing a total of 80 grams. The outer surface of the largest piece is 2.5” x 3” with up to approximately 0.5” of the depth represented from the surface.
Surfaces	The outer surface is roughly planar and compact with a low relief, fine sand exposure. There is also a moderately high abundance of one to two millimeter white binder inclusions exposed on the outer surface. The inner surface is not clearly formed. It is possibly fresh, mostly compact, irregularly planar, and sandy-textured.
Hardness / Friability	The paste is soft, and the mortar is nonfriable. However, it can be easily disaggregated under low to moderate finger pressure. The outer surface is comparatively more cohesive with a moderate hardness.
Appearance	Freshly exposed surfaces have a moderately dull luster and are red-orange in color (Munsell code approximately 7YR 5.5/6.5).
Other Details	The sample contains a low abundance inch-scale, cross-hatched cracking that is visible on the inner surface and perpendicular to the outer surface. No mineral deposits are visible in hand sample, but there is possibly a light gray mineralization on the outer surface. There is a high abundance of millimeter to centimeter-scale red, friable brick inclusions and possibly a low abundance of associated fine brick dust. The sample also contains a moderate abundance white binder inclusions approximately one to two millimeters in diameter. Just below the outer surface there appears to be a less than one millimeter thick horizon of green biological growth. Fresh surfaces are rapidly water absorptive while the outer surface is moderately to somewhat rapidly absorptive.

Sample ID	**M04a (White body coat)**
Description	The sample contains a render with three visible materials weighing a total of 25 grams. These materials include a brick red finish, a white body, and a pink body coat. Only the white body coat is described here, and up to 0.25" depth of this body coat is represented behind the finish coat. Descriptions of the red finish and pink body coats are provided in separate tables.
Surfaces	None of the surfaces of the white body coat are exposed. The inner surfaces are broken and the attachment of the render to the substrate cannot be evaluated. The red finish appears to be well-attached to the white body coat in one piece and partially adhesively disbonded in the other piece. The cross-sectional surfaces of the pieces have a dark brownish gray and black soiling. These could represent surfaces that were exposed or cracked on site.
Hardness / Friability	The paste is moderately soft, yet the render is cohesive and nonfriable.
Appearance	Freshly exposed surfaces have a moderately dull luster and are nearly white in color (Munsell code approximately 2.5Y 8.5/1).
Other Details	No cracks are visible in hand sample. The broken inner surface of the white body coat contains a moderate abundance of fine, white crystals and possibly a low abundance of millimeter-scale white to yellowish-white deposits. There is a moderately low abundance of white binder inclusions approximately one millimeter in diameter as well as a moderately low abundance of red inclusions much less than one millimeter in diameter. The sample also contains a moderate abundance of sharp-textured, reflective black inclusions, all much less than one millimeter in diameter. There is also a single red brick inclusion that is approximately five millimeters in diameter and roughly the same color as the brick in the finish coat. A single two-millimeter long piece of wood cinder is also observed. All surfaces are somewhat rapidly water absorptive.

Sample ID	**M04a (Finish)**
Description	The sample contains a render with three visible materials weighing a total of 25 grams. These materials include a brick red finish, a white body, and a pink body coat. Only the red finish is described here, and its thickness is represented between approximately 1/16" and 1/8" in the sample. Descriptions of the white and pink body coats are provided in separate tables.
Surfaces	The outer surface is smooth and slightly convex with an almost ceramic appearance. The inner surface of the finish coat is not exposed. However, it appears well attached to the underlying body coat in one piece and partially adhesively disbonded in the other piece.
Hardness / Friability	The paste is extremely hard on the outer surface and moderately hard where the finish coat is freshly exposed. The finish coat is nonfriable and cohesive.
Appearance	Freshly exposed surfaces have a slightly subvitreous to moderately dull luster and are light reddish brown in color (Munsell code approximately 3.5YR 6/4). However, the color of the outer surface is a more saturated brick red color (Munsell code approximately 3.5YR 4/4).
Other Details	No cracks are visible in hand sample. The outer surface has voids that are filled with smooth, white, scaly mineral deposits. There is a high abundance white binder inclusions up to one millimeter in diameter along with a high abundance red brick inclusions of similar size. The sample also contains a moderately low abundance of fine black inclusions. All surfaces are very slowly to not noticeably water absorptive.

Sample ID	**M04b (Pink body coat)**
Description	The sample consists of multiple render pieces weighing approximately 12 grams. Though this sample was received in a separate bag, the material is visually consistent with the pink body coat observed in Sample M04a. Upon further investigation, this material is believe to represent a carbonated version of the white body coat.
Surfaces	No formed or tooled surfaces are included. However, there do appear to be exposed surfaces that have some brownish to black soiling.
Hardness / Friability	The paste is soft to moderately soft, yet the render is cohesive and nonfriable.
Appearance	Freshly exposed surfaces have a dull luster and are very pale pinkish brown to nearly white in color (Munsell code approximately 10YR 8/1.5).
Other Details	No cracks, efflorescence, or minerals deposits are visible in hand sample. The sample contains a moderate abundance of fine red inclusions that are much less than one millimeter in diameter as well as a low abundance of angular, reflective black inclusions that are all less than one millimeter in diameter. All surfaces are rapidly water absorptive.

Sample ID	**M05 (Body coat)**
Description	The sample contains multiple reddish body coat pieces and separate white finish coat pieces as well as a moderately high abundance loose powder weighing a total of 25 grams. Only the body is described here while the finish is described in separate table. The body coat pieces have no discernible orientation, but the largest piece is approximately 3/8″ x 3/4″ x 1″.
Surfaces	There are no discernible formed surfaces. All of the surfaces in the provided pieces are mostly compact and sandy-textured.
Hardness / Friability	The paste is soft, yet the render is cohesive and nonfriable. However, it can be disaggregated with low to high finger pressure depending on the piece.
Appearance	Freshly exposed surfaces have a moderately dull luster and are red-orange in color (Munsell code approximately 7.5YR 5.75/6).
Other Details	Cracking cannot be fully assessed due to the small size of the sample pieces. There is a moderately low abundance of white mineral deposits lining air-voids. There is also a low abundance of white binder inclusions and a moderate abundance of red brick inclusions. These are all much less than one millimeter in diameter. All of the surfaces are rapidly water absorptive.

Sample ID	**M05 (Finish)**
Description	The sample contains multiple reddish body coat pieces and separate white finish coat pieces as well as a moderately high abundance loose powder weighing a total of 25 grams. Only the finish is described here while the body coat is described in separate table. The finish coat is approximately 1/8" thick as represented in the sample pieces.
Surfaces	The outer surfaces are planar, compact, sandy-textured and covered with a continuous deposit of light gray mineralizations. The inner surfaces are irregularly planar and sandy-textured with residual reddish body coat attached.
Hardness / Friability	The paste is soft, yet the finish is cohesive and nonfriable. The material appears to be bound cohesively with mineral deposits.
Appearance	Freshly exposed surfaces have a dull luster and are nearly white in color (Munsell code approximately 10YR 8/1).
Other Details	Cracking cannot be fully assessed due to the small size of the sample pieces. No binder or other inclusions are visible in hand sample. There is a continuous light gray mineralization coating the outer surface and part of the inner surface. Fresh surfaces are rapidly water absorptive, but the outer surface that is covered with secondary mineralizations is slowly absorptive.

Appendix II: Photographs and Photomicrographs

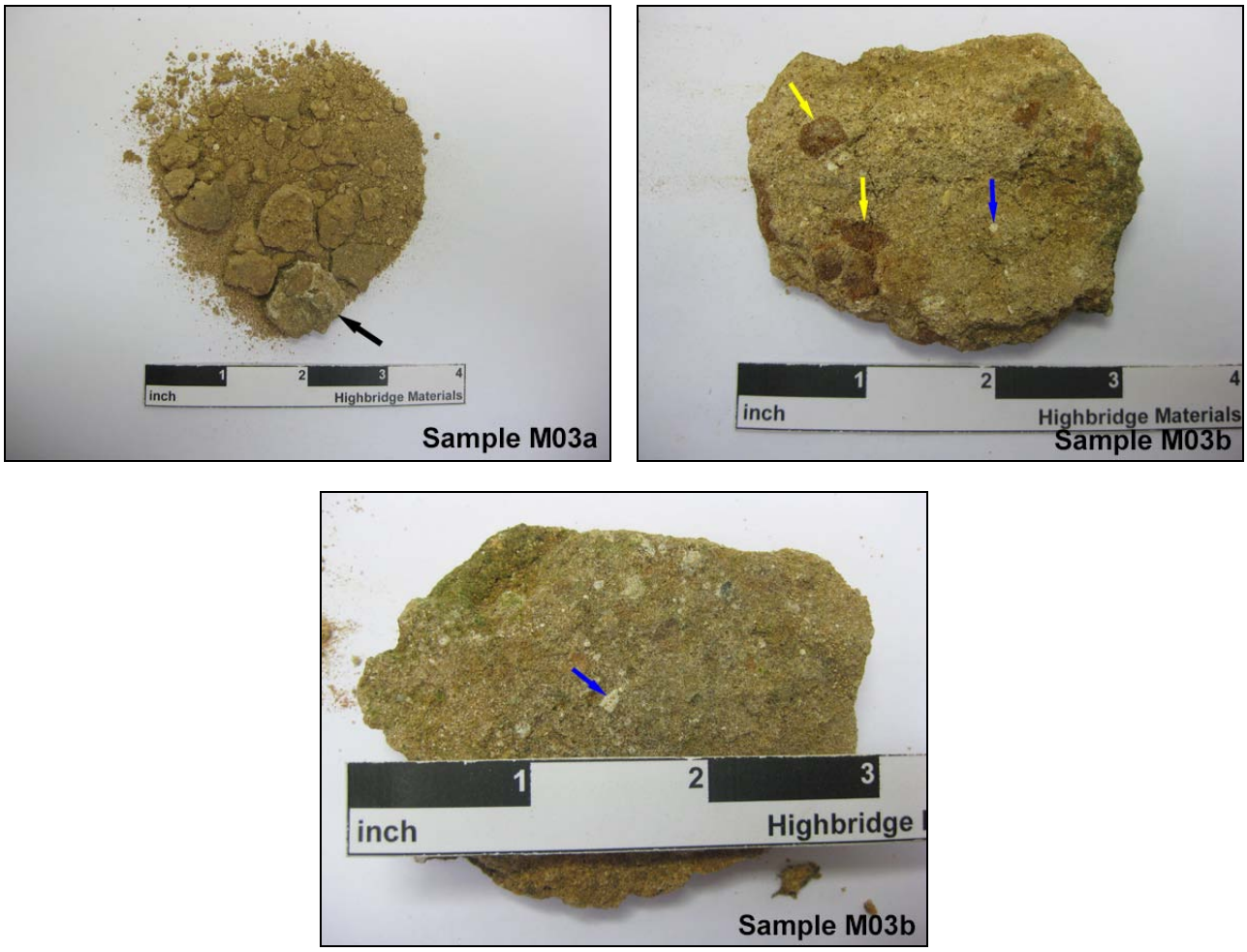


Figure 1: Samples M03a and M03b are similar mixtures of lime and crushed brick representing a mortar and a render respectively. Both have a pastel orange color and a dull, grainy texture. The black arrow in the photograph for Sample M03a indicates a lighter-colored inclusion representing a different lime mortar mixture. This was not examined for this report. Sample M03b is a larger sample that better displays the textural features of the mixture. The brick pozzolan is somewhat crudely crushed resulting in pieces up to a centimeter in size distributed throughout the matrix (yellow arrows). The lime is also not completely dispersed and white lime inclusions contrast against the orange-colored mixture (blue arrows).

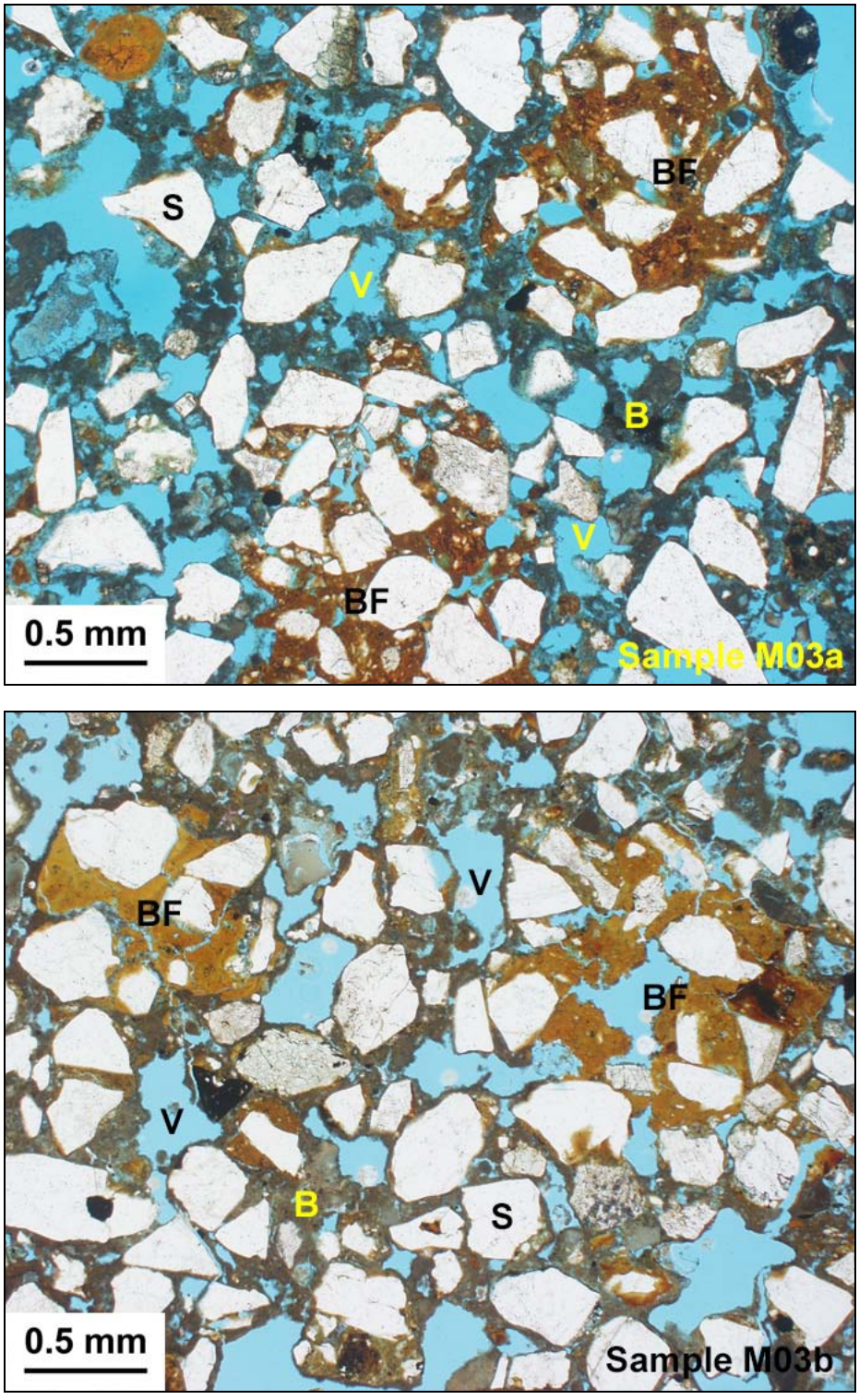


Figure 2: PPL photomicrographs illustrating the microtexture of the two lime-crushed brick mixtures. The samples are impregnated with a low-viscosity, blue-dyed epoxy in order to highlight cracks, pores, and voids. The binder (B) strongly absorbs the dyed epoxy indicating a high capillary porosity. High microporosities are characteristic of lime-based mortars. Sand grains (S) are narrowly graded and densely distributed throughout the mortar. However, these are all shown to be temper particles released from the weak brick matrix when the brick was disaggregated for use in the mixtures. Larger brick fragments (BF) contain the identical sand embedded in a red clay matrix. Though compact in texture, the microscopic consolidation is less ideal and irregularly-shaped air-voids (V) are abundant in both mixes.

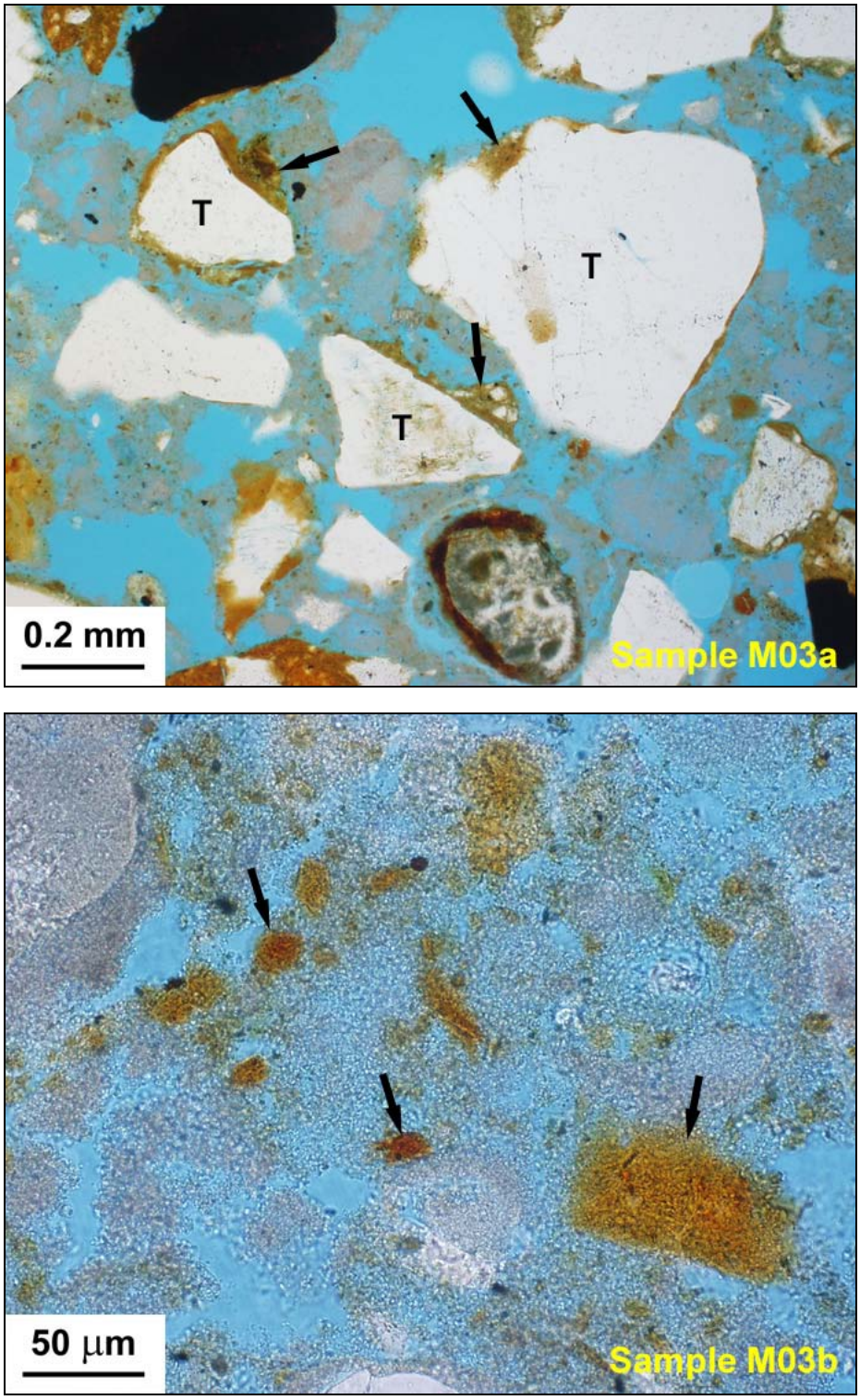


Figure 3: PPL photomicrographs illustrating the qualities of the crushed brick pozzolan in Samples M03a and M03b. (Upper image) Temper particles (T) are separated from the clay matrix but are not crushed. A thin lining of fired clay usually lines the temper particles (arrows) and this demonstrates that all of the sand was derived from the brick. No other aggregate addition is present in these mixtures. (Lower image) The fired clay (arrows) is also present as distributed particulates and powder. These are found blended throughout the lime paste.

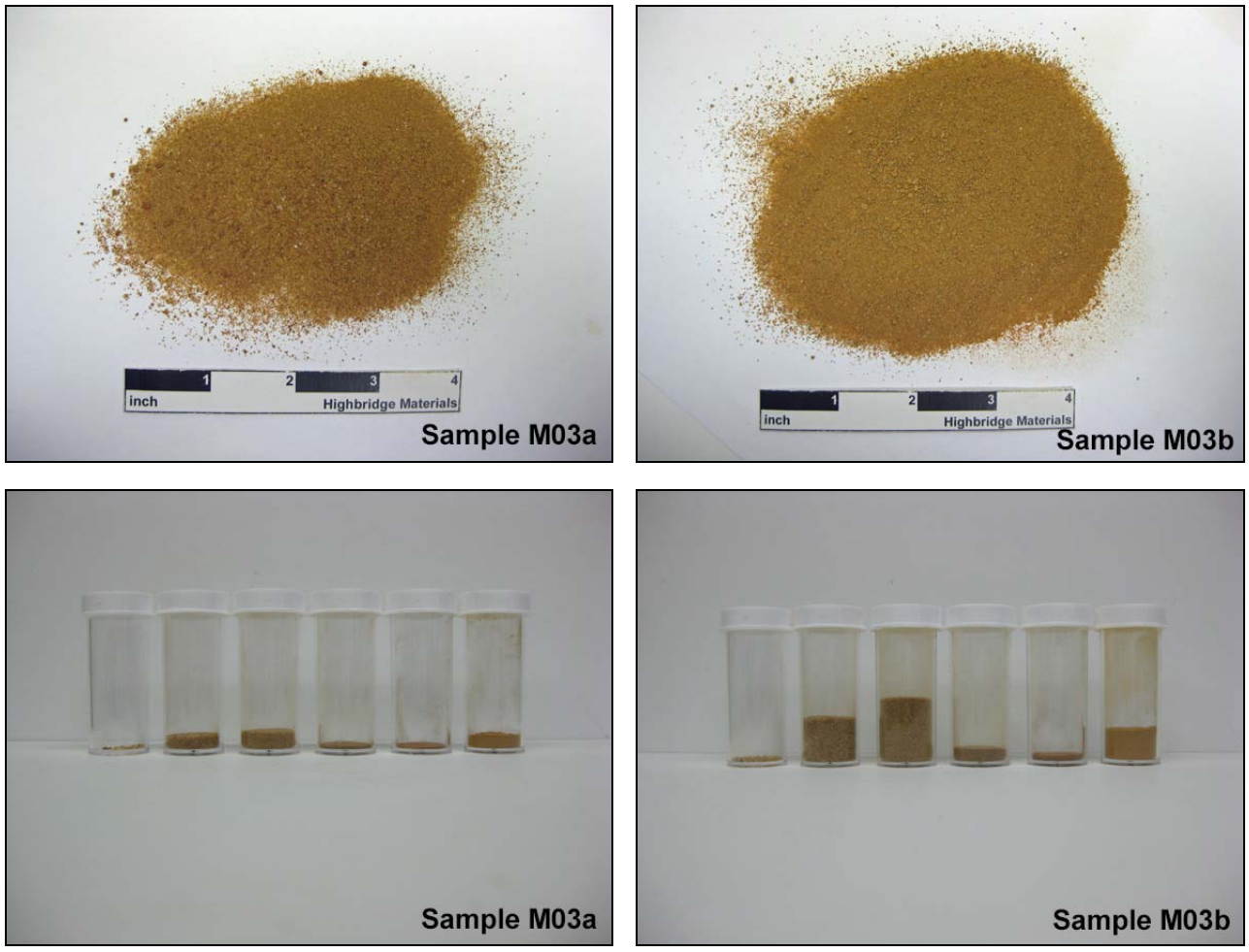


Figure 4: Photographs of the insoluble materials extracted from Samples M03a and M03b after digestion in acid. (Upper images) The materials extracted from the mortars include only the temper and clay from the brick pozzolan. Note that there are no larger particles. The brick is friable and it was not possible to preserve the coarser fragments. (Lower images) The material is shown after gradation through the standard sieve stack used for masonry aggregates. In this case, the particle size distribution reflects the original ingredients of the brick before firing. The vial at the right includes all of the fine powder from the fired clay. All other vials contain temper grains with thin linings of fired clay.

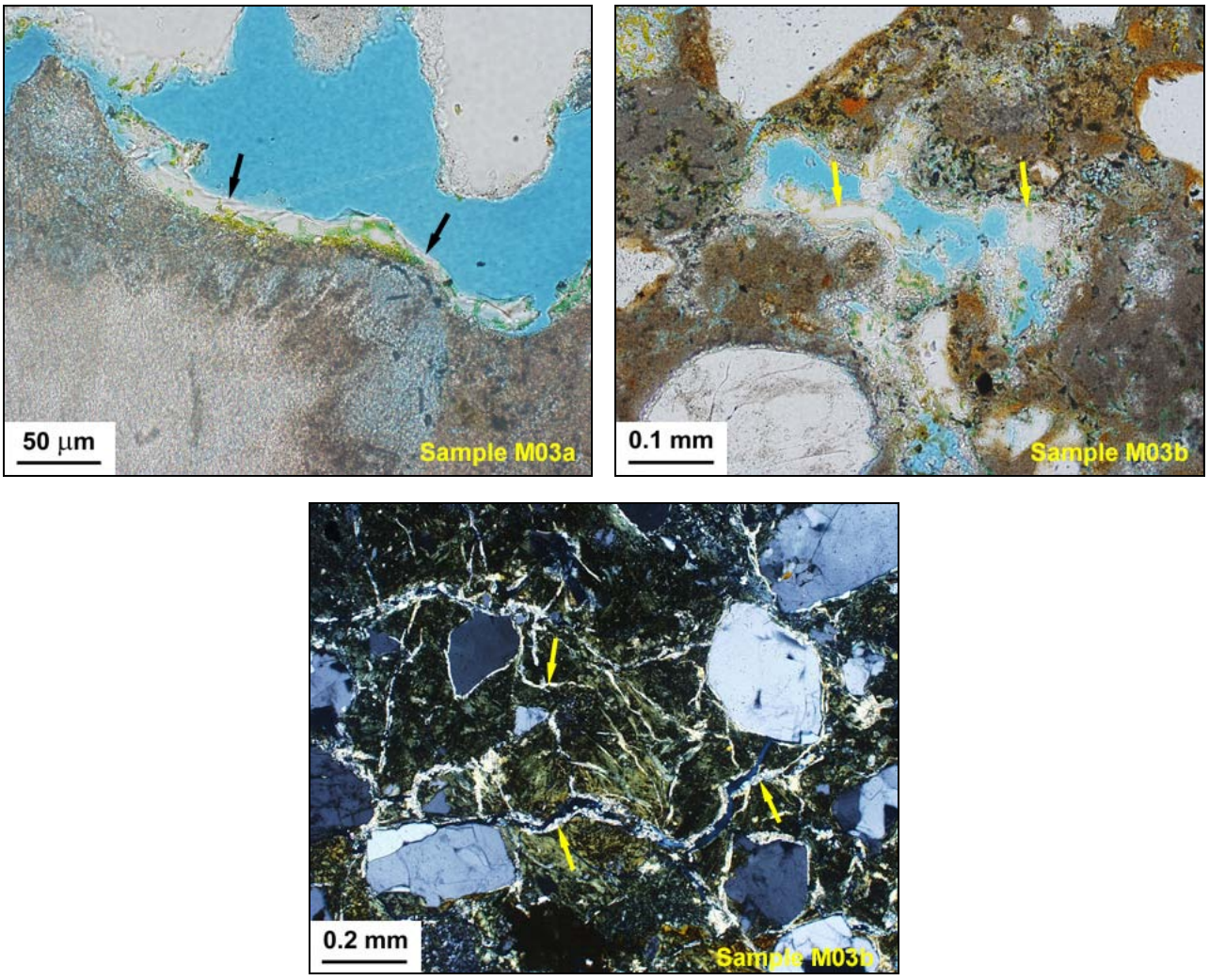


Figure 5: Photomicrographs illustrating trace occurrences of secondary salts in Samples M03a and M03b. (Upper PPL images) The arrows indicate thin salt linings in air-voids. These are probably mixtures of halite and gypsum based on optical properties. (Lower XPL image) The arrows indicate microcracks in a brick fragment that are lined with an unidentified salt phase.

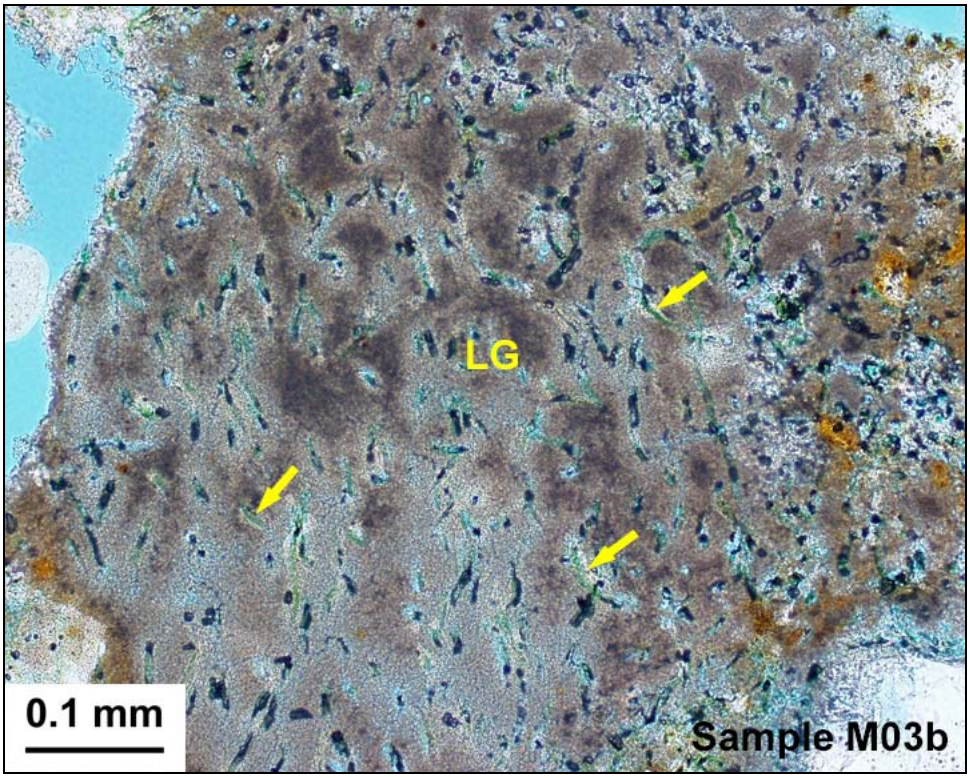


Figure 6: PPL photomicrograph of Sample M03b taken within a lime grain (LG) along the weathered surface of the render. The arrows indicate microscopic channels identified as microbial borings. A greenish colored biota is still present within some of these borings.



Figure 7: Samples M02 and the brown coat of Sample M05 are similar mixtures of lime, crushed brick, and beachrock sand. Both have the same pastel orange color and dull, grainy texture characteristic of Samples M03a and M03b. In Sample M02, there are some larger sandstone fragments presumably represented portions of the masonry (arrows). These are distinguished from the mortar (M). Sample M05 is an interior plaster. Fragments of the white finish coat are also included with the sample (arrow indicates an example).

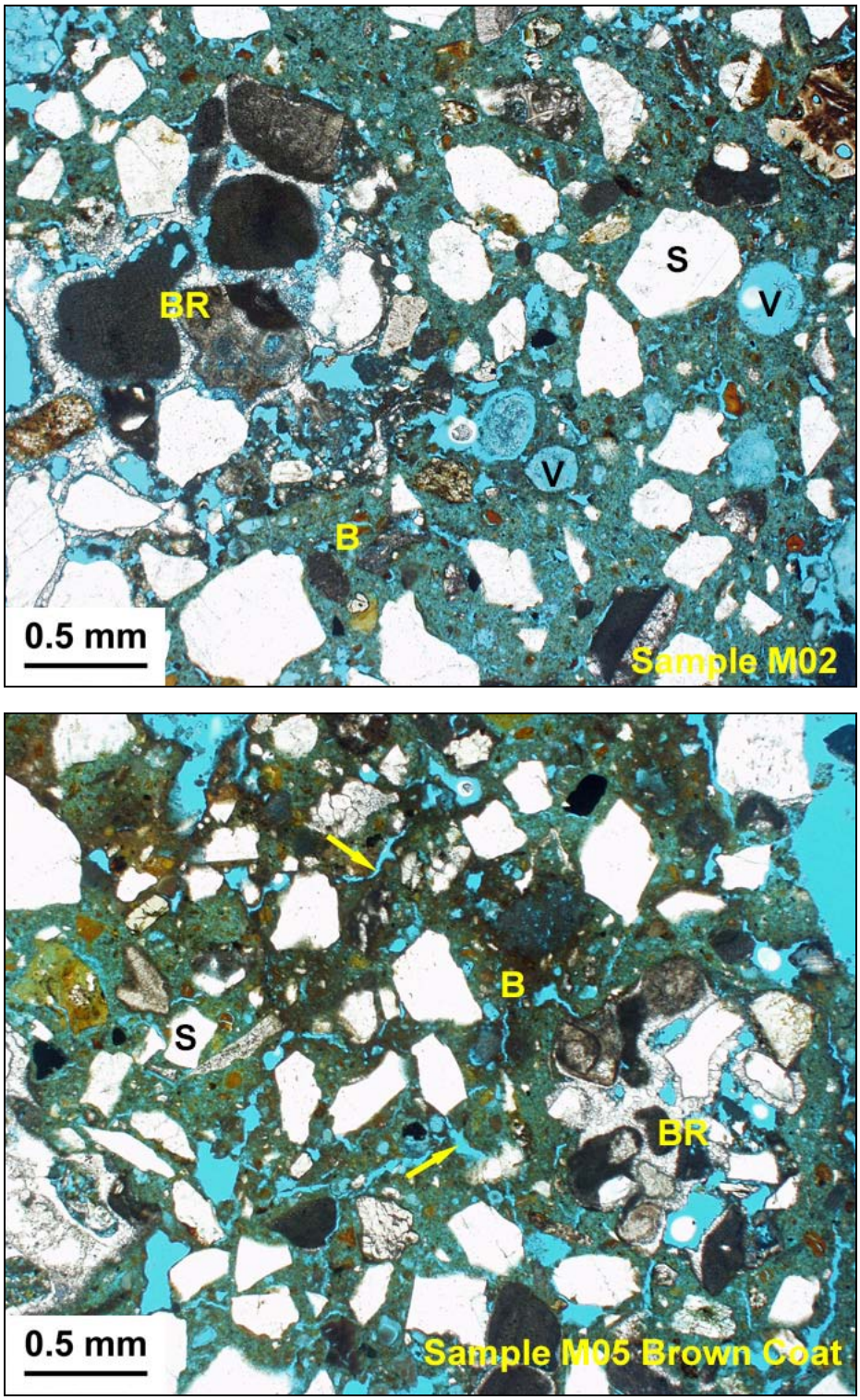


Figure 8: PPL photomicrographs illustrating the microtexture of Samples M02 and the brown coat of Sample M05. The samples are impregnated with a low-viscosity, blue-dyed epoxy in order to highlight cracks, pores, and voids. The binder (B) strongly absorbs the dyed epoxy indicating a high capillary porosity. High microporosities are characteristic of lime-based mortars. Coarser particles of beachrock (BR) are a minor aggregate addition in both samples. Other sand grains (S) are mostly shown to be temper particles derived from the crushed brick. Beachrock particles are also found in this size range but it is typically not difficult to distinguish between these two. More importantly, there is no quartz sand aggregate that is not otherwise associated with these two components. A low abundance of spherical voids (V) are shown for Sample M02. The arrows indicate consolidation voids that are a little more lenticular in shape in the brown coat of Sample M05.

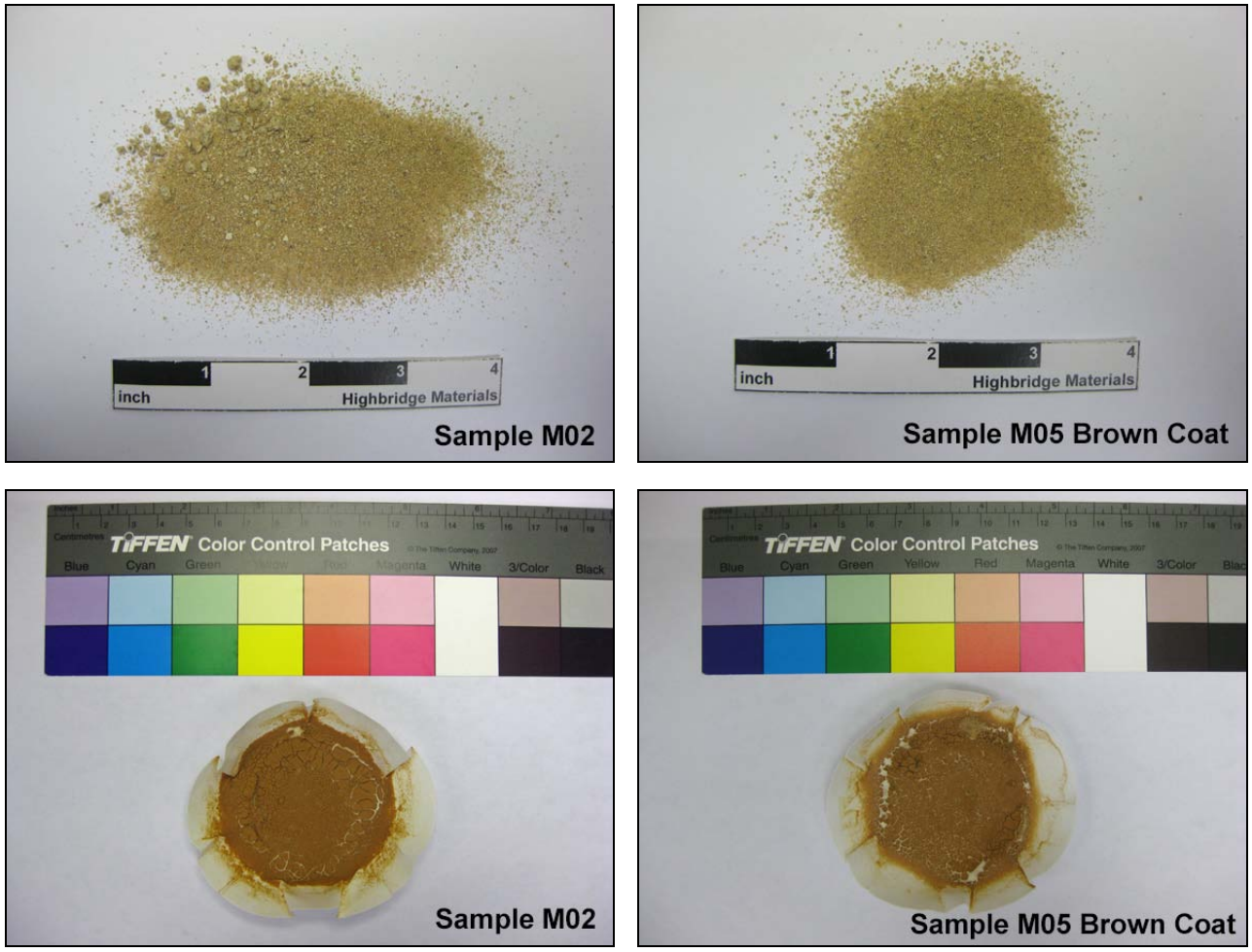


Figure 9: Samples M02 and the body coat of M05 could not be digested in acid without decomposing the beachrock sand. Instead, these were manually disaggregated by hand and passed over a No. 100 sieve. The coarser material was repeatedly rinsed to remove any adherent lime binder. The finer material does not contain any beachrock and could be digested in acid without concern over losing any aggregate or residual pozzolanic material. The cleaned coarser material is shown in the upper images. This is a combination of beachrock sand and brick temper. The finer material is shown in the lower image. This is mostly fired clay along with some finer brick temper. These materials were recombined before gradation.

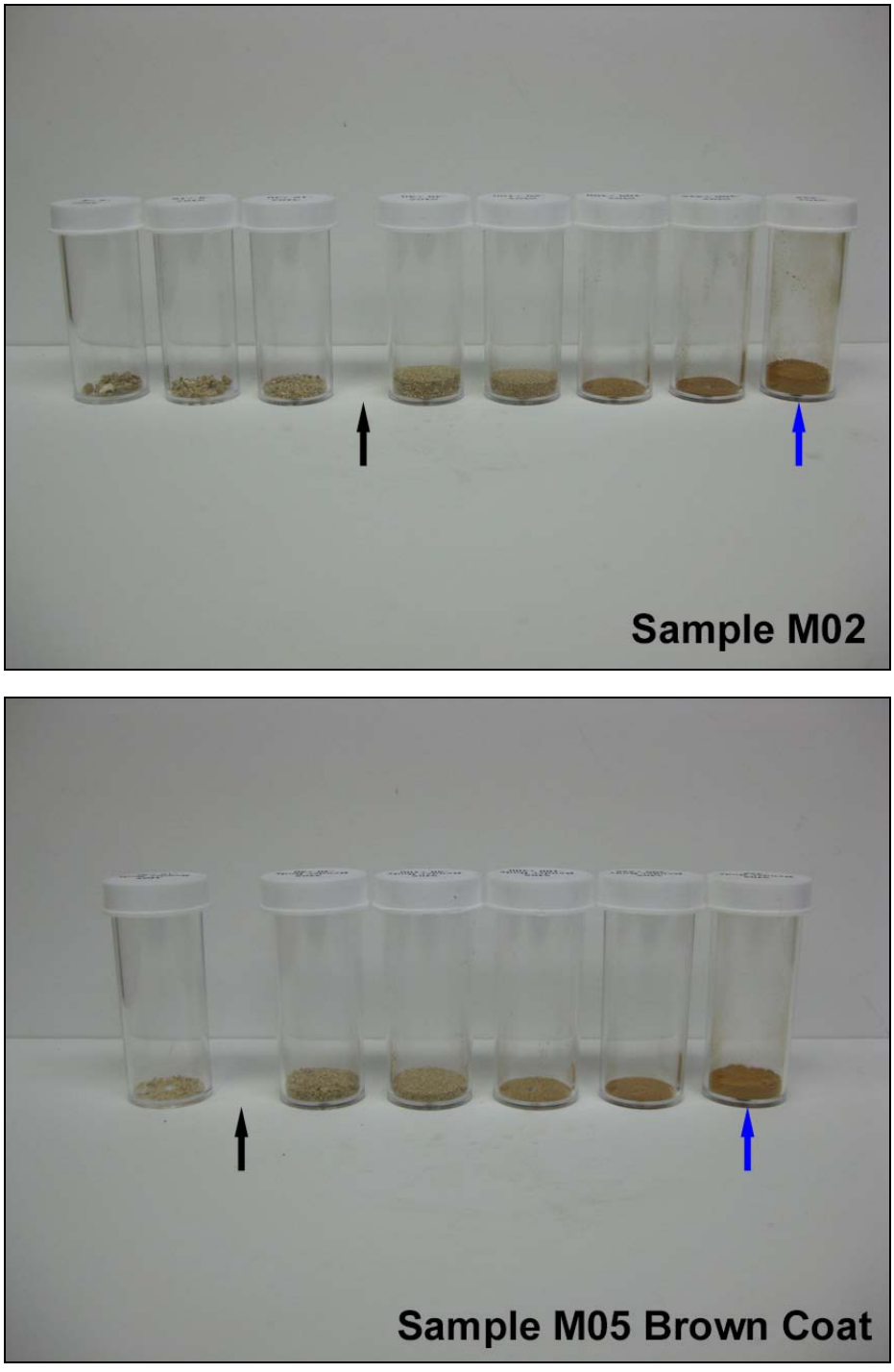


Figure 10: Photographs illustrating the beachrock and crushed brick materials extracted from Samples M02 and M05 after gradation through a standard sieve stack. The black arrows are located at the No. 30 sieve. Most material coarser than this is beachrock and material finer than this is crushed brick. As described for Samples M03a and M03b, any coarser brick fragments were not preserved in the process. The particle size distribution reflects the gradation of the brick temper rather than the crushed brick particles. In these two samples, these are nearly the same thing given the more complete disaggregation of the brick observed throughout the lime matrix. The blue arrows indicate the fine fired clays from the crushed brick.

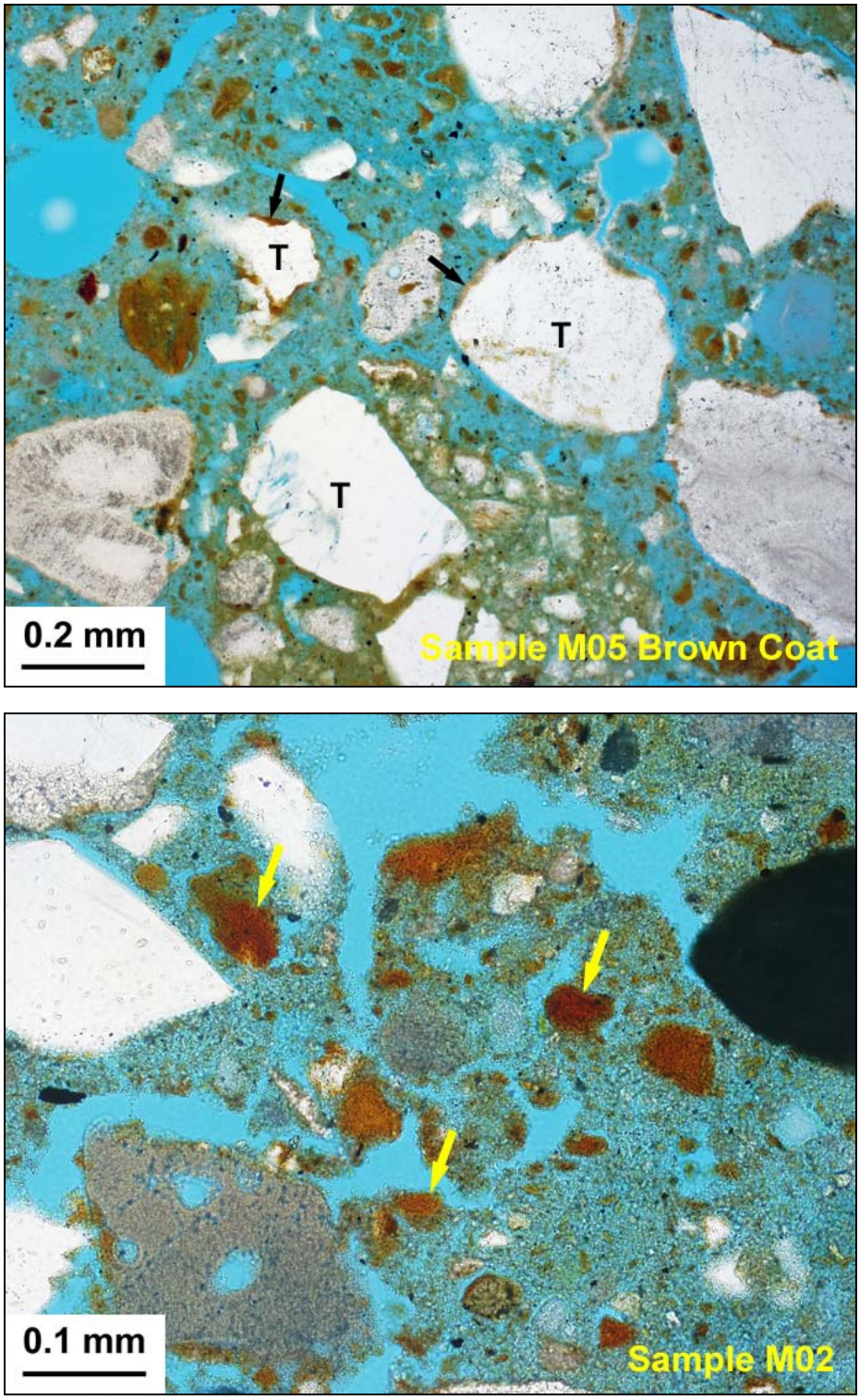


Figure 11: PPL photomicrographs illustrating the qualities of the crushed brick pozzolan in Samples M02 and the brown coat of Sample M05. (Upper image) Temper particles (T) are separated from the clay matrix but are not crushed. A thin lining of fired clay usually lines the temper particles (arrows) and this demonstrates that most of the sand was derived from the brick. The only other aggregate is the beachrock not shown here. (Lower image) The fired clay (arrows) is also present as distributed particulates and powder. These are found blended throughout the lime paste in both samples.

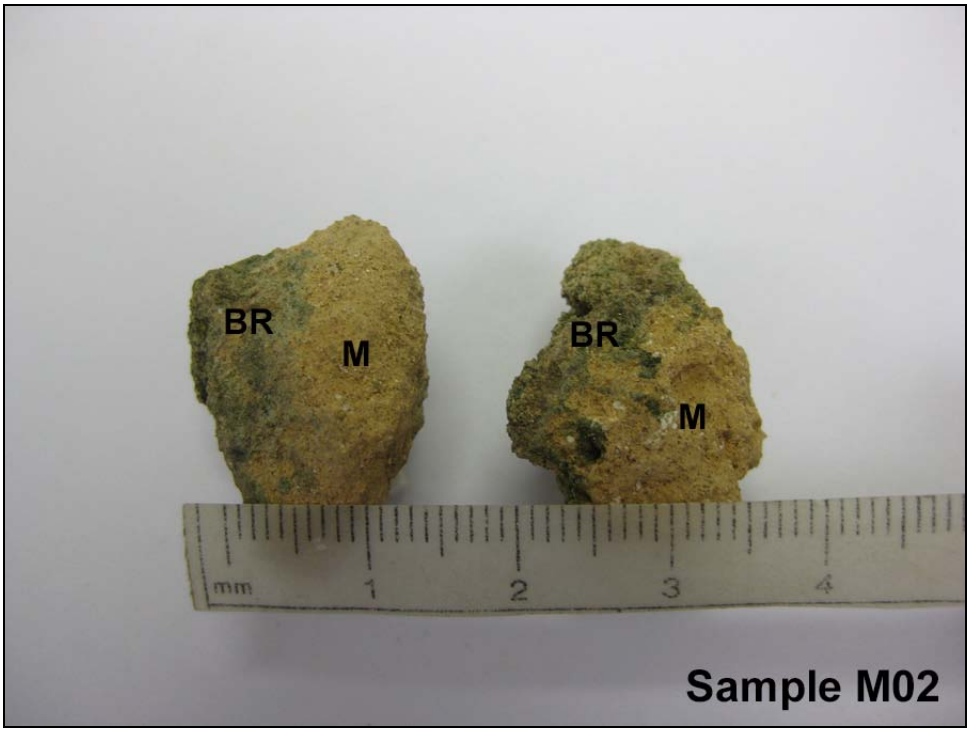


Figure 12: Close-up photograph of Sample M02. The numbered units on the scale bar are in centimeters. Note that some of the mortar (M) has relatively large fragments of beachrock adhered (BR). These are believed to be pieces of the masonry substrate. It is possible that some of the coarser sand-sized pieces of beachrock extracted from this mortar sample are actually pieces of the stone block rather than part of the aggregate. This would mean that the calculated sand might be somewhat overestimated.

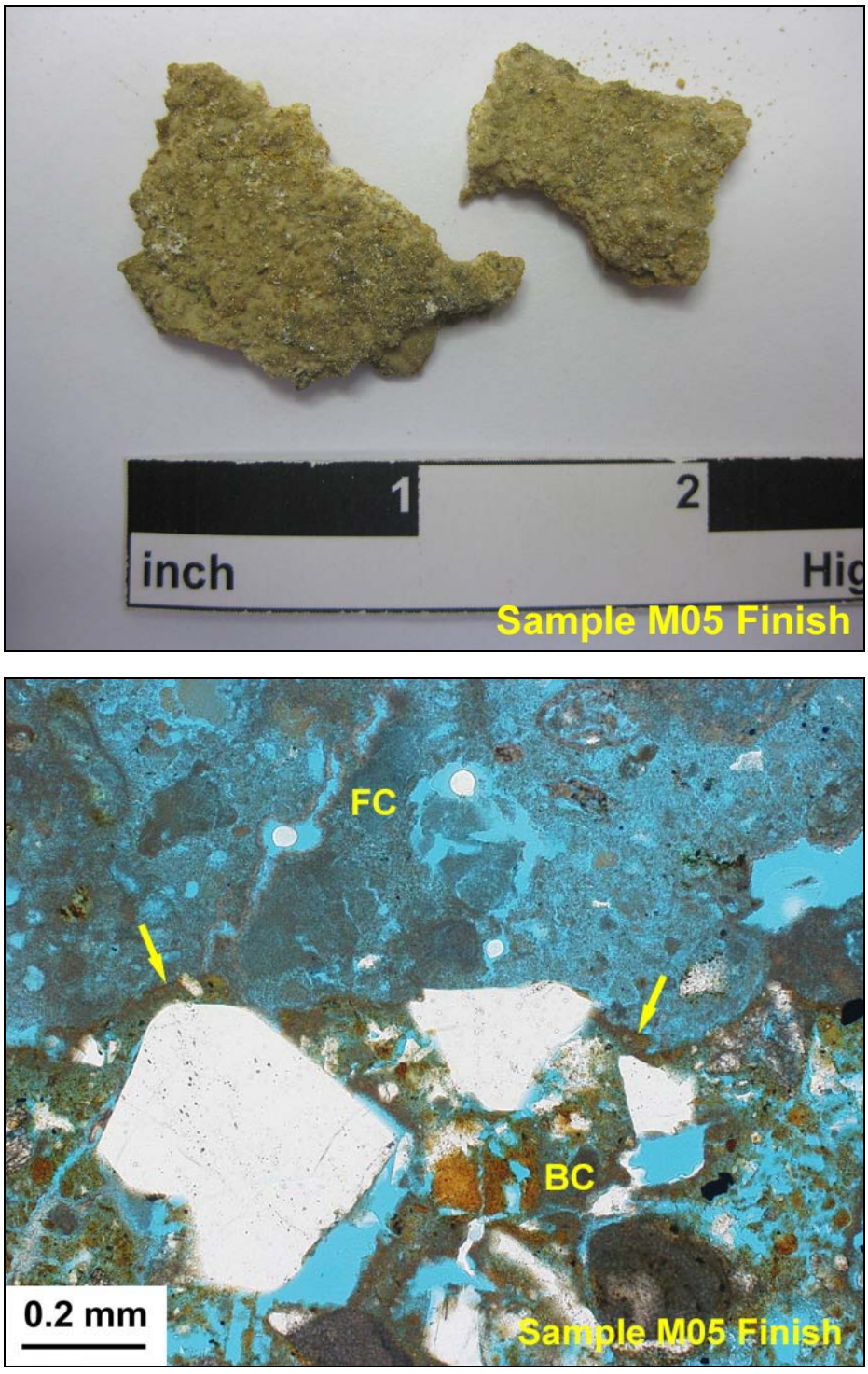


Figure 13: (Upper image) Sample M05 is an interior plaster that has a thin white finish coat. Two small piece of this finish are shown in this photograph. The yellowed color is caused by a continuous gypsum crust. (Lower PPL photomicrograph) The arrows indicate the contact surface between the finish coat (FC) and brown coat (BC). These surfaces are rare in the petrographic sample. However, the lack of any weathering or debris at the interface indicates that the two layers represent a contemporaneous placement.

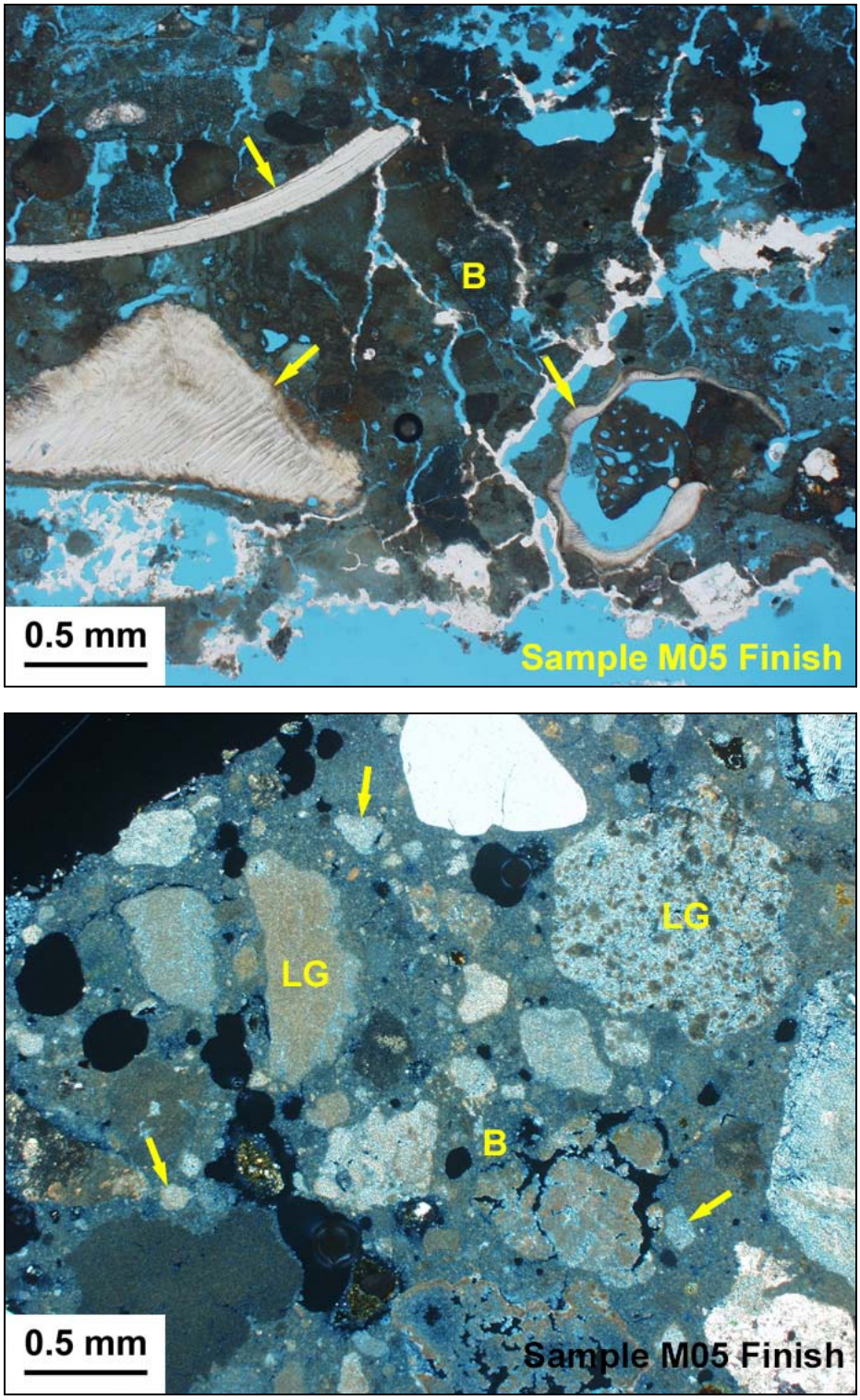


Figure 14: Photomicrographs illustrating the microtexture of the lime plaster finish coat in Sample M05. (Upper PPL image) The binder (B) strongly absorbs the low-viscosity, blue-dyed epoxy used in the sample preparation. This reflects the high microporosity typical of lime-based mixtures. The arrows indicate a variety of shell fragments or "bioclasts". These represent a sparse sand addition to the finish layer. (Lower XPL image) Undispersed lime grains (LG and arrows) are highly abundant and are found in a wide range of sizes. The bright colors indicate that the lime is fully carbonated. The adjacent binder (B) is similarly carbonated.

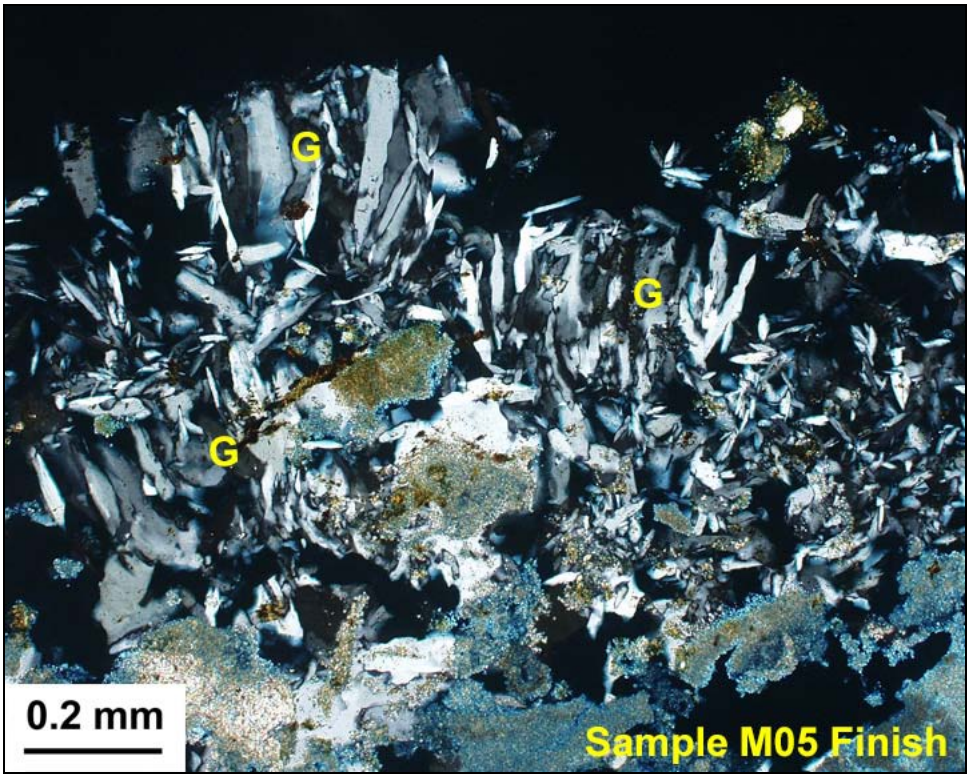


Figure 15: XPL photomicrograph of the finish coat in Sample M05. All of the finish layer pieces are coated with a crust of secondary gypsum (G). The crystals shown here are bladed and have grown perpendicularly to the wall surface.

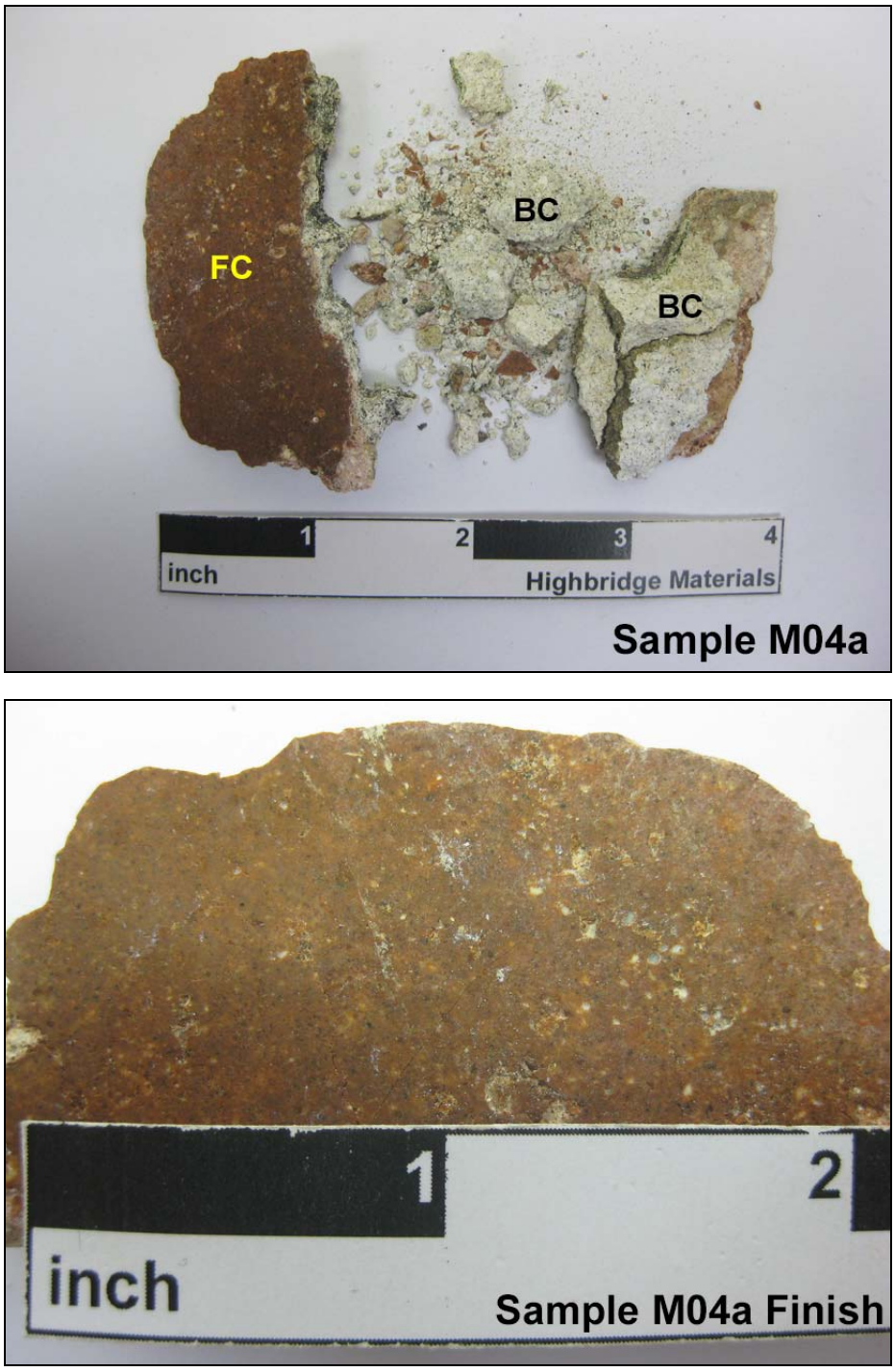


Figure 16: Sample M04a is an exterior render along a string course that contains a light-colored body coat (BC) and a dark red finish coat (FC). The entire sample is shown in the upper image. A close-up of the finish texture is shown in the lower image. Note that the surface is smooth, compact, and planar. If this type of finish were desired today, it would be created with a steel trowel. It is assumed that a similar process might have been used to create the historical finish. Whatever the case, floating of the fine brick dust toward the surface results in a darker color as well as a dense impermeable membrane.

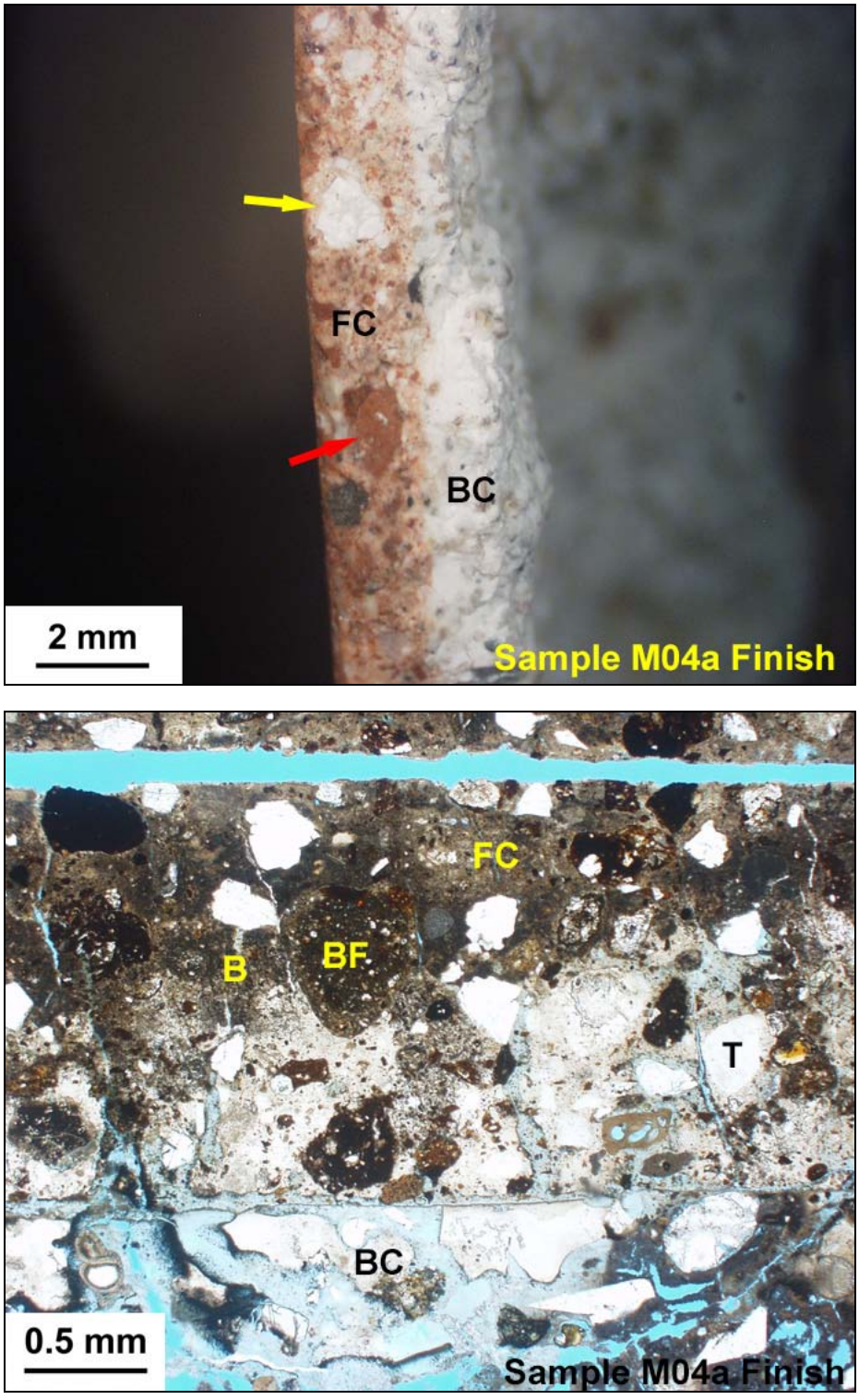


Figure 17: The finish coat of Sample M04a is shown in cross section in these two images. (Upper reflected light photomicrograph) The finish coat (FC) is lighter pink in cross section. Coarser particles of lime (yellow arrow) and crushed brick (red arrow) are visible. Brick fragments are not found in the body coat (BC). (Lower PPL photomicrograph) The finish coat (FC) is tabular in shape and shares a highly planar contact with the body coat (BC). The binder in the finish (B) has a low microporosity as indicated by the minimal absorption of blue-dyed epoxy used in the sample preparation. This has resulted from a highly effective pozzolanic reaction between the lime and the crushed brick. Though the layer has a particulate texture, there is no separate sand addition. Distributed quartz and feldspar particles are actually temper grains (T) derived from the crushed brick. Fine-textured brick fragments are also observed (BF).

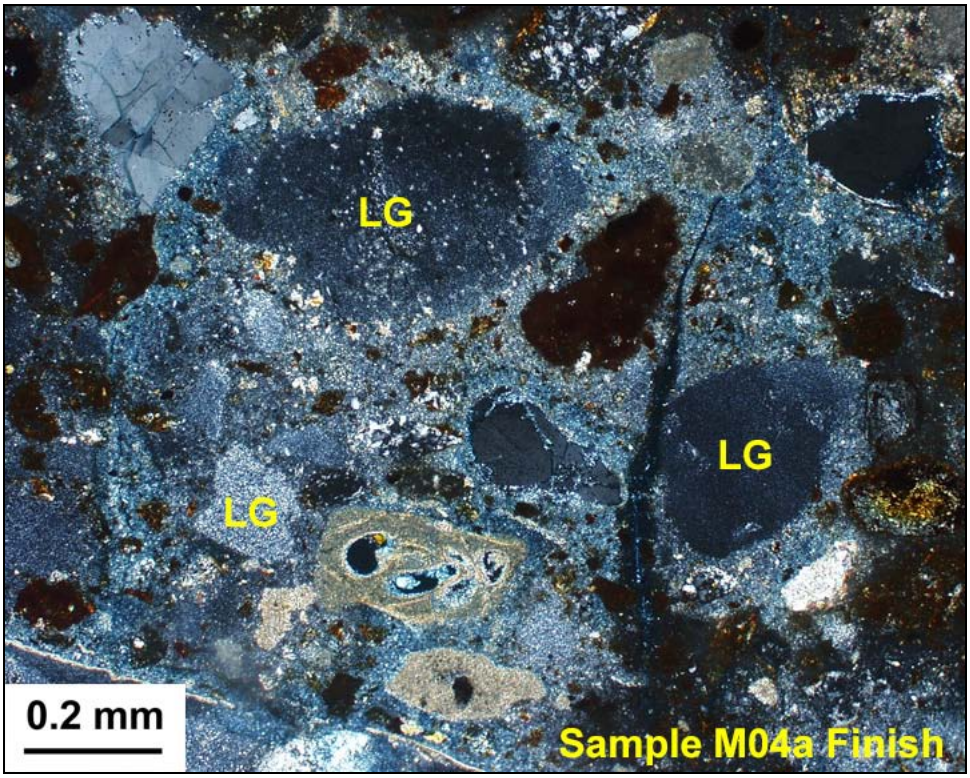


Figure 18: XPL photomicrograph of the finish coat in Sample M04a. Undispersed lime grains (LG) are evident throughout the layer. The darker color under crossed polars indicates that the lime is uncarbonated as is the adjacent matrix. The inhibition of carbonation is attributed to the densifying effect of the pozzolanic reaction. The finish layer is an effective barrier to external agents including carbon dioxide.

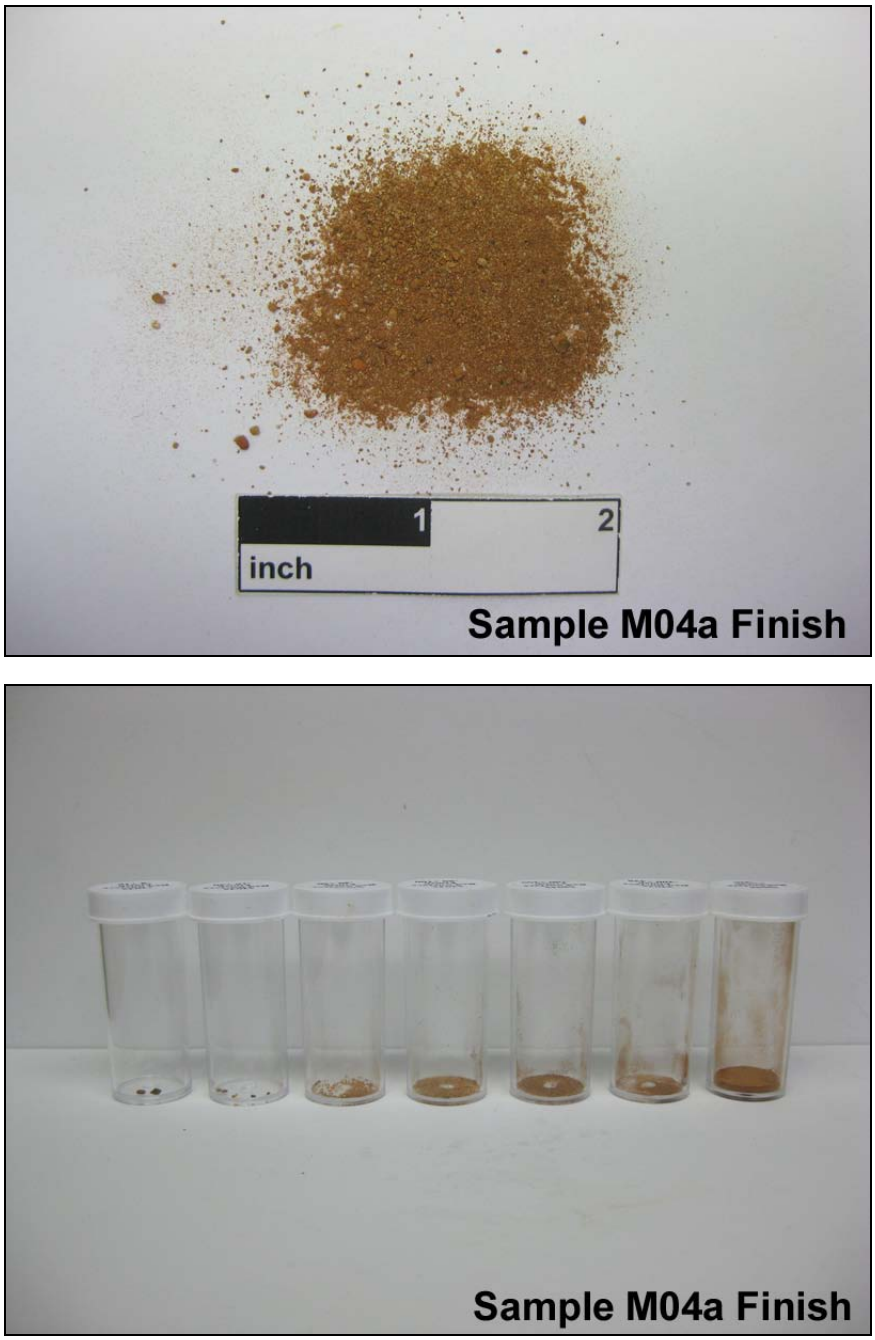


Figure 19: Photographs of the insoluble materials extracted from the finish coat of Sample M04a through acid digestion. (Upper image) The granules and powder extracted from the finish consist solely of broken and crushed brick materials different than those observed in other samples. (Lower image) The same material is shown after gradation through the standard sieve stack used for masonry aggregates. Though there are sand-sized particles in the crushed pozzolan, the majority of the material is a fine powder.

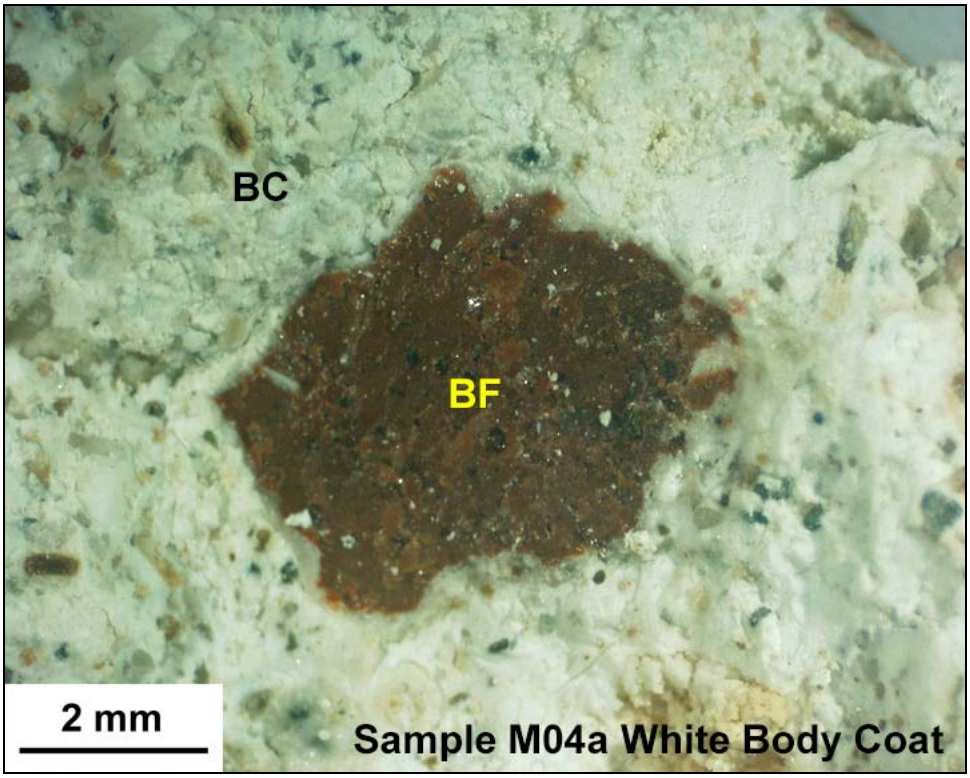


Figure 20: In Sample M04a, a larger brick fragment (BF) was detected in the body coat (BC). It is assumed that this represents the same type of masonry unit used for the brick dust in the finish coat. Note that this brick has a compact, glassy texture and a darker red color. This appearance is much different than the more orange-toned sandy brick found in Samples M02, M03a, M03b, and M05. The brick in the finish coat is clearly a higher-fired product.

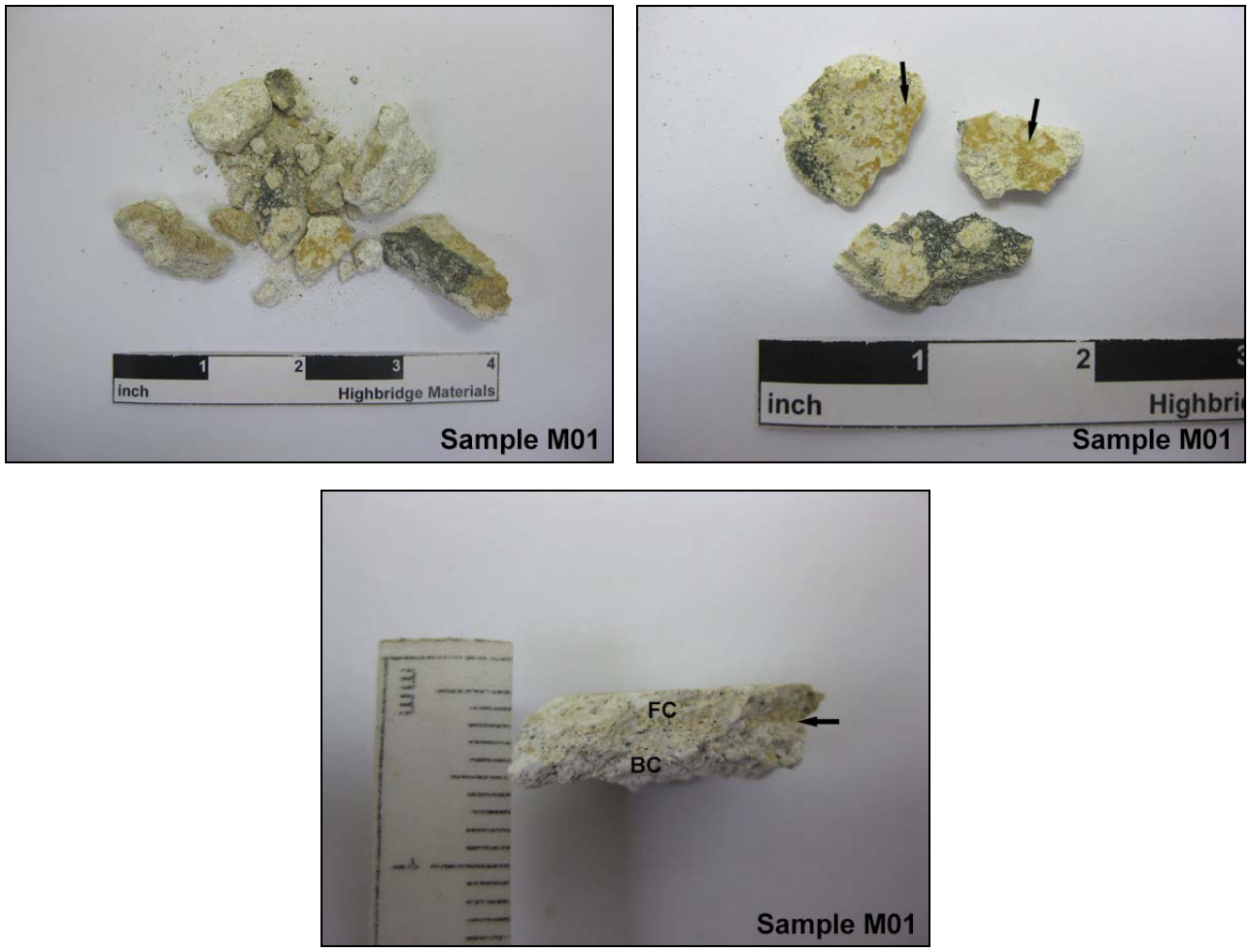


Figure 21: These photographs depict Sample M01 representing the exterior render. This is one of the lime-pozzolan mortars containing a volcanic ash. The entire sample is shown in the upper image. At lower left, the arrows indicate the ochre-colored wash on the presentation face of the render. The render sample is shown in cross section in the lower right image. The arrow indicates the planar boundary between the body coat (BC) and the finish coat (FC). Note that the finish coat is pigmented a pale yellow color.

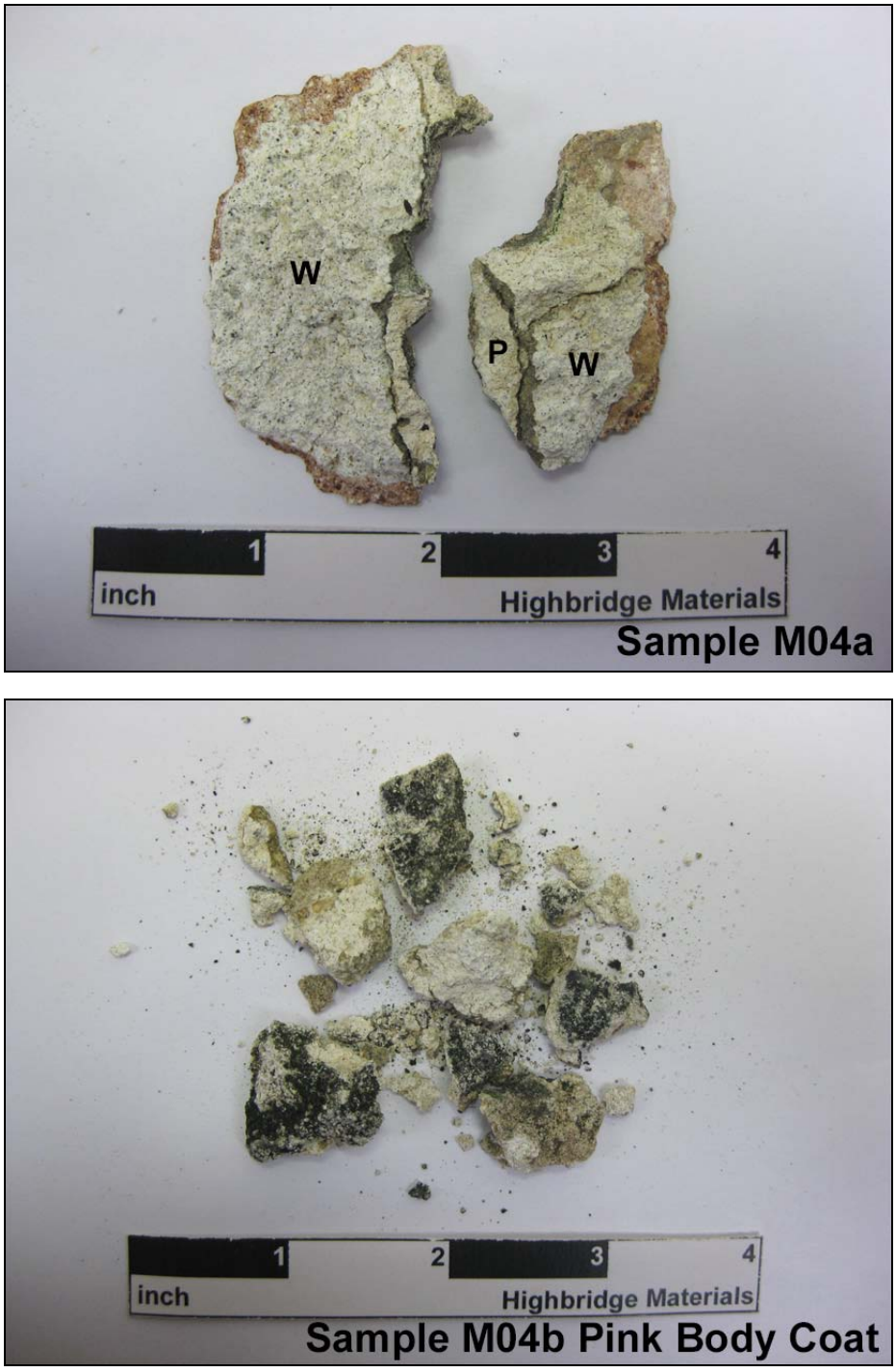


Figure 22: Samples labeled M04 also contain lime-ash mixtures. Sample M04a (upper image) contains a body coat below the red finish layer. The sample is shown from its rear side in this photograph. Some areas are white (W) while others are pink (P). The pink color is attributed to carbonation rather than to a material difference. Sample M04b is fully carbonated and appears more similar to the pink areas of Sample M04a. Sample M04b is shown in the lower image.

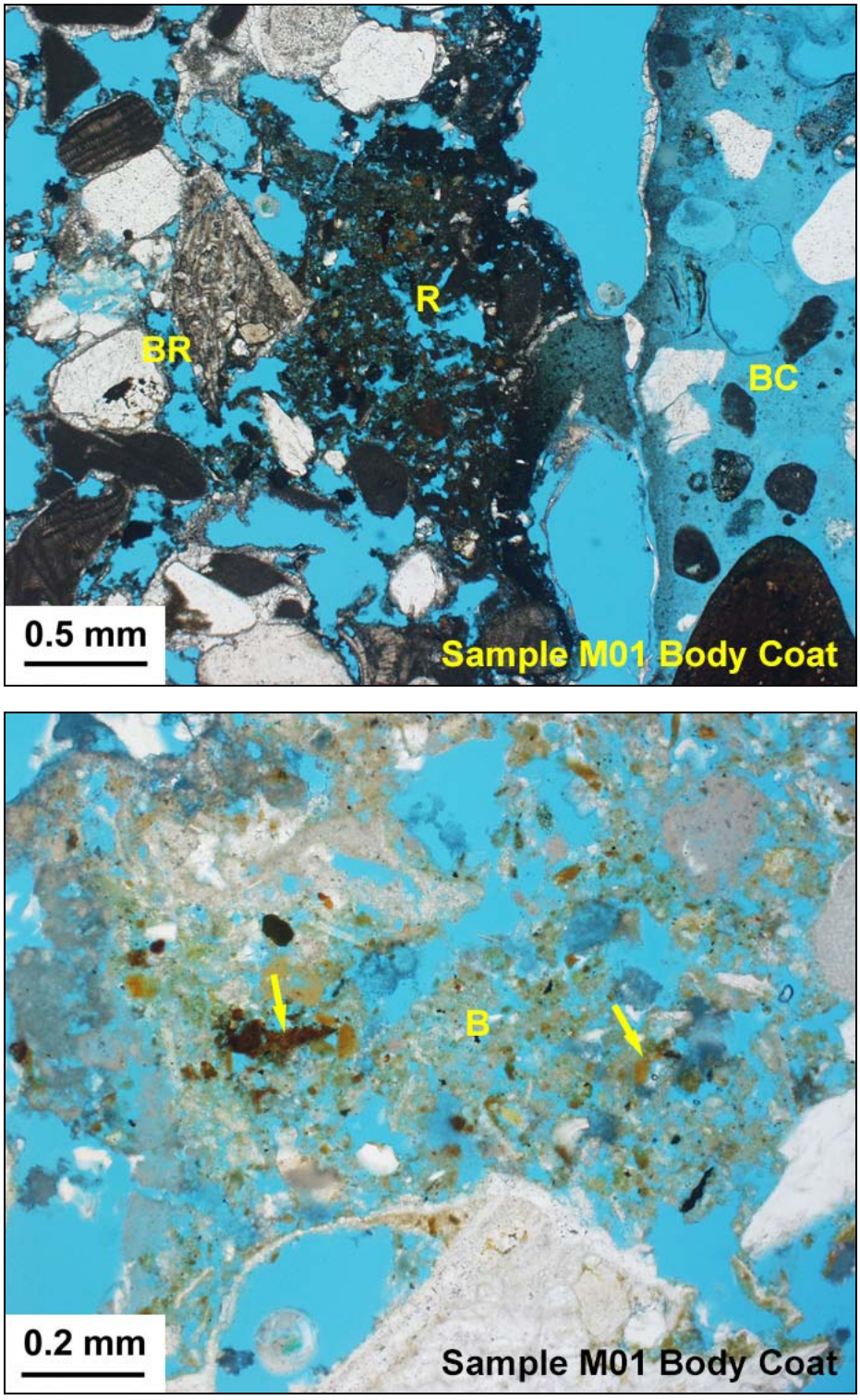


Figure 23: PPL photomicrographs of Sample M01. There is some evidence to suggest that the white render material is not original to the construction. In the upper image, a residue of a different lime-based mixture (R) is identified within the irregular surface embayments of the beachrock (BR) assumed to represent fragments of the underlying masonry substrate. The white body coat (BC) directly overlies this residue. A higher magnification image of the residue is shown in the lower image. The binder (B) is a lime-based matrix. Finely crushed brick dust (arrows) is distributed throughout the lime paste. The residue material appears similar to the lime-brick mixtures identified in Samples M02, M03a, M03b, and the brown coat of M05.

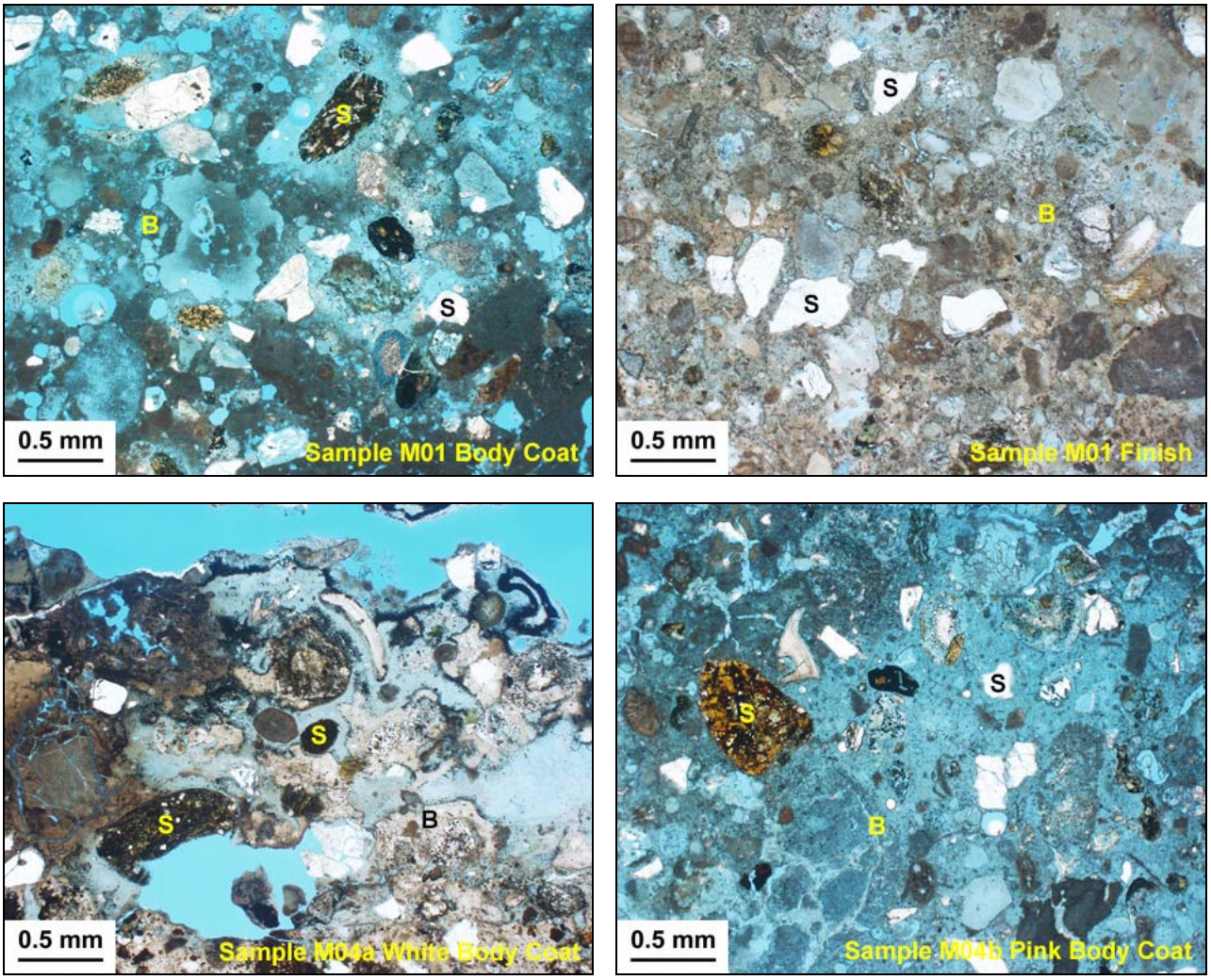


Figure 24: PPL photomicrographs illustrating the microtexture of the lime-pozzolan render mixtures. All of the samples contain a fine-grained sand (S) consisting of volcanic rock grains, bioclasts, and quartz. The sand is sparsely distributed throughout the matrix indicating low sand contents for all samples. The samples are all impregnated with a low-viscosity, blue-dyed epoxy to highlight pore structure. Note that there are different degrees of absorption of this epoxy within the binder in each sample (B). For Sample M04, the pink body coat has a higher capillary porosity likely to be more similar to that of the original material before appreciable pozzolanic reactions had occurred. In contrast, the white layer exhibits a more advanced pozzolanic reaction and contains dense patches of binder that absorb little of the epoxy. Sample M01 tends to be closer in texture to the pink body coat of Sample M04 but there may be a gradient from the finish layer inward in this sample.

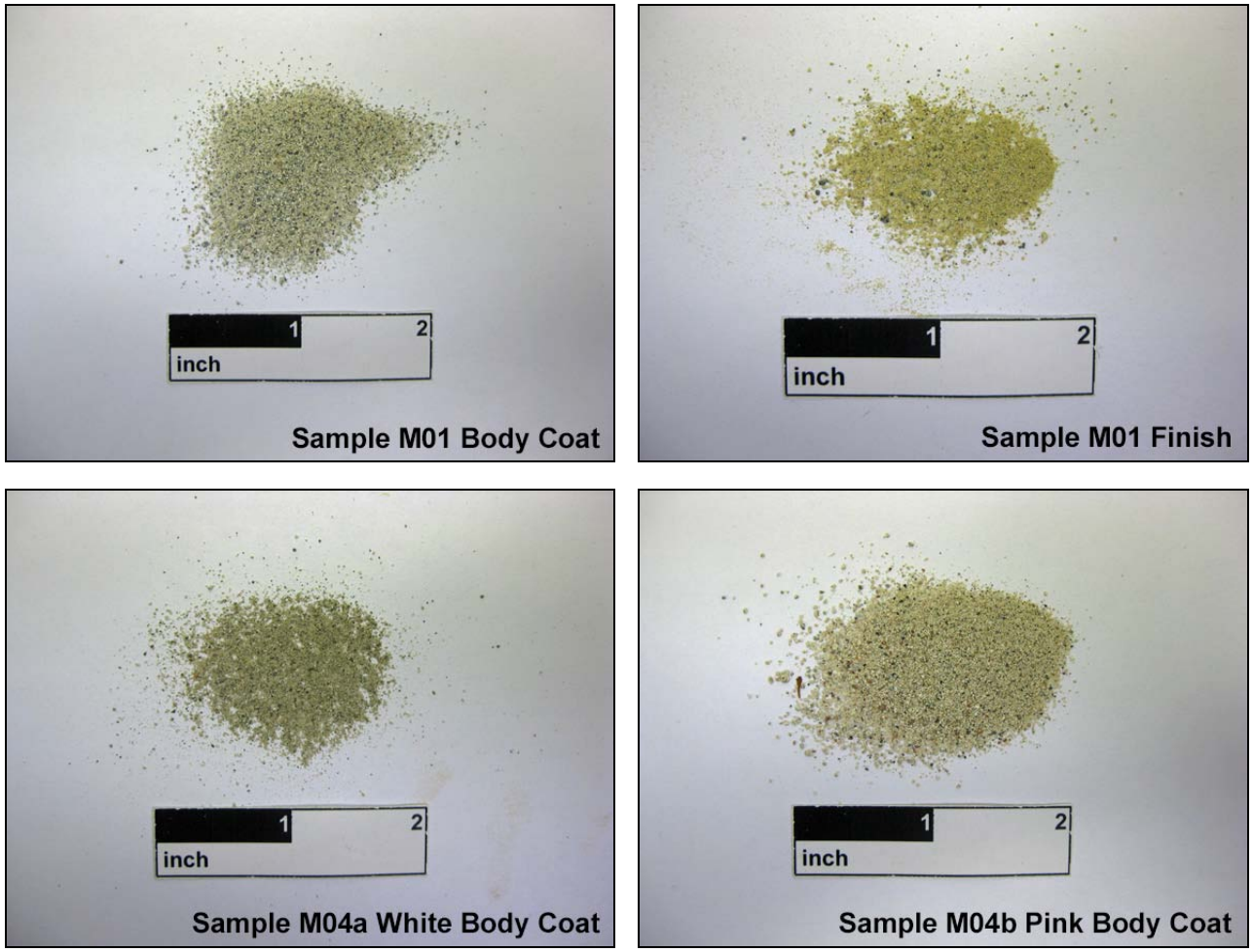


Figure 25: Photographs of the aggregate extracted from the lime-pozzolan samples. The fine-grained sands all have a buff color with a "salt-and-pepper" quality. The finish in Sample M01 is pigmented and the extracted material includes the yellow pigment in addition to the natural sand.

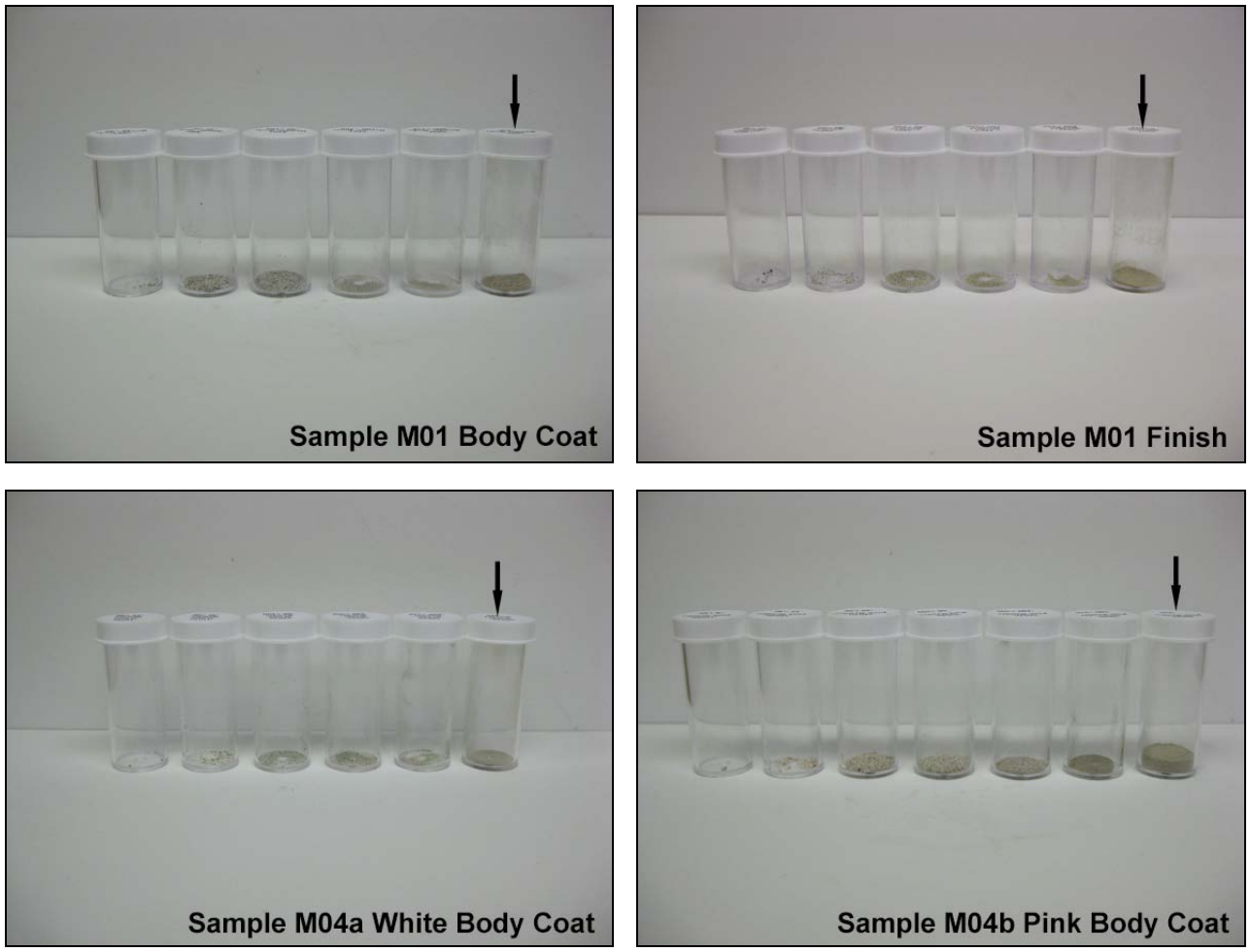


Figure 26: Photographs of the sand extracted from the lime-pozzolan samples after gradation through a standard sieve stack. Most material passes a No. 30 sieve for the four sample layers. It was not always possible to extract a significant amount of material from the renders. Nonetheless, all samples have a "tail" at the fine end of the gradation (arrows). This interval contains a mixture of silt, clay, and volcanic glass.

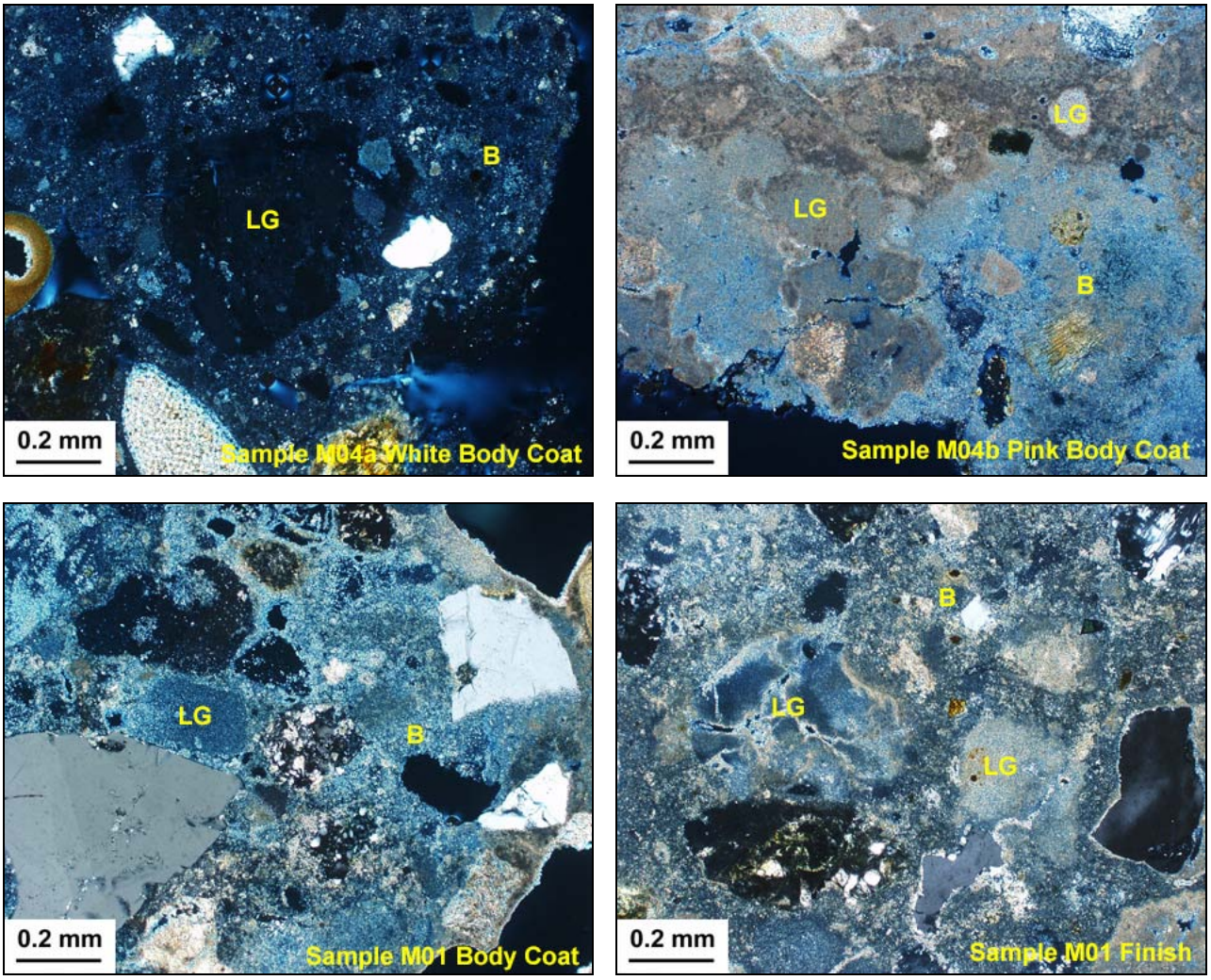


Figure 27: XPL photomicrographs illustrating the qualities of the lime binder in the lime-pozzolan render mixtures. In all images, undispersed lime grains (LG) are shown embedded within a lime-based binder (B). The color differences under crossed polars is indicative of varying levels of carbonation. The white body coat in Sample M04a is dark under crossed polars indicating an absence of any appreciable carbonation (upper left). In contrast, the pinker layer (upper right) has a bright golden color indicative of the presence of ultrafine-grained carbonate crystallites. Individual crystals are too fine to resolve at the light microscope. Sample M01 exhibits a more mottled pattern under crossed polars indicating that carbonation is present but not as well developed.

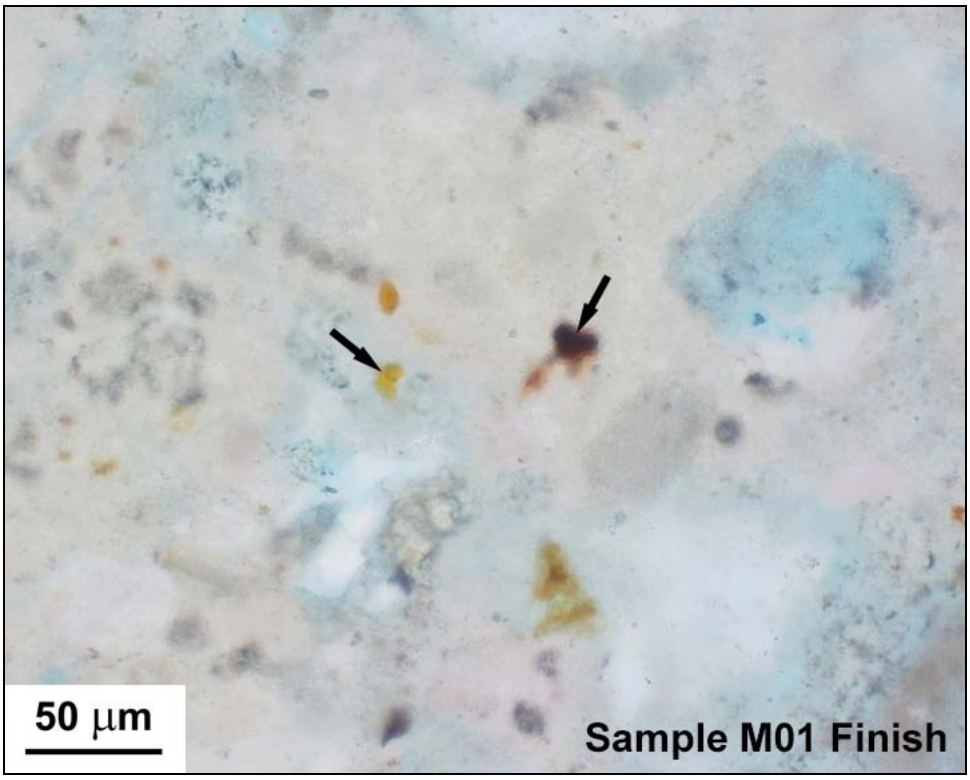


Figure 28: PPL photomicrograph of the finish coat in Sample M01 taken with a condenser lens inserted into the light path. The condenser allows finer particles to be viewed while sacrificing image sharpness. The arrows indicate fine pigment particles present in the finish coat but not identified in the body coat. The sparseness of the particulates is indicative of a relatively low dosage.

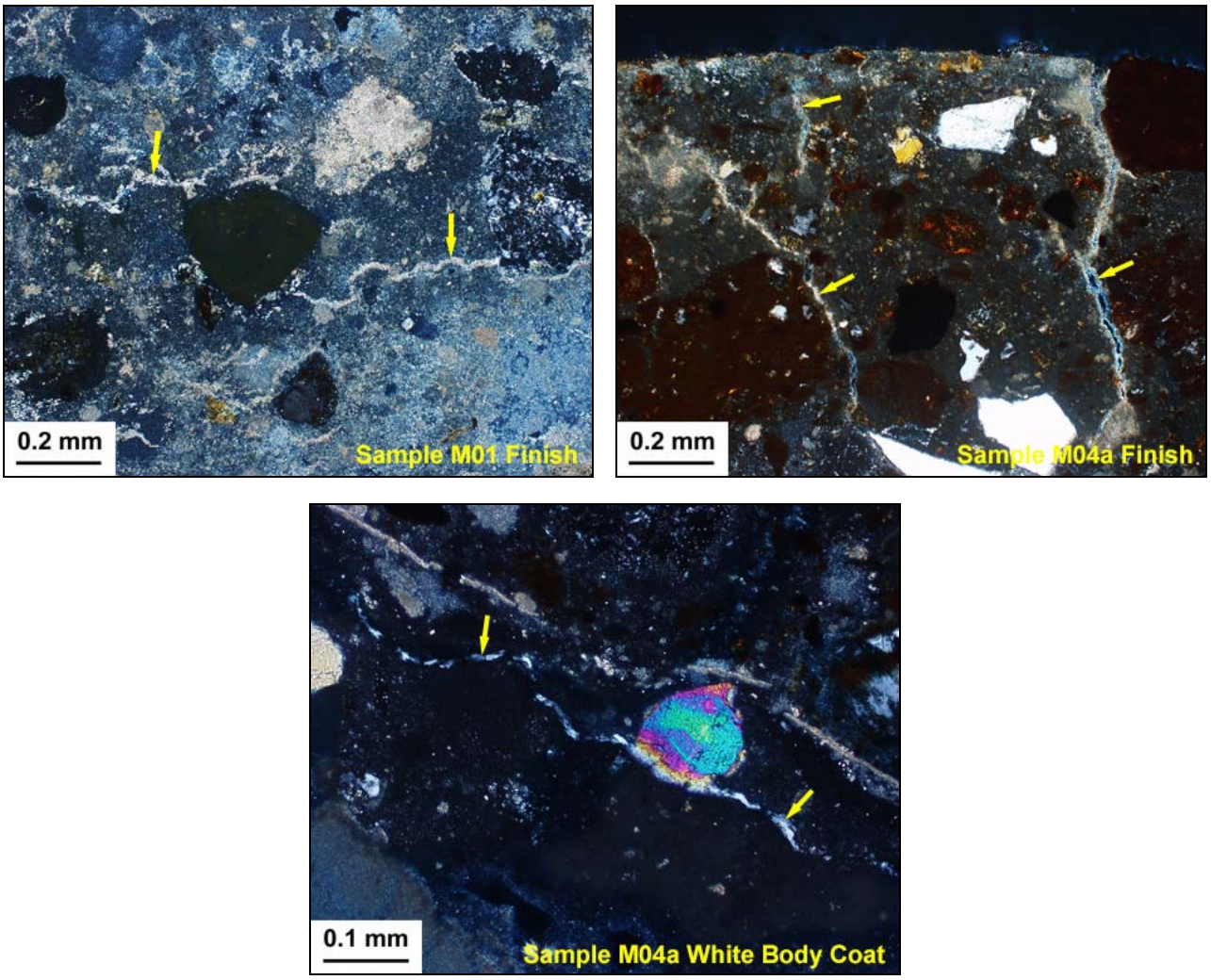


Figure 29: XPL photomicrographs illustrating the occurrence of microcracks in some of the lime-pozzolan render samples. In the upper two images, the arrows indicate microcracks that transect the finish coats in M01 and M04a. These are both lined with secondary calcium carbonate. In the body coat of M04a (lower image), there are microcracks that are surface-parallel and lined with sulfate phases as shown by the arrows.

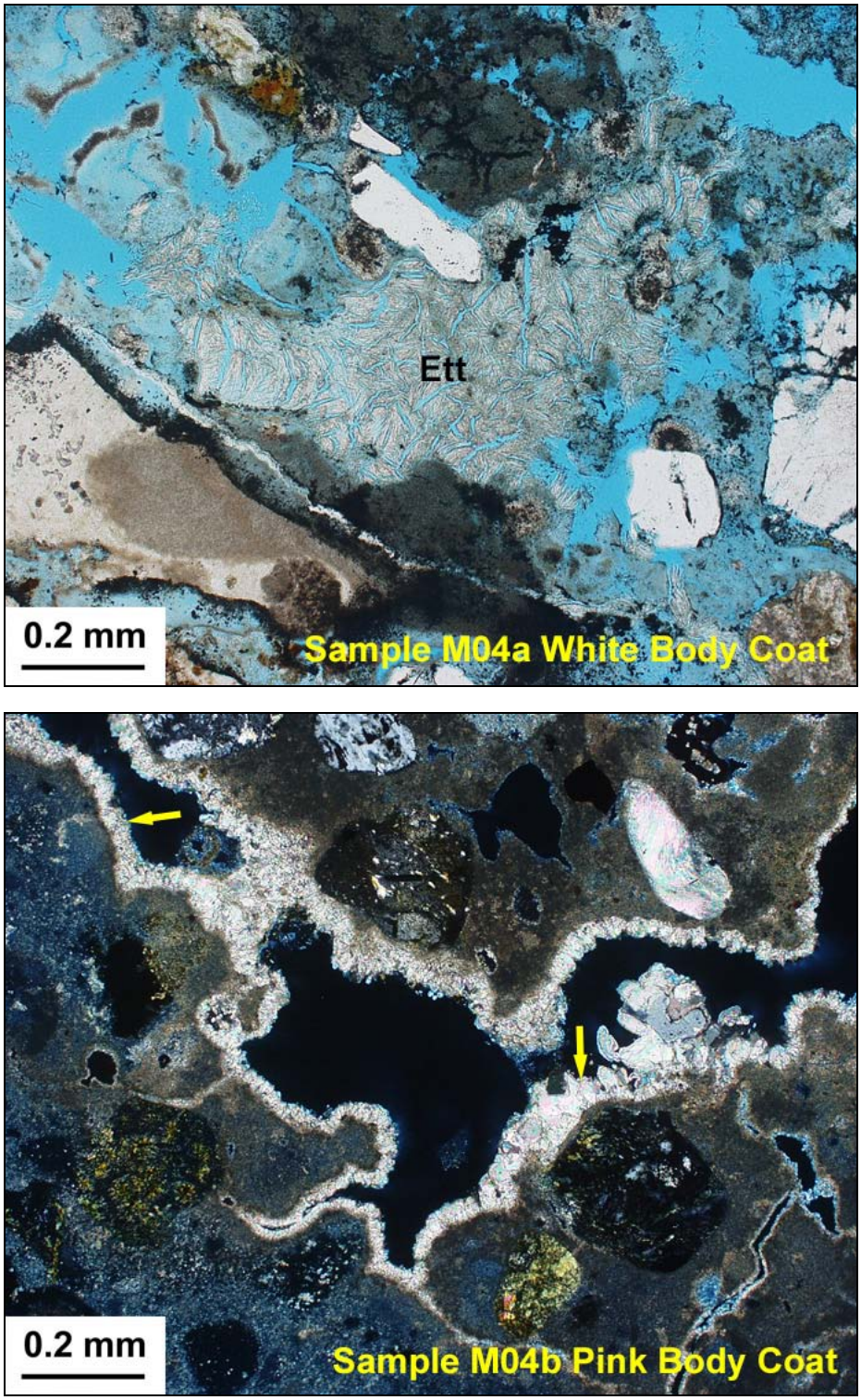


Figure 30: Some minor secondary mineralizations are also identified in the voids of some of the lime-pozzolan mixes. Ettringite (Ett) is found in the uncarbonated body coat of Sample M04a (upper PPL image). In the carbonated layer of this same sample, air-voids are often lined with sparry calcite deposits (arrows in the lower XPL image).

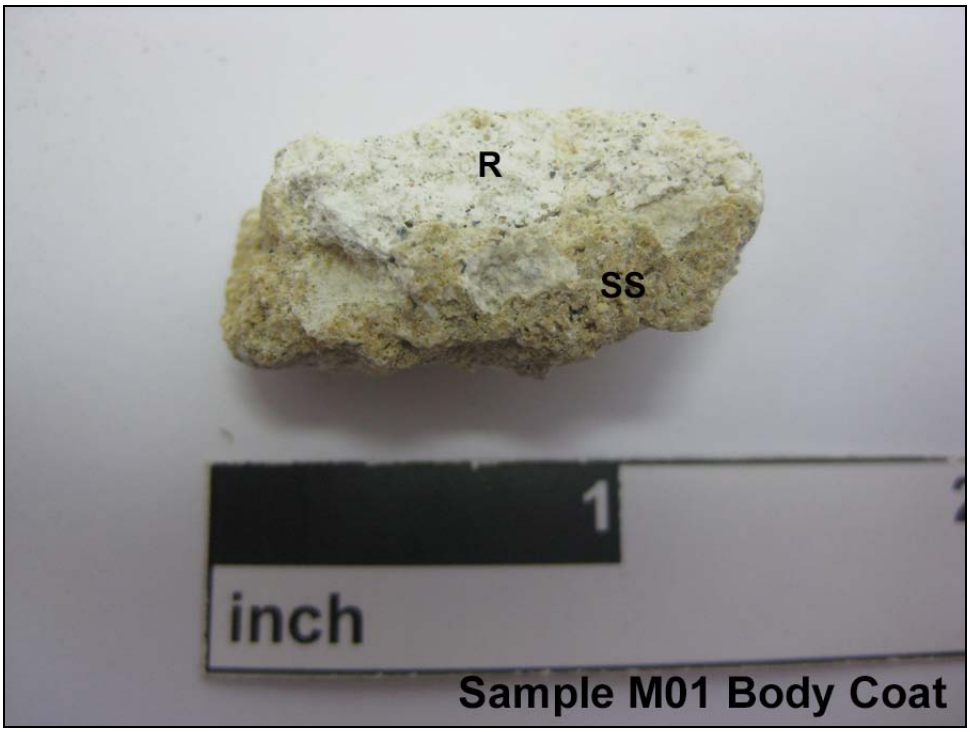


Figure 31: This close-up of a fragment of Sample M01 illustrates a small portion of sandstone (SS) adhered to the white render body (R). The sandstone has an orange hue and a granular appearance. This material matches the description of the substrate masonry as provided by the client.

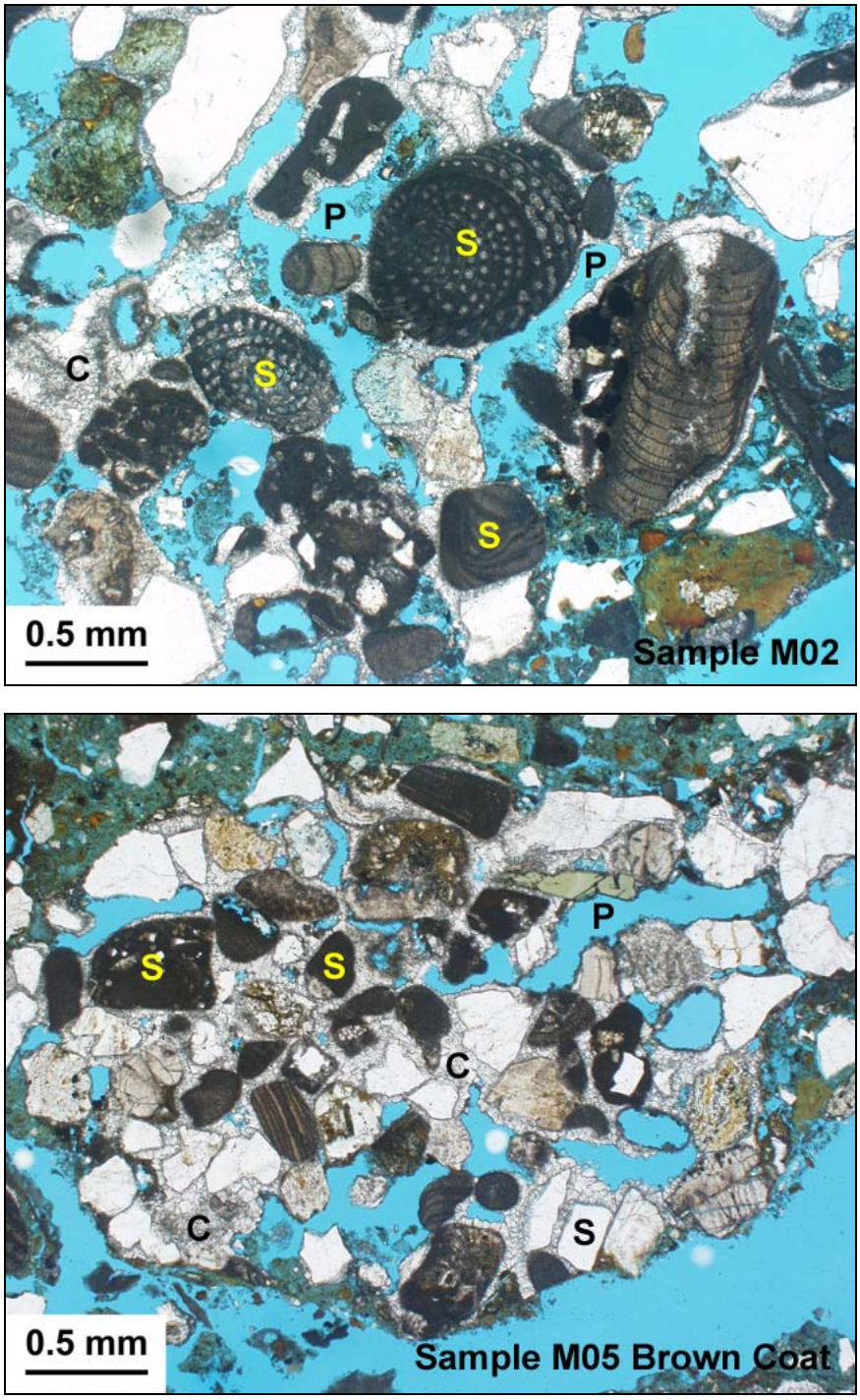


Figure 32: The sandstone is identified as a beachrock. This is essentially an in situ deposit of beach sand that has become cemented in place. These PPL photomicrographs illustrate the beachrock texture. Rounded sand grains (S) are closely packed within the stone. The grains are typically uniform within any one particular area through there is some variation between different fragments. For example, the sand in the beachrock of Sample M02 is coarser than that in M05. The sand is cemented together with a precipitate of sparry calcite (C). The cementation tends to be more complete in beachrock having finer sand grains. Open interstitial pores remain (P) where the cementation is not complete. Most of the pores are likely to be interconnected and this would result in a measurable permeability.

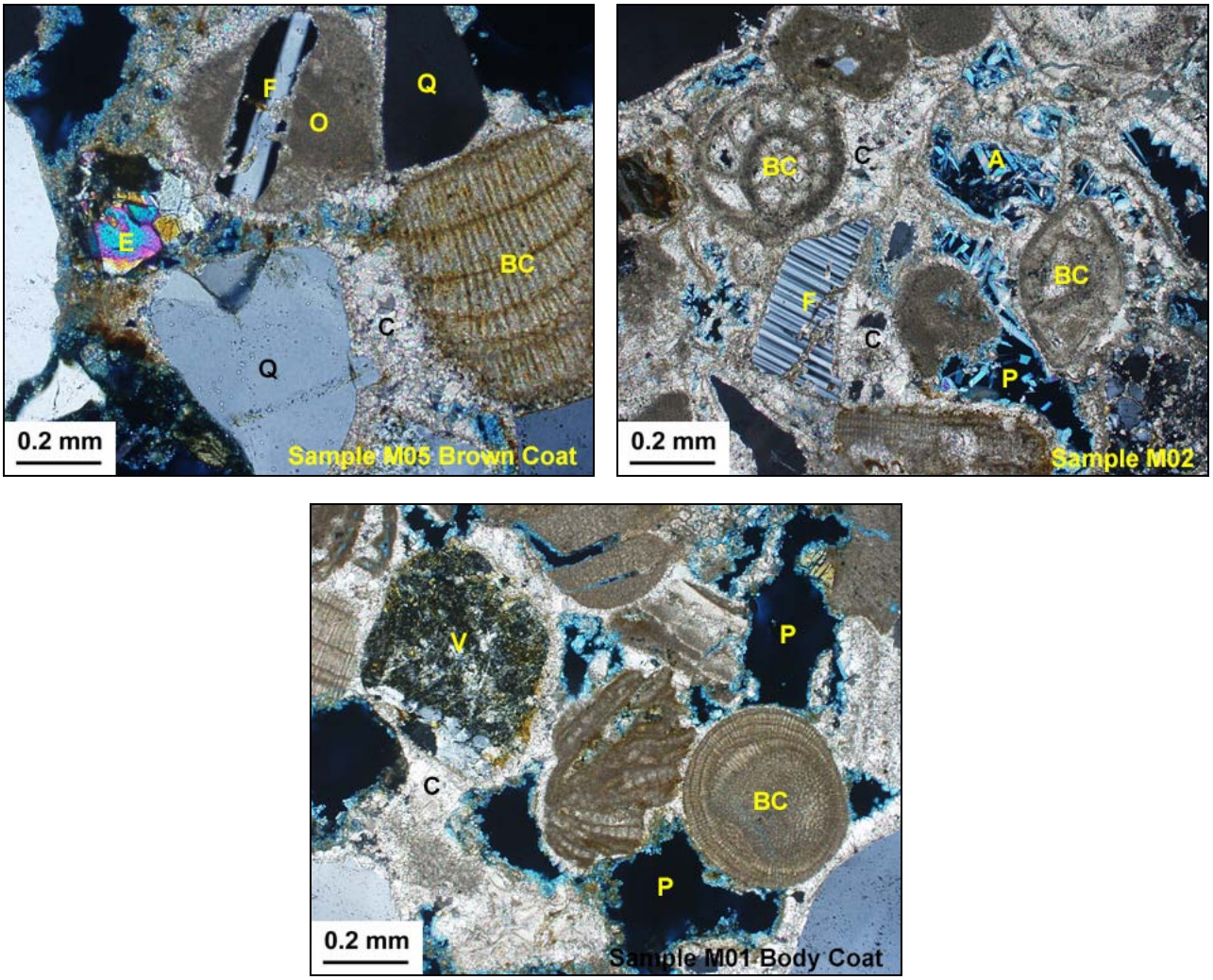


Figure 33: XPL photomicrographs illustrating the types of sand grains identified in the beachrock. (Upper left) Bioclasts (BC) and quartz (Q) are both common and represent the majority of the particles. Epidotite (E) is a relatively minor inclusion in most of the beachrock and probably represents an alteration phase of other volcanic rocks. Oolitic grains are minor grain types noted in this particular sample (O). This oolite has a nucleus of detrital feldspar (F). (Upper right) The bioclasts (BC) generally have rounded shapes due to abrasion in the sedimentary environment. An unweathered feldspar (F) is also shown for this sample. (Lower image) Volcanic rock particles (V) are a trace constituent along with a variety of other rock types. In each of the images shown, the sand grains are bound by calcite cement (C). In some places, this cement completely fills all original interstitial space between sand particles. However, the cement can be thinner in locations as shown in the lower image. Wherever cement has not completely filled the free space, an original pore is left behind (P). These are typically empty though a rare occurrence of secondary aragonite (A) is shown for Sample M02.

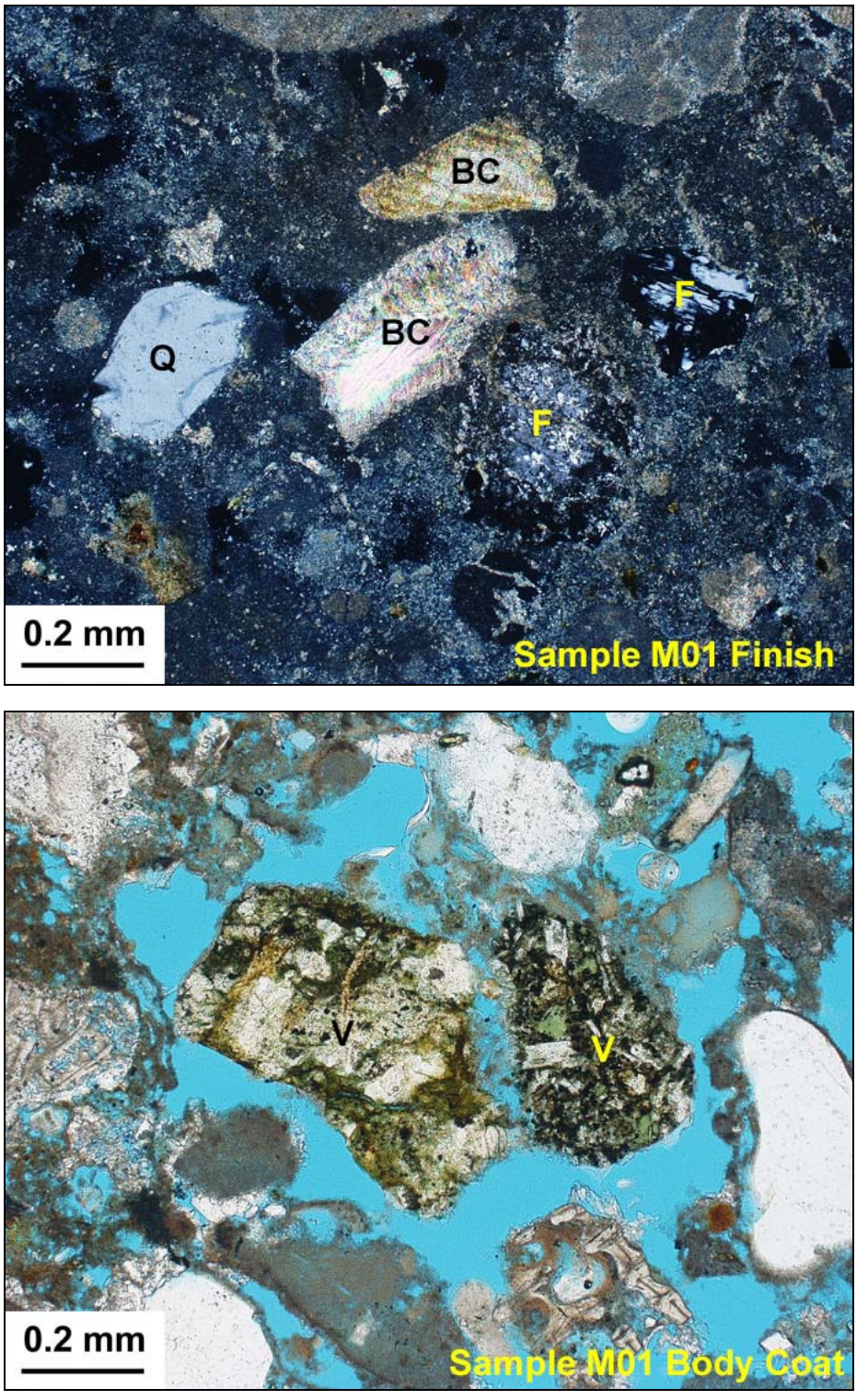


Figure 34: Photomicrographs illustrating the composition of the natural sand in Sample M01. (Upper XPL image) Bioclasts (BC) and quartz (Q) are major constituents of the sand. Feldspar (F) is a common component of volcanic rocks that are also abundant. In this image, the feldspars are corroded due to secondary geological alteration. (Lower PPL image) Two volcanic grains are shown (V). The volcanics all appear to be andesitic in composition. This would be consistent with much of the local geology.

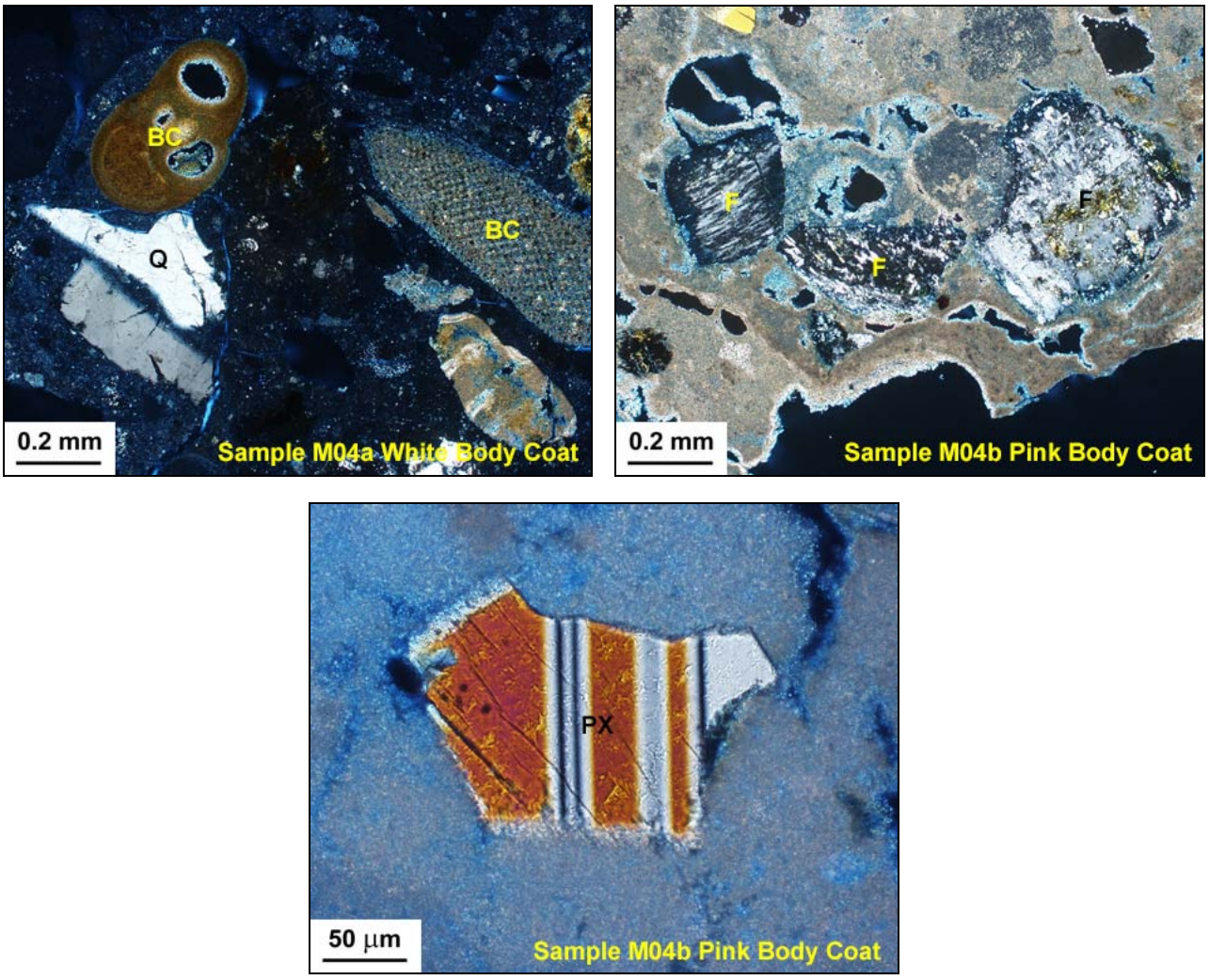


Figure 35: XPL photomicrographs. The sand in Sample M04a and M04b is generally similar to that in Sample M01. As shown in the upper two images, bioclasts (BC), quartz (Q), and corroded feldspar (F) are all identified. However, volcanically derived clinopyroxene (PX) is identified in these samples but not in M01 (lower image).

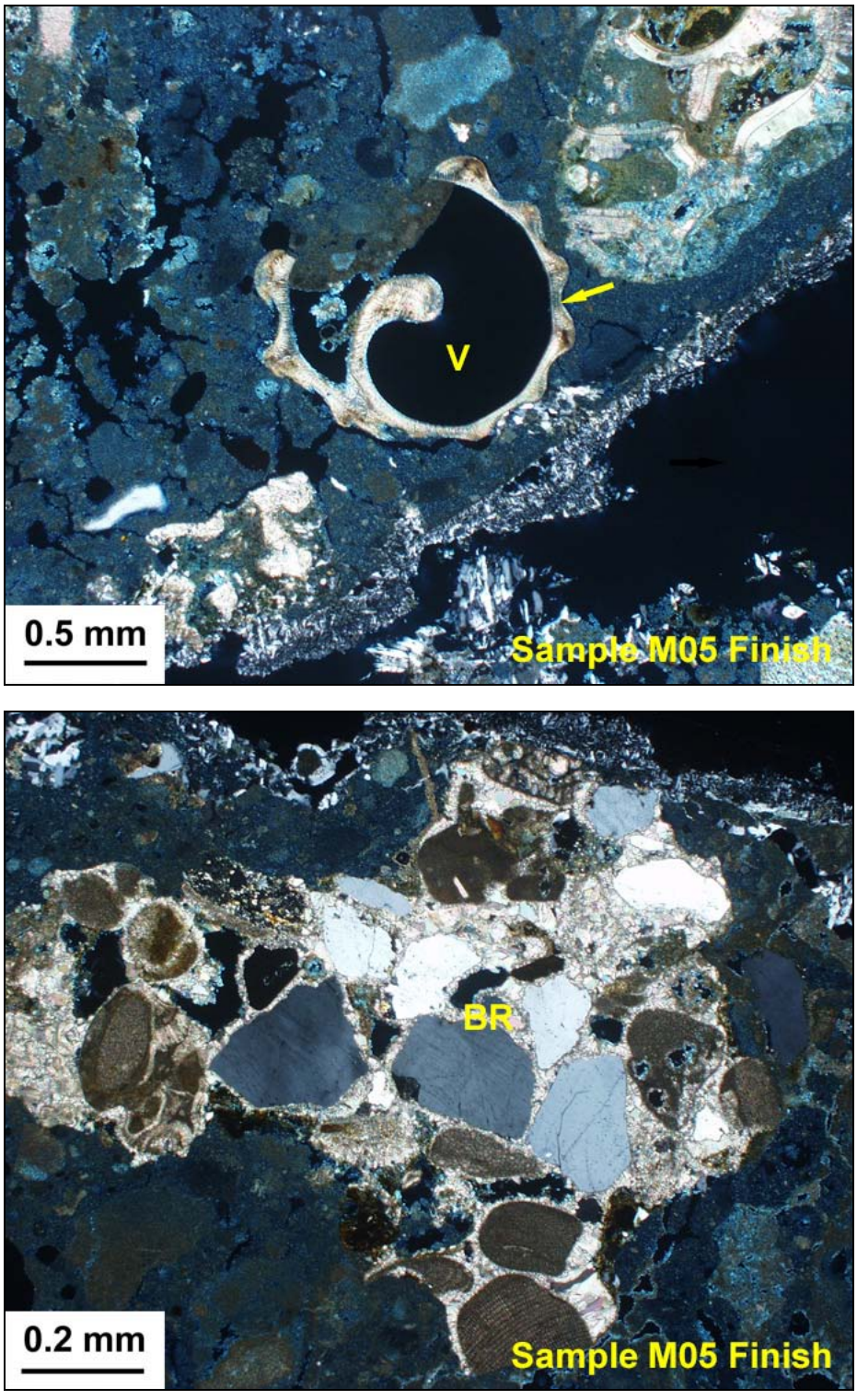
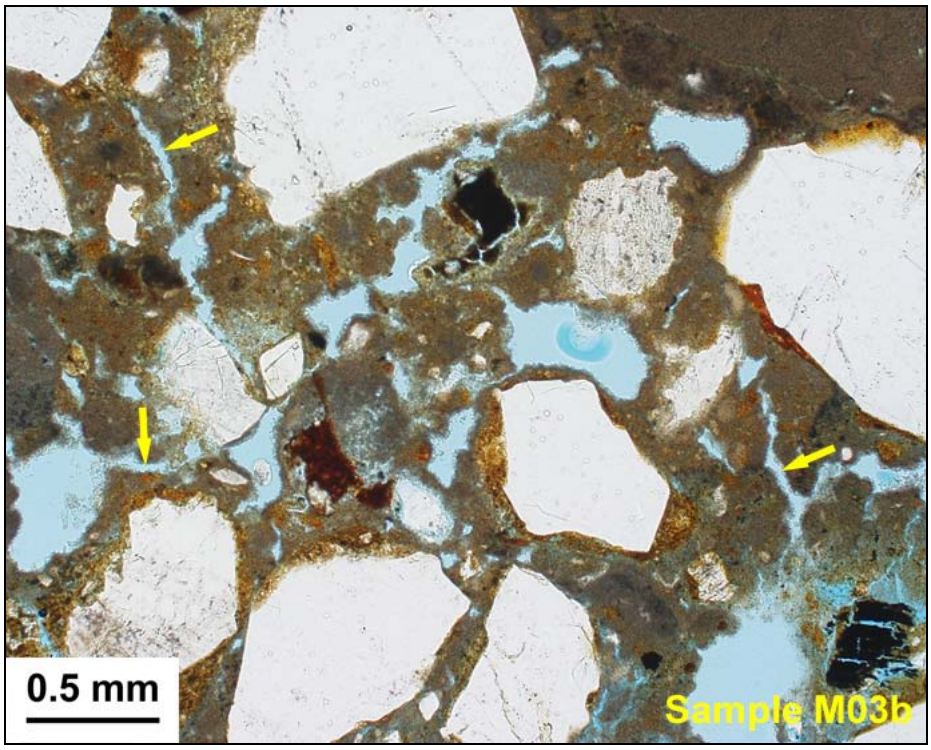


Figure 36: XPL photomicrographs illustrating the aggregate components in the lime finish plaster of Sample M05. (Upper image) Most of the sparse sand consists of broken shells (arrow). Most of these have internal void spaces (V) that remain unfilled by binder. (Lower image) Beachrock grains (BR) are also identified in the finish coat but these are much less abundant. Quartz grains are also a minor component though these are not depicted here.



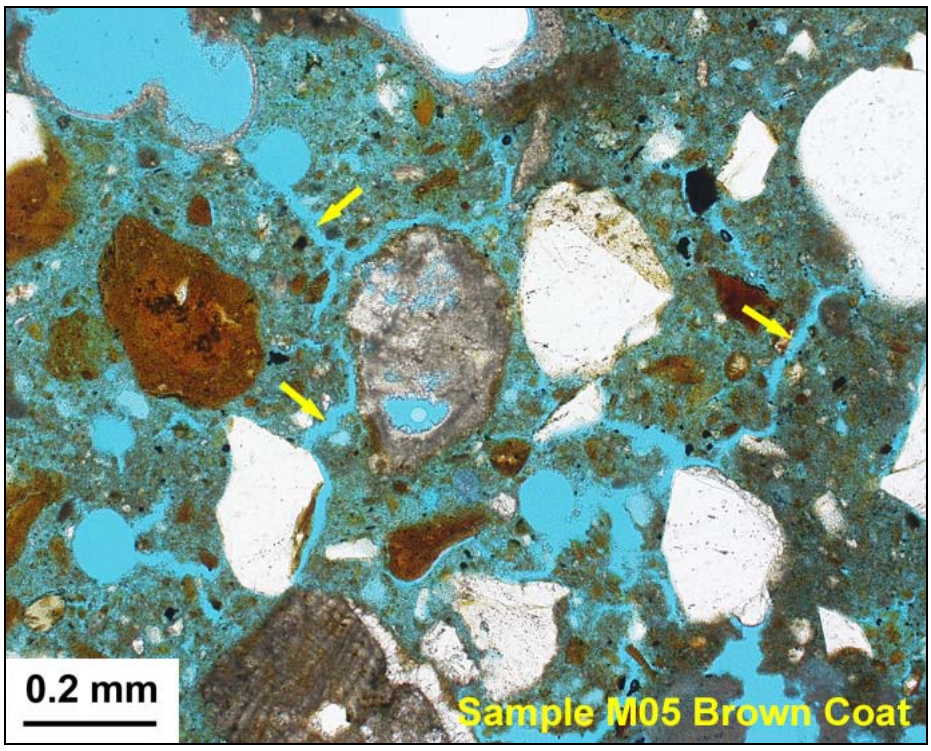


Figure 37: PPL photomicrographs. All of the samples contain lime as the primary binder. While lime is prone to shrinkage, relatively little microcracking is identified in any of the samples. The arrows in these two images provide examples from the two samples that contain the discontinuous polygonal cracks typical of lime shrinkage. The arrows indicate these fine cracks. These are not considered a threat to the continued serviceability of the materials.

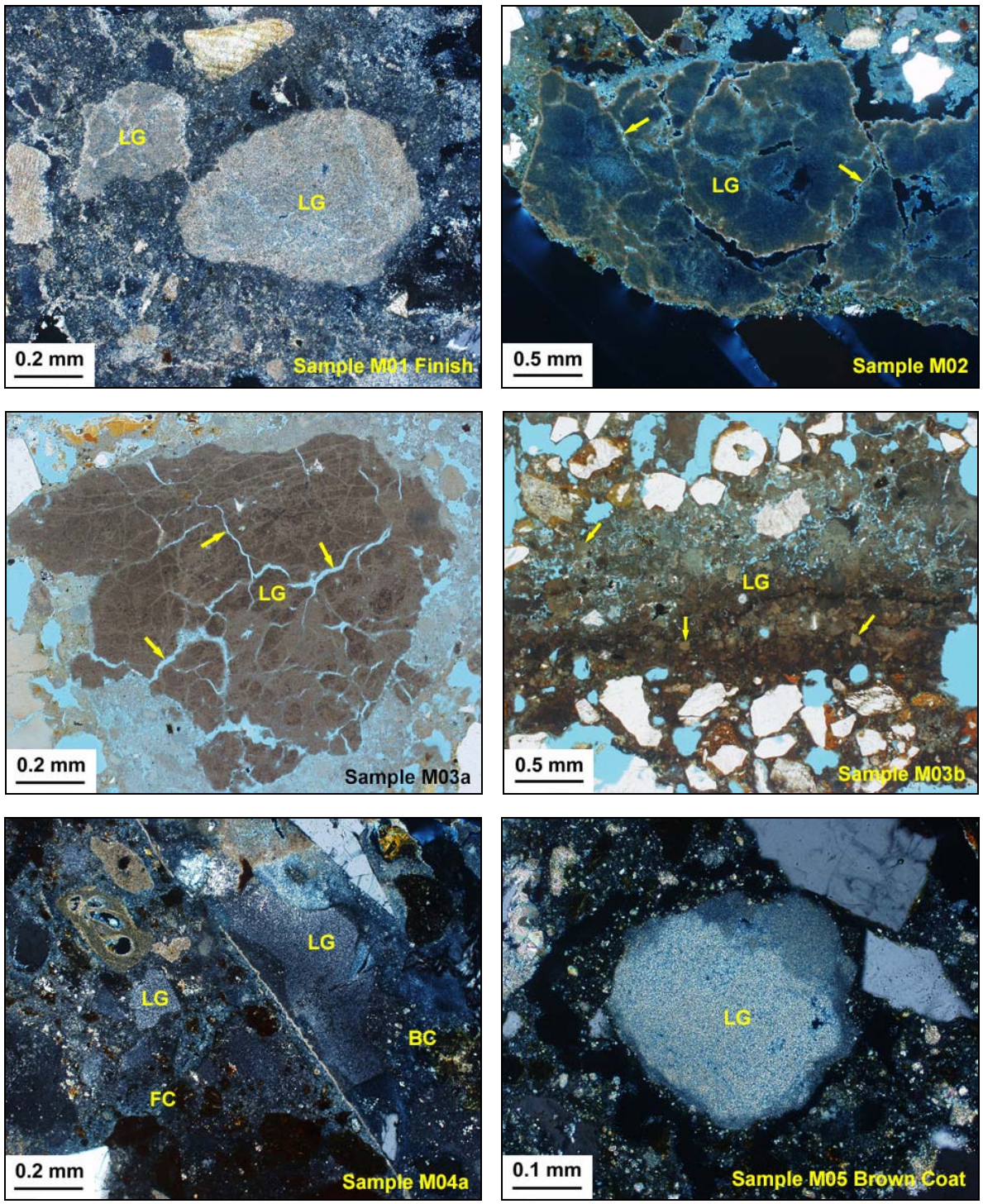


Figure 38: Photomicrographs illustrating some microtextural characteristics of undispersed lime grains (LG) present in all samples. Most grains are more or less nondescript as shown in the upper left and the lower two XPL images. Differences in the colors under crossed polars indicate whether the lime is carbonated. A darker appearance like that shown for Sample M04a is indicative of uncarbonated lime. Note that the lime is uncarbonated in both the body coat (BC) and finish coat (FC). The arrows in the upper right and middle left image indicate disaggregation cracks that define a mosaic pattern related to the original texture of the lime rock. Essentially, the lime particle is exhibiting an incipient dispersal along original grain boundaries. This type of pattern is observed in all samples but in a low proportion of grains. The image at center right depicts a streaky lime residual that itself contains a host of smaller lime lumps (arrows). This may indicate some retempering of the lime for this sample.

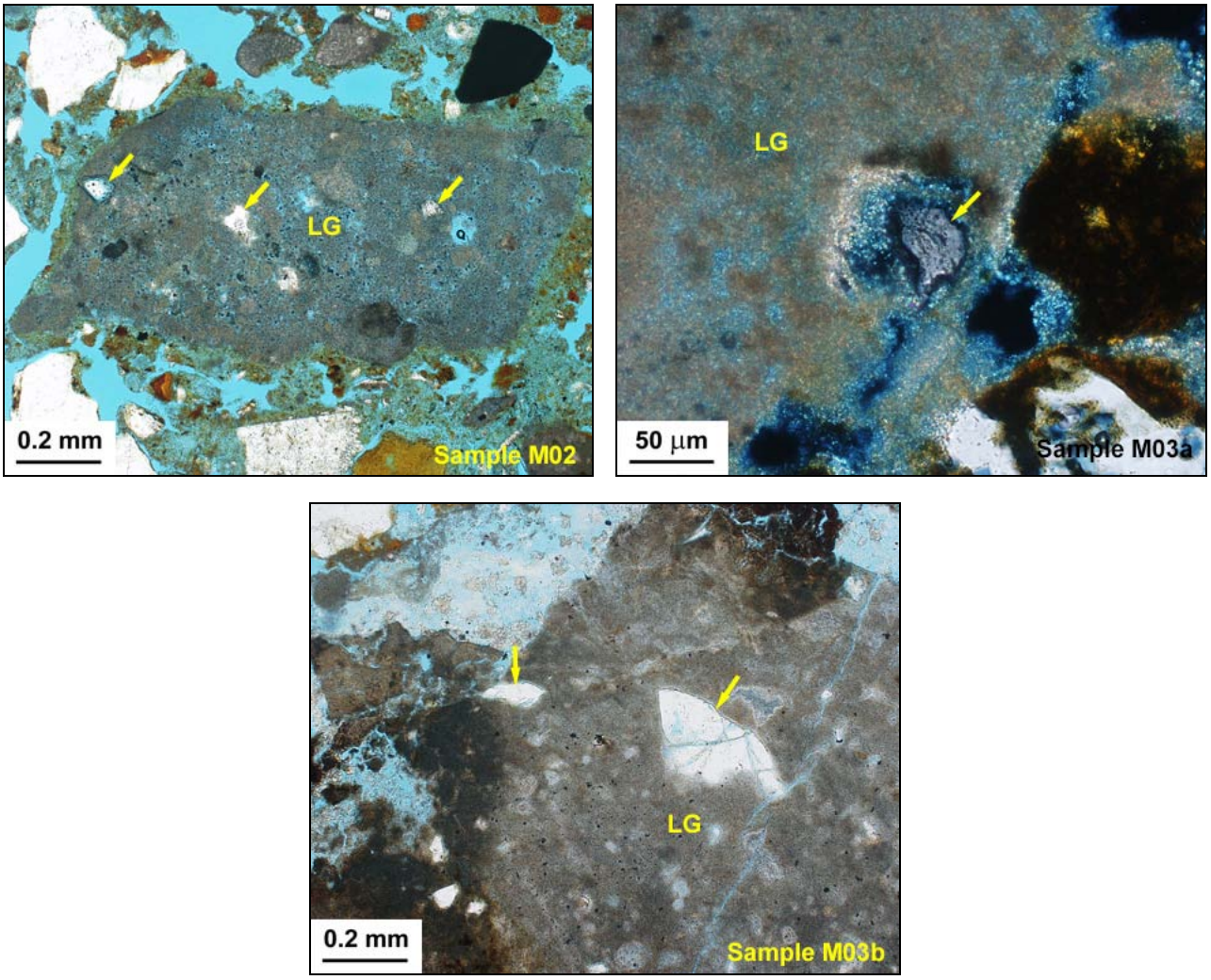


Figure 39: The lime used in all of the construction is interpreted to have been pure. Silicate inclusions are relatively rare in the lime grains (LG). The arrows indicate several examples. A few fine spots are shown in the upper left PPL image. These have fully combined with the surrounding lime to produce some minor hydraulic product. These were likely fine quartz sand grains but the original quartz is no longer evident. The grain shown in the upper left XPL image still has a core of unburned quartz that appears gray under crossed polars. Only a thin reaction rim surrounds the original sedimentary particle. In the lower PPL image, the quartz is coarse-grained and mostly unreacted.

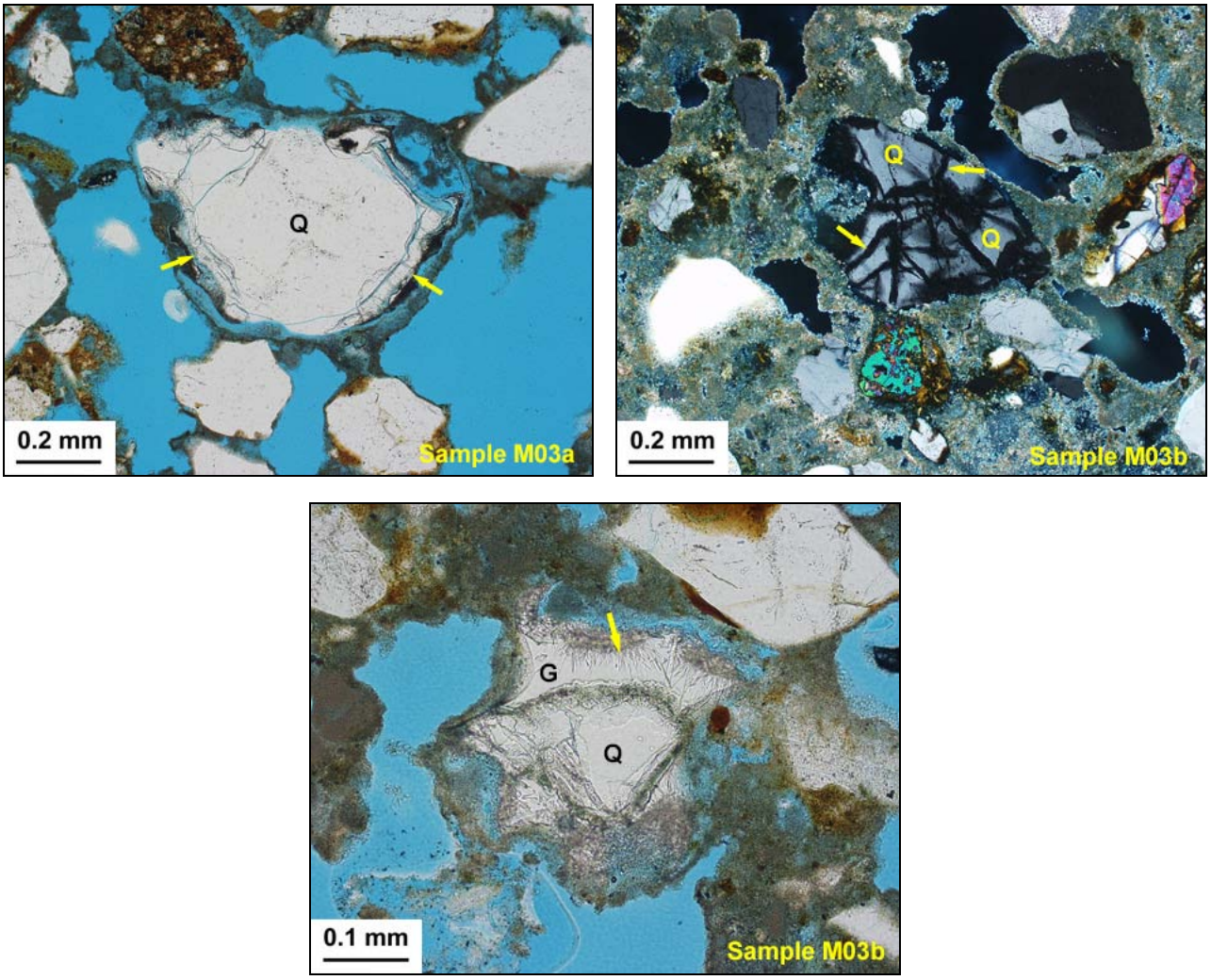


Figure 40: Isolated grains of quartz (Q) found within the binder in some samples display a greater effect of heating in the kiln. These few particles are interpreted to be associated with the lime as well. (Upper left PPL image) The arrows indicate a thin fused rim in an area that had thermally cracked at lower temperature. (Upper right XPL image) Under crossed polars, the pattern of thermal cracking in this quartz grain is quite evident. At higher temperature, the quartz began to fuse along these damaged areas. The presence of a fused glass is indicated by the dark color under crossed polars. (Lower PPL image) Another glass rim (G) is shown surrounding a quartz grain (Q). As the glass quenched, high-temperature mullite crystals had precipitated out of the molten glass (arrow).

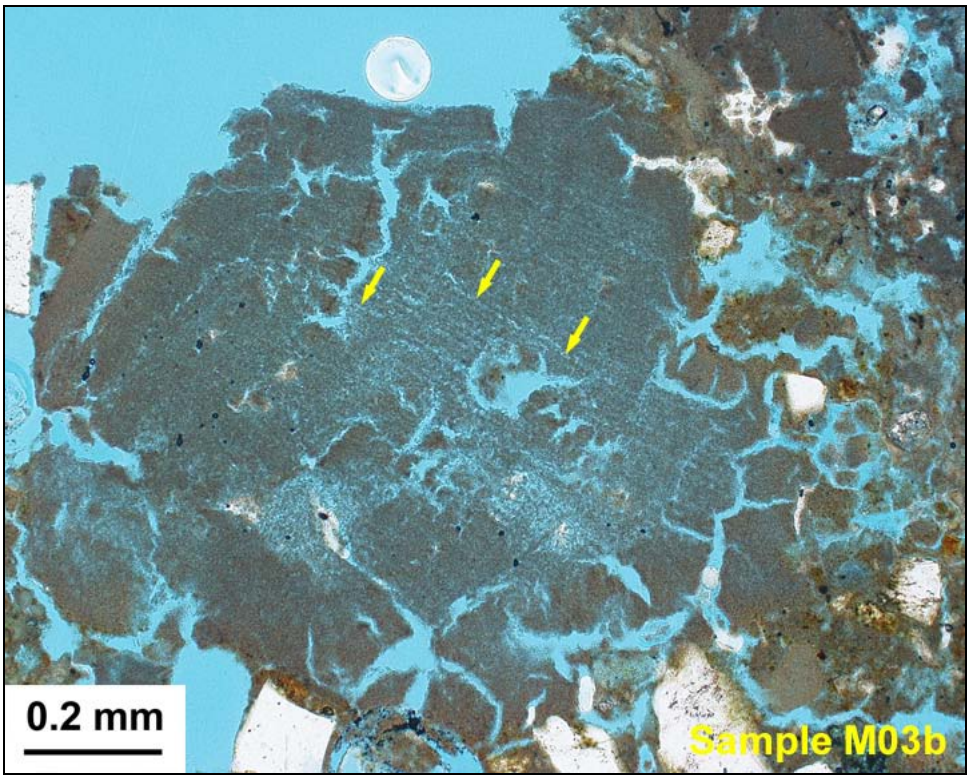


Figure 41: This PPL photomicrograph shows the only example of a residual texture in the lime that might be related to invertebrate fossils present in the original limestone. The arrows indicate fine parallel lines within a lime grain that appear more biological than mineralogical. Still, the source for the lime is interpreted to have been a sedimentary limestone rather than shells.

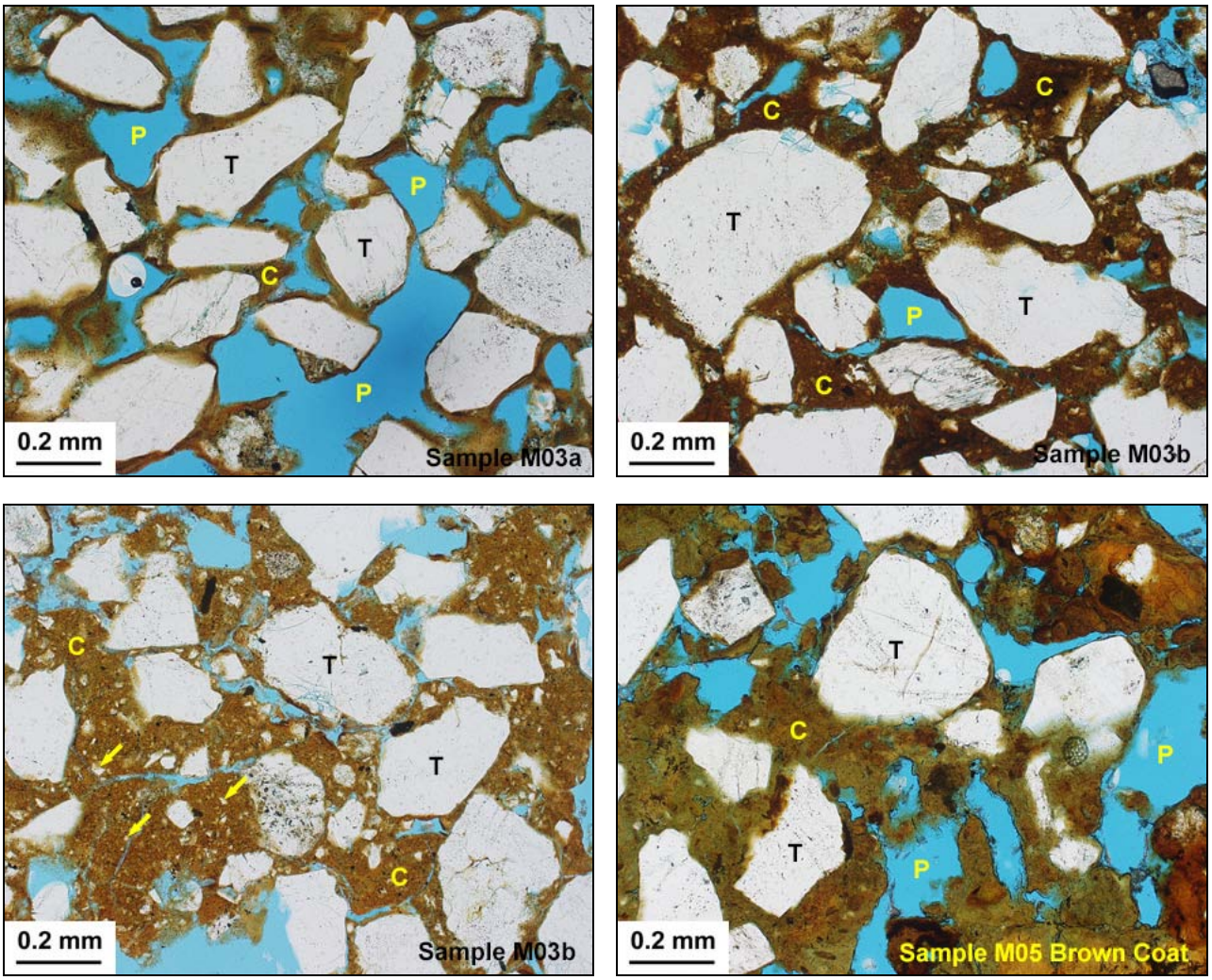


Figure 42: PPL photomicrographs illustrating the microtexture of the soft-fired brick used as a pozzolan for several of the mortars and renders (with the exception of Sample M04a). All of the brick contains a dense distribution of narrowly graded temper (T) that represents over 85% of the solid mass of the material. Some of the brick has a somewhat sparser distribution of temper (e.g., Sample M05) but not by much. The relatively narrow particle size distribution suggests that the temper may have been derived from a beach sand. The temper is bound by a homogenous fired clay matrix (C). In some cases, this is exceptionally uniform and contains no inclusions. In fewer cases, there is some sharp, fine sand evenly distributed throughout the clay. The arrows in the lower left image illustrate an example of this. There is some variability in the degree of original consolidation prior to firing. The original consolidation voids are preserved as rounded to slightly irregular pores (P) in the coarser brick fragments These indicate that the original brick material was probably relatively permeable.

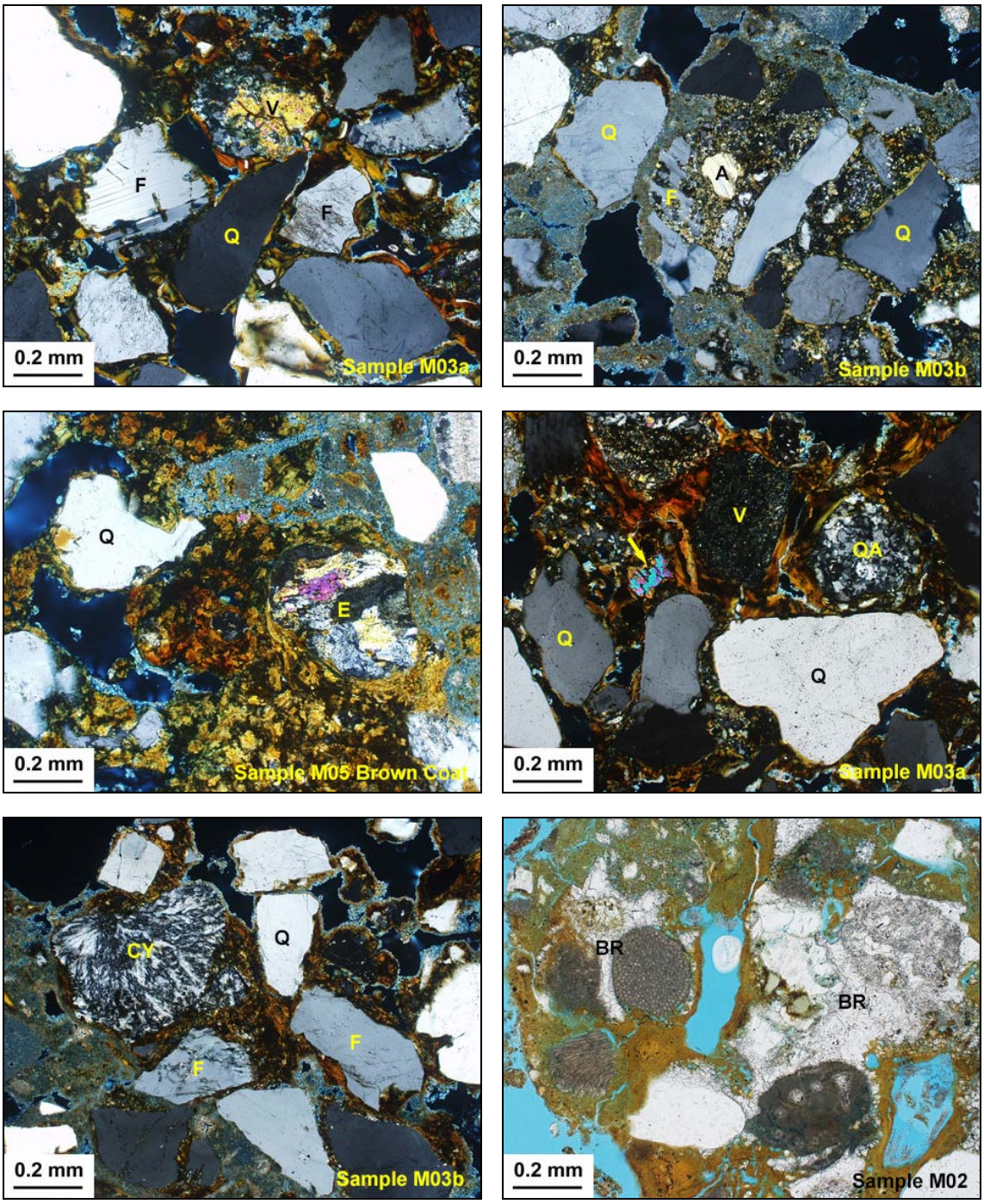


Figure 43: Photomicrographs illustrating the mineralogical constituents of the soft-fired brick temper. Quartz (Q) is the predominant phase in all samples with feldspar present in minor to lesser abundance (F). (Upper left XPL image) Volcanic grains (V) are a minor to trace constituent found in most samples. The grain shown here has partly altered to brightly-colored epidote. (Upper right XPL image) Some trace amphibole is shown (A). The feldspar in this image is skeletal in shape indicating a volcanic origin. (Center left XPL image) Epidotite (E) is a rock composed largely of epidote crystals. Given geological associations identified throughout this study, the epidote appears to be a common alteration phase of the local andesitic volcanic rocks. (Center right XPL image) The arrow indicates another epidote grain. A volcanic rock (V) is highly corroded but not altered to epidote in this case. Quartz arenite (QA) is only identified in Sample M03a. (Lower left XPL image) Chalcedony (CY) is a cryptocrystalline variety of silica that is associated with chert. (Lower right PPL image) Beachrock grains (BR) are actually found embedded within the fired clay matrix in the brick fragments of Sample M02. This further supports an interpretation of a beach sand origin for the temper.

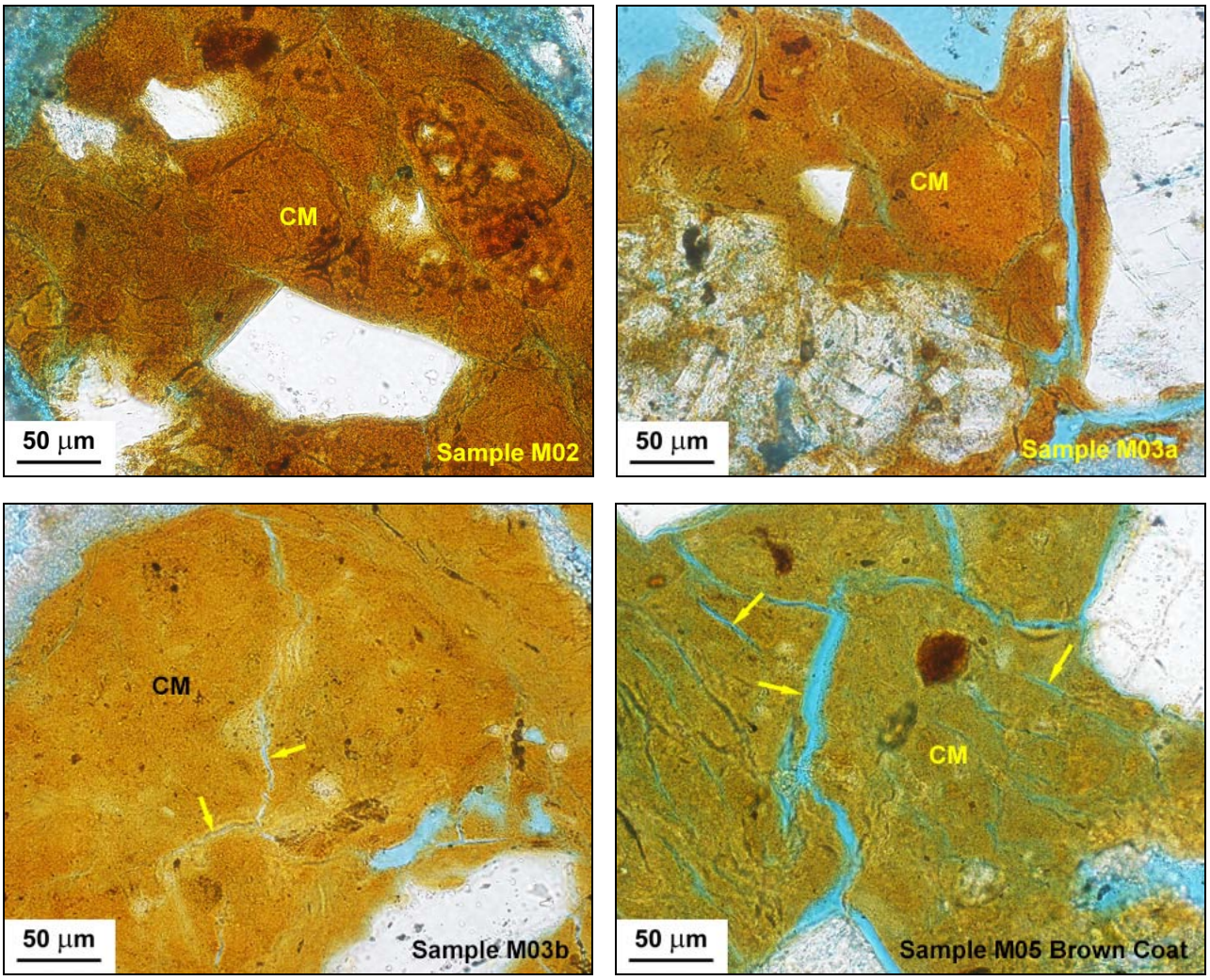


Figure 44: PPL photomicrographs illustrating the qualities of the clay matrix in the soft-fired brick used as a pozzolanic additive in several of the samples. The clay is a uniform orange-red color under plane polarized light. The samples are impregnated with a dyed epoxy but very little of this has penetrated the fired clay. This indicates that the clay has very little microporosity. Mesoscopic pores are also virtually absent. The only void space in the clay (as opposed to between temper grains) is created by minor microcracks such as the ones indicated by the arrows in two of the images.

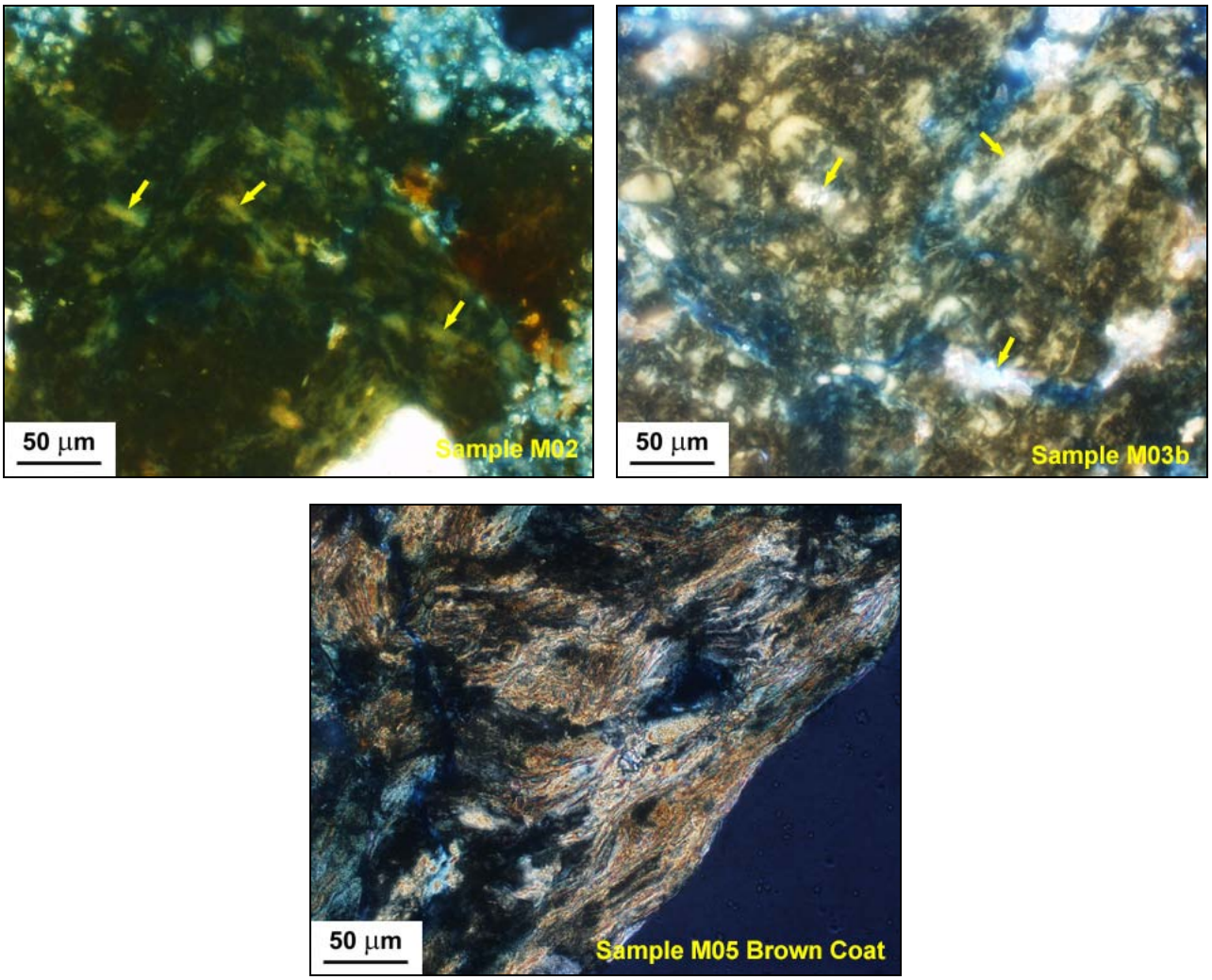


Figure 45: The fired clay in the soft-fired brick contains a residual crystallinity that is detectable under crossed polars as shown in these XPL photomicrographs. The crystallinity is indicative of lower firing temperatures. Different morphologies are identified between samples. In the upper left image, the birefringent material in Sample M02 tends to be plate-like in shape (arrows). Sample M03b (upper right image) contains a higher proportion of patchy crystals (arrows). In the lower image for Sample M05, note the "sheave-like" arrangement of coarser-grained brightly-colored crystals. These are only observed in this sample.

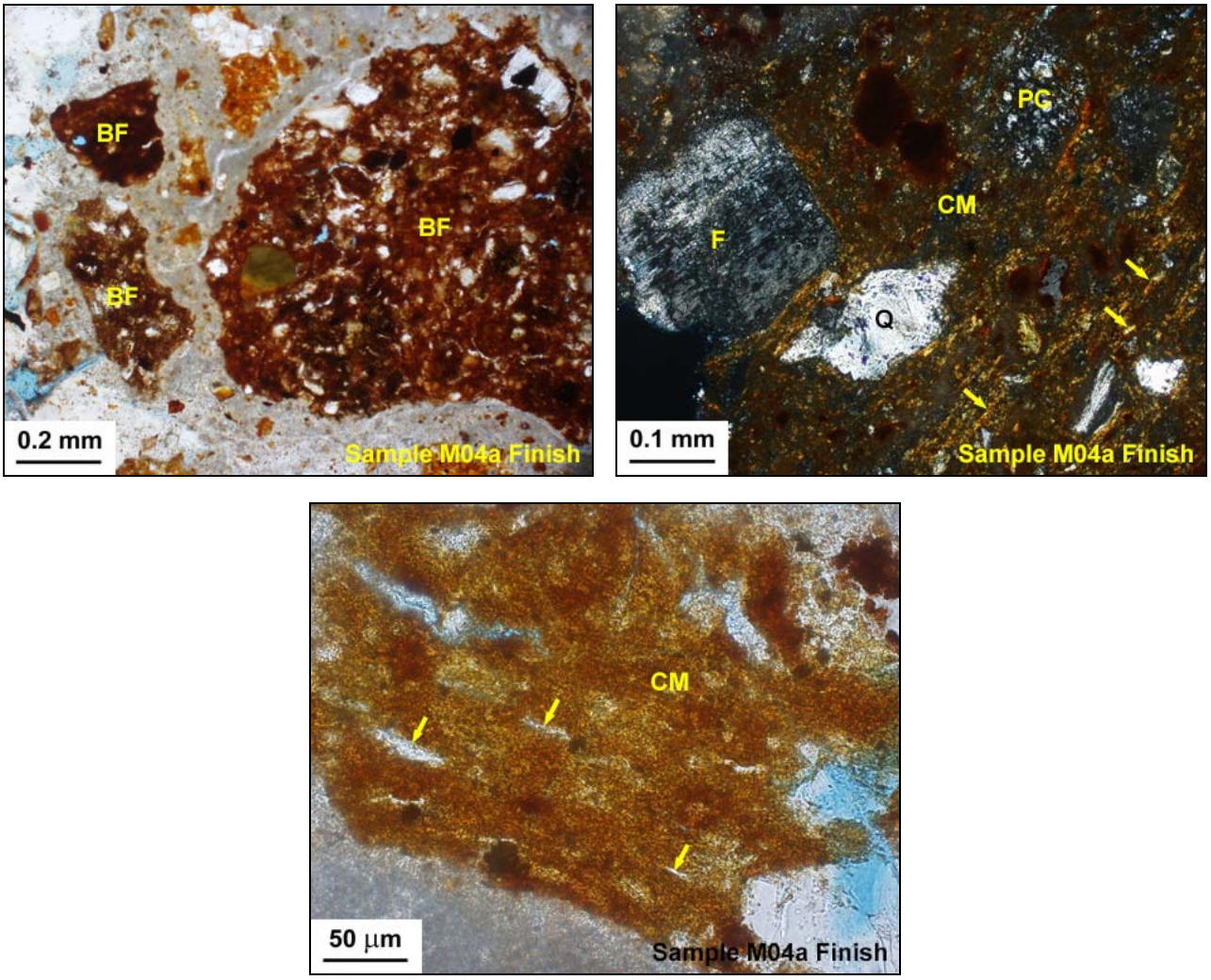


Figure 46: The harder-fired brick used as a pozzolan in Sample M04a has a different microtexture than found in the low-fired brick. (Upper left PPL image) Crushed brick fragments in the render finish (BF) have a compact texture dominated by a darker red clay with subordinate temper. (Upper right XPL image) Temper grains include quartz (Q), feldspar (F), and polycrystalline grains (PC). The clay matrix (CM) is more isotropic in character indicating a higher firing temperature. Still, some relict crystallinity is apparent (arrows). (Lower PPL image) The arrows indicate fine lenticular voids in the clay matrix (CM). These are also more typical of higher firing temperatures.

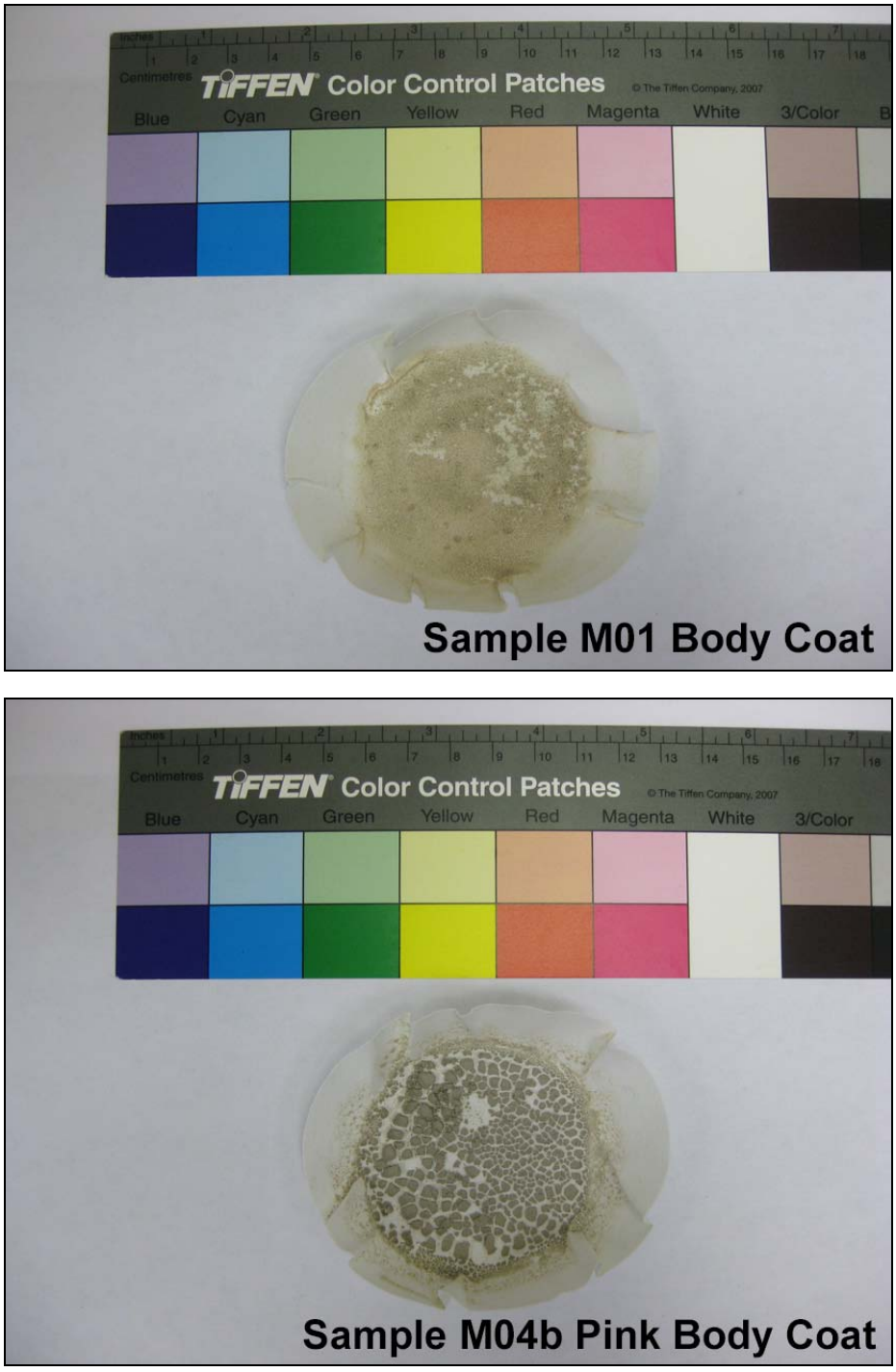


Figure 47: These images illustrate the acid-insoluble fines extracted from two of the four lime-pozzolan renders. While obviously abundant, this material is not apparent in thin section.

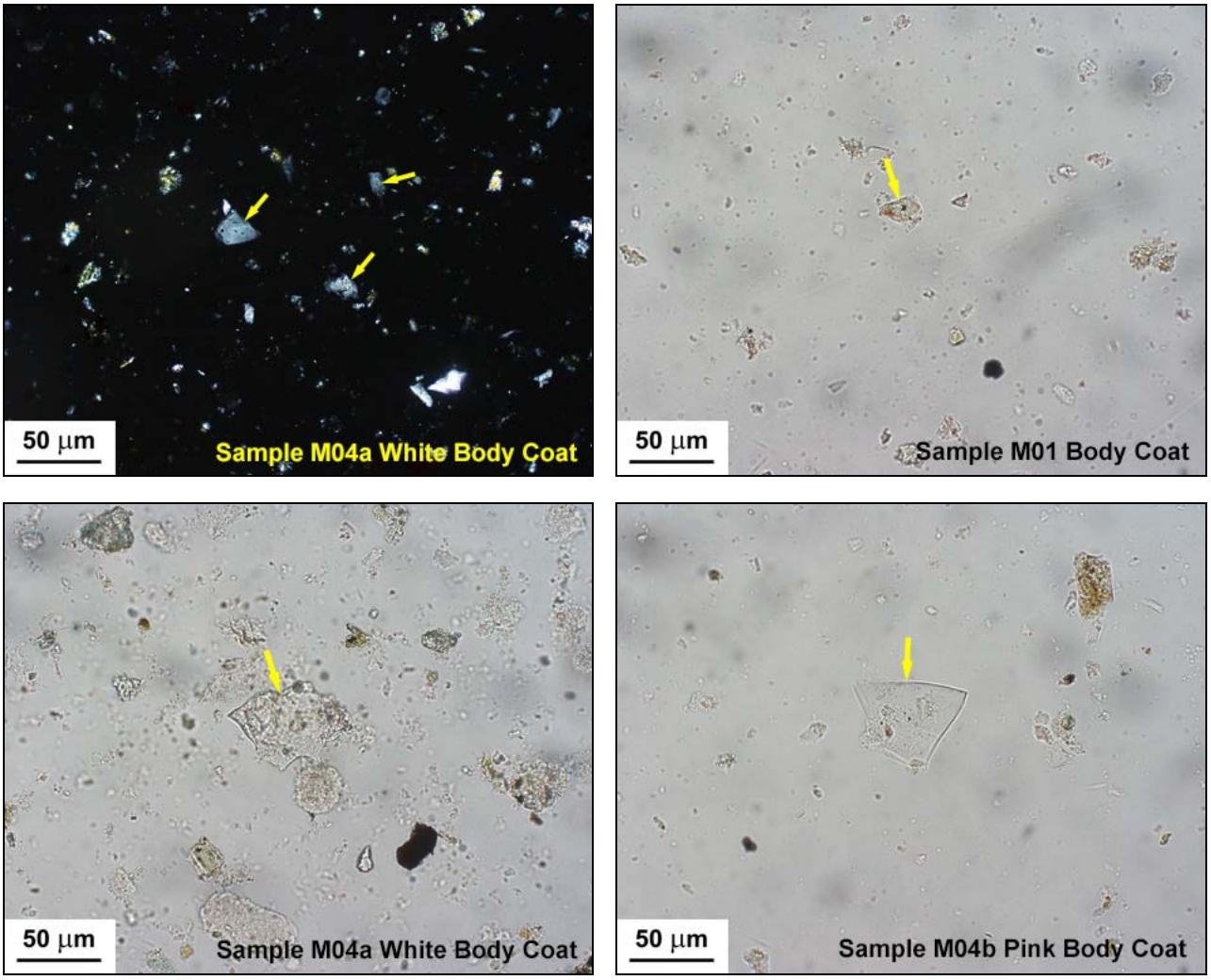


Figure 48: The upper left XPL image provides an example of a microscopic grain mount prepared from the fines extracted from the lime-pozzolan renders. The arrows indicate fine crystalline materials that are present in this fraction. These are simply fine silt grains from the natural aggregate addition. However, a portion of the fines consists of volcanic glass shards as shown in the remaining three PPL photomicrographs. The colorless, non-crystalline materials are indicated by the arrows. The optical properties of the glass indicates a high-silica composition in all cases.

Appendix E: Product Information

D/2 Biological Solution

Discover the D/2 difference!

D/2 Biological Solution is a biodegradable, easy to use liquid that removes stains from mold, algae, mildew, lichens and air pollutants. It is effective on marble, granite, limestone, brownstone, travertine, masonry, terra cotta, concrete, stucco, wood, and other architectural surfaces including monuments, sculpture and headstones. A contact time of only 10 to 15 minutes followed by scrubbing with a soft nylon or natural bristle brush will loosen most biological and air pollutant staining.

D/2 Biological Solution is effective for removing harmful biological and air pollutant staining from many building materials including masonry, marble, granite, limestone, brownstone, travertine, terra cotta, concrete, stucco, wood, canvas and vinyl & aluminum siding.

Features and Benefits

- **Fast acting**: 10 to 15 minutes contact time for great results.
- **Biodegradable**
- **Contains no acids, salts, or chlorine**
- **pH neutral**
- **Will not etch metals or glass**
- **Safer to use around plantings**
- **Is not a hazardous material and requires no special handling or protection**
- **Use full strength, no in-field mixing required**
- **Shelf life of 5 years**

Application Procedures

Always do a spot test sample before proceeding with project. D/2 works best when air and surface temperatures are 45°F or above. Use D/2 undiluted for best results. In the event of excessive plant exposure, rinse all plants and water in all planted ground areas.

Immediate Result Method

1. Apply D/2 Biological Solution with a brush, roller, hand pump sprayer (garden style pump sprayer) or low pressure power sprayer.
2. Allow undiluted D/2 to remain on the surface 10-15 minutes.
3. Apply additional D/2 as necessary to maintain a wet surface.
4. Scrub with soft nylon or natural bristle brush. **DO NOT USE METAL BRUSH.**
5. Lightly mist with water and continue scrubbing.
6. Rinse thoroughly with clean, potable water.

No Scrub/No Rinse Method

1. Apply D/2 Biological Solution with a brush or pump sprayer to a dry surface. Do not pre-wet the surface.
2. Allow to dry. Repeat if there are heavy biological stains.

D/2 works with the elements and results occur within one week to one month depending on severity of growth and weather conditions. The surface will become cleaner over time as the subsurface biological stains release.

Safety Information

D/2 Biological Solution is non-mutagenic, and contains no carcinogenic compounds as defined by NTP, IARC, or OSHA. It is considered essentially non-toxic by swallowing, as it has an oral LD50 of 2.0 g/kg of body weight. No special ventilation is required during use.

D/2 Biological Solutions, Inc. | PO Box 3746, Westport, MA 02790 | (917) 693-7441 | d2bio.com

Packaging and Coverage

D/2 Biological Solution is available in 1 gallon and 5 gallon containers, and 55 gallon drums. The area that can be treated with one gallon of D/2 will vary considerably as a function of the nature and extent of biological deposits, as well as the physical characteristics of the surface. Typical coverage to remove medium deposits will vary from 250 to 350 square feet per gallon.

Technical Data

Physical Form . . . . . Transparent, low viscosity liquid

Color . . . . . Almost colorless

pH 9.5

Specific Gravity 1.01g/cc

Solubility in Water . . . . . Complete

Vapor Pressure . . . . . 25 mm Hg @ 20°C

Notice: The information contained herein is based on our own research and the research of others, and it is provided solely as a service to help users. It is believed to be accurate to the best of our knowledge. However, no guarantee of its accuracy can be made, and it is not intended to serve as the basis for determining this product's suitability in any particular situation. For this reason, purchasers are responsible to make their own tests and assume all risks associated with using this product.

10/2012

D/2 Biological Solutions, Inc. | PO Box 3746, Westport, MA 02790 | (917) 693-7441 | d2bio.com

HBR®

Closed-Cell Polyethylene Backer Rod



HBR® is a closed-cell polyethylene foam backer rod used in concrete construction. HBR acts as a barrier, limits the depth of cold-applied sealant required and prevents excessive sealant use.

PERFORMANCE

HBR helps cold-applied sealants assume the optimum hour glass shape to prolong the sealant service life. It is commonly used in applications such as expansion and contraction joints, curtain walls, construction partitions, parking decks and bridge construction.

HBR is an inert material, and therefore, it is physically and chemically compatible with virtually all known cold-applied sealants including self-leveling types. Sealant compatibility should be confirmed by the sealant manufacturer. Compatibility characteristics of sealants in contact with sealant backings can be determined by ASTM C 1087 test method.

INSTALLATION

Prior to installing HBR, the joints should be cleaned per the sealant manufacturer's recommendations. Thoroughly remove any concrete form-release agents, curing compound reside, laitance or any foreign materials. To ensure a good sealant bond, joints must be clean and dry when the new sealant is installed. Air compressors used for this purpose must be equipped with traps for removal of oil and moisture. Install HBR with a blunt tool to the depth recommended by the sealant manufacturer.

Care should be taken not to puncture or over-compress HBR during installation. Proper size selection is important as it controls the depth of the sealant bead. It must be oversized (25-50%) to fit tightly into the joint and function as a bond-breaker to prevent back-side adhesion of the sealant. HBR is not meant to be used with hot-pour sealants.

DESCRIPTION

FORM: Round Foam Rod.

TYPE: C - Per ASTM C 1330. Cylindrical, flexible sealant backings composed predominantly of closed cell material per ASTM C 1330 for use with cold applied sealants.

TYPE: 3 -Per ASTM D 5249. Round rods of various diameters for use with cold-applied joint sealants.

TEMPERATURE LIMITS: -45°F to +160°F.

Features

- Lightweight
- Water resistant
- Non-exuding
- Easy to use
- Use with cold-applied sealants
- Clean product
- Inert
- Recyclable
- Made in USA

Specification Compliance

- Meets all requirements of the 1990 Clean Air Act
- Is a "Domestic End Product" as defined in Buy American Act, Title 41 USC 10

NOMACO®

HBR®

PHYSICAL PROPERTIES

Property	Value	ASTM Test Methods
Density lb/ft³ (kg/m³), avg.	<1.5 (24)	D 1622
Outgassing (No. of Bubbles)	> 1	C 1253
Compression Recovery, %, min	> 96	D 5249
Compression Deflection psi (kPa)	5.5 (38.2)	D 5249
Tensile Strength psi (kPa)	> 29 (200)	D 1623
Water Absorption (g/cc)	< .03	C 1016 Procedure B

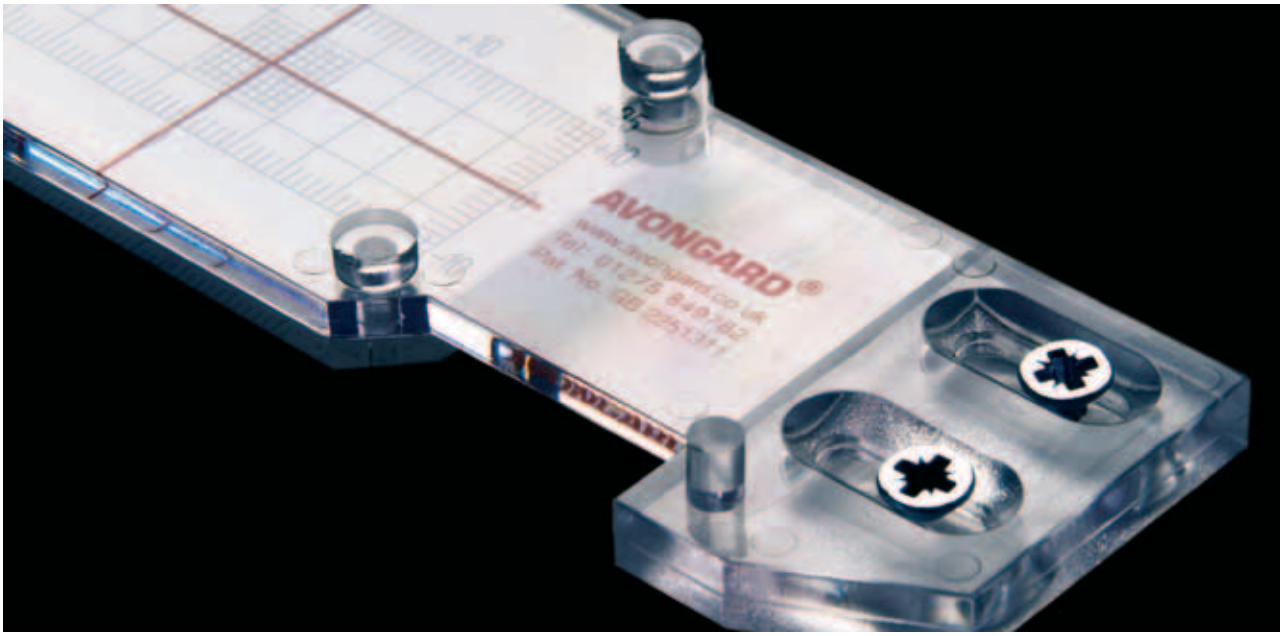
PRODUCT INFORMATION

Product	Unit	Roll Length	Joint Dimension
1/4" (6 mm)	Spool	6400' (1951 m)	3/16" or less (5 mm or less)
1/4" (6 mm)	Handy Pack	2500' (762 m)	3/16" or less (5 mm or less)
1/4" (6 mm)	Poly Bag	500' (152 m)	3/16" or less (5 mm or less)
3/8" (10 mm)	Spool	3600' (1097 m)	1/4" (6 mm)
3/8" (10 mm)	Handy Pack	1400' (427 m)	1/4" (6 mm)
3/8" (10 mm)	Poly Bag	300' (91 m)	1/4" (6 mm)
1/2" (13 mm)	Spool	2500' (762 m)	3/8" (10 mm)
1/2" (13 mm)	Handy Pack	800' (244 m)	3/8" (10 mm)
1/2" (13 mm)	Poly Bag	200' (61 m)	3/8" (10 mm)
5/8" (16 mm)	Spool	1550' (472 m)	1/2" (13 mm)
5/8" (16 mm)	Handy Pack	550' (168 m)	1/2" (13 mm)
5/8" (16 mm)	Poly Bag	150' (46 m)	1/2" (13 mm)
3/4" (19 mm)	Spool	1100' (335 m)	5/8" (16 mm)
3/4" (19 mm)	Handy Pack	400' (122 m)	5/8" (16 mm)
3/4" (19 mm)	Poly Bag	550' (168 m)	5/8" (16 mm)
7/8" (22 mm)	Spool	850' (259 m)	11/16" (18 mm)
1" (25 mm)	Spool	550' (168 m)	3/4" (19 mm)
1-1/4" (32 mm)	Spool	400' (122 m)	7/8" (22 mm)
1-1/2" (38 mm)	Cut Length	552' (168 m)	1-1/8" (29 mm)
2" (51 mm)	Cut Length	360' (110 m)	1-5/8" (41 mm)
2-1/2" (63 mm)	Cut Length	240' (73 m)	2" (51 mm)
3" (76 mm)	Cut Length	144' (44 m)	2-1/2" (64 mm)
4" (102 mm)	Cut Length	90' (27 m)	3" (76 mm)
6" (152 mm)	Cut Length	72' (22 m)	4-1/2" (114 mm)

Storage: Store in a well ventilated area. Do not store products in direct sunlight. Keep away from heat sources and open flames.

501 Innovative Way • Zebulon, NC 27597 • 919.269.6500 • NOMACO.COM
©2017 Nomaco

About Avongard
& Index



Most buildings crack at some time during their service life. Monitoring the changes in the horizontal and vertical movement across a crack will assist in diagnosing the cause of the crack and deciding on the appropriate remedial work.

Index

1. About Avongard
2. Plus Tell-Tale
3. Corner Tell-Tale
4. Displacement Tell-Tale
5. Standard Tell-Tale
6. Crack Monitoring Kit
7. Calipers
8. Caliper Kits
9. Crack Width Gauge
10. Accessories & Fixings
11. How to Buy

About Avongard Tell-Tales

Avongard Tell-Tales are precision gauges that consist of two plates which overlap for a part of their length. The bottom plate is calibrated in millimetres and the top plate is transparent and marked with a hairline cursor in the form of a cross.

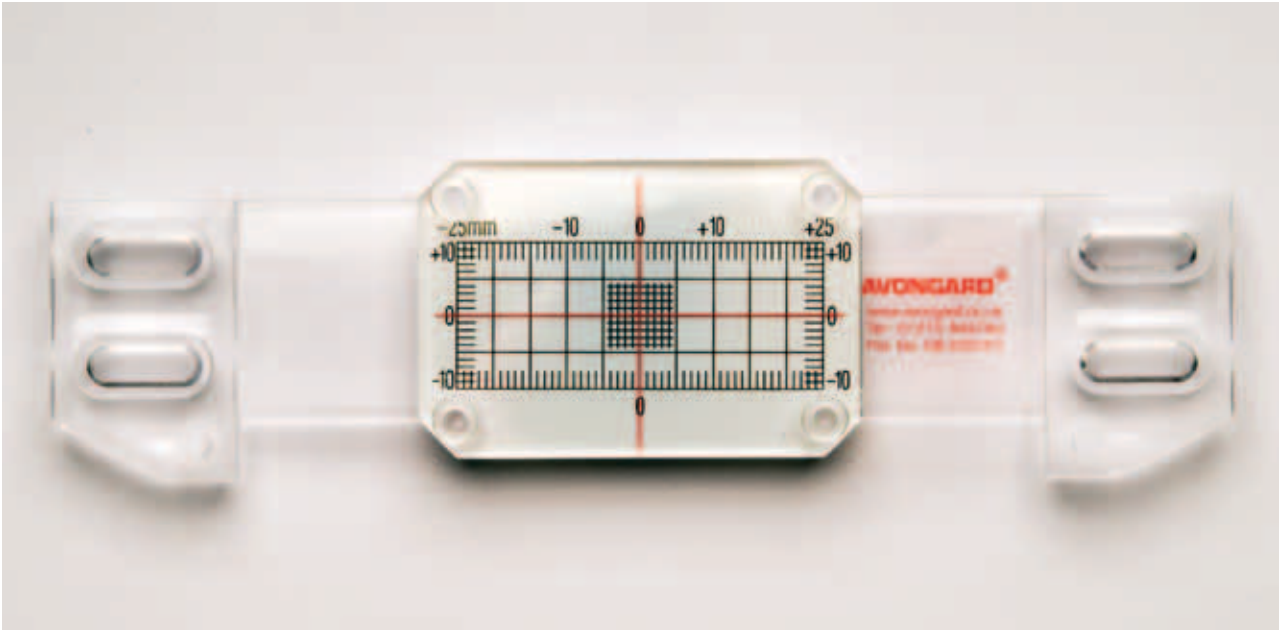
Avongard Tell-Tales are suitable for internal and external use.

The Tell-Tales are manufactured in vandal resistant polycarbonate. The co-efficient of linear thermal expansion is 7.0×10^{-5} cm/cm/^{o}C for ambient temperatures between -30^{o}C to +30^{o}C.

Manufactured to conform to BS EN ISO 9001:2008

(All specifications subject to change without notice.)

Plus Tell-Tale



The Avongard Tell-Tale Plus monitors horizontal and vertical movement across a crack on a flat surface. The Tell-Tale is preset at zero with four pegs. The pegs are removed after the Tell-Tale is fixed across the crack.

Specifications

• Avongard Tell-Tales are precision gauges that consist of two plates which overlap for a part of their length. The bottom plate is calibrated in milli-metres and the top plate is transparent and marked with a hairline cursor in the form of a cross.

• Fix using screws and adhesive (not included). (see page 10).

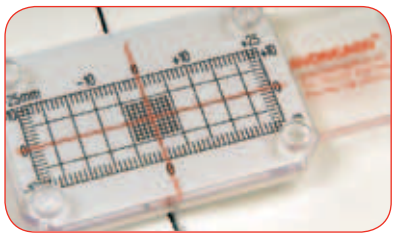
• Supplied with full instructions and Crack Record Sheet.

• Manufactured to conform to BS EN ISO 9001:2008.

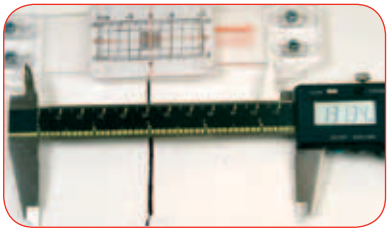
(All specifications subject to change without notice.)

Applications

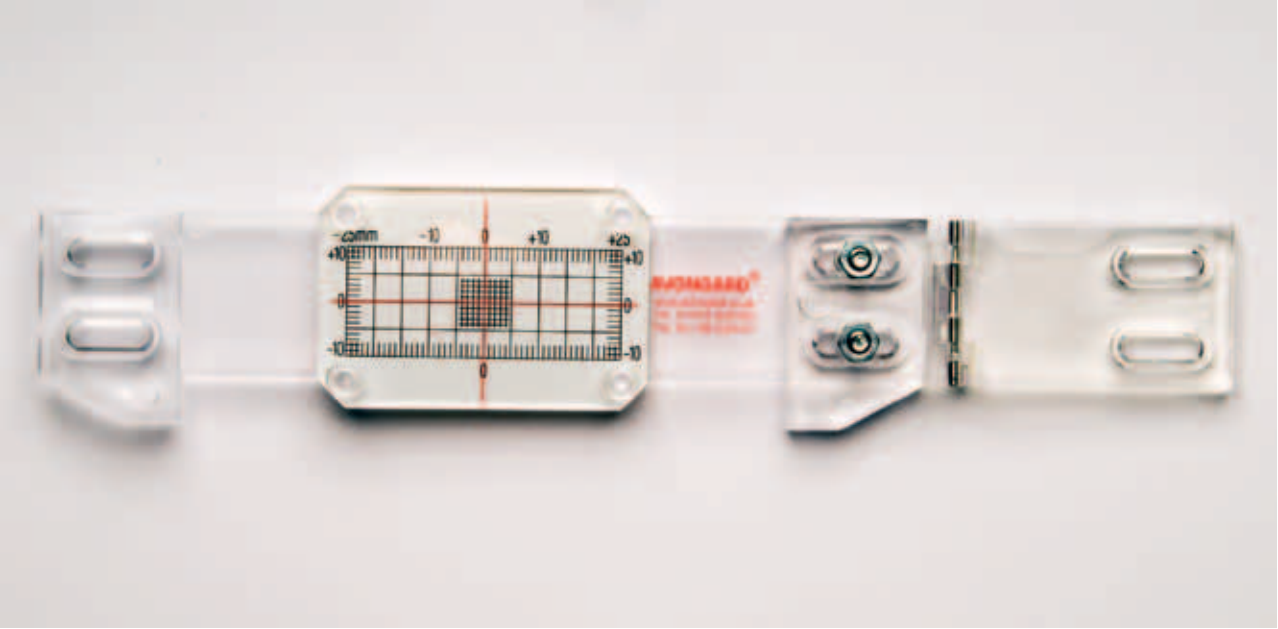
Monitoring cracks to ± 1.0 mm accuracy: As the crack opens, or if vertical movement occurs, the cursor moves relative to the calibration scale. The opening or closing of the crack is then recorded on the crack record sheet supplied.



Monitoring cracks to ± 0.1 mm accuracy: For more accurate monitoring, calipers (see page 7) can be used to measure the distances between the monitoring spigots. The distance between the spigots is then recorded on the crack record sheet supplied.



Corner Tell-Tale



The Avongard Corner Tell-Tale monitors horizontal and vertical movement across a crack in a corner.

Specifications

• The Tell-Tale is hinged enabling it to be used in internal corners of angles between 70^0 and 180^0.

• Monitors both internal and external corners.

• Avongard Tell-Tales are precision gauges that consist of two plates which overlap for a part of their length. The bottom plate is calibrated in milli-metres and the top plate is transparent and marked with a hairline cursor in the form of a cross.

• Fix using screws and adhesive (not included). (see page 10)

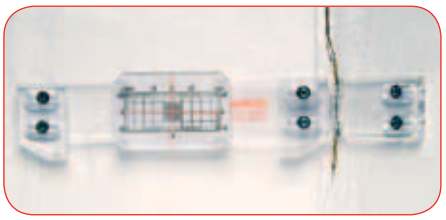
• Supplied with full instructions and Crack Record Sheet.

• Manufactured to conform to BS EN ISO 9001:2008.

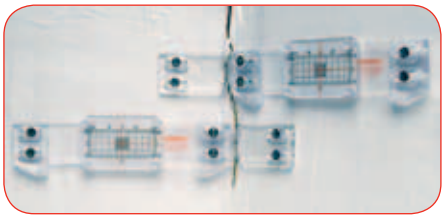
(All specifications subject to change without notice.)

Applications

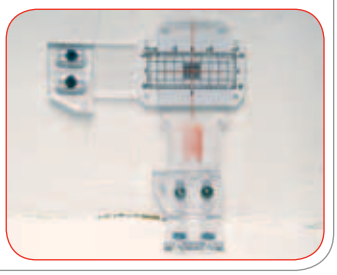
Use singly to monitor two dimensional movement.



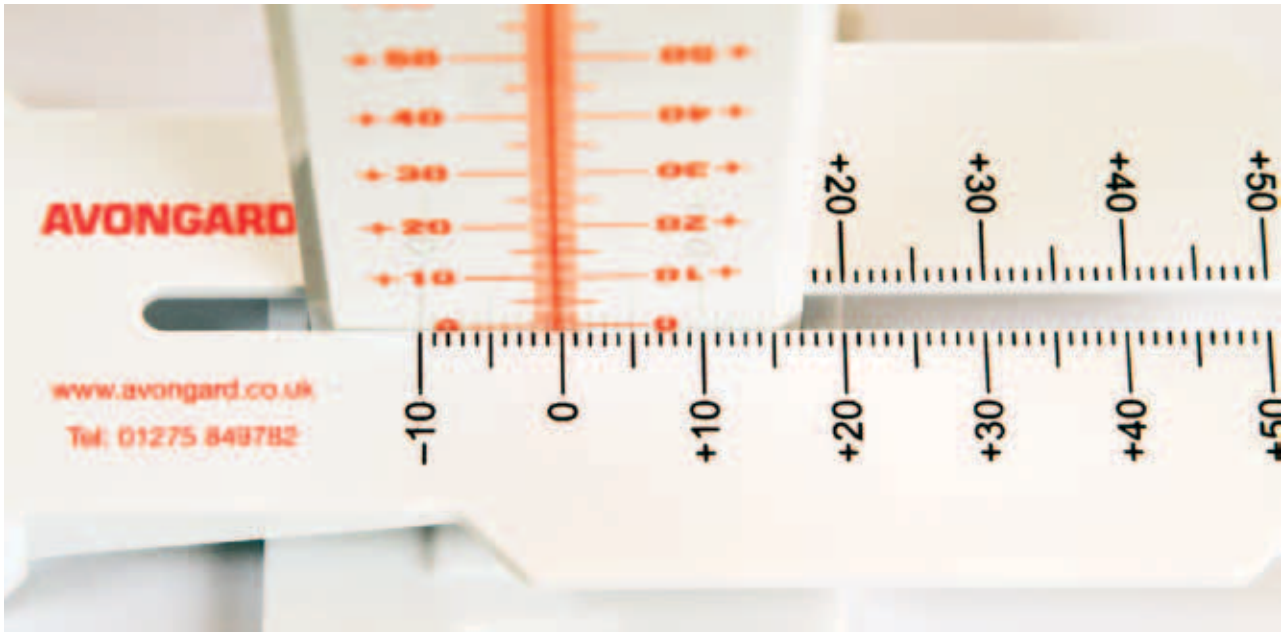
Use in pairs to monitor three dimensional movement.



Re-configure the Tell-Tale components to monitor cracks between ceilings and walls or floors and walls.



Displacement Tell-Tale



The Avongard Displacement Tell-Tale monitors horizontal and displacement movement where there is a "step" across a crack due to displacement or "out of plane" movement. The Tell-Tale consists of three components. A base plate (not calibrated) a top plate (which is calibrated) and a graduated ruler. The ruler is not left on the gauge but is used to measure the relative movement in the two plates.

Specifications

- Calibrated in millimetres.
- Displacement monitoring range of 110mm.
- Horizontal monitoring range of -10mm to +50mm.
- Fix using screws and adhesive (not included). (see page 10)
- Supplied with full instructions and Crack Record Sheet.
- Manufactured to conform to BS EN ISO 9001:2008.

(All specifications subject to change without notice.)

Applications

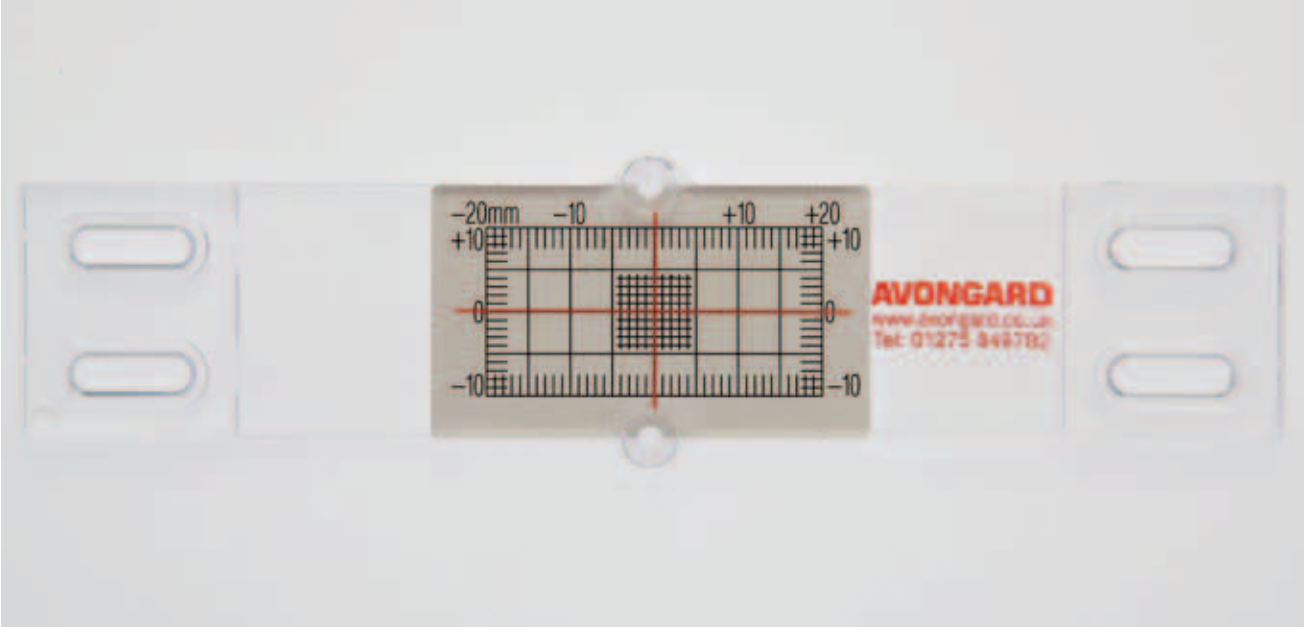
The base plate and horizontal scale are fixed using screws and adhesive each side of the crack to be monitored.



By inserting the graduated ruler, the horizontal and displacement positions can be read and marked on the crack record sheet supplied. The movement of the crack can then be monitored over time.



Standard Tell-Tale



A basic (and the original) calibrated Tell-Tale that monitors horizontal and vertical movement across a crack on a flat surface. The Tell-Tale is preset at zero with two pegs. The pegs are removed after the Tell-Tale is fixed across the crack.

Specifications

• Avongard Tell-Tales are precision gauges that consist of two plates which overlap for a part of their length. The bottom plate is calibrated in milli-metres and the top plate is transparent and marked with a hairline cursor in the form of a cross.

• Fix using screws and adhesive (not included). (see page 10)

• Supplied with full instructions and Crack Record Sheet.

• Manufactured to conform to BS EN ISO 9001:2008.

(All specifications subject to change without notice.)

Applications

The Tell-Tale is fixed across the crack using screws and plugs and/or adhesive.



The two pegs are removed. As the crack opens, or closes, the cursor moves relative to the calibration scale. The opening or closing of the crack is then recorded on the crack record sheet supplied.



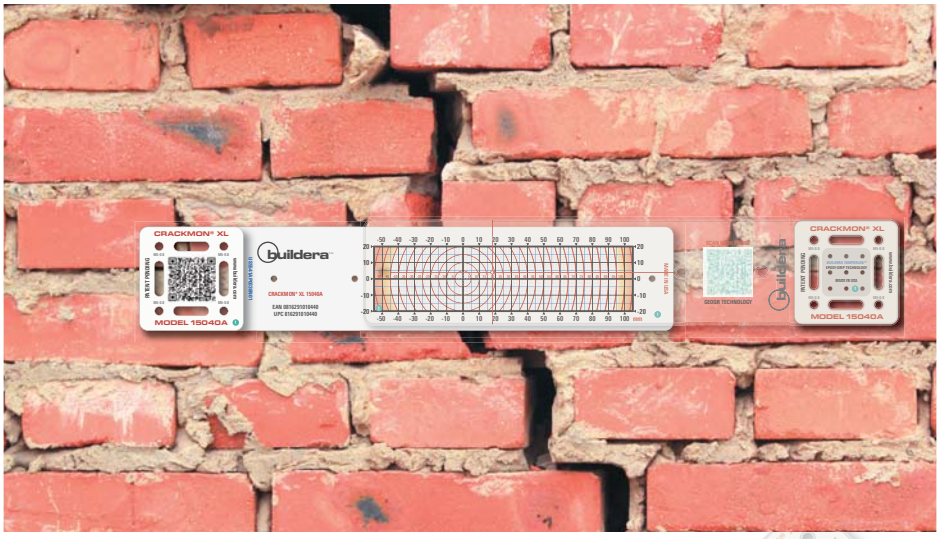
SCAN QR CODE WITH MOBILE PHONE FOR DETAILED
ONLINE DOCUMENTATION AND ORDERING INFORMATION

Data Sheet and Installation Instructions

Patent Pending

CRACKMON® XL 15040A Crack Monitor

Extra-Wide Range for Cracks, Fissures, Expansion Joints, Geophysical Monitoring



Crack-Measurement Forensics for Concrete, Masonry, Plaster and Stucco

- Basements, beams, foundations, retaining walls, seismic retrofits
- Bridges, expansion joints, transportation infrastructure
- Fissures and other wide cracks
- Mine shafts, tunnels, underground support structures
- Sink hole monitoring
- Unreinforced masonry buildings (URM/UMB)

Features and Benefits

- **Dual measurement range**: -55 to +105 mm or -5 to +155 mm (X), ±20 mm (Y)
- **High resolution**: ±1 mm (±0.04") on X-Y axes; ±0.5 mm (±0.02") visual discrimination
- **Accurate**: Vibrant X-Y, and polar-magnitude grid wtih TickPoints™ on 1x1-mm intervals
- **Traceable**: Unique serial ID for engineering and forensic documentation
- **Quality**: Engineered and made in USA from premium materials

Features and Benefits

- **Accurate**: Vibrant X-Y, and polar-magnitude grid wtih TickDots™ on 1x1-mm intervals
- **Traceable**: Unique serial ID for engineering and forensic documentation
- **High-resolution**: ±1 mm (±0.04") on X-Y axes; ±0.5 mm (±0.02") visual discrimination
- **Wide measurement range**: ±20 mm (±0.79") horizontal and ±10 mm (±0.38") vertical
- **Uncompromising quality**: Made in USA from heavy-duty clear polymer

Ordering Information

Model (Qty)	UPC
CRACKMON® XL 15040A (1)	816291010440
CRACKMON® XL 15050A (5)	81629101XXXX
STRUPOXY™ Adhesive (1 Oz)	816291010099

Related Products

Model (Qty)	UPC
CRACKMON® 4020A (18)	816291010013
CRACKMON® 5020AV (1)	816291010389
CRACKMON® 224R (1)	816291010112
CRACKMON® 224R (50-Bulk)	816291010167
CRACKPOINT™ 60ti (10)	816291010303
CRACKPOINT™ 90ti (10)	816291010310
CRACKPOINT™ TR50ti-Kit	816291010334

Engineering Specifications

Parameter	Specification
Dimensions	451 x 64 x 11 mm
Crack-Width Range	160 mm (X), ±20 mm (Y)
Discrimination	±0.5 mm (visual)
Polar Magnitude	-55-105 mm, 5 mm steps
Material	Heavy-duty clear polymer
CoE (ASTM D696)	22 µm/m-°C, -30 to +30°C
Mounting Method	Epoxy and/or fasteners
Fastener Size	(4) #10 x 1-1/2"
Fastener Type	SS Sheet-Metal Hex Head
Anchor	Toggler® A6 (1/4" dia.)
Country of Origin	USA

CRACKMON®, CRACKPOINT™, STRUPOXY™ & TRACARD® are trademarks of Buildera.

©2015 Buildera. All rights reserved. Printed in USA.

SCAN QR CODE WITH MOBILE PHONE FOR DETAILED
ONLINE DOCUMENTATION AND ORDERING INFORMATION

Buildera Data Sheet

Patent Pending

CRACKMON® 4020A Crack Monitor

Traceable Crack Monitor for Concrete Structural Forensics and Seismic Retrofits



Crack-Measurement Forensics for Concrete, Masonry, Plaster and Stucco

- Airports, bridges, dams, highways, power plants
- Basements, beams, foundations, retaining walls, seismic retrofits
- Commercial and residential structures, historic monuments

Features and Benefits

- **Accurate**: Vibrant X-Y, and polar-magnitude grid wtih TickDots™ on 1x1-mm intervals
- **Traceable**: Unique serial ID for engineering and forensic documentation
- **High-resolution**: ±1 mm (±0.04") on X-Y axes; ±0.5 mm (±0.02") visual discrimination
- **Wide measurement range**: ±20 mm (±0.79") horizontal and ±10 mm (±0.38") vertical
- **Uncompromising quality**: Made in USA from heavy-duty clear polymer

Ordering Information

Model (Qty)	UPC
CRACKMON® 4020A (1)	816291010259
CRACKMON® 4020A (3-Kit)	816291010006
CRACKMON® 4020A (18-Kit)	816291010013
CRACKMON® Drill Kit w/ HW	816291010242
StruPoxy™ Adhesive (1 Oz)	816291010099
TraCard® 3D StarterPak (12)	816291010368
TraCard® 3D Refill Kit (50)	816291010082

Related Products

Model (Qty)	UPC
CRACKMON® 224R (1)	816291010112
CRACKMON® 224R (50-Bulk)	816291010167
CRACKMON® 5020AV (1)	816291010389
CrackPoint™ 60ti (10)	816291010303
CrackPoint™ 90ti (10)	816291010310
CrackPoint™ TR50ti-Kit (pair)	816291010334

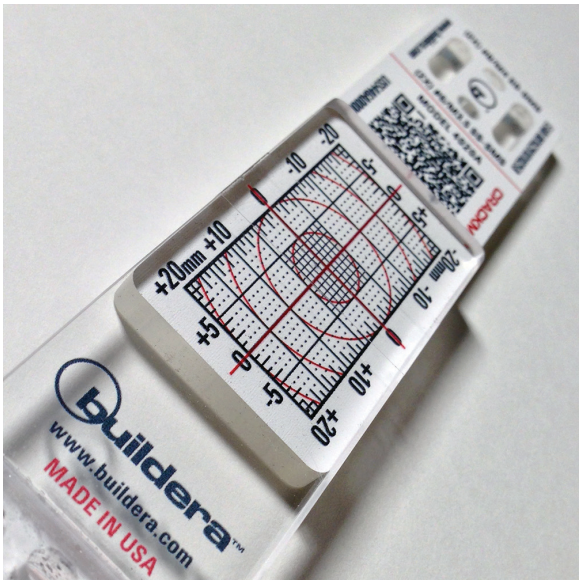
Engineering Specifications

Parameter	Specification
Dimensions	152 x 31 x 8 mm
Crack-Width Range	±20 mm (X), ±10 mm (Y)
Discrimination	±0.5 mm (visual)
Polar Magnitude	0-20 mm in 5 mm steps
Material	Heavy-duty clear polymer
CoE (ASTM D696)	22 µm/m-°C, -30 to +30°C
Mounting Method	Epoxy and/or fasteners
Fastener Sizes	M4 (#8) or M3.5 (#6) SMS
Fastener Type	SS Security Torx® SMS
Anchor	Toggler® A5 (3/16" dia.)
Country of Origin	USA

CRACKMON®, CrackPoint™, StruPoxy™ & TraCard® are trademarks of Buildera.

©2015 Buildera. All rights reserved. Printed in USA.

Product Description



The Buildera CRACKMON® 4020A Crack Monitor is a heavy-duty, commercial-grade crack monitor for the repair, restoration, and long-term monitoring of concrete, masonry, plaster, and stucco structures. Engineered and made in the USA from premium extruded polymer, the new CRACKMON 4020A offers unique features for civil/structural and geotechnical engineers.

X-Y Measurements Plus Polar Magnitude with TickDots™

The X-Y measurement grid includes a new polar-magnitude measurement function that computes the angular hypotenuse (magnitude) of displacement from the zero-crossing. To improve reading accuracy over the entire range, the measurement grid sports variable-length tick marks as well as patent-pending TickDots at 1x1-mm intervals. TickDots improve crack-measurement accuracy as the measurement cross-hairs traverse the grid. This is particularly helpful when the two plates are no longer parallel.

Vibrant, High-Contrast Measurement Grid

We print the CRACKMON 4020A in five process colors, including a high-contrast rich-black text UV-cured over a thick double layer of brilliant opaque white ink. The result is a bright, bold measurement grid with a 2X contrast improvement that is much easier to read over a wide range of lighting.

Engineering Traceability to the Crack

To improve engineering traceability, each CRACKMON 4020A crack monitor features a unique 15-character serial number that tracks the country of origin, design revision, and unique ID. This ensures forensic traceability in the field and offers a significant benefit in report writing and litigation.

Buildera GeoQR™ Mobile Installation Instructions and Ordering

Scan the printed CRACKMON QR code with your mobile phone to access installation instructions and to reorder online.

Tamper-Resistant Mounting Flexibility

Mounting methods include epoxy and/or fasteners. Horizontal and vertical slots are optimally sized to accept four different screw sizes, including US (#8/#6) and metric (M4/M3.5) fasteners. A stainless-steel Torx-Plus® tamper-resistant mounting kit with anchors is also available. To ensure a secure and trouble-free installation, Buildera also offers corrosion-resistant stainless-steel washers to help distribute the load.

Peel-and-Stick Drilling Template

When hammer-drilling hard or rough surfaces like concrete or stucco, the percussive impact from a hammer drill makes it tough to accurately drill holes in the right place. A new impact-absorbing drilling guide (patent pending) features an aggressive adhesive that sticks to concrete, masonry, stucco, steel, wood, and other rough surfaces. Simply peel it, stick it, and drill it. Experience perfect holes every time—saving time and money.

Value for Money

The CRACKMON 4020A offers more value than any crack monitor on the market today. When purchased in bulk, prices are competitive with traditional crack monitors, but with the benefits and premium features that only the CRACKMON 4020A delivers.

Available in Bulk for Distributors and High-Volume End Users

Buy the CRACKMON 4020A online and from our growing list of global channel partners, distributors, and resellers.

Custom Logo and Co-Branding Options

Customize CRACKMON 4020A crack monitors with your company logo and website. Available options include a unique QR code to direct users to your website for re-ordering. Minimum order is 250 pieces. Contact Buildera for options and pricing.

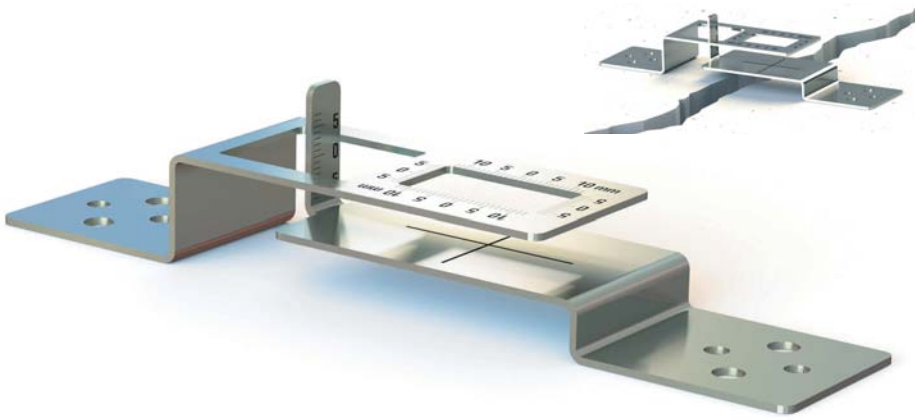
buildera™

SCAN QR CODE WITH MOBILE PHONE FOR DETAILED ONLINE DOCUMENTATION AND ORDERING INFORMATION

Data Sheet and Installation Guide — Model 2412-FSS

CRACKMON® 3D XYZ-Axis Crack Monitor

Industrial-Grade Crack Monitor Measures Crack Displacement on X, Y & Z Axes



3D Crack Measurements for Concrete, Masonry, Plaster, Stucco and Steel

- Airports, bridges, dams, highways, power plants
- Basements, beams, foundations, retaining walls, seismic retrofits, unreinforced masonry
- Commercial and residential structures, historic monuments

Features and Benefits

- **Measure crack displacement in 3D**: Ideal for non-planar offset cracks
- **Crack measurement range**: ±12 mm (X), ±6 mm (Y), ±7 mm (Z-offset)
- **Secure mounting**: Use fasteners and thixotropic epoxy for best results
- **Rugged**: Heavy-duty 18-gauge type-304 stainless steel resists corrosion
- **Corner-mount options**: Order inside (816291010044) and outside (816291010051) corners
- **Proven quality**: Engineered and made in USA

Product Description

The Buildera CRACKMON® 3D Model 2412-FSS is a flat-mount, stainless-steel, industrial-grade crack monitor for the repair, restoration, and long-term monitoring of concrete, masonry, plaster, stucco, and steel structures where 3-axis measurements are required. Most crack monitors or crack meters measure in one or two dimensions, but not all three. The CRACKMON 3D is ideal for foundation and basement restoration, seismic retrofitting, or any structural, geotechnical, or civil engineering project that requires ongoing monitoring of structural defects and cracks in three dimensions.

Buildera manufactures each CRACKMON 3D in the USA using state-of-the-art precision laser cutting. Durable type-304 stainless steel with high-contrast laser-etched markings provide permanent readability even in harsh, corrosive outdoor environments.

Specifications subject to change without notice. Epoxy sold separately.

Ordering Information

Model (Qty)	UPC
CRACKMON® 3D 2412-FSS	816291010037
STRUPOXY™ Adhesive (1 Oz)	816291010099
TRACARD® 3D StarterPak (12)	816291010368

Related Products

Model (Qty)	UPC
CRACKMON® 4020A (1)	816291010259
CRACKMON® 4020A (3-Kit)	816291010006
CRACKMON® 4020A (18-Kit)	816291010013
CRACKMON® 5020AV (1)	816291010389
CRACKMON® XL 15040A (1)	816291010440
CRACKMON® 224R (1)	816291010112
CRACKMON® 224R (50-Bulk)	816291010167
CRACKPOINT™ 60ti (10)	816291010303
CRACKPOINT™ 90ti (10)	816291010310
CRACKPOINT™ TR50ti-Kit	816291010334

Engineering Specifications

Parameter	Specification
Dimensions (at 0,0)	150 mm (L) x 32 mm (W)
Crack Range (XYZ)	±12 mm, ±6 mm, ±7 mm
Discrimination	±1 mm (visual)
Weight	59 g (2.1 oz)
Material	18-gauge type 304 SS
COE	17 µm/m-°C, 0 to +100 °C
Mounting Method	Epoxy and/or fasteners
Fastener Sizes	M4.2 (#8), M3.5 (#6) SMS
Fastener Type	Sheet-metal pan head
Anchor	Toggler® A5 (3/16" dia.)
Country of Origin	USA

CRACKMON®, CRACKPOINT™, STRUPOXY™ & TRACARD® are trademarks of Buildera.

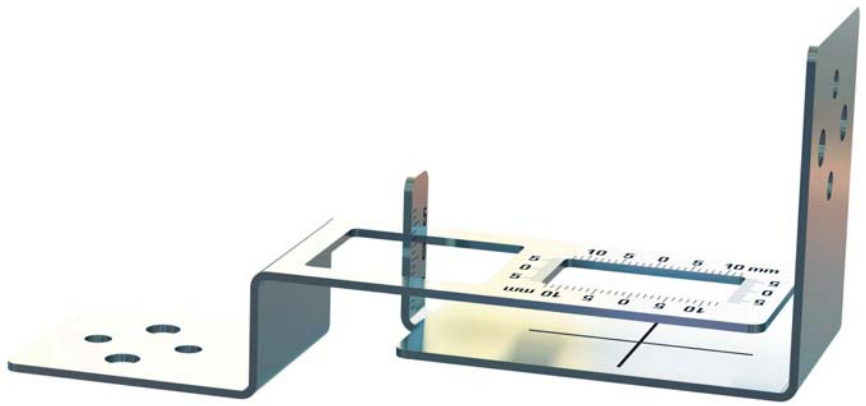
©2015 Buildera. All rights reserved. Printed in USA.

SCAN QR CODE WITH MOBILE PHONE FOR DETAILED ONLINE DOCUMENTATION AND ORDERING INFORMATION

Data Sheet and Installation Guide — Model 2412-ICSS (Inside)

CRACKMON® 3D XYZ-Axis Crack Monitor

Industrial-Grade Crack Monitor Measures Crack Displacement on X, Y & Z Axes



3D Crack Measurements for Concrete, Masonry, Plaster, Stucco and Steel

- Airports, bridges, dams, highways, power plants
- Basements, beams, foundations, retaining walls, seismic retrofits, unreinforced masonry
- Commercial and residential structures, historic monuments

Features and Benefits

- **Measure crack displacement in 3D**: Ideal for non-planar offset cracks
- **Crack measurement range**: -3 to +12 mm (X), ±6 mm (Y), ±7 mm (Z-offset)
- **Secure mounting**: Use fasteners and thixotropic epoxy for best results
- **Rugged**: Heavy-duty 18-gauge type-304 stainless steel resists corrosion
- **Flush and corner options**: Flush (816291010037) and outside corner (816291010051)
- **Proven quality**: Engineered and made in USA

Product Description

The Buildera CRACKMON® 3D Model 2412-ICSS is an inside-corner-mount, stainless-steel, industrial-grade crack monitor for the repair, restoration, and long-term monitoring of concrete, masonry, plaster, stucco, and steel structures where 3-axis measurements are required. Most crack monitors or crack meters measure in one or two dimensions, but not all three. The CRACKMON 3D is ideal for foundation and basement restoration, seismic retrofitting, or any structural, geotechnical, or civil engineering project that requires ongoing monitoring of structural defects and cracks in three dimensions.

Buildera manufactures each CRACKMON 3D in the USA using state-of-the-art precision laser cutting. Durable type-304 stainless steel with high-contrast laser-etched markings provide permanent readability even in harsh, corrosive outdoor environments.

Specifications subject to change without notice. Epoxy sold separately.

Ordering Information

Model (Qty)	UPC
CRACKMON® 3D 2412-ICSS	816291010044
STRUPOXY™ Adhesive (1 Oz)	816291010099
TRACARD® 3D StarterPak (12)	816291010368

Related Products

Model (Qty)	UPC
CRACKMON® 4020A (1)	816291010259
CRACKMON® 4020A (3-Kit)	816291010006
CRACKMON® 4020A (18-Kit)	816291010013
CRACKMON® 5020AV (1)	816291010389
CRACKMON® XL 15040A (1)	816291010440
CRACKMON® 224R (1)	816291010112
CRACKMON® 224R (50-Bulk)	816291010167
CRACKPOINT™ 60ti (10)	816291010303
CRACKPOINT™ 90ti (10)	816291010310
CRACKPOINT™ TR50ti-Kit	816291010334

Engineering Specifications

Parameter	Specification
Dimensions (at 0,0)	150 mm (L) x 32 mm (W)
Crack Range (XYZ)	-3 to +12 mm (X), ±6 mm (Y), ±7 mm (Z)
Discrimination	±1 mm (visual)
Weight	59 g (2.1 oz)
Material	18-gauge type 304 SS
COE	17 µm/m-°C, 0 to +100 °C
Mounting Method	Epoxy and/or fasteners
Fastener Sizes	M4.2 (#8), M3.5 (#6) SMS
Fastener Type	Sheet-metal pan head
Anchor	Toggler® A5 (3/16" dia.)
Country of Origin	USA

CRACKMON®, CRACKPOINT™, STRUPOXY™ & TRACARD® are trademarks of Buildera.

©2015 Buildera. All rights reserved. Printed in USA.

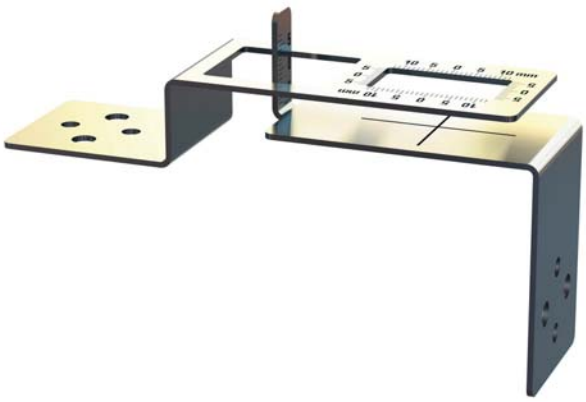
buildera™

SCAN QR CODE WITH MOBILE PHONE FOR DETAILED ONLINE DOCUMENTATION AND ORDERING INFORMATION

Data Sheet and Installation Guide — Model 2412-ECSS (Exterior)

CRACKMON® 3D XYZ-Axis Crack Monitor

Industrial-Grade Crack Monitor Measures Crack Displacement on X, Y & Z Axes



3D Crack Measurements for Concrete, Masonry, Plaster, Stucco and Steel

- Airports, bridges, dams, highways, power plants
- Basements, beams, foundations, retaining walls, seismic retrofits, unreinforced masonry
- Commercial and residential structures, historic monuments

Features and Benefits

- **Measure crack displacement in 3D**: Ideal for non-planar offset cracks
- **Crack measurement range**: ±12 mm (X), ±6 mm (Y), ±7 mm (Z-offset)
- **Secure mounting**: Use fasteners and thixotropic epoxy for best results
- **Rugged**: Heavy-duty 18-gauge type-304 stainless steel resists corrosion
- **Flush and corner options**: Flush (816291010037) and inside corner (816291010044)
- **Proven quality**: Engineered and made in USA

Product Description

The Buildera CRACKMON® 3D Model 2412-ICSS is an exterior-corner-mount, stainless-steel, industrial-grade crack monitor for the repair, restoration, and long-term monitoring of concrete, masonry, plaster, stucco, and steel structures where 3-axis measurements are required. Most crack monitors or crack meters measure in one or two dimensions, but not all three. The CRACKMON 3D is ideal for foundation and basement restoration, seismic retrofitting, or any structural, geotechnical, or civil engineering project that requires ongoing monitoring of structural defects and cracks in three dimensions.

Buildera manufactures each CRACKMON 3D in the USA using state-of-the-art precision laser cutting. Durable type-304 stainless steel with high-contrast laser-etched markings provide permanent readability even in harsh, corrosive outdoor environments.

Specifications subject to change without notice. Epoxy sold separately.

Ordering Information

Model (Qty)	UPC
CRACKMON® 3D 2412-ECSS	816291010051
STRUPOXY™ Adhesive (1 Oz)	816291010099
TRACARD® 3D StarterPak (12)	816291010368

Related Products

Model (Qty)	UPC
CRACKMON® 4020A (1)	816291010259
CRACKMON® 4020A (3-Kit)	816291010006
CRACKMON® 4020A (18-Kit)	816291010013
CRACKMON® 5020AV (1)	816291010389
CRACKMON® XL 15040A (1)	816291010440
CRACKMON® 224R (1)	816291010112
CRACKMON® 224R (50-Bulk)	816291010167
CRACKPOINT™ 60ti (10)	816291010303
CRACKPOINT™ 90ti (10)	816291010310
CRACKPOINT™ TR50ti-Kit	816291010334

Engineering Specifications

Parameter	Specification
Dimensions (at 0,0)	150 mm (L) x 32 mm (W)
Crack Range (XYZ)	±12 mm, ±6 mm, ±7 mm
Discrimination	±1 mm (visual)
Weight	59 g (2.1 oz)
Material	18-gauge type 304 SS
COE	17 µm/m-°C, 0 to +100 °C
Mounting Method	Epoxy and/or fasteners
Fastener Sizes	M4.2 (#8), M3.5 (#6) SMS
Fastener Type	Sheet-metal pan head
Anchor	Toggler® A5 (3/16" dia.)
Country of Origin	USA

CRACKMON®, CRACKPOINT™, STRUPOXY™ & TRACARD® are trademarks of Buildera.

©2015 Buildera. All rights reserved. Printed in USA.

SPECIMEN

PHANTOM®

TERMITICIDE • INSECTICIDE

For sale to, use and storage only by individuals/firms licensed or registered by the state to apply termiticide and/or general pest control products.

Active Ingredient:

Chlorfenapyr: 4-bromo-2-(4-chlorophenyl)-1-(ethoxymethyl) 5-(trifluoromethyl)-1H-pyrrole-3-carbonitrile	21.45%
Other Ingredients:	78.55%
Total:	100.00%

1 gallon contains 2.0 pounds of active ingredient.

EPA Reg. No. 241-392 **EPA Est. No.**

KEEP OUT OF REACH OF CHILDREN.

CAUTION/PRECAUCIÓN

Si usted no entiende la etiqueta, busque a alguien para que se la explique a usted en detalle.
(If you do not understand this label, find someone to explain it to you in detail.)

See inside booklet for complete **First Aid**, **Precautionary Statements**, **Directions For Use** and **Conditions of Sale and Warranty.**

For Product Use Information, Call 1-877-837-6436

In case of an emergency endangering life or property involving this product, call day or night 1-800-832-HELP (4357).

Net Contents:

BASF Corporation
26 Davis Drive
Research Triangle Park, NC 27709

BASF
The Chemical Company

FIRST AID	
If swallowed	• Call a poison control center or doctor immediately for treatment advice. • Have person sip a glass of water if able to swallow. • **DO NOT** induce vomiting unless told to do so by the poison control center or doctor. • **DO NOT** give anything by mouth to an unconscious person.
If on skin or clothing	• Take off contaminated clothing. • Rinse skin immediately with plenty of water for 15-20 minutes. • Call a poison control center or doctor for treatment advice.
If inhaled	• Move person to fresh air. • If person is not breathing, call 911 or an ambulance, then give artificial respiration, preferably mouth-to-mouth, if possible. • Call a poison control center or doctor for treatment advice.
If in eyes	• Hold eye open and rinse slowly and gently with water for 15-20 minutes. • Remove contact lenses, if present, after the first 5 minutes, then continue rinsing eye. • Call a poison control center or doctor for treatment advice.
HOT LINE NUMBER	
Have the product container or label with you when calling a poison control center or doctor, or going for treatment. **In case of an emergency endangering life or property involving this product, call day or night 1-800-832-HELP (4357).**	

PRECAUTIONARY STATEMENTS

HAZARDS TO HUMANS AND DOMESTIC ANIMALS

CAUTION

Harmful if swallowed, inhaled or absorbed through the skin. Causes moderate eye irritation. DO NOT get in eyes, on skin, or on clothing. Avoid breathing vapors or spray mist. Wash thoroughly with soap and water after handling and before eating, drinking, chewing gum or using tobacco. Remove contaminated clothing and wash clothing before reuse.

Personal Protective Equipment (PPE)
Some materials that are chemical-resistant to this product are listed below. If you want more options, follow the instructions for **Category C** on an EPA chemical resistance category selection chart.

All pesticide handlers (mixers, loaders and applicators) must wear:
- Long-sleeved shirt and long pants
- Chemical-resistant gloves such as barrier laminate, butyl rubber or nitrile rubber, neoprene, or polyvinyl chloride (PVC), or viton (≥14 mils).
- Shoes plus socks

Follow manufacturer's instructions for cleaning/maintaining PPE. If no such instructions for washables, use detergent and hot water. Keep and wash PPE separately from other laundry.

In addition, all termiticide handlers must wear a dust/mist filtering respirator (MSHA/NIOSH Approved Number Prefix TC-21C) or a NIOSH approved respirator with any N, R, P or HE filter, when working in a non-ventilated space, including but not limited to crawl-spaces and basements; all termiticide handlers must wear protective eyewear when working in a non-ventilated space when applying termiticide by rodding or sub-slab injection.

User Safety Recommendations
Users should: • Wash hands before eating, drinking, chewing gum, using tobacco or using the toilet. • Remove contaminated clothing. Then wash thoroughly and put on clean clothing. • Remove PPE immediately after handling this product. Wash the outside of gloves before removing. As soon as possible, wash thoroughly and change into clean clothing.

Environmental Hazards
This pesticide is toxic to aquatic organisms, birds and wildlife. **DO NOT** apply directly to water or to areas where surface water is present or intertidal areas below the mean high water mark. **DO NOT** contaminate water by cleaning of equipment or when disposing of equipment washwaters or rinsate.

Physical or Chemical Hazards
DO NOT apply this product around electrical equipment due to the possibility of shock hazard.

Storage and Disposal

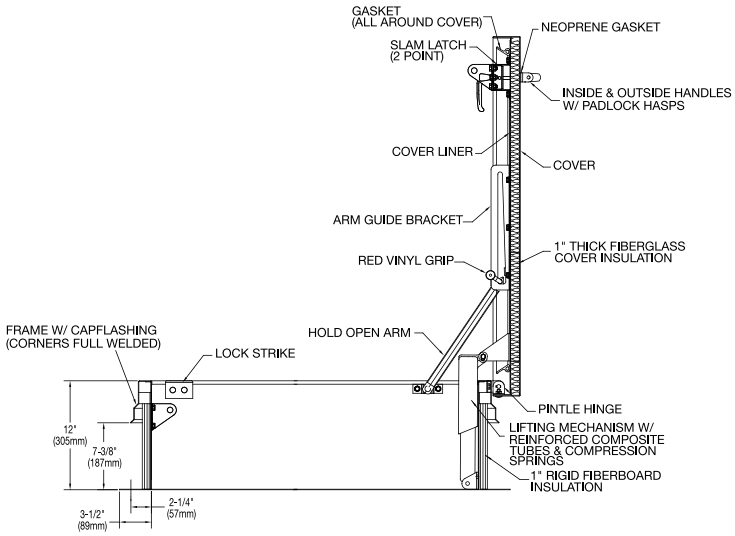
DO NOT contaminate water, food, or feed by storage or disposal.

Pesticide Storage: Store in original container in secure dry storage area. **DO NOT** store below 32 degrees F. **DO NOT** store in direct sunlight or heat.

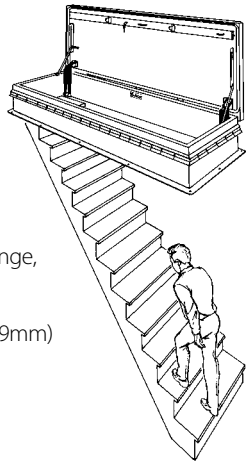
To Contain a Spill: In case of spills, avoid contact and isolate area. To confine spills, dike surrounding area or absorb with sand, cat litter, commercial clay, gel or similar absorbents.

Type L Service Stair Access





Description:
Ideal for installations where frequent use may be expected. Permits easier movement of maintenance personnel, tools and equipment from a full size stairway. Available in galvanized steel, aluminum or stainless steel construction.



Specifications:

Material *(select one)*
- Steel: Cover and frame are 14 gauge (1.9mm) G-90 paint bond galvanized steel
- Aluminum: Cover and frame are 11 gauge (2.3mm) aluminum
- Stainless Steel: Cover and frame are 14 gauge (1.9mm) Type 304 stainless steel

Cover
Brakeformed, hollow-metal design with 1" (25.4mm) concealed fiberglass insulation, 3" (76mm) beaded, overlapping flange, fully welded at corners, and internally reinforced for 40 psf (195 kg/m^2) live load

Curb
12" (305mm) in height with integral capflashing, 1" (25.4mm) fiberboard insulation, fully welded at corners, and 3-1/2" (89mm) mounting flange with 7/16" holes (11mm) provided for securing frame to the roof deck

Gasket
Extruded EPDM rubber gasket permanently adhered to cover

Hinges
Heavy-duty pintle hinges with 3/8" (9.5mm) Type 316 stainless steel hinge pins

Latch
Enclosed two-point spring latch with interior and exterior turn handles and padlock hasps

Lift Assistance
Compression spring operators enclosed in telescopic tubes. Automatic hold-open arm with grip handle release.

Finish
- Steel: Alkyd base red oxide primer
- Aluminum: Mill finish
- Stainless Steel: Type 304 stainless steel with bead blast finish

Hardware
- Steel: Engineered composite compression spring tubes. Steel compression springs. All other hardware is zinc plated/chromate sealed.
- Aluminum: Engineered composite compression spring tubes. Steel compression springs. Type 316 stainless steel hinges. All other hardware is zinc plated/chromate sealed.
- Stainless Steel: Type 316 stainless steel



Standard Sizes and Weights

SIZE		STEEL			STEEL CURB & ALUMINUM COVER			ALUMINUM			STAINLESS STEEL		
(width x length)		Model #	Weight		Model #	Weight		Model #	Weight		Model #	Weight	
inches	mm		lbs.	kg.		lbs.	kg.		lbs.	kg.		lbs.	kg.
30 x 96	762 x 2438	L-20	434	197	L-40	295	134	L-50	253	115	L-90*	434	197

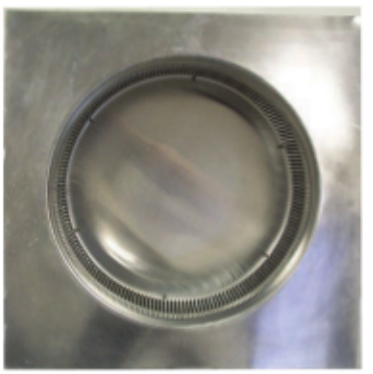
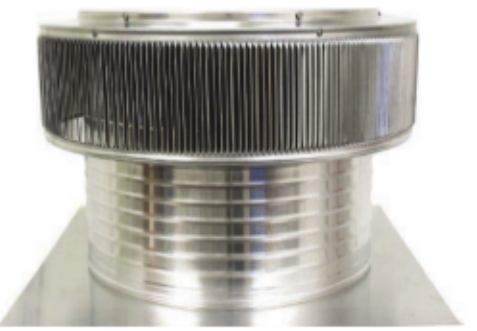
* This model is a special order.

Active Ventilation Products Inc
800-Roof-Vent (766-3836) • 845-565-7770
roofvents.com • sales@roofvents.com

PROUDLY MADE IN THE USA

AV-18-C12 Aura Roof Vent

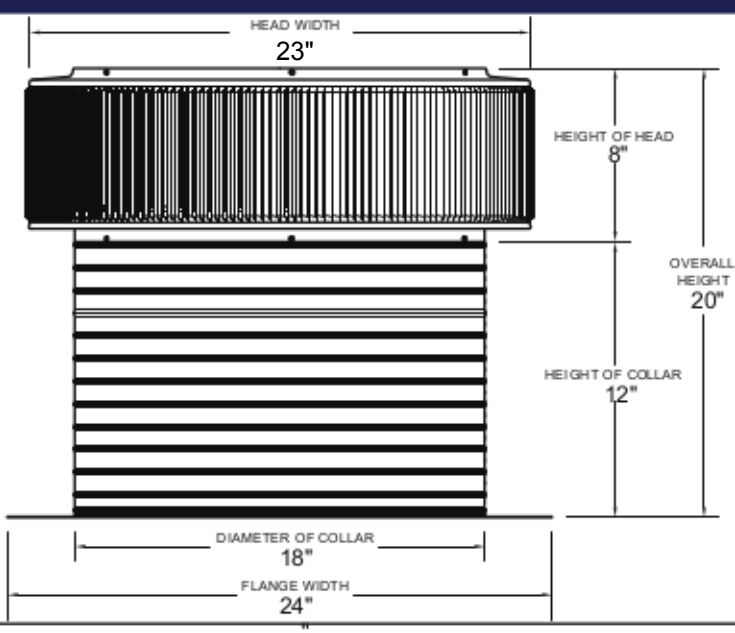
A Roof Vent That Exhausts Air Like a Turbine,
With No Moving Parts, Using Wind, a Renewable Energy Source

- Durable All Aluminum Construction
- Collars Are Available to Increase the Height of the Vent
- Head Assembly is Removable for Easy Installation and Maintenance, Can Be Retrofitted on an Existing Base
- Tested for Texas Insurance, at Wind Speeds up to 200 mph
- Powder Coating Available
- 5 Year Guarantee



DIMENSIONS & SPECIFICATIONS OF THE AV-18-C12



Pitch Capacity		
Min.	Max. (Std Vent)	Max. (Modified)
0/12	5/12	12/12

Net Free Vent Area	
(sq. inches)	(sq. feet)
254	1.76

Application per Sq. Foot	
(1/150)	(1/300)
525	1,050

Weight
12 lbs

CFM Performance Testing using wind only				
4 mph	5.2 mph	7.4 mph	9.8 mph	11 mph
313	352	493	554	634

Active Ventilation Products Inc

800-Roof-Vent (766-3836) • 845-565-7770

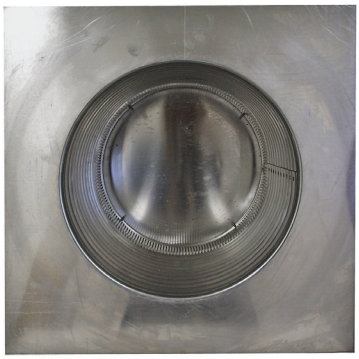
roofvents.com • sales@roofvents.com

PROUDLY MADE IN THE USA

KV-12 Keepa Vent

A Spun Aluminum Gravity Ventilator

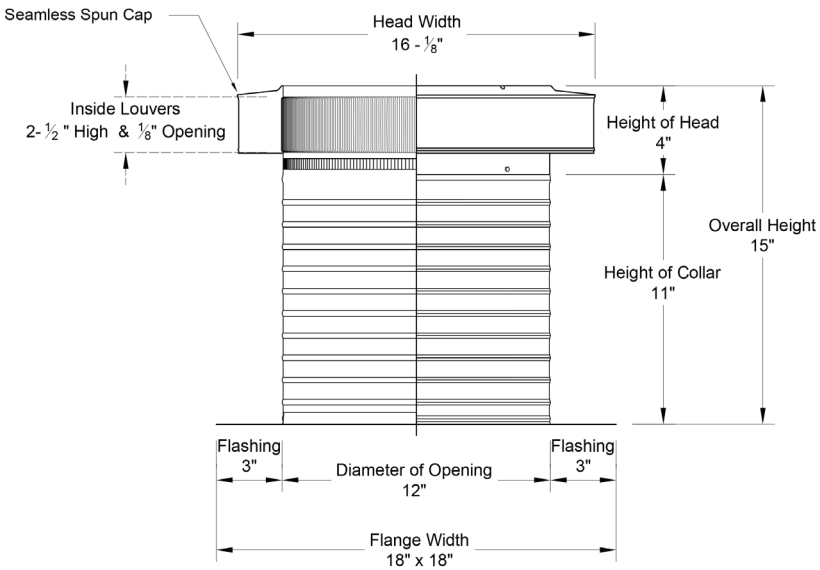






- For Flat Roof Attic Ventilation
- Removes excess heat in the summer and moisture in the winter
- Corrosion Resistant, Rust Free, Heavy Gauge Aluminum Vent that has a durable beaded edge
- Resistant to strong wind & prevents rain or deep snow entering
- Removable vent cap allows for an easy rubber boot installation for membrane roofs
- Inner vertical louvers keep out insects & animals
- Can be used to vent a bathroom and kitchen fans
- Used as Air intake or Exhaust (two-way roof vent)
- 5 year warranty

DIMENSIONS & SPECIFICATIONS OF THE KV-12



Pitch Capacity	
Min.	Max.
0/12	2/12
Net Free Vent Area	
(sq. inches)	(sq. feet)
113	.78
Application per Sq. Foot	
(1/150)	(1/300)
225	450
Weight	
4.5 lbs.	

saju_hsr_back.ai crop marks are black .5 pt lines

National Park Service
U.S. Department of the Interior

San Juan National Historic Site
501 Norzagaray Street
San Juan, PR 00901

www.nps.gov/saju

EXPERIENCE YOUR AMERICA ™